Channel bifurcation and adjustment in multi-channelled floodplain wetlands

Northern Macquarie Marshes, 2017

Neda Yousefi
Bachelor of Agriculture Engineering- Water
Master of Agriculture Engineering- Water Structures

Department of Earth and Environmental Sciences

This thesis submitted for the degree of Doctor of Philosophy, October 2019.

MACQUARIE
University

Table of Contents

Abstract

Multi-channelled rivers and floodplain wetlands are geomorphologically dynamic systems that provide vital resources and habitat. River bifurcation is a critical element of channel formation and adjustment in these systems. Bifurcations may be stable or unstable, leading to anastomosing reaches and also wholesale avulsions that create new channels. The division of discharge, stream power and sediment load between channel branches may be uneven and change over time. Depending on the spatial patterns of branches and the associated processes of channel adjustment, either continuous or discontinuous channels will occur that define the structure of floodplain wetlands into the future. New evidence from the Macquarie Marshes, a large, low energy, floodplain wetland system in semi-arid Australia, demonstrates the importance of bifurcations and return points leading to maintenance of channel capacity despite loss of flow to the floodplain. Estimates of bankfull discharge and unit stream power suggest that channels are able to effectively transmit water and sediment to downstream reaches until a threshold is crossed whereby channels become increasingly inefficient and decline in size rapidly downstream. This ultimately leads to channel breakdown where channels cannot be maintained and where water floods out onto alluvial surfaces at channel termini. The historical trajectory of channel behaviour in hyper-avulsive reaches of this system showed fluctuations in channel capacity adjustment from 1992 to 2018, including large variations in bankfull width, depth and cross-sectional area, as well as bankfull discharge and unit stream power. Erosion is central to the formation of bifurcations and avulsion processes in the Macquarie Marshes. Analysis of erosion risk showed that despite channel ranking according to likelihood and consequence of channel change, few sites experienced significant changes between 2012 and 2018. Overall, understanding the biophysical character and behaviour of multi-channelled floodplain wetlands is important for water resources and environmental management.

Statement of Originality

I hereby declare this thesis, performed by Neda Yousefi, has not previously been submitted for a degree or diploma in any university or institution. To the best of my knowledge and belief, the thesis contains no material previously published or written by another person except where due references is made in the thesis itself.

Neda Yousefi

October 2019

Acknowledgements

Firstly, I would like to give a sincere thanks to my primary supervisor, Tim Ralph, for his continued guidance and professional advice throughout this project. Tim's constant support gave me the opportunity to develop my confidence and ability as a research scientist.

I would like to thank my associate supervisors, Paul Hesse and Michael Chang, for their guidance and assistance.

I also extend my thanks to Will Farebrother and Sam Shumack for their tremendous assistance and advice in GIS issues. Thanks to Will Farebrother, Sana Khan, Carl Helander, Bradley Graves, Zacchary Larkin, Marc Humphries and Tim Ralph for their help in the field.

A special thanks to Tim Hosking, Paul Keyte and Stephanie Suter from the NSW Department of Planning, Industry and Environment (previously the Office of Environment and Heritage) for their logistical support.

The services of a professional editor, Nina Giblinwright, were employed in the production of this thesis, as permitted by Macquarie University policy and compliant with the *Guidelines for editing research theses* (revised 25 February 2019) provided by the Institute of Professional Editors Limited.

Thanks to the "International Macquarie University Research Excellence Scholarship" (iMQRES) for funding this research.

Finally, I truly thank my dear family and in particular my husband, Mehrzad. Thanks, dear Mehrzad, for all of your support, understanding and unwavering love.

Chapter 1: Thesis introduction

1.1 Introduction

This chapter introduces the characteristics and importance of multi-channelled rivers and floodplain wetlands in dry landscapes and describes key concepts related to channel change in these systems. The setting and significance of the Macquarie Marshes, Australia, are introduced, and the main concerns regarding rapid channel change in multi-channelled systems are recognised, leading to the fundamental research question, specific aims and structure of this thesis.

1.2 Multi-channelled rivers and floodplain wetlands

Multi-channelled rivers and floodplain wetlands are geomorphologically dynamic systems that provide vital habitat for fauna and flora (Kingsford and Thomas, 2004; Zedler and Kercher, 2004) and help to maintain local and regional ecological balances (Xue et al., 2008). Multi-channelled rivers typically have anabranching or distributary channel networks and occur in a range of climatic, tectonic and hydrological settings, with variable or seasonal flood and sediment regimes, and a range of channel and bank forms and processes related to erosion and sedimentation (Hooke and Mant, 2000; Larkin et al., 2016; Roy and Sahu, 2015). Anastomosing rivers are a sub-category of anabranching rivers, with multiple channels that are separated by stable islands in low-energy settings dominated by fine, cohesive sediment (Heritage et al., 2016; Nanson and Knighton, 1996). Vegetation type and cover also affects channel morphology by influencing flow resistance and bank strength in these systems (Li et al., 2015; Tooth and Nanson, 2000). Floodplain wetlands are areas of land that are inundated regularly, periodically or irregularly due to flow and flooding from rivers, with inundation-adapted soils and biota (Ralph et al., 2016). Floodplain wetlands are often associated with multi-channelled rivers, especially in arid, semi-arid and sub-humid landscapes (i.e. drylands) (Gell et al., 2009; Ralph et al., 2011). Floodplain wetlands in drylands create highly important ecosystems for agriculture and aquatic species by providing inputs of fresh or saline water in otherwise water-stressed environments (Sandi et al., 2019). It is important to understand these types of rivers and wetlands because their formation and development are strongly influenced by channel change processes that have flow-on effects for habitats and ecosystem functions (Larkin et al., 2016).

The various intrinsic and extrinsic factors influencing multi-channelled rivers and floodplain wetlands causes high levels of variability and unpredictability in the geomorphology of these systems (Ralph et al., 2016). For example, intrinsic processes (e.g. erosion and sedimentation) affect the morphological character (and metrics) of the channels and the development of surrounding wetlands (Larkin et al., 2016; Oyston et al., 2014). External mechanisms (e.g. climate and tectonics) are also important because they control factors such as hydrology, base level and sediment supply (Larkin et al., 2016). These intrinsic and extrinsic factors affect the physical characteristics and biodiversity of the floodplain wetlands (Rolls et al., 2018). Therefore, understanding the behaviour and biophysical character of multi-channelled rivers with floodplain wetlands is important for water resources and environmental management and conservation (Fryirs et al., 2018).

1.3 Overview of channel change in multi-channelled rivers and floodplain wetlands

Processes of erosion and sedimentation are important for the development and maintenance of all rivers and floodplain wetlands (Oyston et al., 2014). Erosion is an inherent process in rivers and floodplain wetlands but anthropogenic impacts (i.e. mining, grazing and river regulation) and natural causes (i.e. climate change, tectonic activity and hydrology shift) instigate variations in the rate, location and distribution of erosion (Yang et al., 2015). Erosion tends to dislodge and remove sediment from the outside of meander bends, from the base of channel beds and from the surface of floodplains (Beneš et al., 2006; Steiger et al., 2003). In doing so, erosion forms and shapes geomorphic units such as ledges, knickpoints, chute channels, meander cut-offs (i.e. oxbows) and flood channels (Kamintzis et al., 2019; Li et al., 2020; Lisenby et al., 2019; Oyston et al., 2014). Sedimentation, the process of sediment deposition in channels and on floodplains or wetlands, is responsible for the growth of geomorphic units, such as point bars and benches within channels and levees on floodplains (Lisenby et al., 2019; Ralph and Hesse, 2010). Together with a range of processes responsible for sediment transport, erosion and sedimentation serve to excavate, redistribute and store sediment in rivers and floodplain wetlands (Oyston et al., 2014).

Alluvial rivers typically respond to changes in external forces or internal processes by adjusting their channel geometry or developing a multi-channelled configuration (Nanson and Knighton, 1996; Savic et al., 2017). Therefore, erosion associated with channel bifurcation (i.e. splitting of flow) and avulsion (i.e. diversion of flow) is particularly important for multi-channelled rivers with floodplain wetlands. Bifurcation is the division of a single channel into two downstream branches in response to hydrological and sedimentological factors (Bolla Pittaluga et al., 2003; Kleinhans et al., 2010). Avulsion is the abandonment of a river channel in favour of a new position that may occur over relatively short reaches, or along whole meander belts, on the floodplain (Hajek and Edmonds, 2014; Heyvaert et al., 2012). A bifurcation may lead to an anabranching or anastomosing channel pattern (where two channels diverge and then reconverge downstream) or a distributary pattern (where two channels diverge but do not reconverge), or it may cause abandonment of the primary channel in favour of the new one (i.e. avulsion) (Gibling et al., 1998; Larkin et al., 2017; Wright, 1977). If a system has very high avulsion frequency, it may be described as hyper-avulsive (Jain and Sinha, 2003). However, irrespective of avulsions, where channels cannot maintain their water and sediment transport capacity, channel breakdown may occur (Ralph et al., 2016). Channel breakdown is a degradation of trunk streams into smaller branches and distributary channels due to a reduction of fluvial efficiency to a point where channelized flow cannot be maintained (Ralph and Hesse, 2010). In some cases, an avulsion may occur when an internal threshold is crossed and channels become very inefficient and/or super-elevated above the floodplain (Tooth, 1999). This may lead to a channel bifurcation and new channel formation on the floodplain, or to water and sediment flooding out of the channel and spreading over adjacent alluvial surfaces in the form of a floodout (Tooth, 1999).

Avulsion is a complex process of channel adjustment and shifting that occurs over a range of spatial and temporal scales (Kleinhans et al., 2010). It impacts upon local floodplain and wetland geomorphology and ecology leading to aquatic habitat changes (Oyston et al., 2014; Sinha et al., 2017). Avulsion also determines channel location and alluvial architecture over the long periods of time by controlling the actual mechanisms of channel evolution and floodplain development (Farrell, 2001; Hajek and Edmonds, 2014). The ability of an alluvial channel to adjust its transport capacity through erosion and sedimentation influences the probability of avulsion occurring (Lisenby et al., 2019). Therefore, understanding the contribution of these processes to channel adjustment in multi-channelled systems is vitally important for their conservation and management.

Few studies have been conducted to characterise patterns and processes of channel erosion, bifurcation and avulsion in contemporary low energy, multi-channelled Australian rivers with significant floodplain wetlands. The Macquarie Marshes are one of the systems in central, semi-arid New South Wales (NSW) that are prone to erosion and avulsion (Ralph et al., 2016). Moreover, there have been no robust or repeat studies conducted that allow for an assessment of channel change over time in this type of system. Therefore, this thesis addresses these knowledge gaps by investigating key patterns of channel bifurcation and adjustment to allow for interpretation of the processes governing channel maintenance (i.e. avulsion and anastomosis) and failure (i.e. channel breakdown) using the Macquarie Marshes as a model system.

1.4 Setting and significance of the Macquarie Marshes

The Macquarie Marshes are one of the largest, perennial floodplain wetland systems with anastomosing and distributary channels in the Murray-Darling Basin (Figure 1.1; Kingsford and Thomas, 1995; Ralph et al., 2016). The Macquarie River, in central NSW, is an inland draining system fed from the Great Dividing Range that flows north-west through a partly-confined, sub-humid valley and out onto a broad, semi-arid alluvial plain (Thomas et al., 2015; Wen et al., 2013). The Macquarie River catchment is situated in a tectonically stable, intra-cratonic (plate centre) setting and the river receives variable rainfall, runoff and discharge from the headwaters (Ralph and Hesse, 2010). River discharge and stream power decline downstream from Dubbo in the Macquarie River system, which leads to a marked decline in the size of the main channel and its subsidiary channels in the lower reaches and in the Macquarie Marshes (Ralph and Hesse, 2010). These intrinsic hydrogeomorphic processes, combined with the minimal lateral migration of the channels and increased sedimentation associated with in-channel vegetation, drive avulsion and channel breakdown in the Macquarie Marshes (Ralph and Hesse, 2010; Yonge and Hesse, 2009). Moreover, evidence exists for the recent abandonment of river channels within the Macquarie Marshes and channel change due to palaeochannel evolution in the landscape (Hesse et al., 2018; Yonge and Hesse, 2009). The position of the abandoned palaeochannels and newly formed channels determines the topography of the system and the location of active and desiccated wetlands in the Macquarie Marshes (Hesse et al., 2018). Over time, these channels change and help to define the structure of the floodplain wetlands in the coming decades (Hesse et al., 2018).

The Macquarie Marshes consist of numerous channels and wetlands that provide unique habitat for many species of aquatic fauna (e.g. migratory waterbirds, including ibis, egrets, herons; native fish, including golden perch, gudgeons, cod) and flora (e.g. river red gum woodlands, Phragmites reed beds, bullrush; see Figure 1.2), and so management of this system is an important issue for nature conservation in both NSW and Australia (Rogers and Ralph, 2011; Wang et al., 2016). Furthermore, channels in this system that have quantifiable rates of erosion, bifurcation and avulsion may be studied to understand the broader processes of river and wetland evolution. Therefore, the Macquarie Marshes is an ideal system for the investigation of contemporary and historical channel character and behaviour, and for assessing the role of erosion when channel change contributes to channel avulsion, anastomosis and breakdown. In particular, the Southern Macquarie Marshes has channels prone to sedimentation, erosion and avulsion (hyper-avulsive behaviour), and so much of the analysis in this thesis is focussed at the sub-system scale of the Southern Marshes.

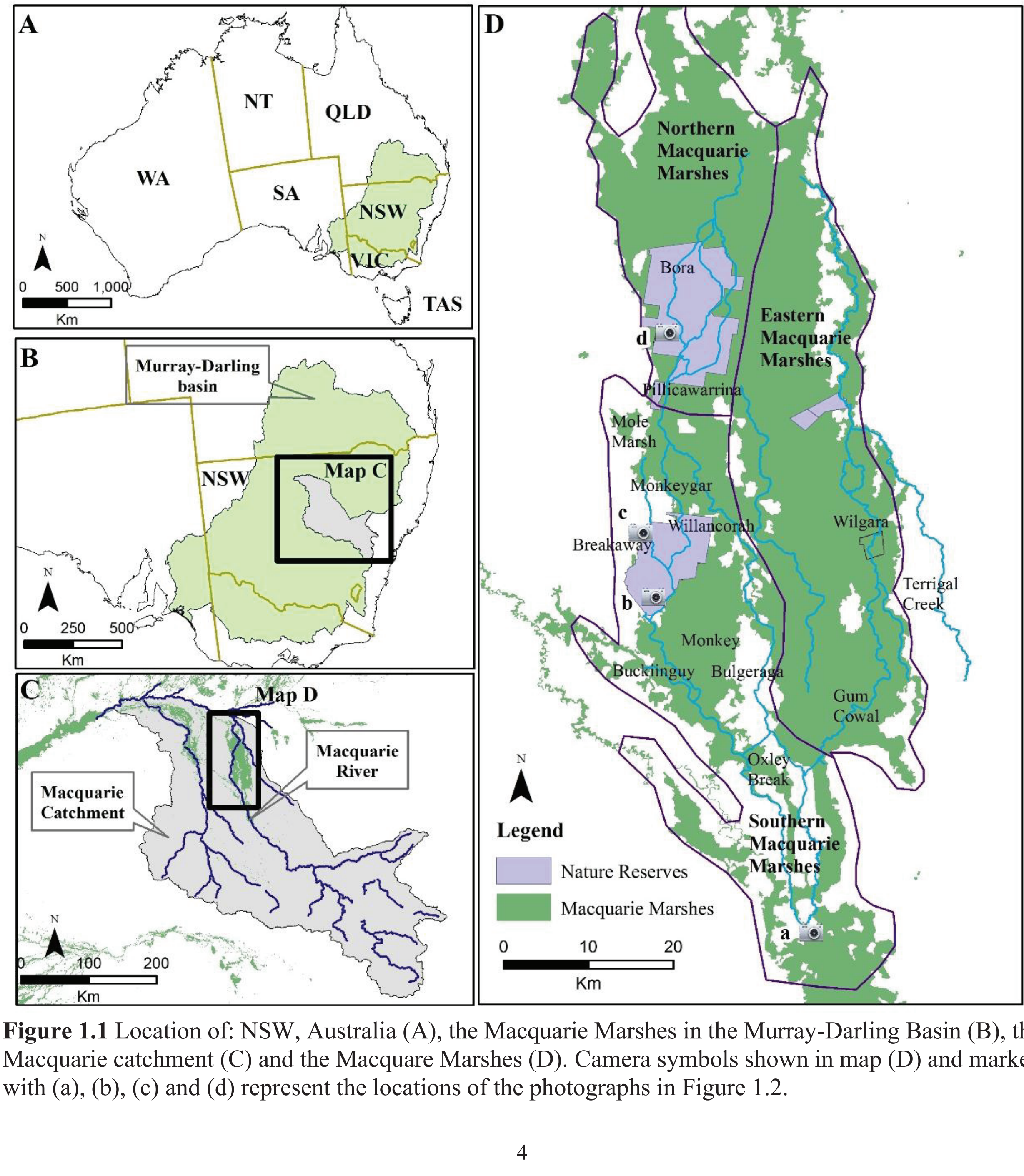

Figure 1.1 Location of: NSW, Australia (A), the Macquarie Marshes in the Murray-Darling Basin (B), the Macquarie catchment (C) and the Macquare Marshes (D). Camera symbols shown in map (D) and marked with (a), (b), (c) and (d) represent the locations of the photographs in Figure 1.2.

a.
b.
c.
d.

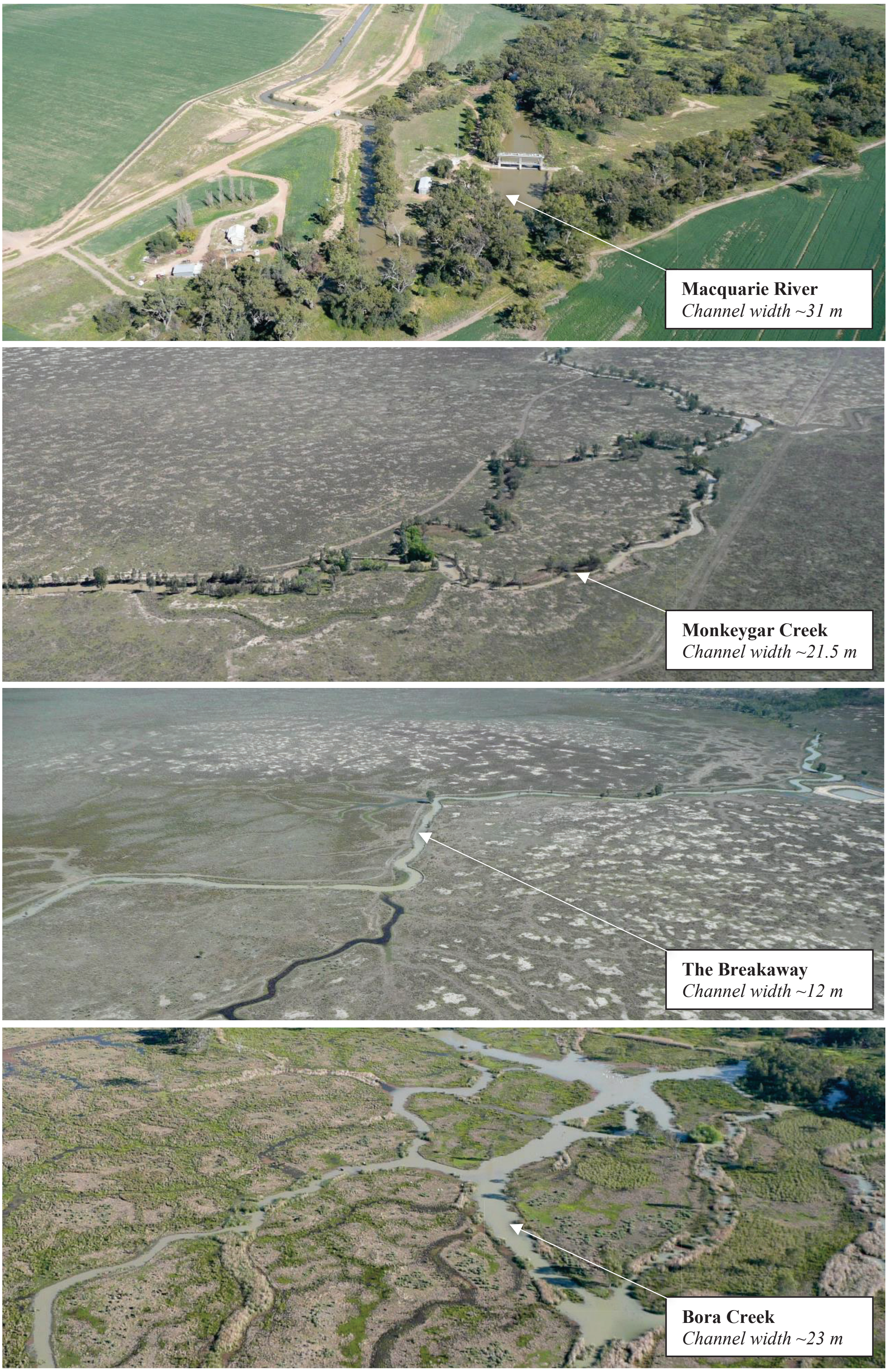

Figure 1.2 Aerial views of the Macquarie River at Marebone Weir, looking downstream and showing the bifurcation of Gum Cowal from the right bank (a), an anastomosing reach of Monkeygar Creek with bifurcation and return points, Southern Macquarie Marshes (b); incised channel of The Breakaway returning to the Old Macquarie River, Southern Macquarie Marshes (c) and shallow anastomosing channels near Bora Creek, Northern Macquarie Marshes (d). All photographs taken in 2008 by Tim Ralph.

1.5 Aims of the thesis

This research aims to understand key patterns and processes of channel change and to define the behaviour of channel bifurcation and avulsion and other modes of channel adjustment by investigating the multi-channelled floodplian wetlands of the Macquarie Marshes.

The specific aims of this research are:

1. *To quantify the spatial patterns of channels and determine the distribution of channel bifurcation and return nodes along major channels within the Macquarie Marshes;*
2. *To define the geomorphic configuration and hydraulic behaviour of channels leading to channel maintenance, avulsion and breakdown in the Macquarie Marshes;*
3. *To identify historical and contemporary trajectories of channel behaviour in hyper-avulsive reaches of the Southern Macquarie Marshes and to explain the role of erosion in the system;*
4. *To assess erosion and sediment deposition risk at key sites in the Southern Macquarie Marshes and to rank channels according to the likelihood and consequences of channel change; and*
5. *To synthesise and understand channel patterns and channel change processes in the Macquarie Marshes that are relevant for water and wetland management.*

1.6 Thesis structure

This thesis is comprised of nine chapters to achieve the aims of the study:

Chapter 1: Introduces key processes of channel change in multi-channelled rivers and floodplain wetlands and outlines the aims of the research.

Chapter 2: Reviews appropriate literature to provide an overview of channel change associated with erosion processes in multi-channelled fluvial systems and summarises key methods of channel change assessment (addresses aims 1 and 5).

Chapter 3: Describes the regional setting of the Macquarie Marshes and outlines the strategy and methods applied in this research (addresses aims 1, 2, 3 and 4).

Chapter 4: Assesses broad patterns of channel expansion and contraction throughout the Macquarie Marshes using field and remote methods (addresses aims 1 and 3).

Chapter 5: Quantifies the distribution of channel bifurcation and return nodes and explains the hydrogeomorphic channel conditions through the Macquarie Marshes (addresses aims 1 and 2).

Chapter 6: Quantifies the geomorphic and hydraulic characteristics of channels in the Southern Macquarie Marshes and presents evidence of recent historical channel changes (addresses aims 2 and 3).

Chapter 7: Determines the key factors affecting bank strength, roughness and channel erosion potential, and assesses and ranks sites in the Southern Macquarie Marshes in terms of erosion risk (addresses aims 3 and 4).

Chapter 8: Discusses the relevance and importance of the results for this system and compares the findings with other research in similar systems (addresses aim 5).

Chapter 9: Synthesises the findings of this thesis and provides recommendations for future research (addresses aim 5).

Chapter 2: Methodological literature review

2.1 Introduction

This chapter provides an overview of fluvial processes and channel change in multi-channelled river systems with floodplain wetlands and discusses some key factors that contribute to fluvial adjustment in these systems. Techniques used to quantify channel change and erosion processes are reviewed and an overview of the key advantages and drawbacks of these approaches is presented to identify appropriate techniques for this research. The thesis aims addressed by this chapter are:

1. *To quantify the spatial patterns of channels and determine the distribution of channel bifurcation and return nodes along major channels within the Macquarie Marshes.*
5. *To synthesise and understand channel patterns and channel change processes in the Macquarie Marshes that are relevant for water and wetland management.*

2.2 Channel change in multi-channelled river systems and floodplain wetlands

Alluvial rivers can produce single (straight, sinuous or meandering) or multi-channelled (braided, anabranching or anastomosing) forms. Studies have shown that very straight or sinuous channels are not stable and modify themselves where possible to a meandering form with moderate sinuosity (Deng and Singh, 1999). However, single meandering alluvial channels adopt multi-channelled patterns when they are not able to transport sediment while maintaining their single channel geometry (Belletti et al., 2015; Bravard, 2010). Multi-channelled systems develop anabranching (anastomosing style in lowland rivers) or distributary forms depending on the flood regime, boundary conditions, channel bank and floodplain composition, mechanism of sedimentation, flow displacement and tectonism processes (Jain and Sinha, 2004). Anabranching patterns form with separated channels within vegetated, semi-permanent islands with specific sinuosity and sediment load characterisation that define their hydrological and morphological properties in multi-channelled systems (Jain and Sinha, 2004). Many lowland-dryland regions are characterised by rivers with stable anabranching patterns while receiving few tributary inputs, leading to downstream declines in discharge and channel transport efficiency, which can cause distributary patterns to develop in these regions (Deng and Singh, 1999; Ralph and Hesse, 2010).

Bank erosion and lateral migration play an important role in controlling channel stability, sediment load and the destruction or reworking of floodplains (Lovric and Tosic, 2016). Eventually, in the case of avulsion, excessive amounts of sediment deposition within the channel will encourage the river to divide (bifurcate) and migrate to a new position on the floodplain (Savic et al., 2017). Avulsion is also a response to a combination of other autogenic and allogenic factors; from river accretion and lateral migration, to climate change and sea level variation (Heyvaert et al., 2012). The frequency of avulsion depends on the vertical sedimentation rate, where slowly or rapidly aggrading river processes causes infrequent and more rapidly avulsion occurrence, respectively (Larkin et al., 2017). Repeated avulsions will expand channel breakdown and floodplain abandonment as a later effect (Ralph and Hesse, 2010). Therefore, understanding erosion and sedimentation processes and quantifying the amount of channel changes associated with channel bifurcation and avulsion is particularly important for multi-channelled rivers with floodplain wetlands.

There are many approaches to erosion measurement in multi-channelled rivers and floodplain wetlands. These procedures may be classified into two main groups, including physical assessments and modelling techniques. Physical assessments of channel change are based on an experimental research procedure that requires direct data extraction from the study area (Lallias-Tacon et al., 2017; Veihe et al., 2011; Xia et al., 2004). Modelling techniques require software to generate and interrogate data remotely, or to test fundamental concepts in fluvial geomorphology (Coulthard and Van de Wiel, 2012).

2.3 Physical assessments for analysis of channel change and erosion processes

Understanding historical channel changes and their main driving factors are critical for floodplain and river management (Ralph et al., 2016). Physical assessments supply a wealth of information through various methods that can be used individually or in combination to provide data that enables the assessment of river patterns and planforms, riparian conditions and channel changes (Lauer et al., 2017; Lu et al., 2016). Generally, data obtained from this approach can be extracted remotely or directly from the field (Lawler, 1993; Rădoane et al., 2017). Table 2.1 synthesises the key methods of physical landscape assessment and their modes of application to rivers, while a brief review of the techniques is provided below.

2.3.1 Field methods

On-ground measurement approaches have been used to generate high-resolution data from the field. These methods are often very precise, although limitations can occur when extrapolating data from a single field site or field season to wider areas and/or time scales (Smith and Vericat, 2015). While many field measurement approaches can be used for geomorphology, vegetation and water condition analysis in rivers, the high cost of some equipment and of having personnel in the field for lengthy periods of time can limit the usage of the techniques (Musa et al., 2015; Smith and Vericat, 2015).

Erosion pin is a simple and inexpensive technique that has been applied to assess bank erosion in short to medium timescales for a wide range of fluvial environments (Foucher et al., 2017; Kearney et al., 2018; Malik and Matyja, 2008). In this method, a 0.25 to 0.5 m long and a 2 mm by 6 mm diameter pin (usually made of metal) is inserted into the riverbank and increased exposure of the pin over time reveals the erosion in the bank (Foucher et al., 2017). Bank erosion rates (and sedimentation rates, if the pin becomes buried) are estimated by repeated measurements of the exposed length of each pin (Steiger et al., 2003).

Table 2.1 Examples of physical assessment methods applied for erosion and channel change measurements.

	Method	System component	Utility	Example Location	Source	Applied in this thesis
Field	Erosion pin	Reaches/sites	Bank erosion	UK (Nant Tanllwyth, Afon Trannon and River Arrow)	Couper et al., 2002	No
	PEEP	Reaches/sites	Historical bank erosion	UK (Trent-Humper system)	Lawler et al., 2001	No
	Field plot	Reaches/sites	Runoff and soil loss	Data from 65 experimental studies conducted worldwide	Smets et al., 2008	No
	Sediment traps	Reaches/sites	Fluvial processes/sediment deposition	Taiwan (northern South China Sea)	Liu et al., 2014	No
	Marker horizons	Reaches/sites	Sediment deposition	USA (Deal Island Wildlife Management Area)	Rooth and Steveson, 2000	No
	Cross-section survey	Reaches/sites	Historical bank erosion/fluvial processes/vegetation cover	UK (River Cole, west midlands)	Gurnell et al., 2006	Yes
	DGPS	Catchments/reaches/sites	Topography data	Scotland (River Feshie)	Brasington et al., 2000	No
Remote	Satellite imagery	Catchments/reaches/sites	River physical dataset/topography	Cambodia, Laos, Thailand (Mekong River)	Gupta and Liew, 2007	No
	Aerial photography	Catchments/landscape/reaches/sites	Topography/land cover	USA (Soda Butte Creek)	Lea and Legleiter, 2016	Yes
	LiDAR	Catchments/landscape/reaches/sites	River physical dataset/Topography/vegetation cover	France (Drôme River and Bléone River)	Lallias-Tacon et al., 2017	Yes
	DoD	Catchments/reaches/sites	Sediment deposition/erosion/ geomorphic changes	Australia (Lockyer Creek, Queensland)	Croke et al., 2013	Yes
	Photogrammetry, structure-from-motion	Catchments/landscape/reaches/sites	Erosion/topography/bank and bed monitoring	USA (Pedernales river)	Fonstad et al., 2013	No

This approach depends on the climatic conditions during the period of measurement. It cannot be performed over long time periods and cannot provide information about historical bank erosion dynamics (Foucher et al., 2017). Erosion pins may be subject to movement in non-cohesive sediment or when they are exposed to floating matter, which introduces error to the technique (Steiger et al., 2003). The elevation of the bank/slope surface may also change, and this may affect the results; or the pin itself may influence local erosion. Pins also protrude different distances into the water column, which may affect local flow patterns and potential erosion and sedimentation rates (Couper et al., 2002; Steiger et al., 2003).

The Photo-Electronic Erosion Pin (PEEP) is a short timescale approach consisting of a sensor with photovoltaic cells that record voltage based on the radiation of cells (Papanicolaou et al., 2017). When facing an eroding surface, more cells will be exposed to light, causing an increase in voltage output from the device (Lawler, 1991). Otherwise, a drop in photovoltaic outputs will provide evidence of deposition (Bandyopadhyay and De, 2017; Lawler et al., 2001). Although quite complex to install, requiring an *in-situ* data logger and buried cables, if set-up properly this approach allows the history of bank erosion and a quasi-continuous time series of erosion/deposition data in rivers to be recorded (Malik and Matyja, 2008; Steiger et al., 2003). Periodically logged data will indicate the magnitude, frequency and timing of erosion and deposition, and provide an estimation of the dynamic of net changes (Lawler, 1991). The scan frequency is normally considered between 1-30 minutes, but it can also be reduced to less than 1 second if required (Lawler et al., 2001). Since the PEEP sensors are photovoltaic devices, they do not need any power supply; this makes it easier to use this technique in the field (Turowski and Cook, 2017). However, the outputs drop to zero at night, which creates hours of data gaps and/or a significant delay for recording nightly events (Lawler et al., 2001).

A field plot of known size, shape and runoff characteristics is a widely used method for investigating geomorphological processes and soil erosion by allowing areal and volumetric estimates of soil surface loss and channel change at specific sites where repeat visits are possible (Fang et al., 2017). This approach has been applied for short timescale analysis and can cause difficulties for the maintenance of long timescale monitoring in the field due to the onerous work required (Boix-Fayos et al., 2006; Fang et al., 2017). The length of the plot is related to runoff and erosion (Chaplot and Le Bissonnais, 2000). Small plots are easier to replicate and the response of a soil surface cover on runoff and soil loss can be measured immediately (Smets et al., 2008). For longer plots, the runoff and soil loss response can be buffered due to the larger possibility for the runoff to infiltrate or for the sediment to be deposited within the plot (Boix-Fayos et al., 2006; Brazier, 2004; Smets et al., 2008). Using a field plot, it is possible to gain an understanding of the individual factors occurring in natural processes. However, sometimes it is difficult to control all the factors present in the field experiments (Boix-Fayos et al., 2006). In terms of spatial scale, this approach is practical for taking direct measurements in natural conditions and may be used in different types of microenvironments, especially small plots. For large plots, this approach may be used to examine the interaction between factors (Boix-Fayos et al., 2006). However, the measurement of different processes depends on the scale (temporal or spatial) and it can be difficult to obtain an accurate representation (Bagarello et al., 2018; Boix-Fayos et al., 2006).

Sediment traps (bottles, cylinders or flat devices) are useful tools for short timescale analysis (one to two years) and for flood-event estimation of sediment transport and deposition (Steiger et al., 2003). Traps with various time ranges are applied to directly collect particles, to measure properties such as volume, depth and calibre, and to analyse the water quality and organic and propagule content of riparian sedimentation, among other things (Liu et al., 2014; Steiger et al., 2003).

A feldspar marker horizon is a medium timescale approach for estimating deposition and sedimentation depth (Kelleway et al., 2017). In this technique, depth is measured through an installed device in the ground that records the amount of newly deposited sediment sitting on top of the buried marker horizon surface. It requires less complex equipment and is a more affordable option than sediment traps (Steiger et al., 2003). The sampling collection and processing procedures are quick and simple (Cahoon and Turner, 1989). This method has a partial impact on the hydraulic resistance of the surface, and the marker horizons may be subject to movement when the energy from flows hit the marker. If this occurs, then the sediment boundary or surface pre-event cannot be identified correctly (Steiger et al., 2003). Other problems encountered include the requirement for large quantities of markers and the possibility of losing the marker in freshwater systems (Knaus and Van Gent, 1989).

Channel cross-section surveys provide information on channel topography (i.e. elevation and distance measures to calculate width and depth) and repeated surveys can be applied for monitoring short-, medium- and long-term geomorphic processes (i.e. erosion, sediment deposition and sediment transport) (Fuller et al., 2003; Lauer et al., 2017). Indeed, channel morphology changes occur in response to sediment and erosion transfer processes and channel cross-sections provide essential morphological information (for example, cross-sectional area, bankfull width and depth and the width:depth ratio) to calculate changes (Fuller et al., 2003; Lauer et al., 2017). In addition, old survey plans, maps, diaries and other data recorded by surveyors and early explorers can provide historical information to compare with channel cross-section surveys. For example, Trimble (1997) analysed long-term channel changes in San Diego Creek in southern California, USA, using data from cross-sectional surveys. Fuller et al. (2002) also surveyed cross-sections along the River Coquet in northern England to calculate sediment budget variations. In large rivers or channels carrying water at the time of analysis, channel surveys could be done with bathymetric instruments (e.g. Arnaud et al., 2017) and/or an acoustic doppler current profiler (e.g. Kimiaghalam et al., 2016). Regardless of the technique used for the survey, there are some issues inherent to the use of channel cross-sections for calculating channel metrics and hydraulic geometry that affect the analysis of reach-scale sediment budgets (Fuller et al., 2003). These include changing roughness over time (i.e. from vegetation) or anthropogenic modifications to channels (Lawler, 1993). Therefore, vegetation evidence from surveys over long timescales (50-100 years) also provides complementary information on channel change (Lawler, 1993). The composition, density and height of different species of vegetation recorded over time and linked to other evidence from cross-sectional surveys can be used to analyse aspects of channel change (Lallias-Tacon et al., 2017).

Differential Global Positioning System (DGPS) is a technique used for acquiring extremely accurate and high-resolution responses to find elevation data at specific sites of interest (Genç et al., 2004). DGPS uses a network of fixed ground-based reference stations to broadcast the differences between the positions indicated by GPS satellites and the known fixed positions (Milan et al., 2011). This method provides improved location accuracy of approximately 10 cm in cases of best implementation and can be used to locate and contextualise sites being studied using all of the aforementioned field methods. DGPS cannot be applied in highly vegetated areas efficiently and is not accurate for fields where there is inaccessible terrain (Rayburg et al., 2009; Reynolds, 2011).

2.3.2 Remote methods

Remote methods, including remote-sensing and airborne photogrammetry, have provided an extensive understanding of historical channel changes and their main driving factors for floodplain and fluvial systems in short to long timescales (Lallias-Tacon et al., 2017). This approach is practical for measuring morphological channel changes because it characterises the rates of planform changes and channel properties in spatial and temporal scales (Lea and Legleiter, 2016; Lu et al., 2016). This technique is also employed for estimating bank erosion intensity on a long timescale for medium and large sized rivers (with a riverbed at least several metres wide) (Malik and Matyja, 2008). Therefore, it gives an insight into sediment transfer over time, rates of bank erosion, variations in transport and storage along the channel, channel widening and changes in channel planforms (Lea and Legleiter, 2016). Although, in the case of poor image quality and dense cover, this method leads to sizable errors for measuring bank migration rates (De Rose and Basher, 2011).

Satellite imagery is a basic physical remote sensing method that provides efficient and rapid datasets at a range of spatial and temporal resolutions (Gupta et al., 2002). Satellite or radar can extract images to provide data for changes in bare ground surfaces, vegetation, water and other features over large areas (Elmi et al., 2016) This method is also useful for the measurement of channels and analysis of their change over time, and for providing variations in river area with appropriate temporal sampling (Elmi et al., 2016). Understanding channel migration through time is a critical issue in geomorphology and river management (Yang et al., 1999), and satellite imagery is often used in systems that are very large or where the field data acquisition is problematic (Gupta and Liew, 2007). Satellite imagery was used to estimate channel depth in the Po River, Italy (Tourian et al., 2017), and the data provided cross-section information along the river. Channel width data was also obtained from satellite imagery to estimate channel discharge in the Niger River, Africa (Elmi et al., 2015), and numerous studies have modelled discharge from remote sensing imagery based on channel metrics observed in imagery (i.e. Di Baldassarre et al., 2009; Larkin et al., 2017). Aerial photography can be used in the same way to provide data over long time scales and large spatial scales (De Rose and Basher, 2011). Channel size, shape, geomorphic units and vegetation can be assessed, as well as information on bankfull geomorphic changes in channels associated with sediment erosion, transfer and deposition (Lauer et al., 2017). For example, De Rose and Basher (2011) used historical aerial photography to map channels and compared this with Light Detection and Ranging (LiDAR) derived data to measure river bank migration over approximately 50 years, while channel width measurements were performed using aerial photographs in Minnesota River, USA, to determine the discharge behaviour of the river and apply the findings for sediment management (Lauer et al., 2017).

LiDAR is an aerial survey technique that uses a laser mounted to a plane or unmanned aerial vehicle (UAV) to collect elevation data (Charlton et al., 2003; Genç et al., 2004). The airborne laser technology in LiDAR surveys enables the measuring of distances between a physical surface and the sensor, via a laser altimeter (Starek, 2016). The time between a laser pulse to the physical surface and its reflected return signal is multiplied by the speed of light twice the distance to the target to calculate the height of objects (Starek, 2016). LiDAR accuracy for data elevation is estimated at 5-11 cm (10-15 cm in some instances) (Rayburg et al., 2009; Reutebuch et al., 2003). Standard LiDAR is not affected by ground-level environmental conditions such as vegetation and difficult terrain; but it cannot penetrate water (Rayburg et al., 2009). Therefore, it can generate suitable coverage and detailed surface topography for dry areas (Rayburg et al., 2009). The LiDAR instrument can store both vegetation and ground returns so that the vegetation canopy height and ground surface elevation can be measured and filtered out of ground return data if warranted. LiDAR can also be used to map areas that are difficult to access (Genç et al., 2004; Lefsky et al., 1999). Other uses of specialist LiDAR technology include the determination of accurate water depths (Cunningham et al., 2016), mapping of wetlands and shallow water (Huang et al., 2014), high-resolution mapping of topography (Tarolli, 2014) and the structural differentiation between forest structures and ages (Bolton et al., 2015). The high positional and vertical accuracies of LiDAR technology and its ability to filter vegetation enables accurate measurements of the position and elevation of banks and of the volumetric erosion rates over annual timescales (De Rose and Basher, 2011).

Digital elevation model (DEM) of difference (DoD) is a repeated topographic survey that is practical in high spatial resolution and over greater spatial extents (Wheaton et al., 2010). DoD has been used for measuring various factors in geomorphological studies, such as sediment budget calculations and geomorphic change determinations (Bezak et al., 2017). It provides assessments of the net landscape changes for sediment budgeting and mapping of morphological changes (Wheaton et al., 2010). Changes in channel banks and beds, and even some larger floodplain variations, have also been detected by DoD (Croke et al., 2013). To gain accurate estimations using DoD, the data sources must be reliable (Schoorl et al., 2000). These sources can be affected by both systematic and random errors via different factors such as the survey point quality, topographic complexity and interpolation methods. The potential impact of these error sources differs depending on the intended application of DoD (Balaguer-Puig et al., 2018; Milan et al., 2011). For instance, studies have shown that random errors (such as an increased level of relative point-to-point accuracy) are more important than systematic errors (such as a high level of absolute accuracy sourced from geomorphological mapping through LiDAR) in river systems in the UK (Croke et al., 2013). Some researchers have declared that LiDAR accuracies play a more important role when morphological budgeting estimations are required (Charlton et al., 2003; Jones et al., 2007). Furthermore, applying an average error for entire DoD studies causes the underestimation/overestimation of elevation changes in some parts of the DoD (Schoorl et al., 2000). DoD accuracy in erosion and sedimentation assessment has not been sufficiently studied in cases of lakes and wetlands (Jones et al., 2007). Therefore, little is known about the suitability of using DoD in such instances.

Photogrammetry is a combined technology of photography and geometry that has been applied for short timescales using optical imagery and laser technology similar to LiDAR (Greaves et al., 2017). This technique can be performed as a terrestrial or aerial survey with data ±5-15 mm data accuracy and 10-10,000 parts/m^2 resolution (Greaves et al., 2017; Peyer et al., 2015). A camera takes numerous photographs from different angles to generate images that can be stitched together to create a three-dimensional (3D) rendering of the site, and/or data to be used for measurements of geometry (Peyer et al., 2015). Aerial photogrammetry can be applied to a large area while terrestrial photogrammetry is suitable for specific structures at smaller scales (Piermattei et al., 2015). However, both types of photogrammetry can create an efficient data set to use in channel change analyses. Structure-from-motion (SfM) is the technique used to reconstitute the 3D geometry from acquired images and to produce high-resolution and accurate topographic data (Tarolli, 2014). For example, Westoby et al. (2012) showed decimetre-scale vertical accuracy with SfM in complex topography systems, and Javernick et al., (2014) suggested errors of only 0.04 m in planar, 0.10 m in elevation and 0.10 m in vertical surface occurring for non-vegetated areas in their analysis.

2.4 Modelling techniques for analysis of channel change and erosion processes

Modelling is a critical approach for understanding river history and evolution (Devia et al., 2015; Matsubara and Howard, 2014). Models provide comprehensive insights into the effects of different conditions in diverse river systems, including the potential for interference from complicated boundary conditions and physical laws (Grenfell, 2015; Nicholas, 2013). To determine the best model for each area, the space and time representation, data availability, calibration and validation and uncertainty of models should be considered (Coulthard and Van de Wiel, 2012). The most practical models in terms of erosion estimation associated with channel change in multi-channelled rivers can be classified into two main groups, hydrodynamic or morphodynamic (Grenfell, 2012; Nabi et al., 2012). Hydrodynamic models simulate the flow and water fluxes through environmental changes, while morphodynamic models investigate changes in landforms and topography (Van de Wiel et al., 2011). Table 2.2 synthesises the key modelling techniques and their modes of application, while a brief review of the techniques is provided below.

Table 2.2 Examples of hydrodynamic and morphodynamic models.

	Model	Field of use	Input requirements/system component	Source
Hydrodynamic	MIKE FLOOD	Flood inundation/flooding depth	Discharge/water level/rainfall/river cross-section/topographic map	Patro et al., 2009
	SWAT	Simulate hydrology and sedimentation	DEM/river network data/land use data	Wang et al., 2016; Wellen et al., 2014
	LISFLOOD-FP	Flood inundation	Floodplain topography/river cross-section/boundary condition/water level	Coulthard et al., 2013; Wood et al., 2016
	HEC-RAS	Flood inundation/flood depth/flow velocities	River cross-section/bed and bank strength/rainfall	Patel et al., 2017; Teng et al., 2017
	TUFLOW	Simulating floods	Rainfall/boundary condition	Morsy et al., 2017
Morphodynamic	LEMs (i.e. CAESAR-Lisflood)	Hydrology/inundation/flood frequency/channel change/floodplain evolution/terrace formation/drainage network/hillslope evolution	LiDAR/river cross-section/reach/catchment/sub-catchment	Coulthard et al., 2013; Hajek and Wolinsky, 2012; Seoane et al., 2015; Van de Wiel et al., 2011
	Alluvial architecture (i.e. Delft 3D)	Floodplain evolution/terrace formation	LiDAR/river cross-section/reach	Coulthard and Van de Wiel, 2012
	CFDs (i.e. STREMR)	Erosion and sedimentation/fluvial landscape evolution	LiDAR/river cross-section/reach/sub-reach	Murray and Paola, 1994; Rodriguez et al., 2004; Seoane et al., 2015; Van de Wiel et al., 2011

2.4.1 Hydrodynamic models

Hydrodynamic models characterise hydrological processes (including catchment hydrology, riverbank erosion and floodplain sediment transport) to predict system behaviours such as the distribution and routing of flow through the catchment (Refsgaard, 1997). These models also represent the frequency and duration of floods and droughts and show the variations in inundation to simulate flood patterns (Gobeyn et al., 2017). The inundation pattern is derived from the calculation of flow in computational cells covering the floodplain and channels (Van de Wiel et al., 2011). These approaches are particularly useful during large, catastrophic floods, which cause flash flooding or dam breaks (Van de Wiel et al., 2011). Topography, roughness, infiltration and rainfall/runoff data for the drainage area are the most important inputs in hydrodynamic models (Coulthard et al., 2013).

Specific models such as MIKE FLOOD are used primarily for simulating flood inundation (Patro et al., 2009). Others, such as the Soil and Water Assessment Tool (SWAT) are used to simulate hydrology (i.e. discharge) and sediment (Wang et al., 2016; Wellen et al., 2014). LISFOOD-FP is a 2D flow model to investigate flood inundation (Coulthard et al., 2013; Wood et al., 2016). Hydrologic Engineering Centre (HEC) developed the River Analysis System (RAS) and HEC-RAS is another model used for a wide range of purposes, including flood inundation, flood depth and flow velocities (Patel et al., 2017; Teng et al., 2017), and Two-dimensional Unsteady Flow (TUFLOW) is used to simulate floods (Morsy et al., 2017). Hydrodynamic models cannot show the geomorphological dynamic of landscapes or the long timescale environmental responses to climate change, and, because they assume a constant topography, cannot accurately simulate areas where changes occur in the topography (Devia et al., 2015; Teng et al., 2017). Integration of hydrodynamic models with high-resolution elevation data could represent the impact of topographic changes on hydraulic characters, such as the effect of topographic changes on the reaches on flood inundation (Marks and Bates, 2000). However, this technology is usually only suitable for smaller floodplains, is computationally expensive and limits the user's ability to analyse the uncertainties of multiple models (Savage et al., 2016).

2.4.2 Morphodynamic models

Morphodynamic models (e.g. Delft 3D) respond to changes through fluid dynamic processes; therefore, these models can simulate changes in landforms and topography, and can predict the evolution of the fluvial landscape, erosion and sedimentation processes (Bogoni et al., 2017). They mostly focus on simulating key modes of change, particularly bank adjustment and bifurcation formation, but are not usually able to simulate the development of full meander bends or avulsion belts (Grenfell, 2015). Understanding the interaction of rivers, as a vital part of fluvial systems and landscapes, is an important issue in morphodynamic modelling (Rousseau et al., 2016).

Landscape evolution models (LEMs) have been used to simulate the geomorphic development of river basins in long timescales (Seoane et al., 2015). LEMs originated from studying the interactions of smaller scale geomorphological sub-processes and show the salient features of the landscape (including hydrological, fluvial and hillslope) (Van de Wiel et al., 2011). These models are capable of simulating all parts of a catchment at various timescales, including channel incision and aggradation, avulsion, breakdowns and river meandering and even the transition between braided and single thread channel patterns (Coulthard et al., 2013; Seoane et al., 2015). Although processes always develop from minor scale processes such as erosion and deposition, they occur over large time scales and LEMs are not able to simulate short-term hydrodynamic effects (Seoane et al., 2015). There are many examples of LEMs including SIBERIA (Hancock et al., 2002; Willgoose et al., 1991), CAESAR (Coulthard et al., 2013) and CAESAR-Lisflood, the latter which was recently used to analyse landscape evolution in the Macquarie Marshes (Seoane et al., 2015).

Alluvial architecture models simulate vertical and horizontal development of alluvial systems through time (Coulthard and Van de Wiel, 2012). These models occur over long timescales and large space scales (Van de Wiel et al., 2011; Williams et al., 2016). They can be used to predict the fluvial landscape evolution, erosion and sedimentation processes, as well as the influence of autogenic and allogenic factors on geomorphology and sedimentology of river systems, including avulsion-prone rivers (Coulthard and Van De Wiel, 2012). However, alluvial architecture models are highly simplified and limit the potential to investigate the responses of river systems to environmental changes (Coulthard and Van de Wiel, 2012; Van de Wiel et al., 2011). Moreover, there is a remarkable disparity between the space and timescales of alluvial architecture models and those associated with reach-scale models and the measurement that can be used to inform them. They mostly consider one style of avulsion (i.e. due to aggradation) and cannot show the impact of in-channel vegetation and other smaller-scale processes (Coulthard and Van de Wiel, 2012; Van de Wiel et al., 2011).

Computational fluid dynamics models (CFDs) include fluid dynamic codes which can be complemented with sediment transport models and provide strong simulations of fluvial responses to environmental changes (Murray and Paola, 1994; Van de Wiel et al., 2011). These models are known as large-scale and short-timescale models and are categorised into reduced complexity models (Coulthard and Van de Wiel, 2012; Seoane et al., 2015).They are able to predict erosion and deposition, model in-channel sediment and fluvial landscape evolution. However, they cannot accurately represent flow depth and flow velocities in channels, and they cannot simulate river evolution (Coulthard and Van de Wiel, 2012).

2.5 Techniques most suitable for this thesis

Due to the various benefits and limitations of the physical assessment and modelling techniques outlined above, it is very important to select the appropriate methods for the task at hand, considering the spatial scale of the system of interest and the timeframe of analysis required. Based on this methodological review, physical assessment methods have been determined to be the most appropriate to use to achieve the overarching aim of this research, which is to understand the key patterns and processes of channel change and to define the behaviour of channel bifurcation and avulsion and other modes of channel adjustment by investigating the multi-channelled floodplain wetlands of the Macquarie Marshes. Because the Macquarie Marshes are a very large system with several hundred channels, small site-scale measurements of change (for example, using erosion pins and sediment mats) are not logistically feasible and would not yield data that is able to be meaningfully and accurately upscaled. Therefore, high-resolution elevation data that can be obtained for a large area is required to determine the spatial patterns of channels and to determine the distribution of channel bifurcation and return nodes linked to hydraulic factors in the system. Therefore, LiDAR-derived data available for the Macquarie Marshes is the best option, which can be interrogated using a DoD methodology as well as by extracting cross-sections at specific sites for morphometric analyses. Estimation of hydraulic factors such as bankfull discharge and stream power linked to these cross-sections is also deemed appropriate, rather than high-resolution modelling of morphological change for every site. Hydrodynamic modelling is not suitable for this purpose, because these models cannot deal with changing topography well, which is precisely what the current study aims to investigate. Repeat cross-section surveys can be used identify historical and contemporary trajectories of channel behaviour and associated hydraulic factors linked to channel cross-sections and changing slope and roughness. A qualitative rapid assessment method tested previously by Ralph et al. (2013) will also be employed to assess erosion and sediment deposition risk at key sites, rather than laborious and logistically demanding erosion and sedimentation measurements.

2.6 Summary

This chapter has given an overview of the character of multi-channelled rivers with floodplain wetlands and reviewed some of the key techniques that can be used to assess erosion and channel change in these systems. Based on this review, selected methods were introduced for the assessment of patterns and processes of channel change in the Macquarie Marshes, as applied in this thesis and described in detail in the next chapter.

Chapter 3: Research sites and methods

3.1 Introduction

This chapter provides a description of the setting and significance of the Macquarie Marshes and introduces the field sites selected for this study. The research strategy and specific methods used to achieve the research aims and questions defined for the project are then described. The thesis aims addressed in this chapter are:

1. *To quantify the spatial patterns of channels and determine the distribution of channel bifurcation and return nodes along major channels within the Macquarie Marshes;*
2. *To define the geomorphic configuration and hydraulic behaviour of channels leading to channel maintenance, avulsion and breakdown in the Macquarie Marshes;*
3. *To identify historical and contemporary trajectories of channel behaviour in hyper-avulsive reaches of the Southern Macquarie Marshes and to explain the role of erosion in the system;*
4. *To assess erosion and sediment deposition risk at key sites in the Southern Macquarie Marshes and to rank channels according to the likelihood and consequences of channel change.*

3.2 Setting and significances of the Macquarie Marshes

The Macquarie Marshes are one of the largest floodplain wetlands in the Murray-Darling Basin (MDB), a wide inland drainage basin in south-eastern Australia, with more than 30,000 wetlands (Rogers and Ralph, 2011) (Figure 3.1). The Macquarie Marshes cover at least 2,000 km^2 when flooded and are located on the lower reaches of the Macquarie River, which drains from the western margin of the Great Dividing Range near the town of Oberon. Runoff and flows for this water-dependent ecosystem are mostly provided from the more humid headwaters upstream of the laterally unconfined reaches of the Macquarie River (Ralph and Hesse, 2010; Seoane et al., 2015). The Macquarie Marshes are recognised under the *Ramsar Convention on Wetlands of International Importance* (hereon, the *Ramsar Convention*) and provide unique habitats for more than 100 species of fauna and flora, including a large population of domestic and international waterbirds (Kingsford and Auld, 2005).

The meandering single channel of the Macquarie River starts to branch on the floodplain near Warren and eventually breaks down into a series of anastomosing and distributary channels with flood outs and wetlands in the Macquarie Marshes (Ralph and Hesse, 2010). Several types of wetlands are supported by the Macquarie Marshes, from permanent to ephemeral and intermittent wetlands that are inundated either frequently or only by the largest floods (Kingsford and Thomas, 1995). Wetlands are made up of reedbeds, grass plains, woodlands and forests (Ralph et al., 2016). There are three main areas within the system, including the Southern Macquarie Marshes, Northern Macquarie Marshes and Eastern Macquarie Marshes, associated with the main branches of the Macquarie River, Monkeygar Creek (an arm of the Macquarie River in the Southern Macquarie Marshes), Bulgeraga Creek, and Gum Cowal-Terrigal Creek (Thomas et al., 2015).

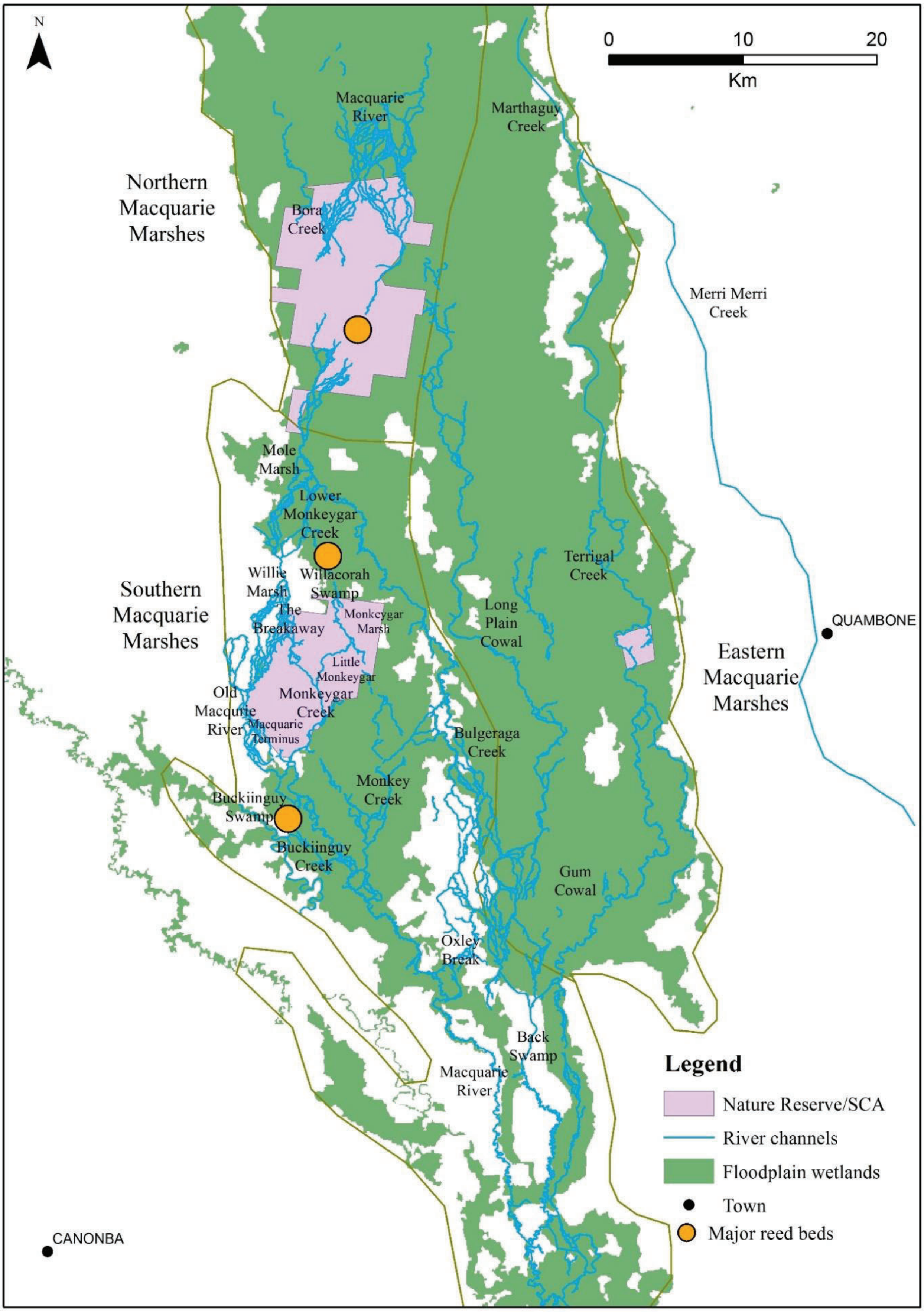

Figure 3.1 Map of the Macquarie Marshes showing major channels and wetlands.

Floodplain wetlands in the Macquarie Marshes are fed by overbank flooding from channels and overland flooding in the terminal reaches of channels. Thus, both major and minor channels feed water into the wetlands. In the Southern Macquarie Marshes, the Macquarie River breaks into several channels that eventually reconverge downstream or terminate in wetlands (Ralph et al., 2016). Oxley Break diverges from the right (eastern) bank and links the Macquarie River to Bulgeraga Creek. Bulgeraga Creek is a large anabranch that leaves the main Macquarie River upstream of the Macquarie River terminus, near Marebone Weir. Monkey Creeks diverges from the right bank downstream of Oxley Break and feeds Monkey Marsh between the Macquarie River and Bulgeraga Creek. Buckiinguy Creek diverges from the left (western) bank of the Macquarie River and runs parallel to the main river but disintegrates in Buckiinguy Swamp.

The Macquarie River terminates where Monkeygar Creek starts (originally Monkeygar was a right bank breach), which in turn feeds Little Monkeygar Creek, The Breakaway, Monkeygar Marsh and Willancorah Swamp, where the channel terminates again. An area of around 6,578 ha in the Southern Macquarie Marshes sits within a nature reserve that has been recognised under the *Ramsar Convention* since 1986 (Murray-Darling Basin Authority (MDBA), 2012; Ralph et al., 2016). A branch of the river, known as the Old Macquarie River, feeds Willie Marsh and Mole Marsh, while channels returning from Buckiinguy, The Breakaway, Willancorah Swamp and Bulgeraga Creek re-join to form another branch of the Macquarie River in the reach just upstream of the Northern Macquarie Marshes (Figure 3.1). The Northern Macquarie Marshes start downstream from Mole Marsh with a complex pattern of anastomosing channels along the Macquarie River and Bora Creek system, which flows to the north past the town of Carinda. An area of around 12,500 ha in the Northern Macquarie Marshes sits within a nature reserve. The Eastern Macquarie Marshes develops along Gum Cowal Creek that continues as Terrigal Creek downstream and joins Marthaguy Creek. In the central part of the marshes, and part of the Eastern Macquarie Marshes, Long Plain Cowal extends to the Northern Macquarie Marshes.

The morphology of an alluvial floodplain depends on its channels and the channel networks that represent the dominant sediment and discharge regime (Ralph and Hesse, 2010). Channel breakdown and termination in the Macquarie Marshes had been linked to a sequence of factors; in particular, the hydrological and geomorphological properties that control the downstream decline in stream power along the Macquarie River and the formation of numerous distributary and anastomosing channels in the Macquarie Marshes that further split flow and energy (Ralph et al., 2016). Reduced water availability due to climatic and anthropogenic disturbances (for example, high water supplements for irrigation or extended droughts) and floodplain earthworks alter the natural erosion and deposition dynamics in the Macquarie Marshes and has been linked to rapid ecological degradation (Kingsford and Thomas, 1995). Therefore, channels and wetlands in the Macquarie Marshes are prone to erosion and sedimentation.

Erosion and sedimentation are natural processes in rivers and floodplain wetlands that explain excavation, redistribution and sediment storage in these systems. Alluvial rivers in the Macquarie Marshes respond to the changes by adjusting channel geometry and developing multi-channelled configuration downstream

(Hesse et al., 2018; Kingsford and Thomas, 1995). However, accelerated rates of erosion could lead to bifurcation and avulsion, which redirect flows and may lead to changes in inundation and wetland areal extent that can lead to depreciation of wetland biota (Henshaw et al., 2013; Oyston et al., 2014). In the Macquarie River, bifurcation and avulsion frequency increases downstream as channel capacity decreases, contributing to greater overbank flow and flood out formation in the Macquarie Marshes (Ralph and Hesse, 2010). Thus, bifurcation and avulsion are the main processes driving channel formation, modification and maintenance in the Macquarie Marshes.

3.3 Research strategy and field sites

The research strategy was designed to address the aim of the study to quantify the spatial patterns of channels and locations of bifurcation and return nodes. It was also aimed to define the morphometric and hydraulic characteristics of these channels related to bifurcation and avulsion. Historical and contemporary trajectories of channel behaviour are identified, and erosion and sediment deposition risk are assessed. These findings will help to understand the relationships between channel pattern and channel changes in the Macquarie Marshes that are critical for water and wetland conservation and management (Table 3.1).

Table 3.1 Research methods in alignment with the aims, and associated field sites.

Aim	Method used	Site selection	Related result chapter
Spatial pattern of channels and distribution of bifurcation and return nodes	Analysis from LiDAR-derived DEM	Whole area of the Macquarie Marshes	Chapter 5
Geomorphic and hydraulic behaviour of channels leading to channel maintenance, avulsion and breakdown	Analysis from LiDAR-derived DEM	Whole area of the Macquarie Marshes	Chapters 4 and 5
Historical channel behaviour related to channel erosion and sedimentation	Comparison between channel surveys from 1992 and new channel surveys in 2018	Hyper-avulsive reaches in the Southern Macquarie Marshes	Chapter 6
Contemporary channel behaviour related to channel erosion and sedimentation	Comparison between LiDAR-derived DEM data in 2008 and 2015, and new channel surveys in 2018	Hyper-avulsive reaches and 19 key sites on major channels in the Southern Macquarie Marshes	Chapters 4, 5 and 6
Erosion and sediment deposition risk	Field risk assessment analysis in 2018, and comparison with 2012 risk assessment	20 key sites on major channels in the Southern Macquarie Marshes	Chapter 7

Initially, flow accumulation modelling, channel mapping and morphometric analyses were undertaken using the data from LiDAR-derived DEMs, old topographic surveys and new data collected from field surveys. Analyses were performed for the entire area of the Macquarie Marshes and continued at subscales of the southern, northern and eastern sections, and were finalised by reach scale analysis. LiDAR-derived DEMs were obtained from the Office of Environment and Heritage (OEH) from 2008 and 2015. Changes in the geometric character (channel width, depth, area and width/depth ratio) for 19 sites in the Southern Macquarie Marshes were investigated over the six-year interval of the LiDAR datasets applying DEM-of-

Difference analysis (see the results in Chapter 4, Table 3.2 and Figure 3.2A). Then, using the spatial pattern of channels and locations of bifurcation and return nodes, the channel morphology and behaviour associated with these nodes was analysed for the whole Macquarie Marshes (see the results in Chapter 5 and Figure 3.2B). Recent historical channel changes (26 years from 1992 to 2018) were then interpreted for key sites on the main channels in the Southern Macquarie Marshes using repeat topographic surveys based on data collected in 1992 by Brereton (Brereton, 1994). In total, 62 cross-sections were resurveyed on the ground, using Leica digital level sprinter offering 1 mm deviation in height and distance measurements, to measure elevation and distance data so that geometric parameters (i.e. channel width, depth, area, width/depth ratio, bed height and bank height) and hydraulic parameters (i.e. channel bankfull discharge and unit stream power) could be calculated (see the results in Chapter 6 and Figure 3.2C). Twenty sites in the Southern Macquarie Marshes were used for the erosion risk assessment analysis based on repeat field assessments from 2012 (Ralph et al., 2013) and 2018 (see the results in Chapter 7, Table 3.2, Table 3.3 and Figure 3.2A). The rapid assessment process considered impacts of existing works in the study area (including where structures were present), likely changes to channel cross-sections and long-profiles over time, the potential consequences of changes to flow in the channels and the inundation of the floodplain. Evidence of current or ongoing bed and bank erosion was a focus of the field assessment. These study areas were identified based on the high priority for consideration of potential works, measurements from previous studies and knowledge of experts (see Ralph et al., 2013, Table 3.2 and the field survey form in Appendix 1).

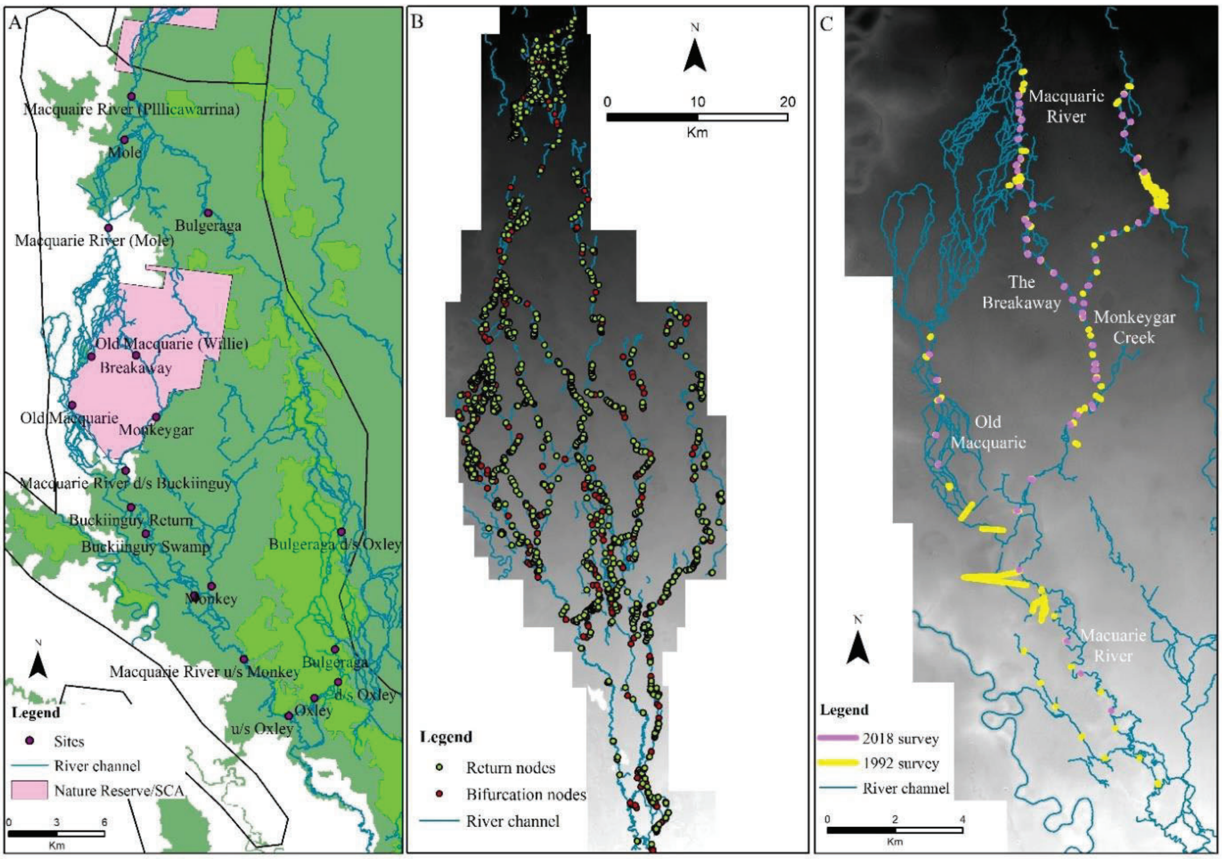

Figure 3.2 Map showing study sites in Chapters 4 and 7 (A), Chapter 5 (B) and Chapter 6 (C).

Table 3.2 Site selection strategy for Chapters 4 and 7.

Selected channels and sites	Priority for consideration
Oxley Break	Erosion and increased flow
The Breakaway	Erosion, increased flow and existing works
Buckiinguy Return	Erosion, increased flow and existing work
Buckiinguy Creek	Sedimentation and decreased flow through Buckiinguy swamp
Monkeygar Creek	Erosion upstream and sedimentation downstream of The Breakaway
Old Macquarie River	Sedimentation and decreased flow
Monkey Creek	Sedimentation and decreased flow
Old Macquarie River near Willie	Sedimentation and decreased flow
The Mole reed bed return channels	Erosion and existing works

Table 3.3 Site identification with specific codes.

Site code	Site name
SMM001	Upper Oxley Break
SMM002	Middle Oxley Break
SMM003	Lower Oxley Break
SMM004	Bulgeraga Creek downstream of Oxley Break
SMM005	Monkey Creek
SMM006	Macquarie River downstream of Oxley Break and upstream of Monkey Creek
SMM007	Macquarie River downstream of Monkey Creek and downstream of Buckiinguy Creek
SMM008	Buckiinguy Creek
SMM009	Bulgeraga Creek downstream of Oxley Break
SMM010	Bulgeraga Creek at Willancorah (downstream of Gibson Way)
SMM011	The Breakaway
SMM012	The Mole reed bed outflow channels
SMM013	Macquarie River at Maxwelton and The Mole
SMM014	Macquarie River at Pillicawarrina
SMM015	Old Macquarie River in Nature Reserve (near Willie)
SMM016	Old Macquarie River in Nature Reserve (Boss' Crossing)
SMM017	Monkeygar Creek upstream of The Breakaway in Nature Reserve
SMM018	Buckiinguy Return and Buckiinguy Runner
SMM019	Macquarie River downstream of Monkeygar Creek and downstream of Buckiinguy Creek
SMM020*	Buckiinguy Swamp

* Site added in 2013 by Oyston (2014).

3.4 Methods

3.4.1 DEM of Differences (DoD)

Two LiDAR-derived DEMs acquired by the NSW Government OEH in 2008 and 2015 were used for the morphometric analysis of the channels. In 2008, LiDAR data acquisition with associated high-resolution aerial photography and ground truthing/control surveys was conducted during the period February to September 2008 utilising Leica ALS50-IIM ALS, Leica ADS40 digital sensor and Spectrum medium format digital cameras (2008 LiDAR metadata report). In 2015, LiDAR data and associated imagery and ground surveys were obtained during the period March to April 2015 (2015 LiDAR metadata report). Channel cross-sections were extracted from the LiDAR-derived DEMs at 19 representative sites in the Southern Macquarie Marshes. Transect lines were inserted across the channel and the “stack profile” tool was used in ArcGIS to extract distance and elevation data for each transect. Analyses of the channel geometry including bankfull width, bankfull depth and width:depth ratio were undertaken using standard methods (Ralph and Hesse, 2010) (explained in Section 3.4.5). Comparisons of cross-section metrics from 2008 and 2015 were used to calculate changes in channel width and depth that occurred during the six-year period. The LiDAR-derived DEM data has ±15 cm vertical accuracy and ±45 cm horizontal accuracy. This translates to thresholds of detectible change equivalent to 30 cm vertical and 90 cm horizontal when considering differences between cross-sections extracted from the DEMs. A DoD was created by subtracting the LiDAR-derived elevations in 2015 from those in 2008 for the entire area covered by LiDAR-derived data using the “raster calculation” tool in ArcMap 10.3. The potential vertical error for DoD values based on the two LiDAR-derived acquisitions is up to ±30 cm vertical and 90 cm horizontal, and values less than these thresholds measured by DoD were categorized as a non-detectible change.

3.4.2 Flow accumulation model and channel delineation

LiDAR-derived DEM data from 2008 were used to produce a channel layer for the Macquarie Marshes based on flow accumualtion modelling parameters. Several sections of the 2015 LiDAR-derived DEM were not well represented and were deemed to be inaccurate due to inundation and in some cases dense vegetation, and so the 2008 LiDAR-derived data was used for all further analysis (Figure 3.3). The following methods used for channel delineation were based on those developed by Farebrother and Ralph (2017) for low-gradient fluvial systems with multiple, branching channels.

GRASS GIS contains over 350 modules to render maps and images and extract the channel lines that are suitable for raster and point data analysis. The r.watershed algorithm in GRASS was run to identify flow accumulation paths and used to delineate channel lines from the void-filled 2008 LiDAR-derived DEM. The GRASS r.watershed model was chosen as it does not require sinks in the DEM to be filled, unlike many of the other commonly available flow accumulation models (such as those found within ArcMap and SAGA GIS), because it utilizes a least-cost path methodology (GRASS Development Team, 2018). Within complex reticulate drainage systems, such as those found in the Macquarie Marshes, the act of filling sinks in the DEM usually results in a loss of detail and accuracy because shallow (e.g. <1 m deep) or obstructed flow paths are filled to the point that the modelled drainage lines may be over-straightened and incorrectly shown on the floodplain, and the derived channel system is drastically simplified. The r.watershedmodel also considers multiple flow directions, unlike other more simplistic models (such as those found in ArcGIS- pre version 10.6). Within the r.watershed “accumulation” tool there is also a tuning parameter (convergence factor) that enables the derived flow accumulation to model differing degrees of convergent/divergent flow (ranging from 1 = most divergent flow to 10 = most convergent flow). The flow accumulation model was run iteratively using all 10 convergence factor values and the outputs were visually compared for differences. It was found that there was a negligable difference between the models. Therefore, the default convergence factor of 5 in GRASS was utilised for the channel mapping in this study.

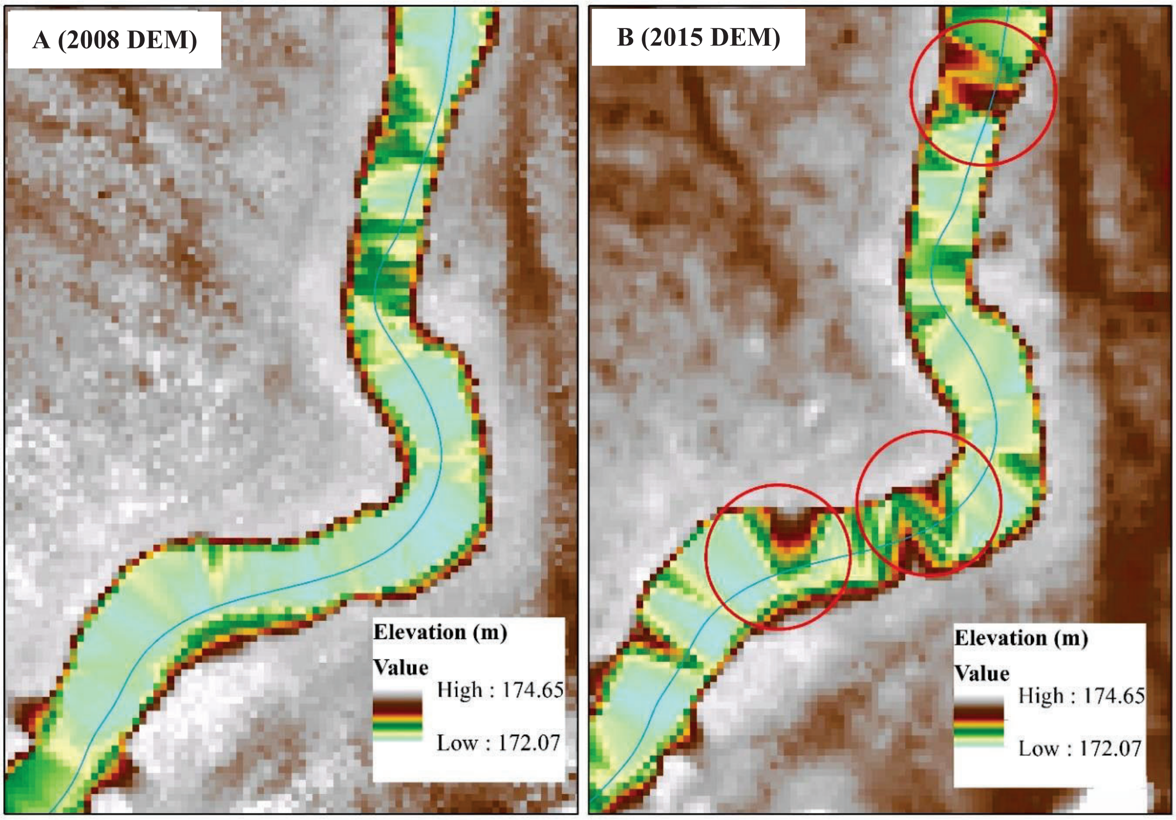

Figure 3.3 LiDAR-derived DEM from 2008 (A) and 2015 (B) showing the inaccurate data in 2015 due to water and/or dense vegetation in the channels (red circles).

Flow accumulation raster cells with an accumulation threshold of ≥1,000,000 m^2 were extracted using the "CON" tool in ArcMap and the output raster was thinned using the "r.thin" tool in GRASS so that channel segments were only one cell thick. The thinned raster was then converted to polyline vector data using the "raster to line" tool in ArcMap. To obtain channel segments representative of the known main channels within the study area, any line within 10 m of the OEH Smarshed Network (a vector dataset provided by OEH used in their hydrodynamic modelling) was selected using the "select by location" tool in ArcMap. Additionally, channels that were affected by vegetation and inundation issues within the DEM were manually digitised in ArcMap through visual analysis of the DEM outputs and aerial imagery obtained with the LiDAR-derived data from OEH (2008).

Next, the polylines were checked for connectivity and channel segments that were inaccurately modelled as being discontinous were linked by manual digitisation through visual analysis of the aerial imagery and DEM in ArcMap. Small dangles (minor flowlines <50 m and up to 100 m long flowing into/out of the channel segments) were deleted. Once the stream segment dataset was checked, the polylines were merged into a single feature and then planarized in ArcMap, which created a new line each time an intersection between 2 or more polylines occured. The planarized dataset was smoothed using the Polynomial Approximation with Exponential Kernel (PAEK) method, which smooths polygons using a smoothing tolerance (20 m in this study). The smoothing tolerance parameter controls the length of a moving path used in calculating the new vertices. Any inundated sections of the drainage line that impacted the accuracy of the channel segment or that were not smoothed using the PAEK method were manually checked and, where necessary, manual digitisation was performed through visual analysis of the DEM and aerial imagery.

3.4.3 Bifurcation and return points

After producing the channel layer, the “feature vertices to points” tool in ArcMap was used to create points at the start and end of each line segment (representing the bifurcation and return nodes). The “collect events” tool in ArcMap helped to remove non-bifurcation and/or return points (for example, areas of channel breakdown/termination); locations with “> = 3 nodes/points” were extracted. Missing bifurcation and/or return points (or extra selected points) were then manually added or deleted as needed in ArcMap to create the best bifurcation and return dataset that approximates reality. All output points were inspected manually (through expert knowledge, checking flow direction and channel slope by use of the LiDAR-derived DEM and aerial imagery) to distinguish whether the point was a bifurcation or return. Nodes that were considered altered by anthropogenic means (i.e. in close proximity to anthropogenic banks) were removed from the analysis. Finally, all bifurcation and return points were then exported in separate layers to perform more in-depth analysis of channel metrics such as channel width, depth and cross-sectional area.

3.4.4 Channel cross-section transects

For further analysis, cross-sections were extracted from the LiDAR-derived DEM in ArcMap upstream and downstream of each bifurcation or point to explore the effect of channel splitting and re-joining on channel connection and channel form. Each node was given a universal identifier (UID) number so that cross-section data and derived metrics could be managed consistently. The UID was obtained through ranking the node location from south (upstream) to north (downstream). The different buffer distances were checked to see which distance could capture all of the reaches around each point without interfering with another node’s area and a 50 m distance buffer was created around each point. The intersection points of the buffer and channel layer (polyline) were utilised to extract a transect perpendicular to the channel segment direction at that point (Figure 3.4). A new field called UID_TRAN was then added in the attribute table in ArcMap to provide a dedicated number for each transect. Where a transect was not perpendicular to channel direction, and/or where one or both banks were not captured by the 50 m transect length and/or where a transect was missed, a new transect was determined by creating a new point (within 10 m of the original transect) and a revised perpendicular transect was extracted in the new location with the same size (in some places with longer lengths to capture the banks). In total, 2,667 transects at bifurcation nodes and 2,934 transects at return nodes were extracted and analysed in ArcMap. Of these, approximately 160 transects were fixed prior to analysis to meet the accuracy criteria.

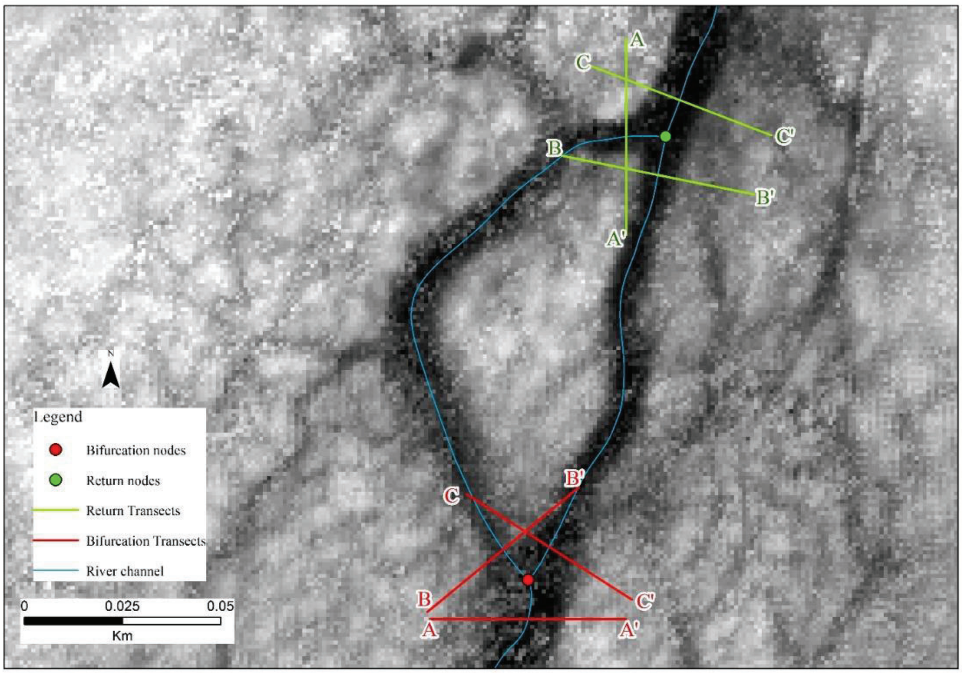

Figure 3.4 Transects upstream and downstream of bifurcation and return nodes.

3.4.5 Channel geometry data

Once all the transect locations were checked, the "stack profile" tool in ArcMap was used to export distance and elevation data for each cross-section at the bifurcation and return nodes. Then, channel geometry, including bankfull width, bankfull depth and cross-sectional area, were measured using a semi-automated system in MATLAB. In MATLAB, elevation and distance data for each cross-section was read from an Excel .csv file and plotted visually in an X, Y scatter plot for each channel separately; this allowed manual identification and selection of the left and right banks at each cross-section from which a MATLAB script enabled the calculation of all the aforementioned channel metrics. The formulas used in MATLAB for the key channel metrics were:

$$\text{Bankfull width (m)} = \text{Distance top of right bank} - \text{distance top of left bank} \qquad \textbf{Eq.1}$$

$$\text{Bankfull depth (m)} = \text{Maximum elevation of the lowest bank} - \text{minimum elevation of the bed} \qquad \textbf{Eq.2}$$

$$\text{Bankfull area (m}^2\text{)} = \text{Polyarea between the top of right bank and top of left bank (calculated by area within the curve)} \qquad \textbf{Eq.3}$$

Because investigating the effect of channel breakdown and channel connection demanded a special arrangement of transects from upstream to downstream, and because they were not necessarily numbered in order, all transects were inspected manually to recognise the main streams and their secondary branches. Final measurements were made for calculating channel change between primary channels and their branches downstream for each bifurcation and return node in terms of bankfull width, depth and area.

3.4.6 Manning's n estimates

Manning's n is a parameter often used to estimate the resistance (roughness) coefficient in alluvial channels and is a preferred approach for calculating hydraulic parameters, which can control sediment transport capacity and plays a vital role in sedimentation and erosion processes, in open channel flow fields (Arcement, 1989; Barness, 1849). Various factors (including surface material, surface irregularity, variation of channel cross-sections, obstructions, vegetation and the degree of meandering) have an impact on Manning's n value.

Manning's n values were derived for this study in two stages. First, data collected in the field during the rapid assessment field survey in 2012 (Ralph et al., 2013), and checked again in January 2018 (see Chapter 7; Appendix 1), were used to define Manning's n values for 20 field sites based on the method outlined in the Geomorphological Field Manual (Dackombe and Gardiner, 1983). A vegetation visual estimate was also undertaken at all of the sites in conjunction with the Manning's n estimate, considering habitat type (aquatic, riparian or terrestrial), structural type (herbs, grasses, shrubs or trees) and dominant species (native or alien) (Appendix 1). Second, the field-derived Manning's n data was used to create a ranked list of Manning's n values and associated site characteristics (Table 3.4), with a range of values between 0.025 and 0.07 allocated to nine groups related to channel types. All bifurcation and return sites were then inspected manually using high resolution aerial imagery (OEH, 2008) and compared to the group values in the table. The suitable Manning's n value was then applied for each bifurcation or node site and extrapolated systematically to other similar sites in the system (Figure 3.5).

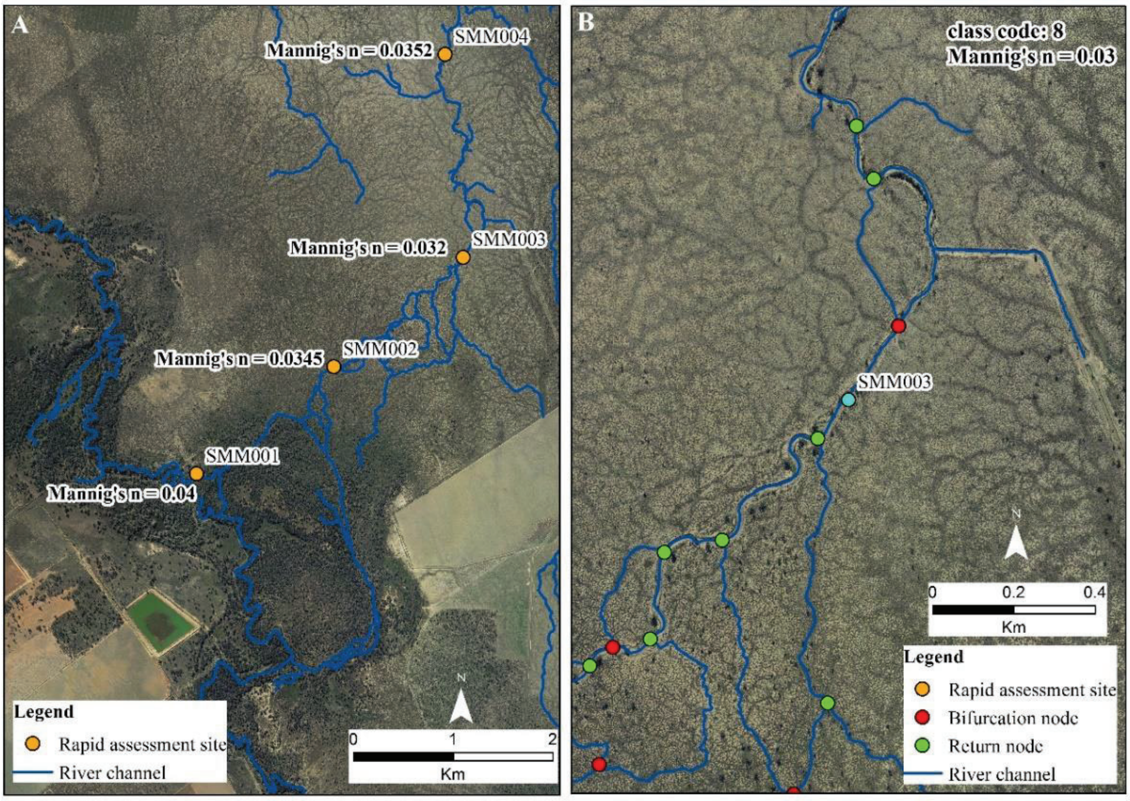

Figure 3.5 An example of rapid assessment sites overlain on aerial imagery (OEH, 2008), describing characteristics of recorded Manning's n (A), and bifurcation and return nodes along aerial imagery to

extrapolate Manning's n values (B).**Table 3.4** Categories of Manning's n value derived for the Macquarie Marshes.

Reference site types	Actual value	Class value	Description
Channels blocked by reeds	N/A	0.07	Shallow, sinuous or straight channel in dense reeds with significant obstructions by leafy vegetation
Channels lined by reeds	N/A	0.065	Shallow, sinuous or straight channel with dense reeds at margins
Monkeygar upstream The Breakaway	0.057	0.06	Sinuous channel with very dense woody vegetation along margins and in channel
The Breakaway	0.055	0.05	Straight channel with obstructions (rocks)
Mole outflow channels	0.049		
Buckiinguy Swamp	0.046	0.045	Sinuous channel with dense woody vegetation along margins, or straight channel with dense woody vegetation along margin and in channel
Buckiinguy Creek	0.042		
Upper Oxley Break	0.04	0.04	Straight channel with sparse woody vegetation along margins, or straight channel with dense woody vegetation on one bank only
Old Macquarie (Boss's Crossing)	0.04		
Macquarie River downstream Monkeygar	0.04		
Macquarie River downstream Oxley Break	0.038		
Macquarie Branch downstream Monkey Creek	0.038		
Buckiinguy return	0.037		
Macquarie River at Maxwelton	0.037		
Monkey Creek	0.037		
Macquarie River at Pillicawarrina	0.036	0.035	Sinuous channel with very sparse woody vegetation along margins, or dense woody vegetation on one bank only
Bulgerera Creek downstream Oxley Break (upper reach)	0.035		
Bulgerera Creek at Willancorah	0.035		
Middle Oxley Break	0.034		
Lower Oxley Break	0.032	0.03	Straight channel with no woody vegetation along margins, or very sparse woody vegetation on one bank only
Bulgerera Creek downstream Oxley Break (middle reach)	0.029		
Old Macquarie near Willie	0.025	0.025	Shallow sinuous or straight channel with very sparse vegetation

3.4.7 Longitudinal channel slope

To calculate channel slope (a key input for discharge and stream power calculations), multiple methods were explored, including "zonal statistics" and the "slope tool" in ArcMap. However, these were found to provide inaccurate values (i.e. significantly higher than would be expected for a system of this type, as confirmed by previous fieldwork; see Table 3.5). This was concluded to be due to underlying issues with the DEM, such as erroneous elevation values due to inundation and dense vegetation, and the way slope is calculated using the "slope tool" in ArcMap. In ArcMap, slope is calculated for each cell by considering the maximum change in elevation over the distance between that cell and its neighbour, and the steepest slope is extracted as a percentage or degree. In this study, distance and elevation data were extracted manually using the "stack profile" tool in ArcMap for each reach of the main river channels in the Macquarie Marshes and an elevation-distance graph was plotted for all data in Excel. The reaches were identified by assessing and marking significant breaks in slope along the channels. The equation of a linear trendline was fitted for each reach to find the slope value for that reach, as follows:

$$y = mx + b \qquad \textbf{Eq.4}$$

where y = elevation (m), m = channel slope (m/m), x = distance (m) and b = y intercept (m).

A single trendline and therefore slope value was suitable for some reaches (Figure 3.6A), but not for others where marked changes in gradient occurred, and so these were divided into segments and slopes were calculated for the different segments by obtaining different trendlines (Figure 3.6B). After finalising the slope value for each segment, the "near table" tool in ArcMap was used to determine and attribute the slope values related to each bifurcation or return point and the associated transects.

Table 3.5 Comparison of values for slope (m/m) from different methods (range of all reaches).

"Zonal statistics"	"Slope tool" in ArcMap	Linear regression	(Ralph, 2008)
0.01-0.2	1.53-2.6	0.0000002-0.002	0.00005-0.005

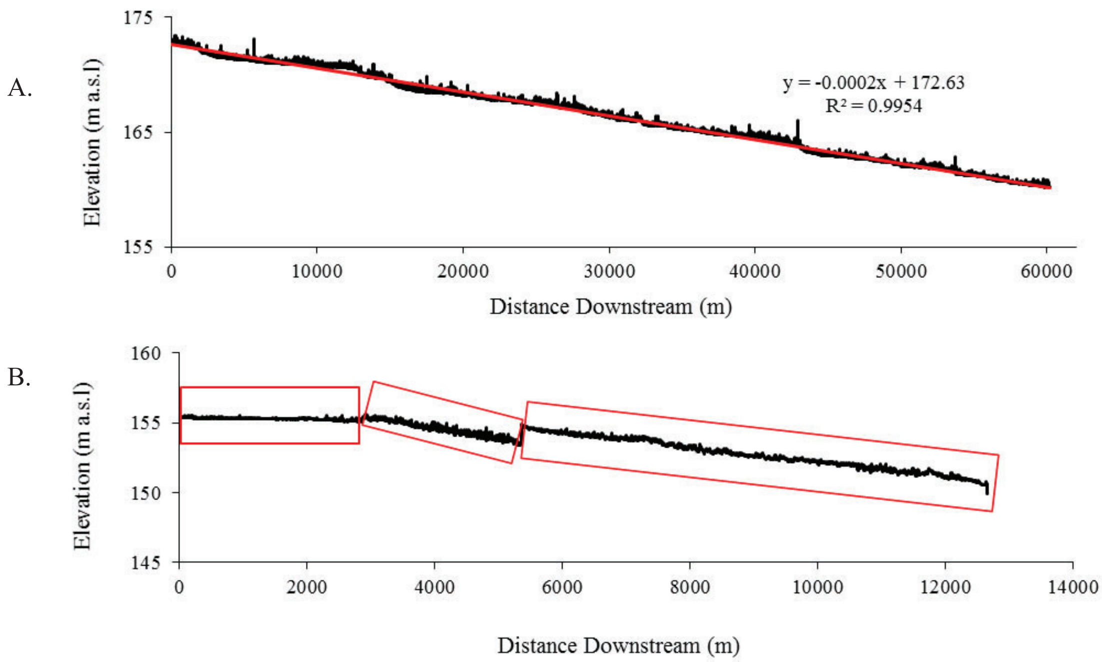

Figure 3.6 Downstream elevation data to calculate slope for a reach with one value in the Macquarie River upstream of Buckiinguy (A), and downstream elevation data to calculate slope for a reach with three values in the middle of Bulgeraga Creek (B).

3.4.8 Channel hydraulic data

Channel hydraulic parameters were calculated using the following equations to define the channel bankfull conditions related to periods of maximum flow energy. The estimation of bankfull discharge will help to predict the maximum potential capacity of the channel to transport sediment before splitting due to overbank flow conditions (Larkin et al., 2017). The equations below are based on the relationship between channel hydraulic character, channel geometry parameters (i.e. channel width, depth and area), bed gradient and roughness.

Discharge:

$$Q = \frac{1}{n} A D^{2/3} S^{1/2} \qquad \textbf{Eq.5}$$

where Q = bankfull discharge (m^3/s), n = Manning's n value, A = channel bankfull cross-sectional area (m^2), D = channel depth (m) and S = channel slope (m/m).

Stream power:

$$\Omega = \rho g Q S \qquad \textbf{Eq.6}$$

where Ω = stream power (W/m), ρ = density of water (1,000 kg/m^3), g = acceleration due to gravity (9.8 m/s^2), Q = discharge (m^3/s) and S = channel slope (m/m).

Unit stream power:

$$\omega = \Omega / W \qquad \textbf{Eq.7}$$

where ω = unit stream power (W/m^2), Ω = stream power (W/m^2) and W = channel width (m).

3.5 Rapid assessment

Risk is a function of the likelihood and consequences of a hazard occurring (Middlemann, 2007). Hazards and risks associated with channel erosion, sedimentation and overall geomorphic change will vary between sites, over time and under different management and intervention scenarios in the Macquarie Marshes. Therefore, geomorphic site assessments, geomorphic mapping and subsequent analyses were used to inform the risk assessment, following the protocol developed by Ralph et al. (2013). A rapid field-based risk assessment was carried out in 2012 and 2018 at 20 sites in the Southern Macquarie Marshes (three measurements at representative places for each site) to identify the context, potential hazards and the likelihood and consequences of hazards related to erosion and geomorphic change. Fieldwork was undertaken in January 2018 to assess the channel conditions in detail to help refine the erosion risk assessment method. Bank shape, erosional features, depositional features, anthropogenic modifications to the channels and their impacts, vegetation and roughness were investigated using the same assessment template (see Appendix 1). Water temperature, pH and electrical conductivity were also measured using handheld meters within the channel baseflow as an indicator of current water quality conditions. Soil surface characteristics, including cracking, biotic crust, salt crust and saline discharge, were also surveyed.

A handheld penetrometer was used to measure soil compressive strength, where a telescoping rod was pushed into sediment of the banks repeatedly to yield a mean compressive strength value (kg/cm^2). A handheld shear vane was used to measure undrained soil shear strength, where a rod with vanes mounted to it was inserted into the banks and rotated to the point of failure repeatedly to yield a mean shear value (kPa). The full form used for on-site geomorphic assessment is provided in Appendix 1.

Based on all of the information gathered during the geomorphic field assessments and subsequent analyses, a level of likelihood (1 = rare to 5 = almost certain; Table 3.6) and consequence (1 = insignificant to 5 = extreme; Table 3.7) were assigned for bed and bank erosion, flow capture, in-channel sedimentation and channel blockage and other factors affecting the channels. An erosion risk assessment matrix (1 = very low to 5 = very high; Table 3.8) was then built based upon the integration of the levels of likelihood and consequence. Study sites were then ranked according to the risk and assessed in terms of the priority/need for future land and water management to maintain and/or improve the site's geomorphic condition. The risk assessment data from 2018 was compared with the results from Ralph et al. (2013), which was undertaken in October 2012, to update the erosion risk assessment ranked list and to explore any short-term trends or trajectories for the Southern Macquarie Marshes. In broad terms, for very high- and high-risk sites, urgent or immediate action and a high level of management is recommended. For medium-risk sites, management action may be needed, and for low- and very low-risk sites, routine monitoring and management may be needed.

Table 3.6 Likelihood framework for the Southern Macquarie Marshes erosion risk assessment.

Level	Descriptor	Definition
1	Rare	May occur only in exceptional circumstances
2	Unlikely	Could occur at some time
3	Possible	Might occur at some time
4	Likely	Will probably occur in most circumstances
5	Almost certain	Is expected to occur in most circumstances

Note: from Ralph et al. (2013), as adapted from AS/NZS 4360 (2004) and MDBA (2011).

Table 3.7 Consequence framework for the Southern Macquarie Marshes erosion risk assessment.

Level	Descriptor	Definition
1	Insignificant	Negligible impact on channel and/or wetland environmental values
2	Minor	Localised short-term damage to channels and/or wetland environmental values
3	Moderate	Short-term damage to channel and/or wetland environmental values; on-site impacts can be contained and/or managed
4	Major	Long-term damage to channels and/or wetland environmental values; off-site impacts with no detrimental effects
5	Extreme	Irreversible damage to channels and/or wetland environmental values; severe off-site impacts with detrimental effects

Note: from Ralph et al. (2013), as adapted from AS/NZS 4360 (2004) and MDBA (2011).

Table 3.8 Risk matrix for the Southern Macquarie Marshes erosion risk assessment.

Likelihood	**Consequence**				
	1. Insignificant	**2. Minor**	**3. Moderate**	**4. Major**	**5. Extreme**
1. Rare	Very low	Very low	Low	Medium	High
2. Unlikely	Very low	Low	Medium	Medium	High
3. Possible	Low	Low	Medium	High	High
4. Likely	Low	Medium	Medium	High	Very high
5. Almost certain	Low	Medium	High	Very high	Very high

Note: from Ralph et al. (2013), as adapted from AS/NZS 4360 (2004) and MDBA (2011).

3.6 Summary

This chapter described the research strategy, study sites and methods used in this study to understand the geomorphic and hydraulic characteristics of channels within the Macquarie Marshes and the likely role and risk of erosion in this system. The next chapter (chapter 4) presents results from spatial analysis of patterns of channels and an assessment of their recent expansion and contraction throughout the Macquarie Marshes using DEMs. Chapters 5, 6 and 7 then present results and discussion to address and answer the remaining research questions.

Chapter 4: Assessment of recent channel change using DEMs

4.1 Chapter introduction

This chapter assesses broad patterns of channels throughout the Macquarie Marshes and evidence for their recent expansion and contraction using LiDAR-derived DEM analysis. Understanding channel change in floodplain wetlands is critical because this can lead to alterations in inundation patterns and habitat degradation or loss. While some channels in the wetlands clearly experience channel change, it is important to determine whether cross-sections extracted from DEMs and DEM of Difference (DoD) analysis can resolve these types of fine-scale channel adjustments over a short timeframe (i.e. 2008-2015 ”as an error it is written 2014 in this paper”). The thesis aims addressed in this chapter are:

1. *To quantify the spatial patterns of channels and determine the distribution of channel bifurcation and return nodes along major channels within the Macquarie Marshes;*
3. *To identify historical and contemporary trajectories of channel behaviour in hyper-avulsive reaches of the Southern Macquarie Marshes and to explain the role of erosion in the system.*

This chapter is published as:

Yousefi, N., Ralph, T.J., Farebrother, W., Chang, H-C. & Hesse, P.P. 2018. Assessment of channel expansion and contraction using cross-section data from repeated LiDAR acquisitions in the Macquarie Marshes, NSW. Proceedings of the 9th Australian Stream Management Conference: 12–15 August 2018, Hobart, Tasmania. Vietz, G. J. & Rutherfurd, I. D. (eds.). Melbourne, Victoria: River Basin Management Society, p. 103-110.

Available online: http://9asm.org.au/assets/9ASM-Complete-Proceedings-2018-Final.pdf

4.2 Author contributions

Yousefi, N. – conducted all data analyses and interpretation, wrote the draft manuscript, drafted the figures and tables, edited the final manuscript (75% of all work).

Ralph, T.J. – reviewed and edited the draft and final manuscripts, edited figures, and contributed to GIS and channel data analysis and interpretation (10% of all work).

Farebrother, W. – reviewed and edited the draft and final manuscripts, and contributed to GIS data analysis (10% of all work).

Chang, H-C. – reviewed and edited the final manuscript and contributed to GIS data interpretation (2.5% of all work).

Hesse, P.P. – reviewed and edited the final manuscript and contributed to channel data interpretation (2.5% of all work).

Assessment of channel expansion and contraction using cross-section data from repeated LiDAR acquisitions in the Macquarie Marshes, NSW

Neda Yousefi, Timothy J. Ralph, William Farebrother, Hsing-Chung Chang and Paul P. Hesse

Department of Environmental Sciences, Macquarie University, NSW 2109, Australia, neda.yousefi@hdr.mq.edu.au

4.3 Abstract

Floodplain wetlands have alluvial channels that change over time due to both erosion (sediment export) and sedimentation (sediment accumulation). Adjustments in channel capacity resulting from erosion and sedimentation influence the timing and extent of floodplain wetland inundation and alter in-channel and other habitats and their ecological processes, and are a key factor in river and floodplain management. Nineteen sites in the southern Macquarie Marshes were studied, some with multiple channels and others with a single channel, yielding 54 channel cross-sections in all. Two Light Detection And Ranging (LiDAR) Digital Elevation Model (DEM) datasets acquired in 2008 and 2014 were used to assess changes in channel size and shape due to erosion and sedimentation. Channel depth measurements could not resolve any changes in depth, and were not accurate when channels contained water. Comparisons of channel width measurements showed that 17% of channels experienced expansion over the 6 year period between LiDAR acquisitions, while 5% had a reduction in channel width, and 78% had no measureable change. The trunk streams of the Macquarie River and Bulgeraga Creek and a return channel of Buckiinguy expanded, suggesting erosion, whereas one reach of Bulgerara Creek and the distributary channel Monkey Creek contracted, suggesting sedimentation. Analysis of a DEM of Difference (DoD) for the whole area covered by the Macquarie Marshes LiDAR data was not able to produce reliable results for vertical level changes (deposition or degradation), particularly where water and dense vegetation were present. It is inferred from the DoD that any sedimentation or erosion in the system during this brief time window was beyond the limits of detection (±15 cm vertical; ±45 cm horizontal) and was not significant.

Keywords: Channel capacity, channel change, erosion, floodplain wetlands, DEM, sedimentation, wetland in drylands

4.4 Introduction

Floodplain wetlands provide unique habitat for water-dependent flora and fauna. Channels supply floodplain wetlands with water and play a critical role in maintaining ecological and geomorphological conditions, although, they are at the risk from natural disturbances and human impacts (Ralph et al., 2016). Channel change due to erosion and sedimentation is a concern in floodplain wetlands, especially where changes in channel capacity may affect the depth, extent and timing of floodplain or wetland inundation. Therefore, understanding channel behavior and the patterns of erosion and sedimentation in alluvial channels is helpful when managing wetlands.

Several methods have been introduced to assess channel expansion and contraction due to erosion and sedimentation in rivers and wetlands. For example, erosion pins (Palmer et al., 2014, Foucher et al., 2017), field plots (Smets et al., 2008, Smith and Vericat, 2015), cross-section surveys (Hupp et al., 2015), remote sensing and satellite imagery (Patro et al., 2009, Rowland et al., 2016), analysis of aerial photographs and historical maps (Ralph et al., 2016, Lallias-Tacon et al., 2017), Light Detection And Ranging (LiDAR) surveys (Croke et al., 2013, Huang et al., 2014), and Digital Elevation Models (DEMs) and DEMs of Difference (DoDs) (Bezak et al., 2015). Of these, LiDAR and DoD approaches are being widely applied due the growing availability of high resolution digital elevation data, for example, Croke et al., (2013 used LiDAR to assess basin-scale erosion and deposition in the Lockyer River valley in Queensland, Australia. Erosion and deposition patterns have also been quantified using LiDAR in Colorado (Brogan et al., 2015), while LiDAR and historical aerial photos have been used to reconstruct floodplain formations (Lallias-Tacon et al., 2017).

Although these techniques have been used worldwide, they have not been widely applied in multi-channeled floodplain wetland systems to help understand patterns of channel erosion and sedimentation. Therefore, the channel-dependent floodplain wetlands of the Macquarie Marshes were selected for this study, and cross-sections extracted from LiDAR-derived DEMs were used to calculate metrics and to assess channel changes over a 6 year period (2008-2014). A DoD analysis was also undertaken through the comparison of the repeated LiDAR-derived DEMs. The aim was to determine whether significant channel change could be detected, and if so, whether these changes signified hotspots of erosion and/or sedimentation that may be relevant for river and wetland management.

4.5 Study Sites and methods

4.5.1 Study sites

The Macquarie Marshes are one of the largest semi-permanent inland floodplain wetlands in south-eastern Australia, spanning an area of >2,000 km^2 when in flood. The wetlands are located on the lower reaches of the Macquarie River in the Murray-Darling Basin, New South Wales, Australia (Figure 4.1). Sediment erosion and deposition dynamics in the Macquarie Marshes lead to channel adjustment, channelization of wetlands, and avulsion, the relocation of channels from one part of the floodplain to another (Ralph et al., 2011, Ralph et al., 2016). The Macquarie Marshes have three core regions, the southern Macquarie Marshes, northern Macquarie Marshes and eastern Macquarie Marshes (Figure 4.1C), and patterns of flow and flooding throughout the wetlands are variable and have changed over time (Thomas et al., 2011).

In the southern Macquarie Marshes, the trunk stream of the Macquarie River breaks down into a few major distributary channels including Oxley Break, Monkey Creek, Buckiinguy Creek, Monkeygar Creek and The Breakaway (Ralph and Hesse, 2010). Some of these distributaries break down again into smaller marsh channels and almost all discharge into significant wetlands, where, in many cases, return channels flow from the wetlands back into the trunk streams. Bulgeraga Creek is a major anabranch of the Macquarie

River in this region and is also considered as a trunk stream. Nineteen key sites on ten major channels in the southern Macquarie Marshes were assessed in this study (Figure 4.1D), all downstream of Marebone Weir. The hydrological record for the Macquarie River at Marebone Weir for the period of our study shows that drought conditions prevailed in 2008/09, before flood conditions occurred in 2010/11 and 2012/13 (Figure 4.2).

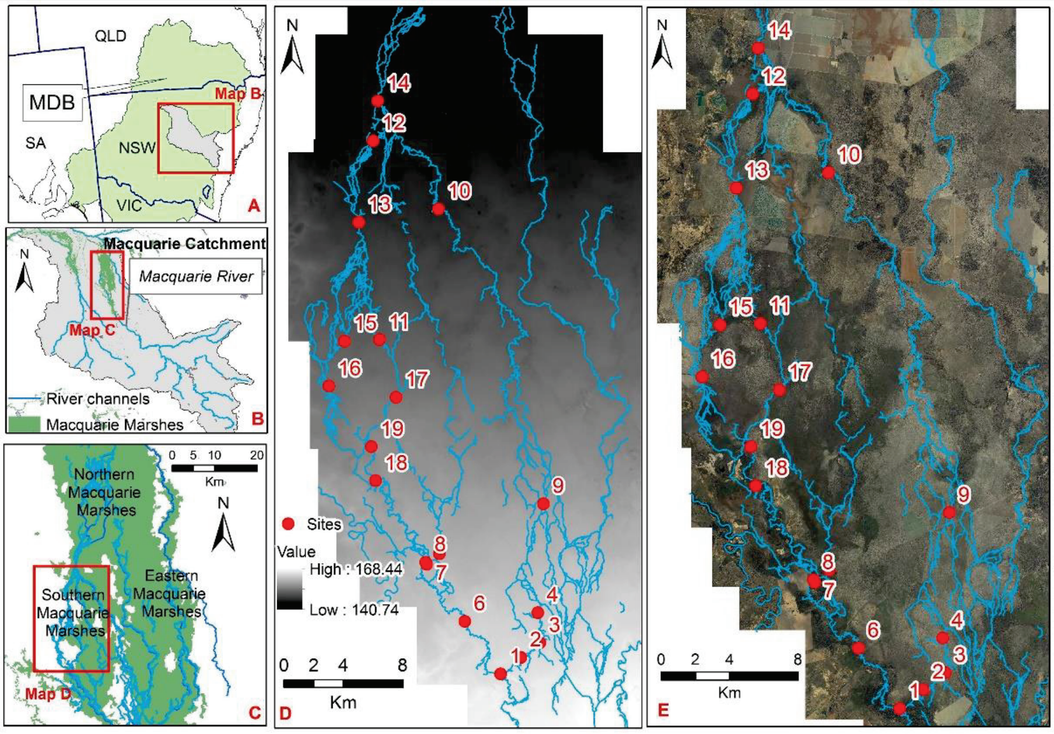

Figure 4.1 Location of the Macquarie Marshes in the Murray-Darling Basin (A), in the Macquarie catchment (B), the southern Macquarie Marshes study area (C), 19 study sites (D), and aerial imagery (E).

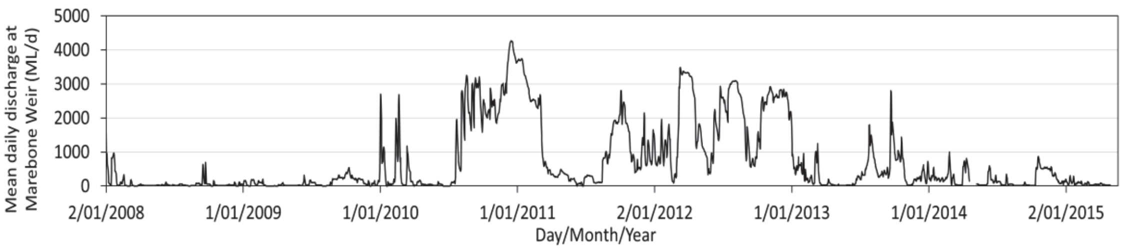

Figure 4.2 Mean daily discharge entering the Macquarie Marshes (Marebone Weir) from 1/1/08 to 30/4/15.

4.5.2 Methods

Two LiDAR-derived DEMs acquired by the NSW Government Office of Environment and Heritage (OEH) in 2008 and 2014 were used for the morphometric analysis of the channels. The LiDAR-derived DEM data has ±15 cm vertical accuracy and ±45 cm horizontal accuracy. This translates to thresholds of change equivalent to 30 cm vertical and 90 cm horizontal when considering differences between cross-sections extracted from the DEMs. Channel cross-sections were extracted from the LiDAR-derived DEMs at 19 representative sites using ArcGIS. Analyses of the channel geometry including bankfull width, bankfull depth and width/depth ratio were undertaken using standard methods. Comparison of cross-section metrics from 2008 and 2014 were used to calculate changes in channel width and depth that occurred during the 6-year period.

A DoD was created by subtracting the LiDAR-derived elevations in 2014 from LiDAR-derived elevations in 2008 for the entire area covered by LiDAR data using the raster calculation tool in ArcMap 10.3. The potential vertical error for DoD values based on the two LiDAR acquisitions is up to ±30 cm vertical and 90 cm horizontal, and values less than these thresholds measured by DoD were categorized as no change.

4.6 Results and discussion

4.6.1 Cross-section morphology and change

Trunk streams in the study area (i.e. the Macquarie River, Bulgeraga Creek, Old Macquarie River) had channels with a mean width of ~39 m, mean depth of ~2 m and mean width/depth ratio (w/d) of ~21. Distributary channels (i.e. upper and middle Oxley Break, Monkey Creek, Monkeygar Creek, Buckiinguy Creek) had a mean width of ~23.5 m, mean depth of ~2 m and mean w/d ratio of ~13. Return channels (i.e. Mole Marsh, Buckiinguy Return, lower Oxley Break) had a mean width of ~21 m, mean depth of ~1.6 m and a mean w/d ratio of 13.4 (Table 4.1). The channel width was therefore the main factor that could be used to differentiate channels in terms of their morphology.

Table 4.1 Common channel types and key metrics from the 2008 LiDAR-derived DEM.

Metrics from 2008 LiDAR-derived DEM	Trunk streams	Distributary channels	Return channels
Mean channel width (m)	38.9 *(4.4)*	23.5 *(2.5)*	21.2 *(1.9)*
Mean channel depth (m)	2.1 *(0.1)*	2.1 *(0.2)*	1.6 *(0.1)*
Mean width/depth ratio	20.7 *(2.6)*	12.9 *(2)*	13.4 *(1)*

Note: Values in parentheses represent standard error of the mean.

Three types of channel change were observed at the 19 sites between 2008 and 2014 (Table 4.2). The results showed an apparent contraction in channel width for just 5% of channels, possibly representing a dominance of sedimentation during the 6 year period. One reach of the trunk stream of Bulgerara Creek and the distributary channels of Monkey Creek and Buckiinguy Creek experienced channel contraction. Conversely, 17% of channels experienced channel expansion, including the trunk streams of the Macquarie River, Bulgeraga Creek and the Old Macquarie River, the major distributary channel Monkeygar Creek, and the return channel Buckiinguy Return, possibly due to erosion. However, the vast majority of sites (78%) had no detectable change during the 6 year period. This suggests that most of the channels in the southern Macquarie Marshes are either relatively stable over this short timeframe and/or that the methods used to detect change were not of sufficient resolution to detect fine-scale, subtle changes.

No channels exhibited measureable changes in depth using the LiDAR-derived DEM data. The results also show that depth measurements are unreliable when channels contain water, or when there is dense vegetation present in the channel or on the floodplain. For example, the cross-section extracted for site 9 shows a flat bottom which is due to water inside the channel, which is confirmed by imagery taken at the time of LiDAR acquisition (Figures 4.3A and 4.3B). Therefore, the actual depth of the channel could not be measured at this site. At site 6, however, measurements were not affected by water, but by dense vegetation, again leading to poor channel detection (Figures 4.3C and 4.3D).

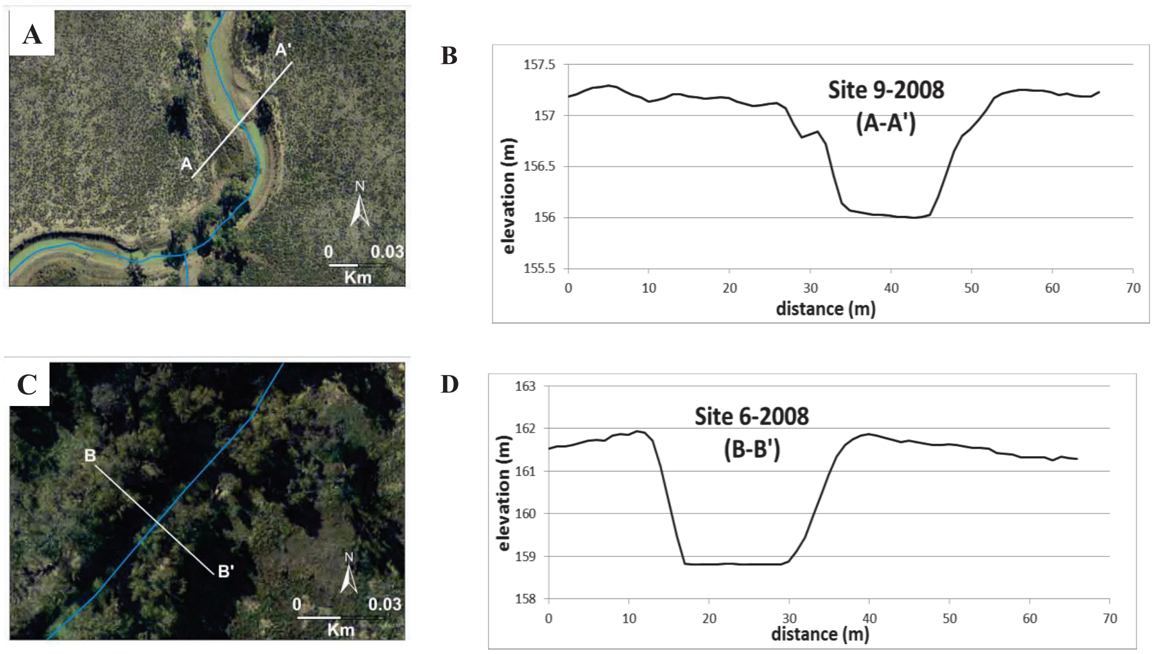

Figure 4.3 Imagery and cross-sections extracted from site 9 and site 6 showing the effects of water and vegetation on elevation data.

4.6.2 DEM of Differences

The results of the DoD analysis for the whole Macquarie Marshes LiDAR acquisition area showed that the DoD could not accurately identify increases or decreases in elevation due to erosion or sedimentation because of the low resolution and detection limits of the data, in particular, where water or dense vegetation was present in either LiDAR acquisition. While reliable data was attainable in an ideal location (i.e. along a road that had not changed between 2008 and 2014; Figure 4.4A), channels and wetlands with dense vegetation gave misleading results (Figure 4.4B), as did areas with inundation at the time of acquisition (Figure 4.4C).

Table 4.2 Channel types and results of cross-section analysis from 2008 and 2014 LiDAR-derived DEMs.

Site number	Site name	Channel type	Cross section (SMM)	Measured change in depth (m)	Change in depth >DEM threshold	Measured change in width (m)	Change in width >DEM threshold
1	Upper Oxley Break	Distributary	1-1	0	-	0.08	-
			1-2	0.001	-	0	-
			1-3	0.031	-	-0.01	-
2	Middle Oxley Break	Distributary	2-1	0.003	-	-0.12	-
			2-2	-0.005	-	0.08	-
			2-3	0	-	0	-
3	Lower Oxley Break	Return	3-1	-0.001	-	0.01	-
			3-2	0.008	-	0.14	-
			3-3	-0.021	-	-0.68	-
4	Bulgeraga Creek downstream of Oxley Break	Trunk	4-1	-0.006	-	-0.27	-
			4-2	0.004	-	-0.86	-
			4-3	-0.001	-	0.99	contraction
5	Monkey Creek	Distributary	5-1	-0.001	-	1.49	contraction
			5-2	0.003	-	0.06	-
			5-3	0.016	-	1.03	contraction
6	Macquarie River downstream of Oxley Break and upstream of Monkey Creek	Trunk	6-1	0.005	-	0	-
			6-2	0	-	0.03	-
			6-3	0.013	-	-0.13	-
7	Macquarie River downstream of Monkey Creek and upstream of Buckiinguy Creek	Trunk	7-1	0.012	-	0.03	-
			7-2	0.003	-	-0.04	-
			7-3	0.012	-	-0.18	-
8	Buckiinguy Creek	Distributary	8-1	-0.005	-	0	-
			8-2	0	-	0.01	-
			8-3	0.001	-	0.96	contraction
9	Bulgeraga Creek downstream of Oxley Break	Trunk	9-1	-0.003	-	-1.15	expansion
			9-2	-0.018	-	-0.86	-
			9-3	0	-	-0.17	-
10	Bulgeraga Creek at Willancorah	Trunk	10-1	0.005	-	0.18	-
			10-2	-0.021	-	-1.05	expansion
			10-3	-0.075	-	-4.02	expansion
11	The Breakaway	Distributary	11-1	-0.006	-	-0.19	-
12	The Mole reed bed outflow channels	Return	12-2	0.011	-	-0.04	-
			12-3	-0.002	-	-0.04	-
13	Macquarie River at Maxwelton and the Mole	Trunk	13-1	0	-	-0.79	-
			13-2	-0.003	-	-0.07	-
			13-3	-0.021	-	-0.65	-
14	Macquarie River at Pillicawarrina	Trunk	14-1	-0.013	-	-1.95	expansion
			14-2	0.003	-	0.04	-
			14-3	-0.11	-	0.03	-
15	Old Macquarie River in Nature Reserve near Willie	Trunk	15-1	-0.008	-	-0.85	-
			15-2	0.001	-	-0.92	expansion
			15-3	0.002	-	0.16	-
16	Old Macquarie River in Nature Reserve	Trunk	16-1	0.006	-	0.04	-
			16-2	0.014	-	-0.38	-
			16-3	-0.007	-	-0.20	-
17	Monkeygar Creek upstream of The Breakaway	Distributary	17-1	0	-	-0.05	-
			17-2	0.012	-	-0.02	-
			17-3	-0.003	-	-1.35	expansion
18	Buckiinguy Return and Buckiinguy Runner	Return	18-1	0	-	-0.01	-
			18-2	0.001	-	0.02	-
			18-3	-0.006	-	-1.03	expansion
19	Macquarie River downstream of Monkey Creek and downstream of Buckiinguy Creek	Trunk	19-1	-0.011	-	0.07	-
			19-2	-0.083	-	-1.04	expansion
			19-3	0.014	-	0.07	-

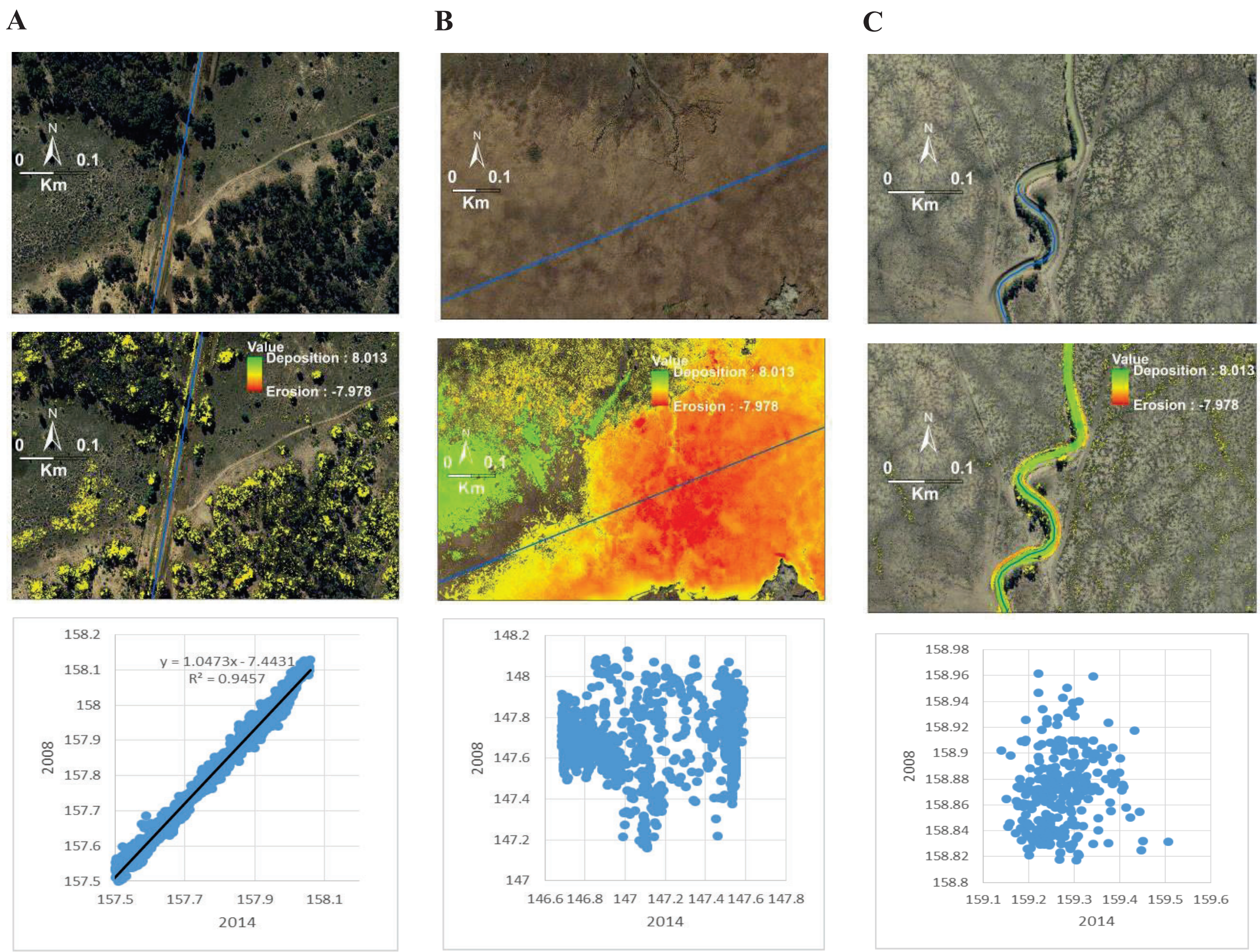

Figure 4.4 DoD results for a road (A), a densely vegetated area of wetland (B), and a channel with water (C).

4.7 Interpretations

In the six year period channel change in the Southern Macquarie Marshes was observed as minor adjustments in depth and width. The pattern of the channels in the southern Macquarie Marshes represents the dominant of the trunk stream channels in this area, where tributary and distributary junctions joined them. Regards the type of the channel, they could be eroded or deposited. Trunk stream channels and tributary channels which provide the majority of flow and incoming discharge exhibit channel erosion and expansion. Despite the findings of some eroded channels, distributary channels are more likely to exhibit deposition as the flow decreases because of channel branching. These results confirm a direct relation between flow and sediment transportation, increased flow leading channels towards higher risk of erosion. LiDAR-derived DEMs could not provide precise data on floodplain and channel changes because of the limitation of the threshold accuracy. Based on this restriction the data suggest mostly unchanged cross-sections for the majority of sites.

4.8 Conclusion

Nineteen sites located in the southern Macquarie Marshes were studied to assess channel change in a six year period between 2008 and 2014. Although previous research has shown that channels in this system are highly dynamic (Ralph et al., 2016), results from two LiDAR-derived DEM surveys showed that the majority of channels did not change and of the changes that did occur, most suggested channel expansion. While LiDAR is a useful and important tool for understanding fluvial geomorphology and for measuring the size and shape of channels and other landforms, short-term repeated LiDAR acquisition and channel cross-section analysis yielded results that were not highly resolved, and in most cases potential changes in channel width and depth did not exceed the limits of detection. The DoD analysis was inconclusive during this short-term analysis of channel change likely due to the low-gradient nature of this environment. Further detailed research is required to apply high resolution LiDAR-derived DEMs in the Macquarie Marshes, and to test their validity for change detection over longer timescales.

4.9 Chapter summary

This chapter assessed recent channel changes in the Macquarie Marshes using DEMs, showing that few significant changes in channel width and depth were detectable using a DoD approach over a relatively short six-year timeframe. The next chapter presents the results from a system-wide analysis of channel bifurcation and return points in the context of channel patterns in the Macquarie Marshes.

Chapter 5: Spatial pattern of channel bifurcation and return nodes in the Macquarie Marshes

5.1 Introduction

This chapter quantifies the distribution of channel bifurcation and return nodes and describes the anastomosing channel pattern leading to anabranching and distributary channels and zones of channel breakdown in the Macquarie Marshes. A detailed description of channel analysis is presented that focuses on comparisons of channel morphology and capacity (i.e. width, depth, area, slope), roughness (Manning's n) and hydrological character (discharge and stream power) at and between bifurcation and return points in the system. These findings are interpreted in relation to the (non) equilibrium condition of channels in the Macquarie Marshes. In this chapter, following aims of the thesis are answered addressed.

1. *To quantify the spatial patterns of channels and determine the distribution of channel bifurcation and return nodes along major channels within the Macquarie Marshes.*
2. *To define the geomorphic configuration and hydraulic behaviour of channels leading to channel maintenance, avulsion and breakdown in the Macquarie Marshes.*

5.2 Channel delineation and pattern

Channel lines extracted for the whole Macquarie Marshes, using flow accumulation modelling for the LiDAR-derived DEM from 2008 (methods in Chapter 3; Section 3.4.2), show that an anastomosing pattern dominates the channels in the Southern, Northern, and Eastern Marshes (Figure 5.1a). Overall, 4,248 individual river channel segments were considered for inclusion in the major channels layer, equating to 1,499.25 km of channel length. These major channels align closely with observable channels in the system (Figures 5.1b and 5.1c). Also, smaller channel segments that were considered to be too short (less than 50 m) or too isolated and/or disconnected to warrant inclusion as a major channel were thus excluded from further analysis.

5.3 System-wide arrangement and morphology of bifurcation and return nodes

Analysis of bifurcation and return patterns and associated channel metrics provides an understanding of the spatial variability of channels and their morphology (i.e. size, shape, arrangement), as well as a way to interpret key geomorphic processes and aspects of channel adjustment. The spatial arrangement of channel bifurcation and return nodes shows a similar pattern in the Southern, Northern and Eastern Macquarie Marshes (Figure 5.2).

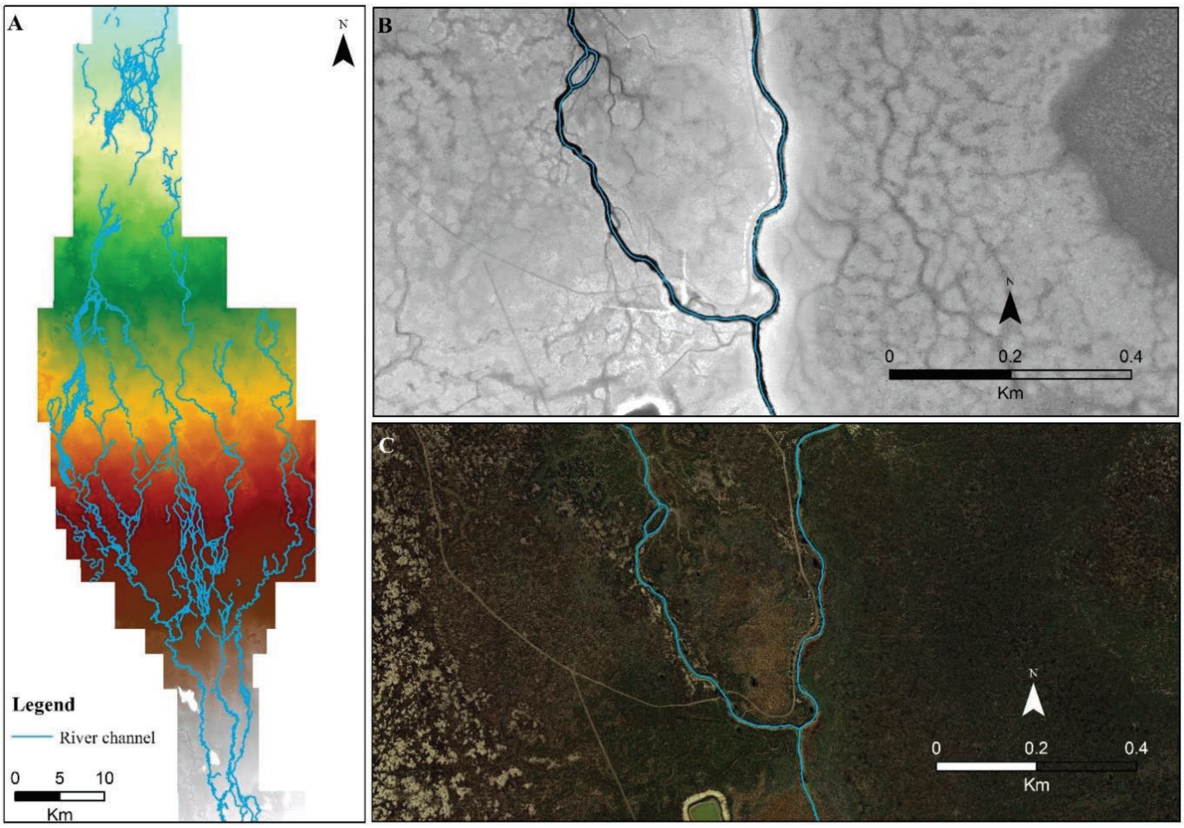

Figure 5.1 Major river channels (polylines) delineated for the Macquarie Marshes (A), river channel polyline at the avulsion point of Monkeygar Creek and The Breakaway overlain on LiDAR-derived DEM (B), and river channel polyline at the same location overlain on aerial photography (C).

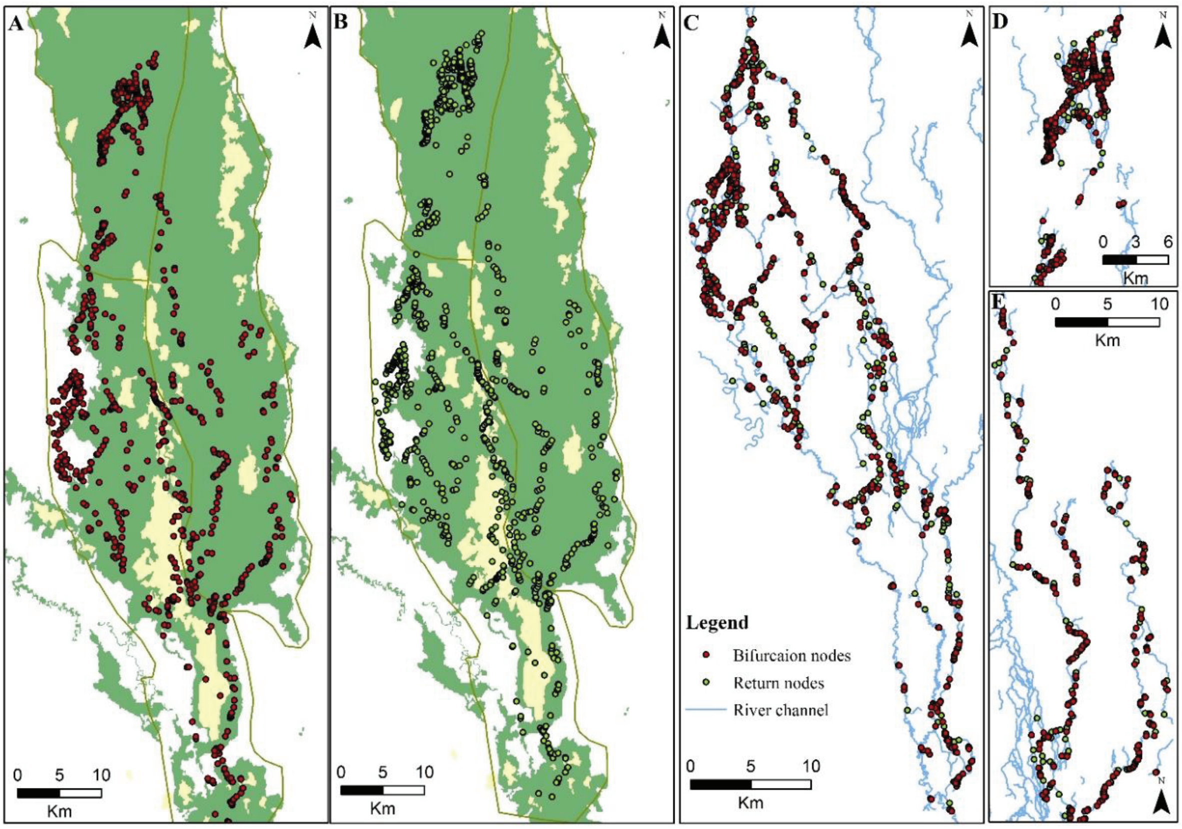

Figure 5.2 Channel bifurcation nodes (A) and return nodes (B) in the whole Macquarie Marshes, in the Southern Macquarie Marshes (C), in the Northern Macquarie Marshes (D) and in the Eastern Macquarie Marshes (E).

Comparison of the total number of channel bifurcations and returns through the main rivers in the entire Macquarie Marshes and the sub-systems of the Southern, Northern and Eastern Macquarie Marshes shows that ~50% or more of the bifurcations and returns occur in the Southern Macquarie Marshes, while ~30% of bifurcations and returns occur in the Northern section and ~20% of bifurcations and returns occur in the Eastern section (Table 5.1). In the whole system, and also in each of the sub-systems, returns outnumber bifurcations. However, there is a relatively equivalent ratio of channel bifurcations and returns in the Northern and Eastern Macquarie Marshes, while the Southern section has a lower ratio (Table 5.1).

Table 5.1 Proportion of bifurcations and returns and their key morphometrics in the whole Macquarie Marshes and sub-systems.

		System scale			
	Morphometric parameter	Whole Macquarie Mashes	Southern Macquarie Marshes	Northern Macquarie Marshes	Eastern Macquarie Marshes
Bifurcations	Number of bifurcations	889	440	260	189
	% of total bifurcations	-	49.5	29.2	21.3
	Channel width mean ± standard deviation (m)	19.7±8.4	19.5±8.8	21.2±8	17.9±7.6
	Channel width range (m)	2.8-78.3	3.5-78.3	2.8-64.8	4.6-67.1
	Channel depth mean ± standard deviation (m)	0.7±0.6	0.9±0.8	0.5±0.2	0.5±0.3
	Channel depth range (m)	0.01-5.03	0.02-5.03	0.05-1.67	0.06-2.55
	Channel cross-sectional area mean ± standard deviation (m^2)	8.5±11.8	11.8±15.4	5.9±4.3	4.6±5.6
	Channel cross-sectional area range (m^2)	0.04-122.9	0.04-122.9	0.11-30.8	0.11-75.1
	Channel bed slope mean ± standard (m/m)	0.0004±0.0001	0.0004±0.0001	0.0004±0.0002	0.0003±5E-05
	Channel bed slope range (m/m)	2E-05-0.002	3E-05-0.002	2E-05-0.0007	0.0003-0.0004
Returns	Number of returns	977	509	276	192
	% of total returns	-	52.1	28.2	19.7
	Channel width mean ± standard deviation (m)	17±7	17.3±7.5	18.8±6.2	13.9±5.6
	Channel width range (m)	3.6-55.4	4- 46.8	5.1-55.4	3.6-47.7
	Channel depth mean ± standard deviation (m)	0.7±0.6	0.9±0.7	0.4±0.3	0.4±0.2
	Channel depth range (m)	0.03-4.57	0.04-4.57	0.03-1.65	0.03-1.48
	Channel cross-sectional area mean ± standard deviation (m^2)	7±9.7	9.8±12.3	4.9±3.9	2.8±2.9
	Channel cross-sectional area range (m^2)	0.02-117.7	0.02-117.7	0.1-32.2	0.06-31.9
	Channel bed slope mean ± standard (m/m)	0.0004±0.0002	0.0004±0.0002	0.0004±0.0002	0.0003±5E-05
	Channel bed slope range (m/m)	2E-05-0.002	0.0001-0.002	2E-05-0.0007	0.0003-0.0004
Bifurcation: return ratio		0.91	0.86	0.94	0.98

Channel morphometric factors including bankfull width, bankfull depth and bankfull cross-sectional area, and longitudinal slope were calculated for the channels upstream and downstream of each bifurcation and return node (within 50 m distance around each point). Considering all transects upstream and downstream of bifurcation and return nodes (three transects per node), 2,667 transects at bifurcations and 2,931 transects at returns were analysed. The findings reveal that channels at bifurcation nodes have a greater range of width compared to channels at return nodes, while cross-sectional area and depth show a similar pattern at the scale of the whole system. However, the Southern Macquarie Marshes contains the deepest channels with generally larger cross-sectional area, while channels in the Northern and Eastern Marshes have lower mean depth and cross-sectional area, and overall have more similarity to each other in terms of their morphometric character. The Northern Macquarie Marshes has the smallest variation in channel width, but greater mean width and the Eastern Macquarie Marshes has the least mean width at both bifurcations and returns. Overall, mean cross-sectional area for returns is less compared to bifurcations for the whole system and its sub-systems (Table 5.1). The Southern Macquarie Marshes has a greater range of channel bed slope while mean slope in the Southern and Northern Marshes are similar, with more variation for the bifurcations in the Northern Marshes. The Eastern Macquarie Marshes has the lowest mean slope among all sub-systems (Table 5.1).

Morphometric results for all of the transects show that channels with width of 10-20 m are dominant in the whole Macquarie Marshes and its three major sub-systems. There are more returns with width less than 20 m and bifurcations generally have greater widths than returns (Figure 5.3). The majority of channels in the Macquarie Marshes are less than 1 m deep and the largest portion of the channels with depth between 1-3 m are in the Southern section (Figure 5.3). The only channels greater than 3 m deep were also in the Southern Macquarie Marshes. Channels with cross-sectional area less than 10 m2 dominate the whole Macquarie Marshes and the sub-systems, and few channels have cross-sectional area greater than 30 m2, although the majority of these larger channels occur in the Southern Macquarie Marshes (Figure 5.3).

5.4 System-wide hydraulic characteristics

Channel hydraulic factors including bankfull discharge and unit stream power were calculated for the transects upstream and downstream of each bifurcation and return node based on channel morphometrics. These estimates assume flow in a downstream direction at each site, and do not consider backwater effects. The findings show highly variable values for bankfull discharge in the whole system for transects at both bifurcation and return nodes (Table 5.2). The Southern Macquarie Marshes experiences a greater range and variability of bankfull discharge conditions while the Northern and Eastern Marshes have generally lower and less variable discharge with a more limited range of values. Average discharge in the Southern Macquarie Marshes is ~4 times greater than at bifurcations and returns in the Northern and Eastern Marshes (Table 5.2). Discharge at bifurcations tends to exceed discharge at returns in the Southern and Eastern Macquarie Marshes, while discharge at returns exceeds that at bifurcations in the Northern Marshes. Unit stream power behaves similarly to bankfull discharge at all system scales, with the highest and most variable values in the Southern Macquarie Marshes, and lowest values in the Eastern Marshes. Variation of unit stream power is more remarkable in bifurcation areas compared to return areas (Table 5.2).

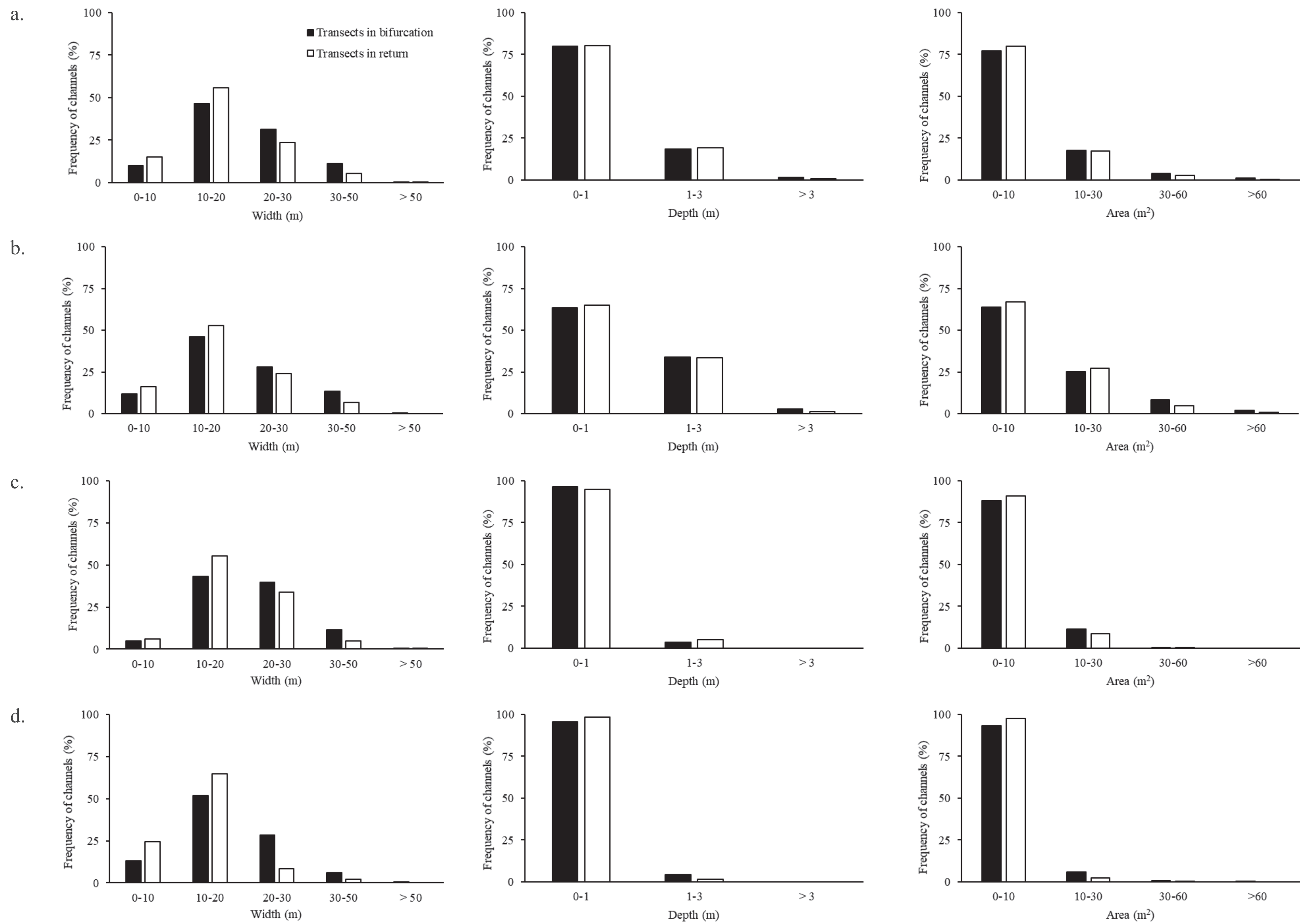

Figure 5.3 Frequency of channels with different bankfull width, bankfull depth and bankfull cross-sectional area in the whole Macquarie Marshes (row a), Southern Macquarie Marshes (row b), Northern Macquarie Marshes (row c) and Eastern Macquarie Marshes (row d).

Table 5.2 Hydraulic characteristics of the whole Macquarie Marshes and sub-systems.

	System scale	Whole Macquarie Mashes	Southern Macquarie Marshes	Northern Macquarie Marshes	Eastern Macquarie Marshes
Bifurcations	Bankfull discharge mean ± standard deviation (m^3/s)	5.4±11.2	8.8±14.7	2.1±2.6	2.1±4.5
	Bankfull discharge range (m^3/s)	0.002-132.5	0.002-132.5	0.004-20.2	0.01-81
	Unit stream power mean ± standard deviation (W/m^2)	0.8±1.4	1.2±1.8	0.4±0.6	0.3±0.4
	Unit stream power range (W/m^2)	0.0001-24	0.0009-24	0.0001-5	0.009-5.7
Returns	Bankfull discharge mean ± standard deviation (m^3/s)	4.7±9.9	7.5±12.9	1.9±2.8	1.2±2
	Bankfull discharge range (m^3/s)	0.002-124.6	0.002-124.6	0.003-39.2	0.005-17.5
	Unit stream power mean ± standard deviation (W/m^2)	0.9±1.7	1.3±2.2	0.4±0.7	0.2±0.2
	Unit stream power range (W/m^2)	0.0003-31.5	0.0001-31.5	0.0003-6.8	0.003-2.1

Hydrological results for all extracted transects show that bankfull discharge less than 5 m^3/s and unit stream power less than 1 W/m^2 are dominant hydrological characteristics in the whole system and its sub-systems (Figure 5.4). Greater discharge and unit stream power characterise the Southern Macquarie Marshes while the other two sections show only a few channels with relatively high discharge and unit stream power (Figure 5.4).

5.5 Overall effect of bifurcations and returns on channel capacity, discharge and stream power

Bifurcations and returns affect the morphometric and hydraulic characters of the river channels. Channels can increase or decrease after bifurcations and returns or they can be without change if parameters are within defined threshold. The LiDAR-derived DEM data has ±0.15 m vertical and ±0.45 m horizontal accuracy. Therefore, thresholds for change are identified for meaningful differences in channel bankfull width (0.45 m), bankfull depth, (0.15 m), cross-sectional area (0.07 m^2), bankfull discharge (0.02 m^3/s) and unit stream power (0.04 W/m^2). This means that if the net change in channel width, depth, cross-sectional area, discharge or unit stream power at a bifurcation or return falls below these thresholds, then no change can be ascribed at that point in the system.

The results show that channels are more likely to increase in bankfull width, depth and cross-sectional area after bifurcations, and to decrease in these metrics after returns, in the whole system and its sub-systems (Figure 5.5). Fewer changes in depth occur at bifurcations and returns as opposed to changes in width and cross-sectional area. Changes in bankfull discharge at bifurcations and returns are less pronounced in the whole system and sub-systems (Figure 5.6). However, unit stream power tends to increase after bifurcations and decreases after returns across the system. Fewer channels decrease in stream power at returns in the Northern Marshes, where outflow is generally more stable, compared to the other sections (Figure 5.6).

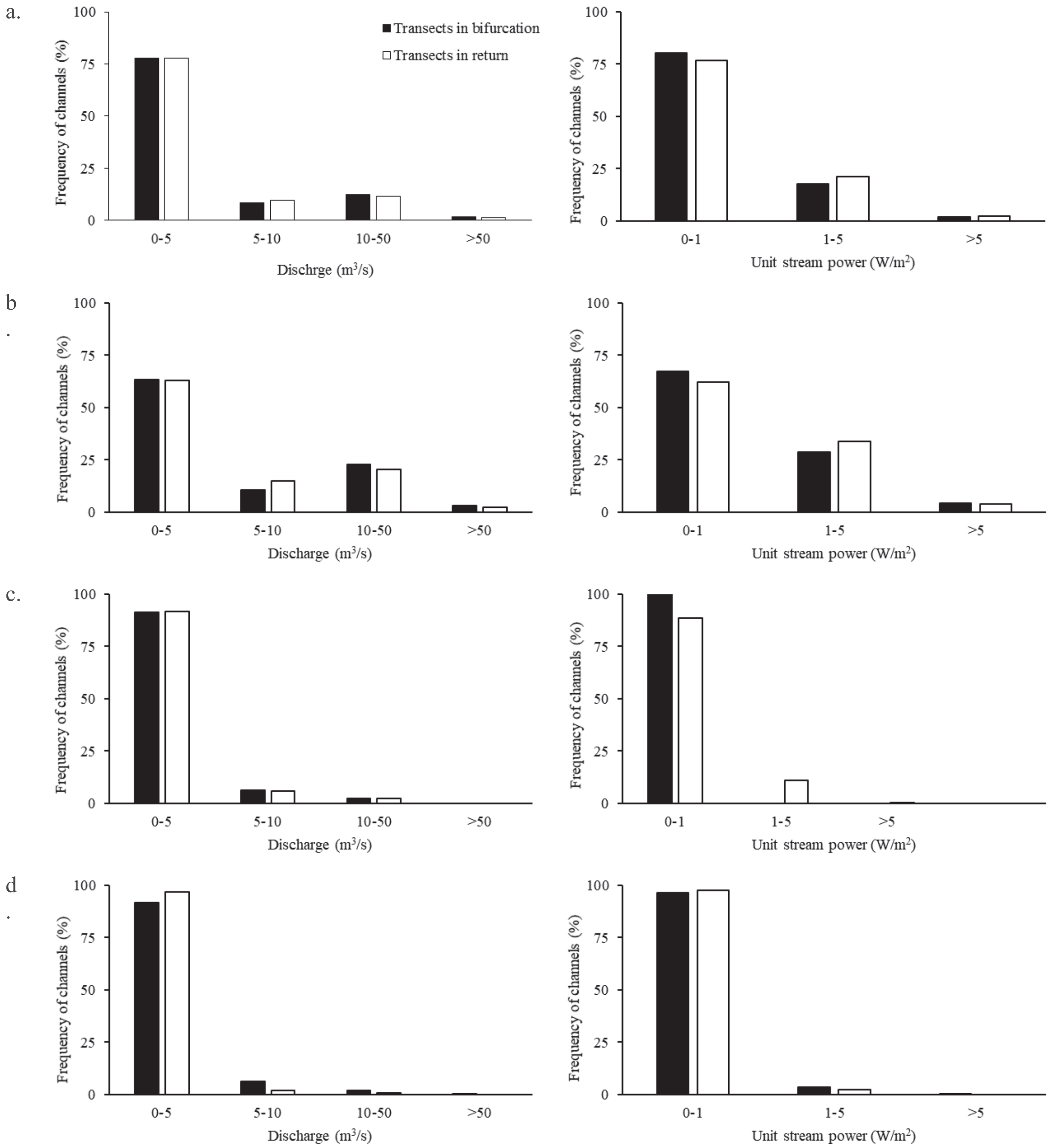

Figure 5.4 Frequency of channels with different bankfull discharge and unit stream power in the whole Macquarie Marshes (row a), Southern Macquarie Marshes (row b), Northern Macquarie Marshes (row c) and Eastern Macquarie Marshes (row d).

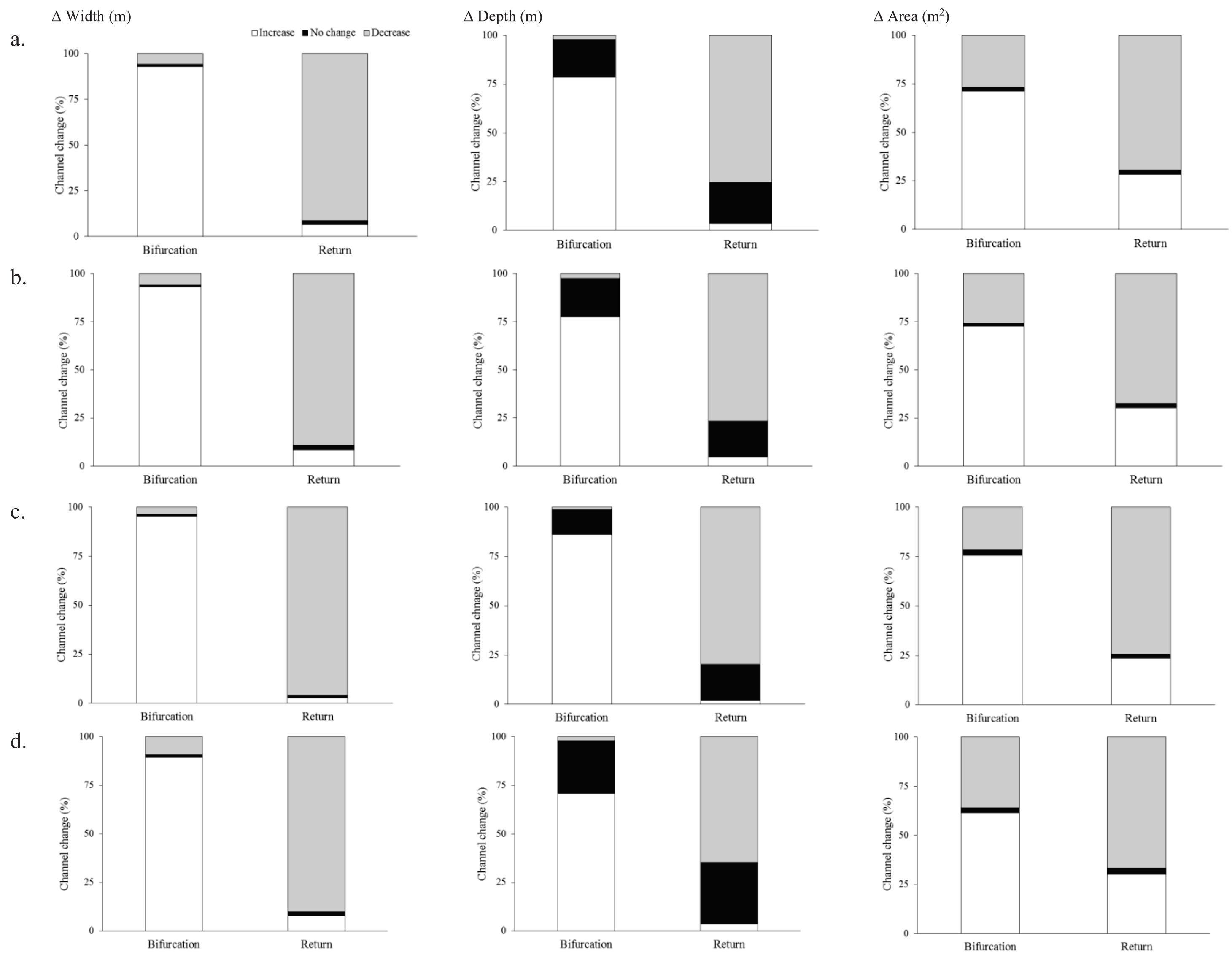

Figure 5.5 Percentage of channel morphometric changes affected by bifurcations and returns in the whole Macquarie Marshes (row a), Southern Macquarie Marshes (row b), Northern Macquarie Marshes (row c) and Eastern Macquarie Marshes (row d).

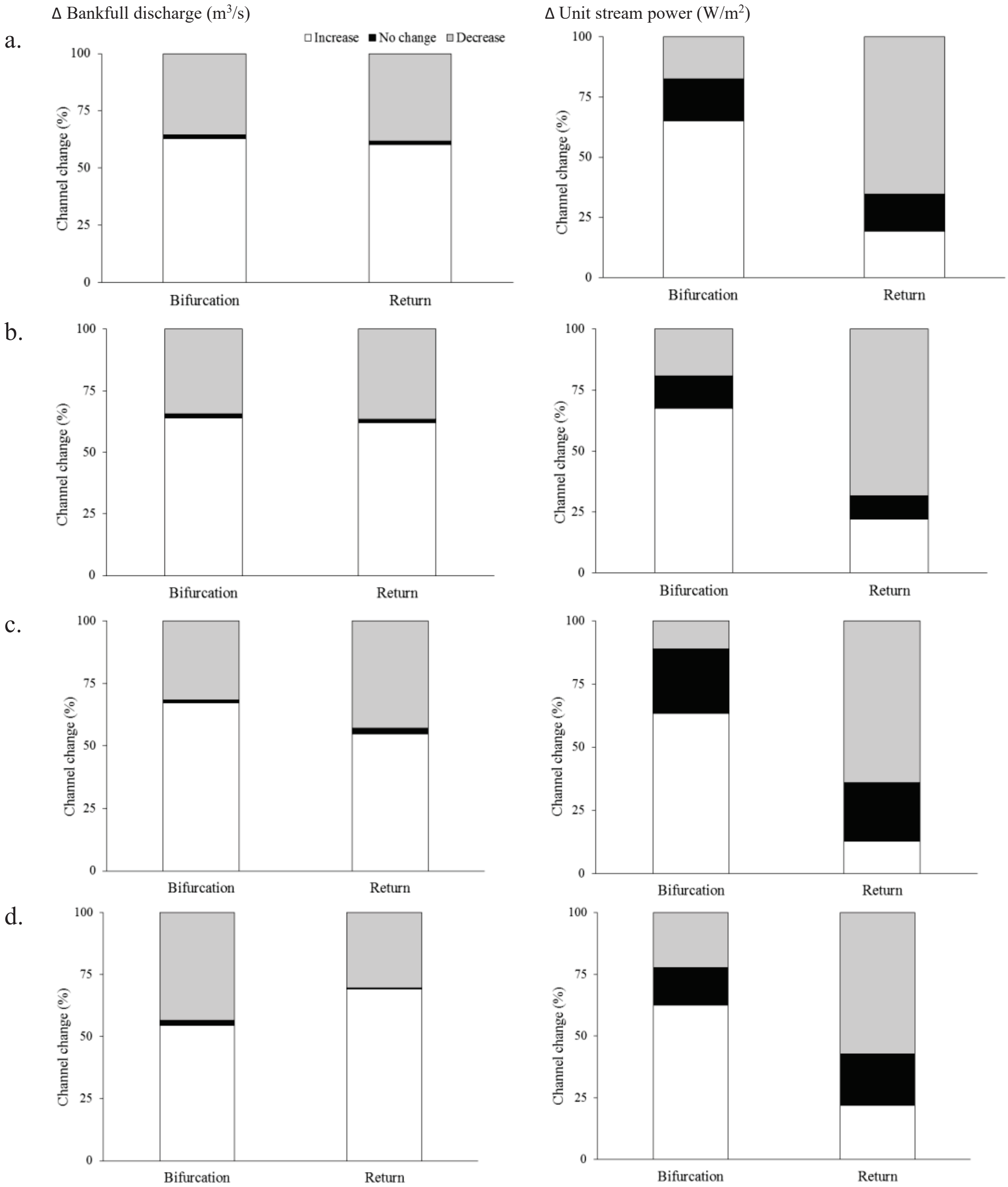

Figure 5.6 Channel hydraulic changes affected by bifurcations and returns in the whole Macquarie Marshes (row a), Southern Macquarie Marshes (row b), Northern Macquarie Marshes (row c) and Eastern Macquarie Marshes (row d).

5.6 River- and reach-scale downstream effects of bifurcations and returns

In this section, a series of morphometric and hydraulic parameters are compared downstream for sixteen main river channels in the Macquarie Marshes. Downstream analysis reflects the role of the distributary and tributary flows that affect channel hydraulic and geomorphological character leading to changes in channel capacity which may be inferred as being related to equilibrium (i.e. channel maintenance) or non-equilibrium (i.e. channel decline and/or termination) conditions.

The Macquarie River enters the Southern Macquarie Marshes and Back Swamp and Bulgeraga Creek break from its right (eastern) bank, flowing to the north (Figure 5.7a). Oxley Break links the Macquarie River to Bulgeraga Creek further to the east upstream of Monkey Creek and Buckiinguy Creek, which diverge from the right and left banks of the Macquarie River, respectively. The Macquarie River then breaks down to form Monkeygar Creek and its wetlands, as well as the Old Macquarie River. The Breakaway diverges form the left bank of Monkeygar Creek and joins to the Old Macquarie River which continues to another reach of the Macquarie River further downstream. Monkeygar Creek continues into Willancorah Swamp, where it breaks down into a non-channelized wetland, before eventually remerging to join Bulgeraga Creek downstream. The Macquarie River downstream of the Old Macquarie feeds into Mole Marsh which reconnects to another section of the Macquarie River near the confluence of Monkeygar Creek and Bulgeraga Creek.

The Macquarie River continues in the Northern Macquarie Marshes past Pillicawarrina until it dissipates in the extensive reed bed, while Bora Creek diverges from the left side of the Macquarie River and eventually re-joins branches of the Macquarie River downstream of the reed bed. In the northern part of this section, multiple channels converge and lead out of the Northern Macquarie Marshes (Figure 5.7b).

Gum Cowal leaves the Macquarie River near Marebone weir upstream of the Southern Macquarie Marshes, and feeds into Gum Cowal, Terrigal Creek, and Long Plain Cowal in the Eastern Marshes. Water from Gum Cowal-Terrigal Creek system feed to the north and join Marthaguy Creek, while Long Plain Cowal is a palaeochannel that is occasionally inundated and flows toward the Northern Marshes (Figure 5.7c).

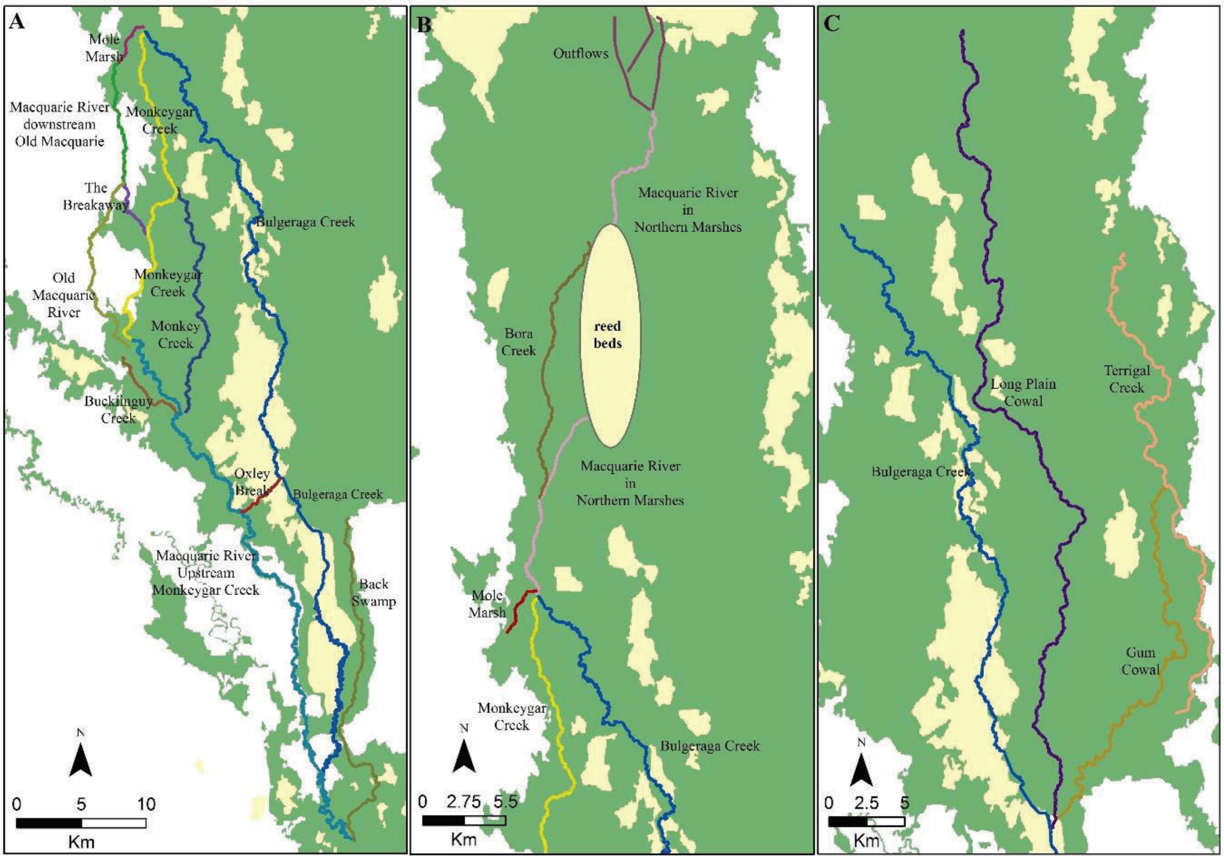

Figure 5.7 River channels studied in the Southern Macquarie Marshes (A), Northern Macquarie Marshes (B) and Eastern Macquarie Marshes (C). Distances downstream referred to in subsequent sections and figures stem from the polylines (coloured differently) for each of the channels shown in this figure.

5.6.1 Southern Macquarie Marshes

5.6.1.1 Macquarie River upstream Monkeygar

Channel bifurcations exceed returns along the Macquarie River upstream of Monkeygar Creek (bifurcation:return ratio greater than 1), although at ~25 km downstream a cluster of returns occur which causes the bifurcation:return ratio become closer to 1 (Figures 5.8a and 5.8b). Bifurcations and returns tend to occur in clusters with long distances in between in the upper and middle reaches, with exceptions occurring between 20 and 30 km and ~60 km where the nodes occur closer together. However, the number of bifurcations and returns increase markedly in the lower reach, from ~75 km downstream, as the channel enters a major anastomosing reach and then enters the wetlands of the Southern Macquarie Marshes Nature Reserve (Figure 5.8a). Channel bankfull width, bankfull depth and bankfull cross-sectional area are highly variable, but decrease slightly downstream and there are noticeable local declines in all three parameters at ~25.5 km, ~40 km and after ~75 km downstream (Figures 5.8c, 5.8d and 5.8f). Width:depth ratio is fairly constant along the whole reach except for the end of the reach with a variable pattern (Figure 5.8e). Discharge and unit stream power follow the same downstream trends as channel width, depth and area, and both are lower where the channel becomes smaller (Figures 5.8g and 5.8h). There are significant positive correlations between channel width and depth, width and discharge, width and unit stream power and depth and area, and significant negative correlation between width:depth ratio and unit stream power for the Macquarie River upstream of Monkeygar Creek (Appendix 2; Figure A2.1).

5.6.1.2 Buckiinguy Creek

Channel bifurcations exceed returns along the length of Buckiinguy Creek (bifurcation:return ratio greater than 1), until the channel terminates in the reed beds of Buckiinguy Swamp (Figures 5.9a and 5.9b). Three returns occur in the middle reach, causing the bifurcation:return ratio to approach 1, and then a cluster of returns occur downstream of the reed beds where outflowing channels converge to create the Buckiinguy Return, which feeds water back into the Macquarie River (Figure 5.9a). Channel bankfull width, bankfull depth and bankfull cross-sectional area decrease downstream along Buckiinguy Creek until the channel enters the dense wetlands, and then all these metrics markedly increase downstream of the reeds at the Buckiinguy Return (Figures 5.9c, 5.9d and 5.9f). Width:depth ratio increases downstream until the channel terminates and decreases sharply after Buckiinguy Swamp where the returns occur (Figure 5.9e). Discharge and unit stream power follow the same downstream declining trends as channel width, depth and area, and are generally lower where the channel is smaller, until they too sharply increase at the outflowing return channels (Figure 5.9g and 5.9h). There are significant positive correlations between channel width and area and depth and area, and significant negative correlation between width:depth ratio and unit stream power for Buckiinguy Creek (Appendix 2; Figure A2.2).

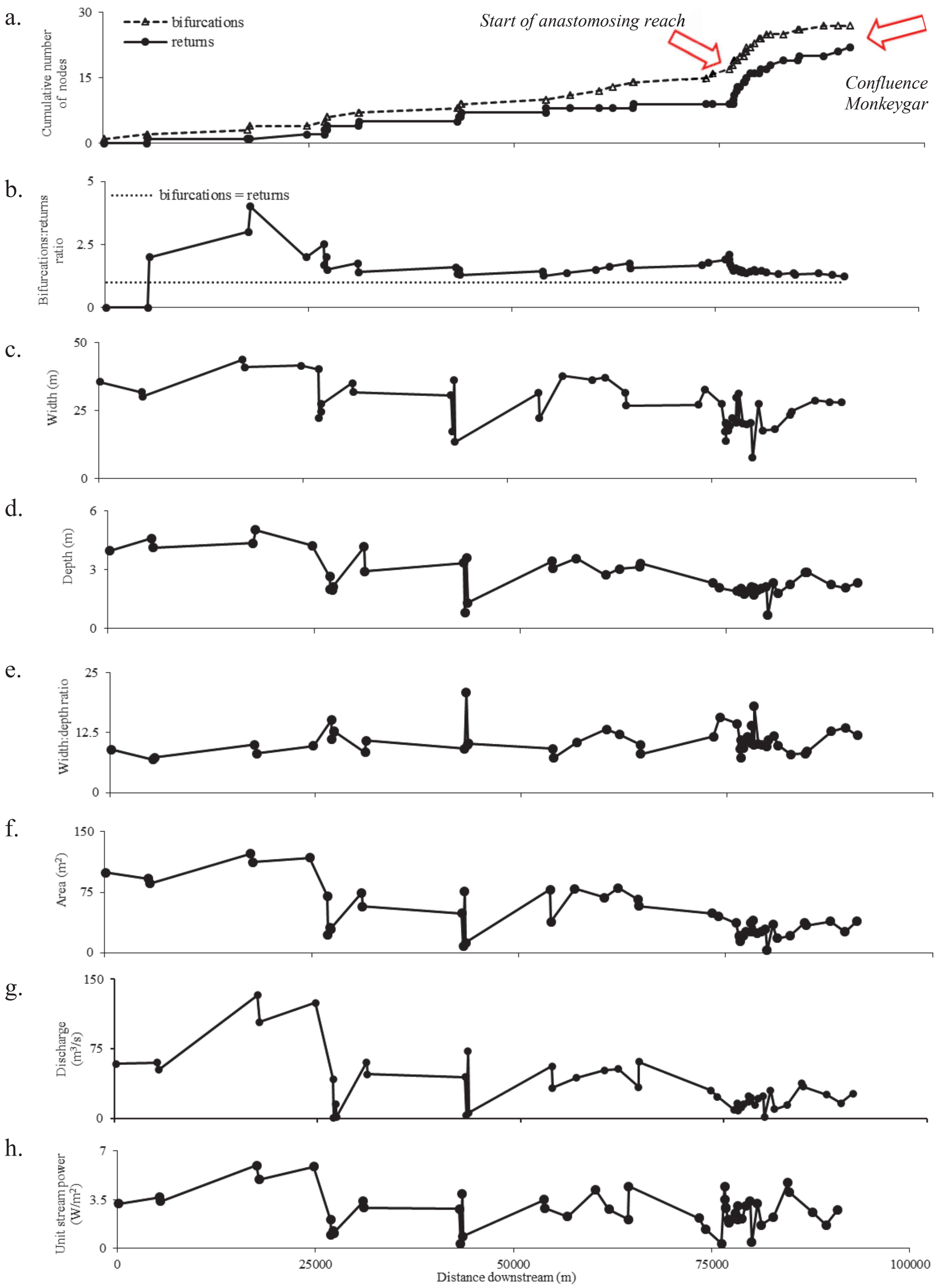

Figure 5.8 Downstream trends along the Macquarie River upstream Monkeygar Creek for the distribution of bifurcation and return nodes (a), bifurcation:return ratio (b), channel bankfull width (c), channel bankfull depth (d), channel width:depth ratio (e), channel bankfull cross-sectional area (f), bankfull discharge (g) and unit stream power (h). Distance downstream on the X-axis is derived from the start of the polyline for this channel, shown in Figure 5.7.

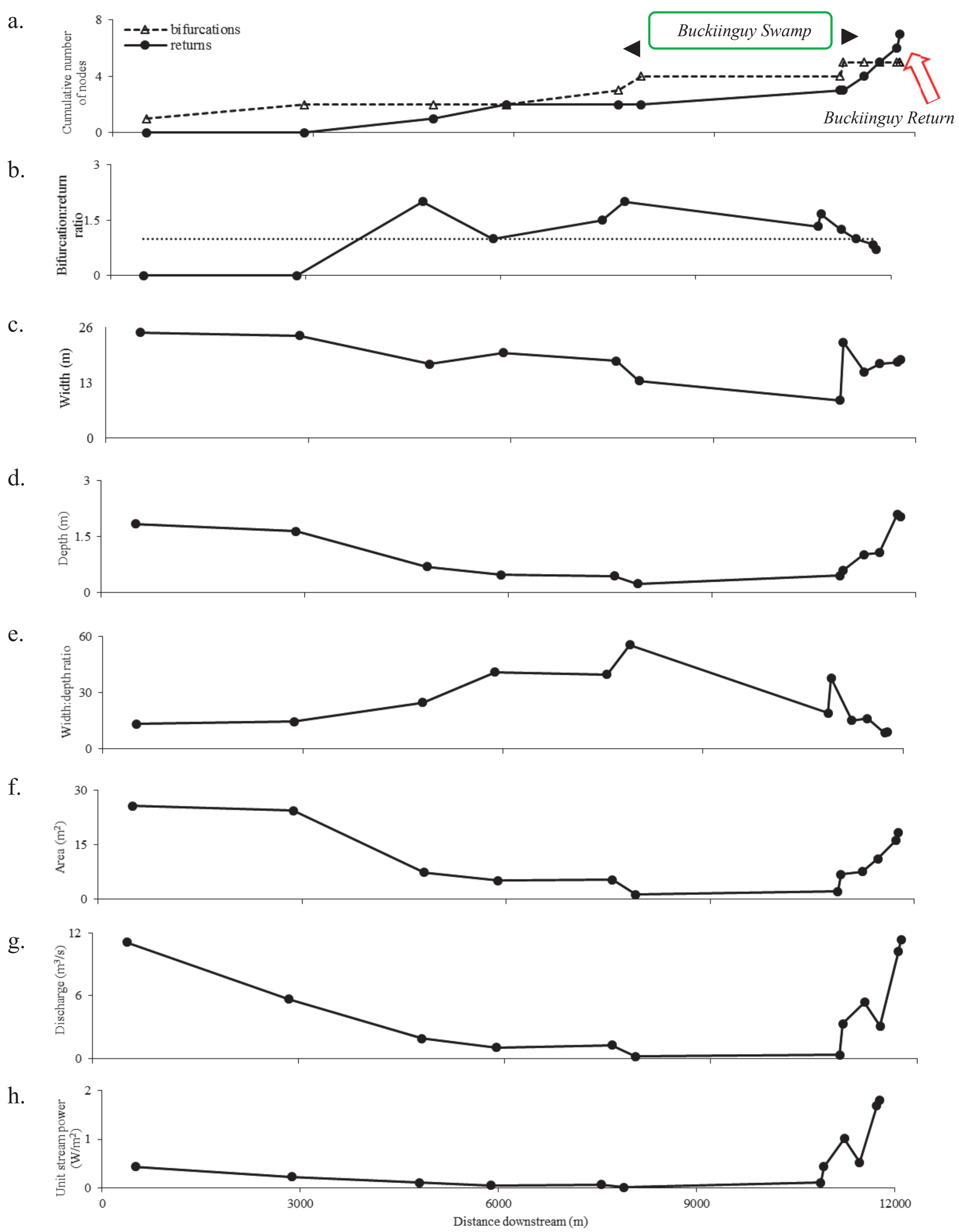

Figure 5.9 Downstream trends along Buckiinguy Creek for the distribution of bifurcation and return nodes (a), bifurcation:return ratio (b), channel bankfull width (c), channel bankfull depth (d), channel width:depth ratio (e), channel bankfull cross-sectional area (f), bankfull discharge (g) and unit stream power (h). The symbol ◀ represents a point of channel termination, and the symbol ▶ represents a point of channel reformation. Distance downstream on the X-axis is derived from the start of the polyline for this channel, shown in Figure 5.7.

5.6.1.3 Old Macquarie River

Channel bifurcations initially exceed returns along the Old Macquarie River, until ~4.5 km downstream where a cluster of returns occur which causes the bifurcation:return ratio to drop below 1 (Figure 5.10a and 5.10b). Bifurcations occur throughout the middle reach, however two large clusters of returns increase occur ~9 km and ~18 km downstream, as the channel nears and then is joined by The Breakaway in the Southern Macquarie Marshes (Figures 5.10a and 5.10b). Channel bankfull width, bankfull depth and bankfull cross-sectional area are highly variable, but decrease slightly downstream and there are noticeable local variations in the pattern in between ~10 to ~15 km downstream (Figures 5.10c, 5.10d and 5.10f). Width:depth ratio is fairly constant along the whole reach with a slight decline to the middle reaches and a slight increase in the second half of the reach (Figure 5.10e). Discharge and unit stream power follow the same downstream trends as channel width, depth and area, and both are lower where the channel becomes smaller, and show nan increase where channel area is larger around 13 km downstream (Figures 5.10g and 5.10h). There are significant positive correlations between channel width and depth, width and area, width and discharge, width and unit stream power and depth and area, and significant negative correlation between width:depth ratio and unit stream power for the Old Macquarie River (Appendix 2; Figure A2.3).

5.6.1.4 Macquarie River downstream of the Old Macquarie River

Channel returns exceed bifurcations along the Macquarie River downstream of the Old Macquarie River (bifurcation:return ratio less than 1), except for ~1 km downstream where a cluster of bifurcations occur which causes the bifurcation:return ratio exceed 1 briefly (Figures 5.11a and 5.11b). Bifurcations and returns tend to occur in clusters with long distances in the middle reach, and in closer distances in upper and lower reach which causes the bifurcation:return ratio become closer to 1 (Figures 5.11a and 5.11b). However, the number of returns increase markedly in the lower reach, from ~11.5 km downstream, as the channel nears and then enters the Mole Marsh in the Southern Macquarie Marshes (Figure 5.11a). Channel bankfull width and bankfull cross-sectional area are variable, they increase slightly in the upper and middle reaches and decrease slightly downstream at the lower reaches (Figures 5.11c and 5.11f). Channel bankfull depth is also variable, it increases slightly for ~3 km with local noticeable decline at ~2 km and then decreases slightly downstream through the middle and lower reaches (Figure 5.11d). Width:depth ratio is fairly constant along the upper and middle reaches, except for the local increase at ~2 km, and then increases in the lower reach (Figure 5.11e). Discharge and unit stream power follow the same downstream trends as channel width, depth and area, and both are lower where the channel becomes smaller, declining into the wetlands of Mole Marsh (Figures 5.11g and 5.11h). There are significant positive correlations between channel width and depth, width and area, width and discharge, width and unit stream power and depth and area for the Macquarie River downstream of the Old Macquarie River (Appendix 2; Figure A2.4).

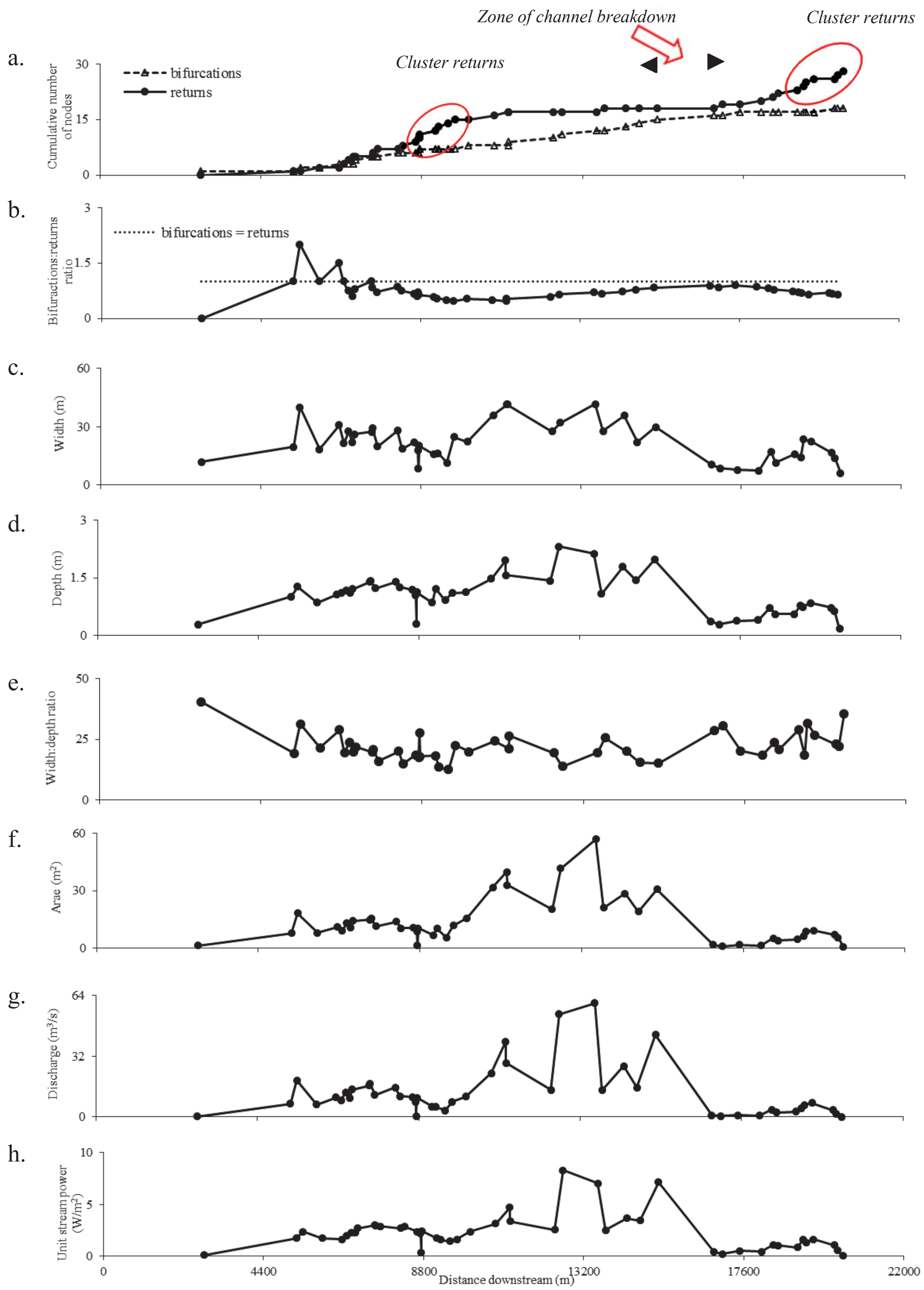

Figure 5.10 Downstream trends along the Old Macquarie River for the distribution of bifurcation and return nodes (a), bifurcation:return ratio (b), channel bankfull width (c), channel bankfull depth (d), channel width:depth ratio (e), channel bankfull cross-sectional area (f), bankfull discharge (g) and unit stream power (h). The symbol ◀ represents a point of channel termination, and the symbol ▶ represents a point of channel reformation. Distance downstream on the X-axis is derived from the start of the polyline for this channel, shown in Figure 5.7.

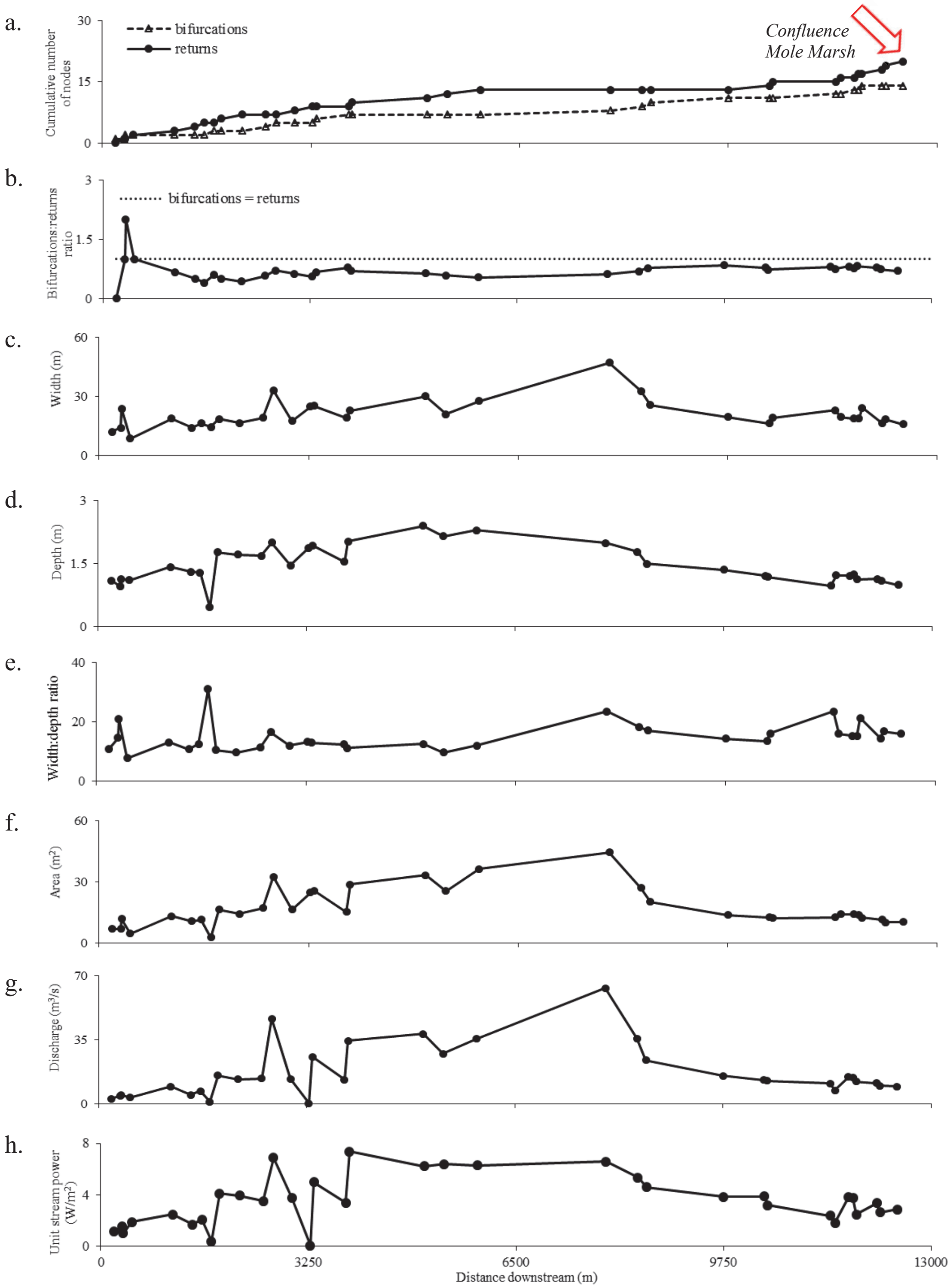

Figure 5.11 Downstream trends along the Macquarie River downstream of the Old Macquarie River for the distribution of bifurcation and return nodes (a), bifurcation:return ratio (b), channel bankfull width (c), channel bankfull depth (d), channel width:depth ratio (e), channel bankfull cross-sectional area (f), bankfull discharge (g) and unit stream power (h). Distance downstream on the X-axis is derived from the start of the polyline for this channel, shown in Figure 5.7.

5.6.1.5 Mole Marsh

Channel bifurcations initially exceed returns along the Mole Marsh, until ~800 m downstream where bifurcations stay constant and a cluster of returns occur which causes the bifurcation:return ratio drop below 1 (Figures 5.12a and 5.12b). Returns are evenly spaced in the middle and lower reaches, with exceptions occurring between 2.6 and 2.8 km where channels enter the wetland, before the channel joins Monkeygar Creek and Bulgeraga Creek downstream, heading to the Macquarie River in the Northern Marshes (Figure 5.11a). Channel bankfull width, bankfull depth and bankfull cross-sectional area are highly variable, in particular cross-sectional area, but decrease slightly downstream, and there are noticeable local declines in width and depth at ~200 m downstream (Figures 5.12c, 5.12d and 5.12f). Channel bankfull width and cross-sectional area increase before entering the wetland and bankfull depth increases after that at the lower reach (Figures 5.12c and 5.12d). Width:depth ratio is fairly constant along the whole reach except for the middle of the reach where it increases slightly (Figure 5.12e). Discharge and unit stream power follow the same downstream trends as channel area, and both are lower where the channel becomes smaller (Figures 5.12g and 5.12h). There are significant positive correlations between channel width and area, width and discharge, and depth and area for Mole Marsh (Appendix 2; Figure A2.5).

5.6.1.6 The Breakaway

Channel bifurcations initially exceed returns along The Breakaway, until ~4 km downstream where a cluster of returns occur which causes the bifurcation:return ratio to drop below 1 (Figures 5.13a and 5.13b). Bifurcations and returns tend to be evenly spaced, with longer distances between each node in the lower reach. However, the number of bifurcations and returns increase as the channel joins the Old Macquarie River downstream (Figure 5.13a). Channel bankfull width, bankfull depth and bankfull cross-sectional area are fairly constant, but decrease slightly downstream and there are noticeable local increase in width and area at ~4.2 km downstream, and local decline for all parameters at the end of the reach (Figures 5.13c, 5.13d and 5.13f). Width:depth ratio is fairly constant along the whole reach with more variation from ~4.2 km (Figure 5.13e). Discharge and unit stream power follow the same downstream trends as channel width, and both are lower where the channel becomes smaller (Figures 5.13g and 5.13h). There are significant positive correlations between channel width and area and depth and area for The Breakaway (Appendix 2; Figure A2.6).

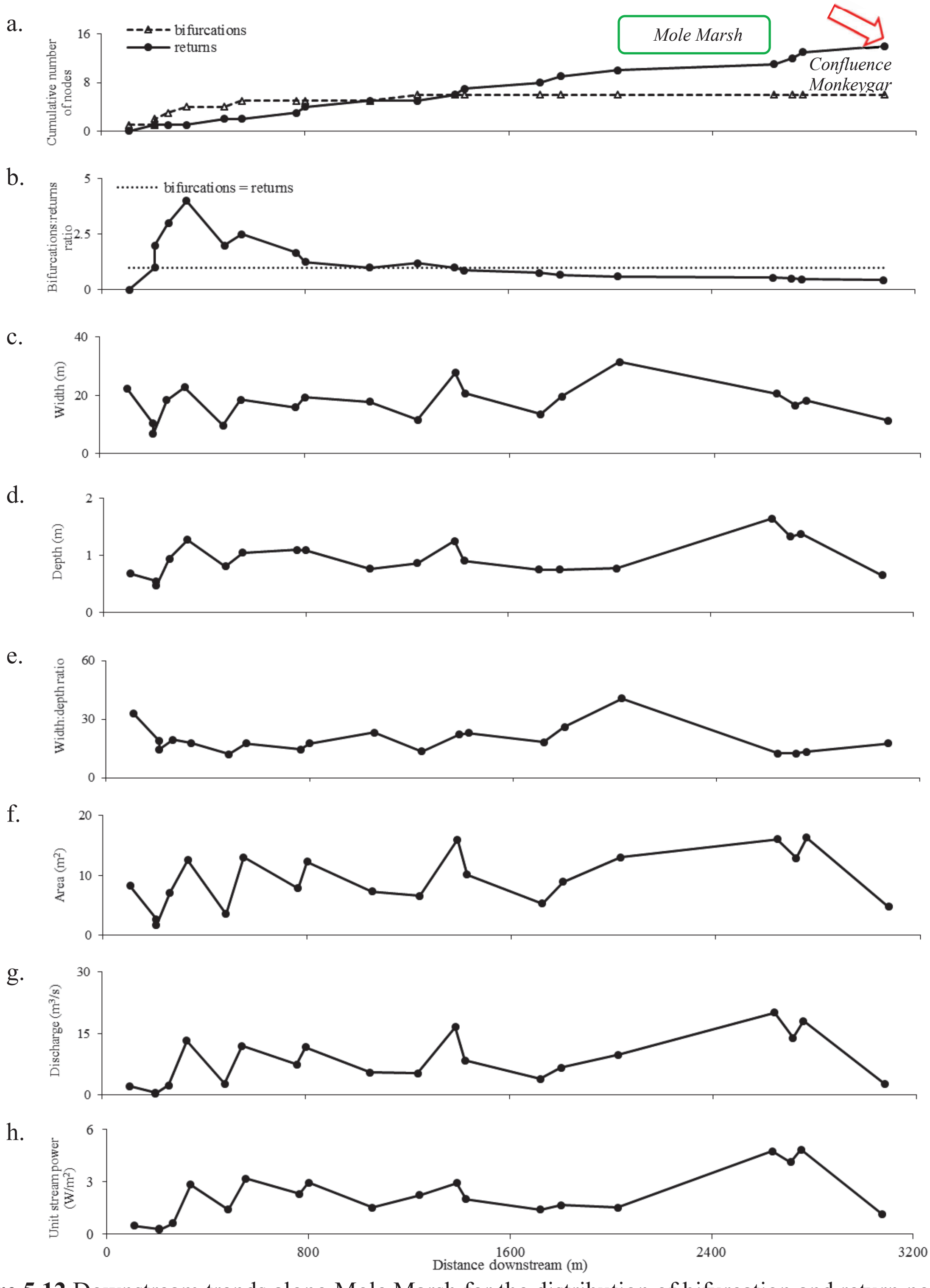

Figure 5.12 Downstream trends along Mole Marsh for the distribution of bifurcation and return nodes (a), bifurcation:return ratio (b), channel bankfull width (c), channel bankfull depth (d), channel width:depth ratio (e), channel bankfull cross-sectional area (f), bankfull discharge (g) and unit stream power (h). Distance downstream on the X-axis is derived from the start of the polyline for this channel, shown in Figure 5.7.

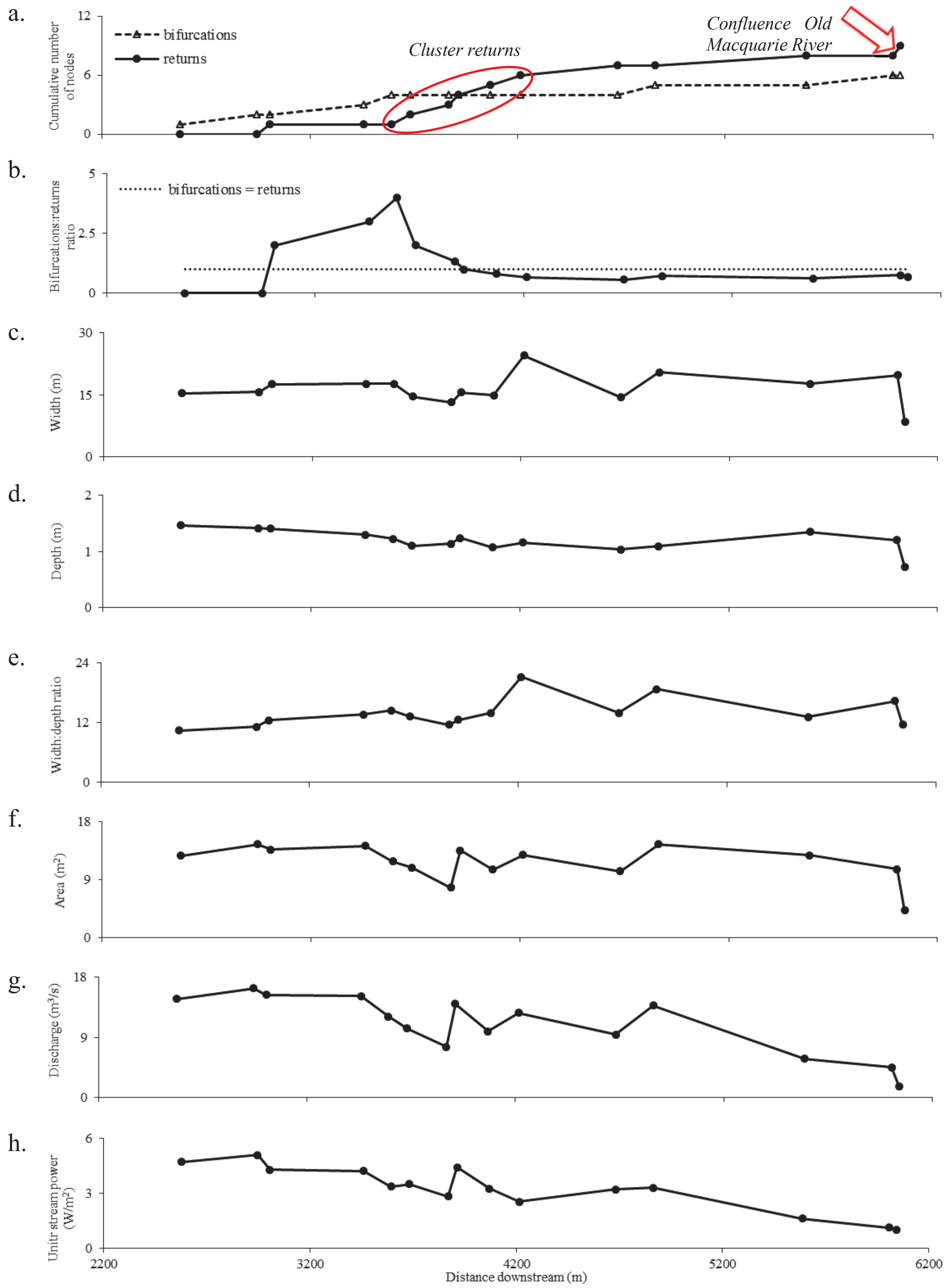

Figure 5.13 Downstream trends along The Breakaway for the distribution of bifurcation and return nodes (a), bifurcation:return ratio (b), channel bankfull width (c), channel bankfull depth (d), channel width:depth ratio (e), channel bankfull cross-sectional area (f), bankfull discharge (g) and unit stream power (h). Distance downstream on the X-axis is derived from the start of the polyline for this channel, shown in Figure 5.7.

5.6.1.7 Monkeygar Creek

Channel bifurcations initially exceed returns along Monkeygar Creek, until a cluster of returns occur which causes the bifurcation:return ratio become closer to 1 at ~7 km downstream (Figures 5.14a and 5.14b). Bifurcations and returns occur in clusters with close distances in between in the upper and middle reaches, with exceptions occurring between ~8.5 and ~15.5 km where the nodes occur in longer distances from each other. However, the number of bifurcations and returns increase markedly in the middle reach, from ~16 km downstream, as the channel nears and then enters the reed beds (Figure 5.14a). Channel returns and bifurcation again occur after reed beds and returns exceed along the lower reach of the Monkeygar Creek with the bifurcation:return ratio is less than 1 (Figures 5.14a and 5.14b). Channel bankfull width, bankfull depth and bankfull cross-sectional area are highly variable in upper and middle reaches, but decrease downstream, while width is more variable in the middle reach and all parameters are more stable in the lower reach (Figures 5.14c, 5.14d and 5.14f). Width:depth ratio is fairly constant in the upper and lower reaches and higher and more highly variable in the middle reach (Figure 5.14e). Discharge and unit stream power follow the same downstream trends as channel depth both are lower where the channel becomes smaller, declining downstream overall (Figures 5.14g and 5.14h). There are significant positive correlations between channel width and depth, width and area, width and discharge, width and unit stream power and depth and area, and significant negative correlation between width:depth ratio and unit stream power for Monkeygar Creek (Appendix 2; Figure A2.7).

5.6.1.8 Monkey Creek

Channel bifurcations exceed returns along the Monkey Creek, until ~6 km downstream where a cluster of returns occur which causes the bifurcation:return ratio become closer to 1, and then more returns ~20 km downstream cause the bifurcation:return ratio to drop below 1 (Figures 5.15a and 5.15b). Bifurcations and returns occur in clusters (~5, 10, 17 and 25 km) with long distances in between in the upper and middle reaches. However, the number of bifurcations and returns increase markedly in the lower reach, from ~23 km downstream, as the channel joins Monkeygar Creek in the Southern Macquarie Marshes (Figure 5.15a). Channel bankfull width, bankfull depth and bankfull cross-sectional area are variable, but decrease slightly downstream, and there are noticeable local jumps in all three parameters at ~3.5 km, ~10 km downstream and a highly variable pattern in the lower reach (Figures 5.15c, 5.15d and 5.15f). Width:depth ratio is fairly constant along the whole reach except for sudden jump where the channel becomes narrower and shallower ~15 km downstream (Figure 5.15e). Discharge and unit stream power follow the same downstream trends as channel width, depth and area, and both are lower where the channel becomes smaller (Figures 5.15g and 5.15h). There are significant positive correlations between channel width and area, width and discharge and depth and area, and significant negative correlation between width:depth ratio and unit stream power for Monkey Creek (Appendix 2; Figure A2.8).

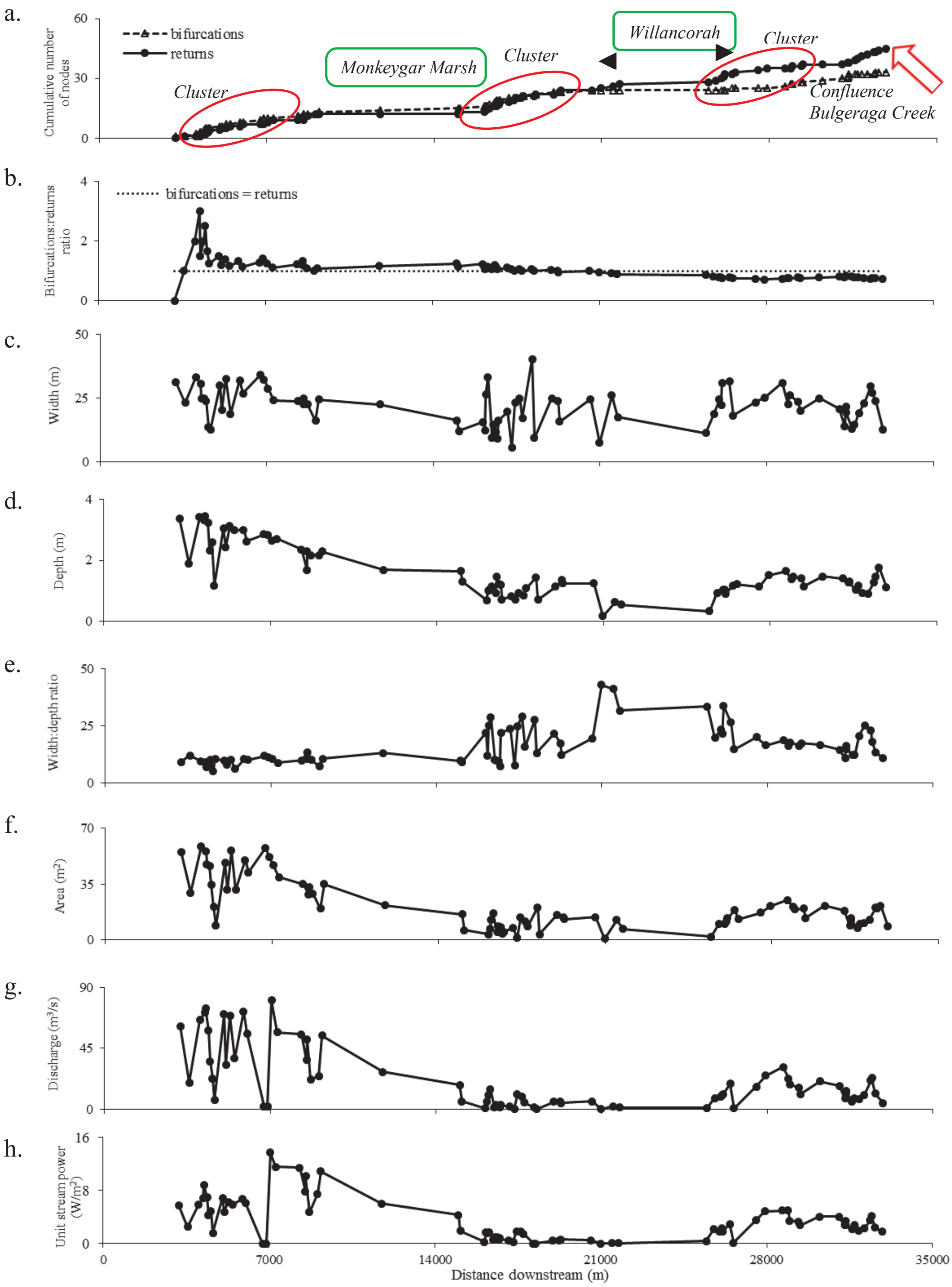

Figure 5.14 Downstream trends along Monkeygar Creek for the distribution of bifurcation and return nodes (a), bifurcation:return ratio (b), channel bankfull width (c), channel bankfull depth (d), channel width:depth ratio (e), channel bankfull cross-sectional area (f), bankfull discharge (g) and unit stream power (h). The symbol ◀ represents a point of channel termination, and the symbol ▶ represents a point of channel reformation. Distance downstream on the X-axis is derived from the start of the polyline for this channel, shown in Figure 5.7.

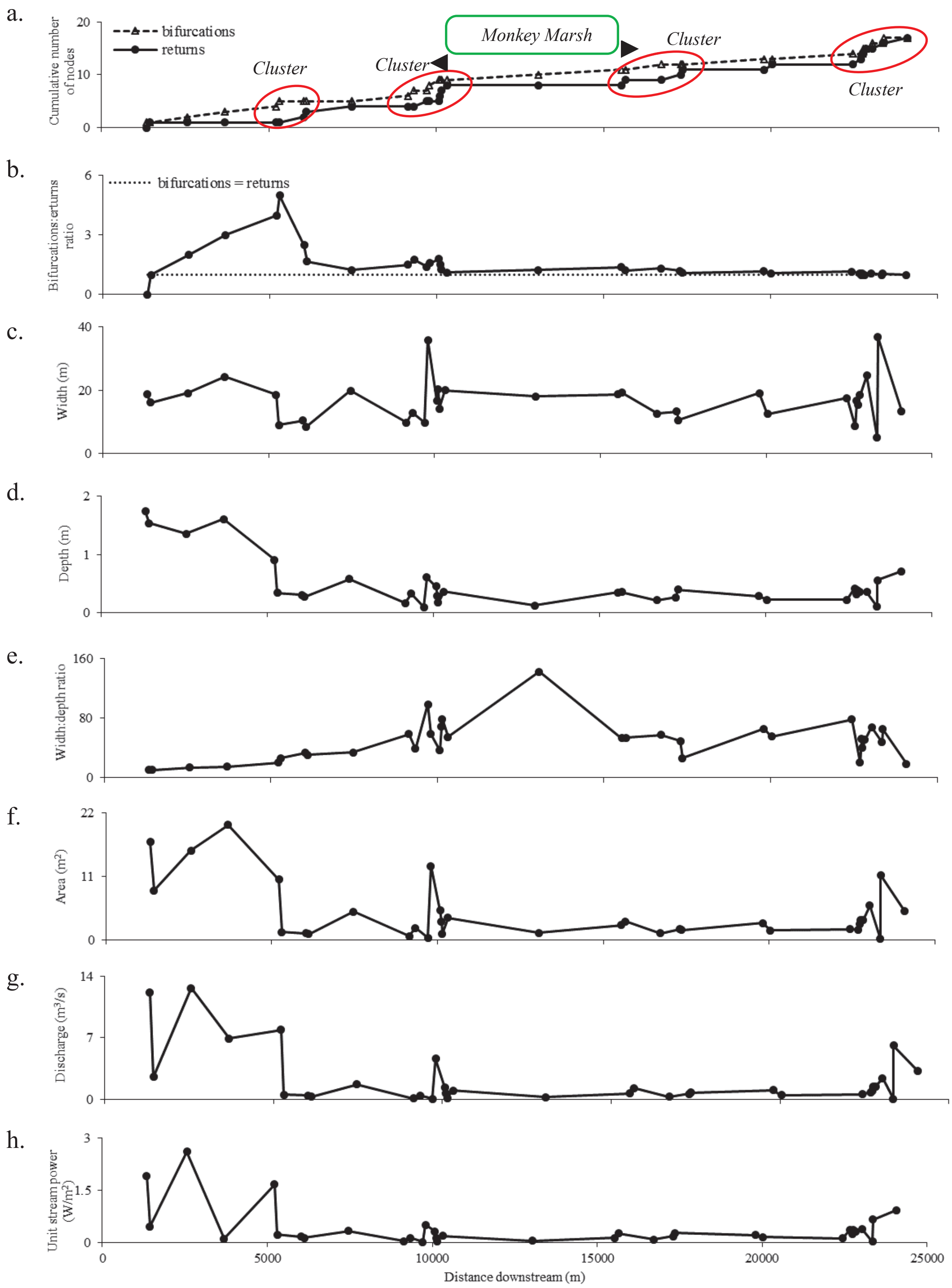

Figure 5.15 Downstream trends along Monkey Creek for the distribution of bifurcation and return nodes (a), bifurcation:return ratio (b), channel bankfull width (c), channel bankfull depth (d), channel width:depth ratio (e), channel bankfull cross-sectional area (f), bankfull discharge (g) and unit stream power (h). Distance downstream on the X-axis is derived from the start of the polyline for this channel, shown in Figure 5.7.

5.6.1.9 Oxley Break

Channel returns exceed bifurcations along the whole of the Oxley Break and bifurcation:return ratio is under 1 for the whole reach, and close to 1 when bifurcations and returns increase in number markedly between 3 and 3.5 km downstream (Figures 5.16a and 5.16b). Bifurcations and returns tend to occur in a cluster ~3.5 km downstream but are otherwise evenly spaced. The number of returns increase in lower reach while bifurcations are fairly constant (Figure 5.16a). Channel bankfull width, bankfull depth and bankfull cross-sectional are variable, but become more so at ~3.5 km in the middle reach (Figures 5.16c, 5.16d and 5.16f). Channel width does increase slightly downstream, while depth decreases (Figures 5.16c and 5.16d). Width:depth ratio is increases slightly along the whole channel and is most variable in the middle reach (Figure 5.16e). Discharge and unit stream power follow the same downstream trends as channel area, and both are lower where the channel becomes smaller (Figures 5.8g and 5.8h). There are significant positive correlations between channel width and area, width and discharge and depth and area, and significant negative correlation between width:depth ratio and unit stream power for Oxley Break (Appendix 2; Figure A2.9).

5.6.1.10 Bulgeraga Creek

Channel bifurcations initially exceed returns along Bulgeraga Creek, until ~65 km downstream where a cluster of returns occur which causes the bifurcation:return ratio become closer to 1 and remains less than 1 along the rest of the reach (Figures 5.17a and 5.17b). Bifurcations and returns occur with long distances between them in the upper reach, however, the number of bifurcations and returns increase markedly in the middle and lower reach, as the channel joins Monkeygar Creek and Mole Marsh heading to the Northern Marshes (Figure 5.17a). Channel bankfull width, bankfull depth and bankfull cross-sectional area are highly variable, particularly in the middle reach, but decrease slightly downstream (Figures 5.17c, 5.17d and 5.17f). Width:depth ratio is fairly constant along the upper reach and highly variable for the rest of the channel (Figure 5.17e). Discharge and unit stream power are also highly variable, but generally follow the same trends as channel width, depth and area, and both are lower where the channel becomes smaller (Figures 5.17g and 5.17h). There are significant positive correlations between channel width and depth, width and area, width and discharge, depth and area, and significant negative correlation between width:depth ratio and unit stream power for Bulgeraga Creek (Appendix 2; Figure A2.10).

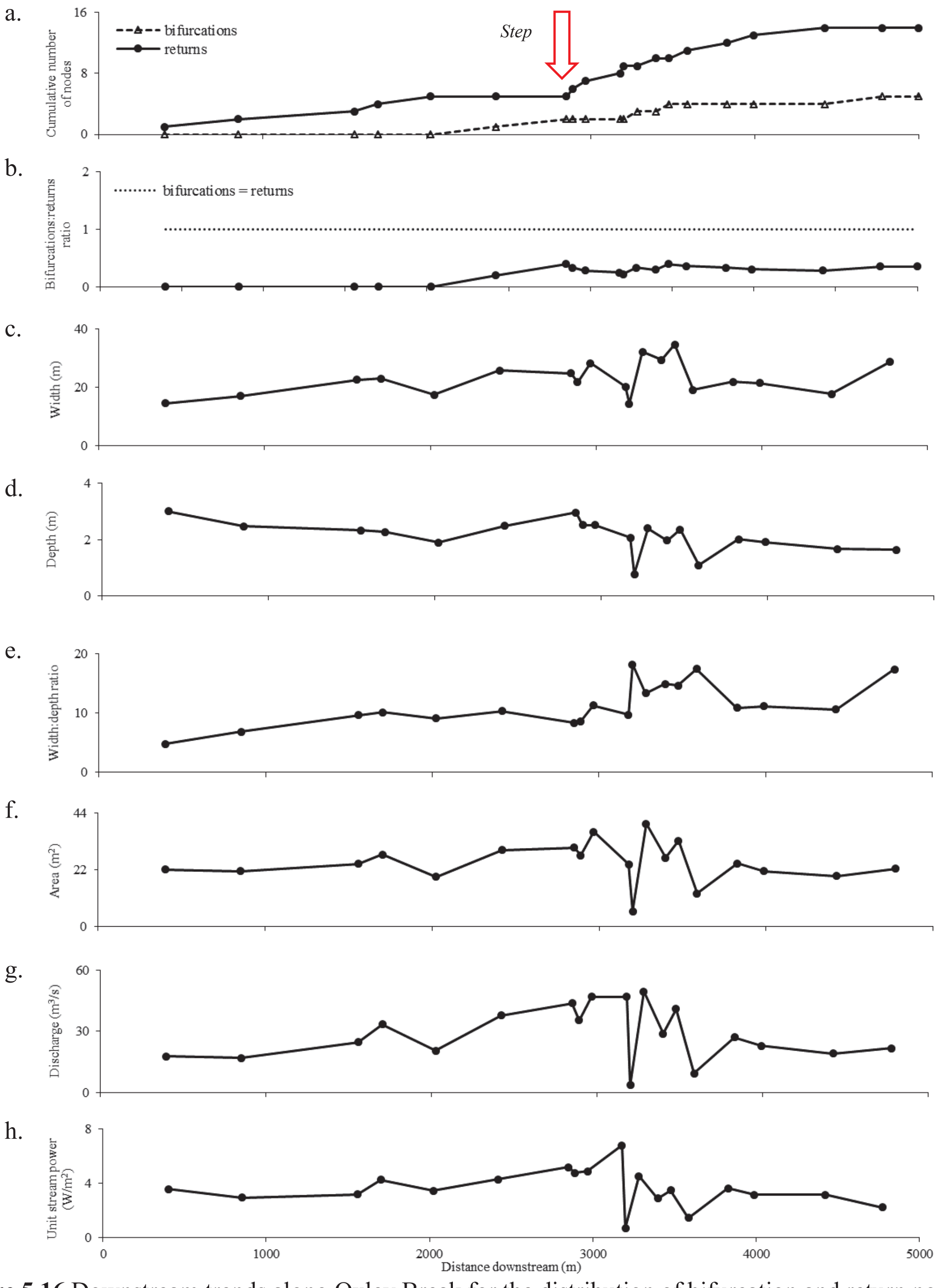

Figure 5.16 Downstream trends along Oxley Break for the distribution of bifurcation and return nodes (a), bifurcation:return ratio (b), channel bankfull width (c), channel bankfull depth (d), channel width:depth ratio (e), channel bankfull cross-sectional area (f), bankfull discharge (g) and unit stream power (h). Distance downstream on the X-axis is derived from the start of the polyline for this channel, shown in Figure 5.7.

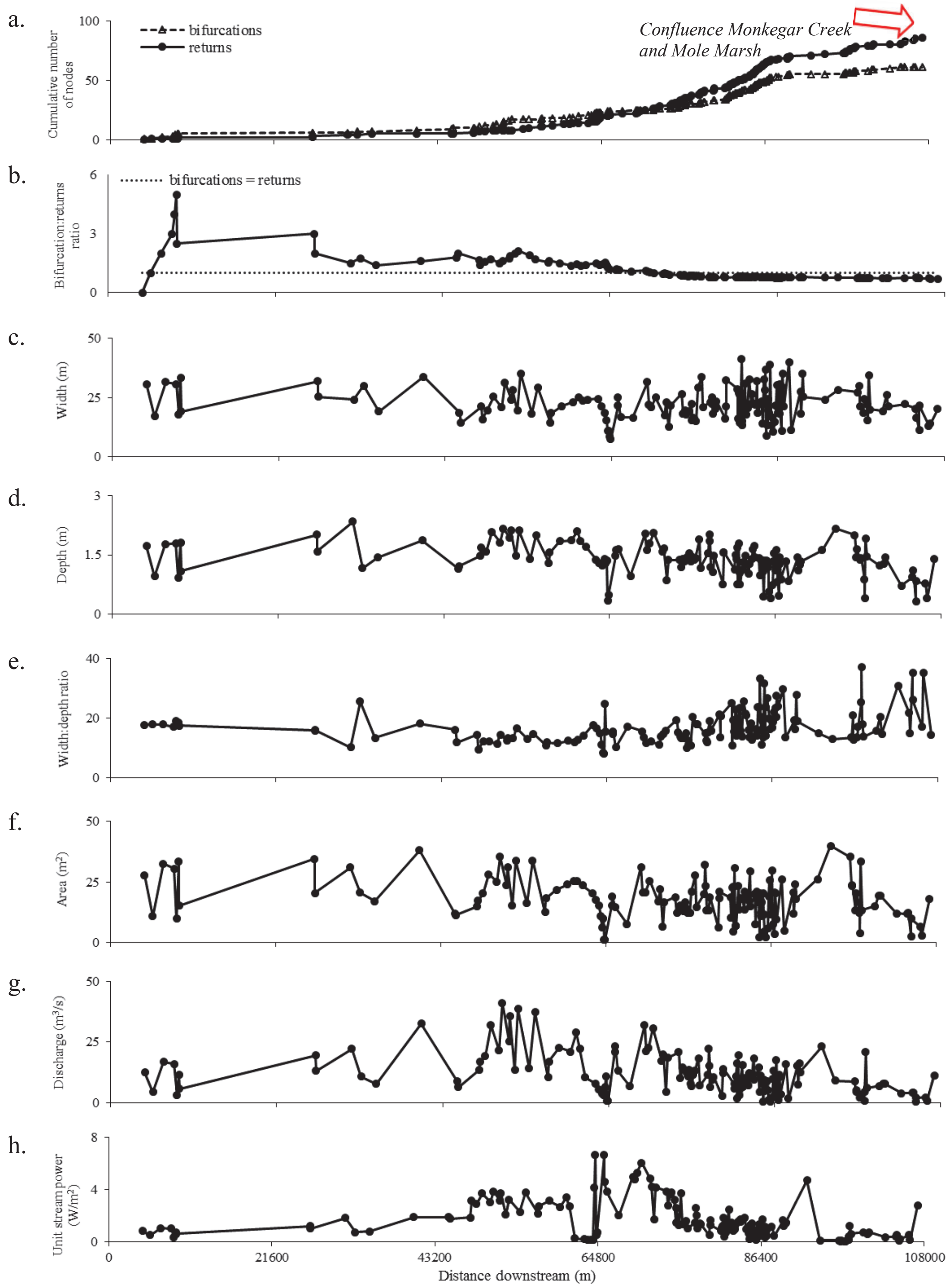

Figure 5.17 Downstream trends along Bulgeraga Creek for the distribution of bifurcation and return nodes (a), bifurcation:return ratio (b), channel bankfull width (c), channel bankfull depth (d), channel width:depth ratio (e), channel bankfull cross-sectional area (f), bankfull discharge (g) and unit stream power (h). Distance downstream on the X-axis is derived from the start of the polyline for this channel, shown in Figure 5.7.

5.6.1.11 Back Swamp

Channel bifurcations initially exceed returns along the Back Swamp, until ~12 km downstream where a cluster of returns cause the bifurcation:return ratio become closer to and then less than 1, and it remains in the same range for the rest of the channel (Figures 5.18a and 5.18b). Bifurcations and returns tend to occur in large clusters although there are some places when none occur for several kilometres. However, the number of bifurcations and returns increase slightly along the channel and returns increase sharply at the end of the lower reach (Figure 5.18a). Channel bankfull width, bankfull depth and bankfull cross-sectional area are highly variable, but decrease slightly downstream and there are noticeable local increases in all three parameters between ~13 and ~17 km downstream (Figures 5.18c, 5.18d and 5.18f). Width:depth ratio is fairly constant along the whole reach except for the sudden jump where the channel becomes narrower and shallower ~10 km downstream (Figure 5.18e). Discharge and unit stream power follow the same trends as channel width, depth and area, and both are lower where the channel becomes smaller (Figures 5.18g and 5.18h). There are significant positive correlations between channel width and depth, width and area, width and discharge, width and unit stream power, depth and area, and significant negative correlation between width:depth ratio and unit stream power for Back Swamp (Appendix 2; Figure A2.11).

5.6.2 Northern Macquarie Marshes

5.6.2.1 Macquarie River in the Northern Marshes

Channel returns initially exceed bifurcations along the Macquarie River in the Northern Marshes (bifurcation:return ratio less than 1), until ~10 km where a cluster of bifurcations occur and the main channel terminates in reed beds which causes the bifurcation:return ratio to exceed 1. Through the reed beds, small clusters of bifurcations and returns occur holding the bifurcation:return ratio just above 1 (Figures 5.19a and 5.19b). Numerous channels converge in the lower reach, where returns accumulate flow and lead out of the Northern Marshes (Figure 5.19a). Several bifurcations also occur downstream of the reed bed, but the bifurcation:return ratio drops below 1. Channel bankfull width, bankfull depth and bankfull cross-sectional area are variable, but decrease markedly downstream into the reed beds before increasing in the lower reach downstream of the reed beds (Figures 5.19c, 5.19d and 5.19f). Width:depth ratio increases downstream and becomes more variable as the channel enters the reed beds and becomes less variable in the lower reach (Figure 5.19e). Discharge and unit stream power have a local peak before the reed beds, and both decline sharply downstream into the reeds and then increase and become more variable in lower reach (Figures 5.19g and 5.419h). There are significant positive correlations between channel width and depth, width and area, width and discharge, and depth and area, and significant negative correlation between width:depth ratio and unit stream power for the Macquarie River in the Northern Marshes (Appendix 2; Figure A2.12).

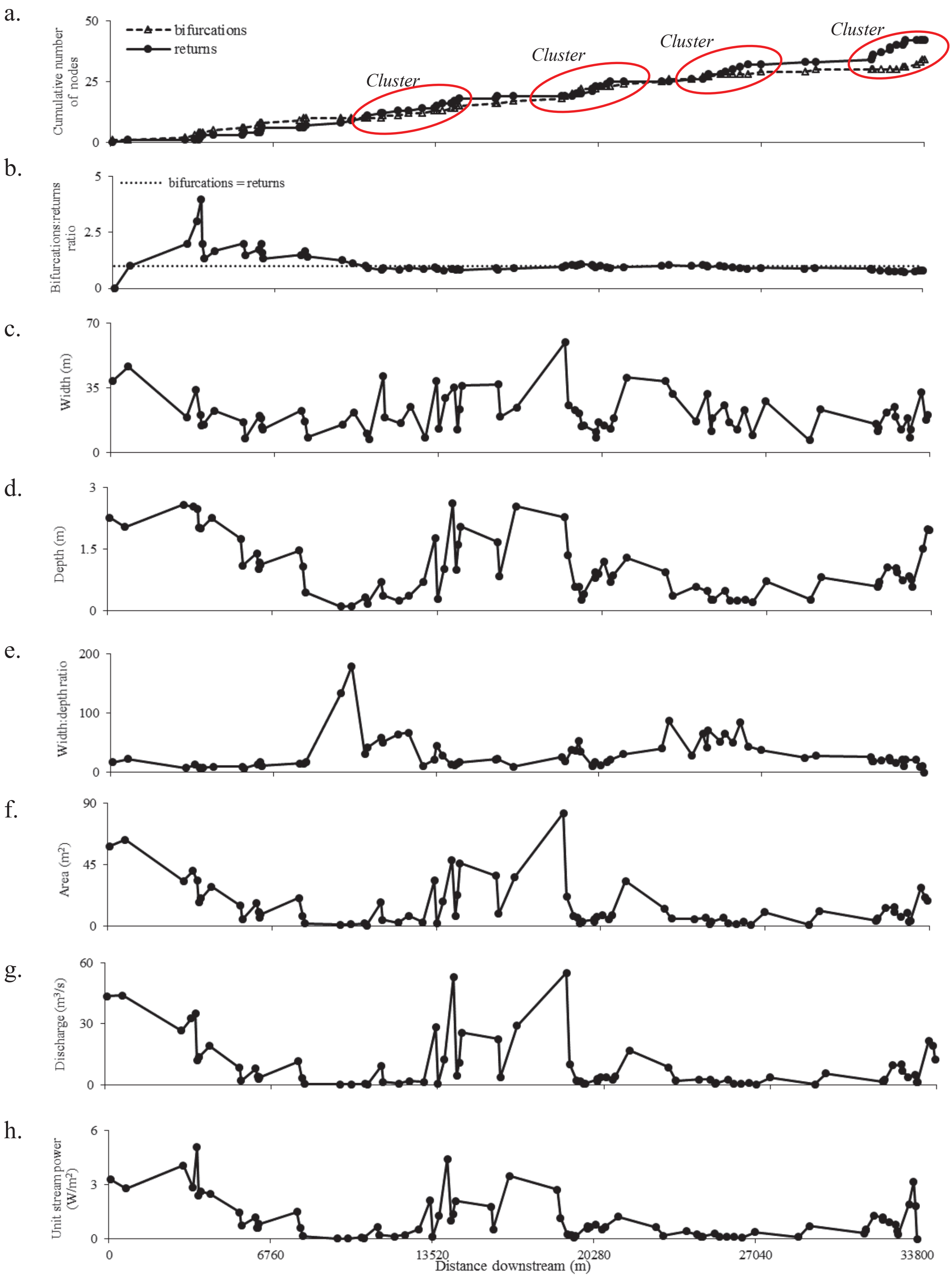

Figure 5.18 Downstream trends along Back Swamp for the distribution of bifurcation and return nodes (a), bifurcation:return ratio (b), channel bankfull width (c), channel bankfull depth (d), channel width:depth ratio (e), channel bankfull cross-sectional area (f), bankfull discharge (g) and unit stream power (h). Distance downstream on the X-axis is derived from the start of the polyline for this channel, shown in Figure 5.7.

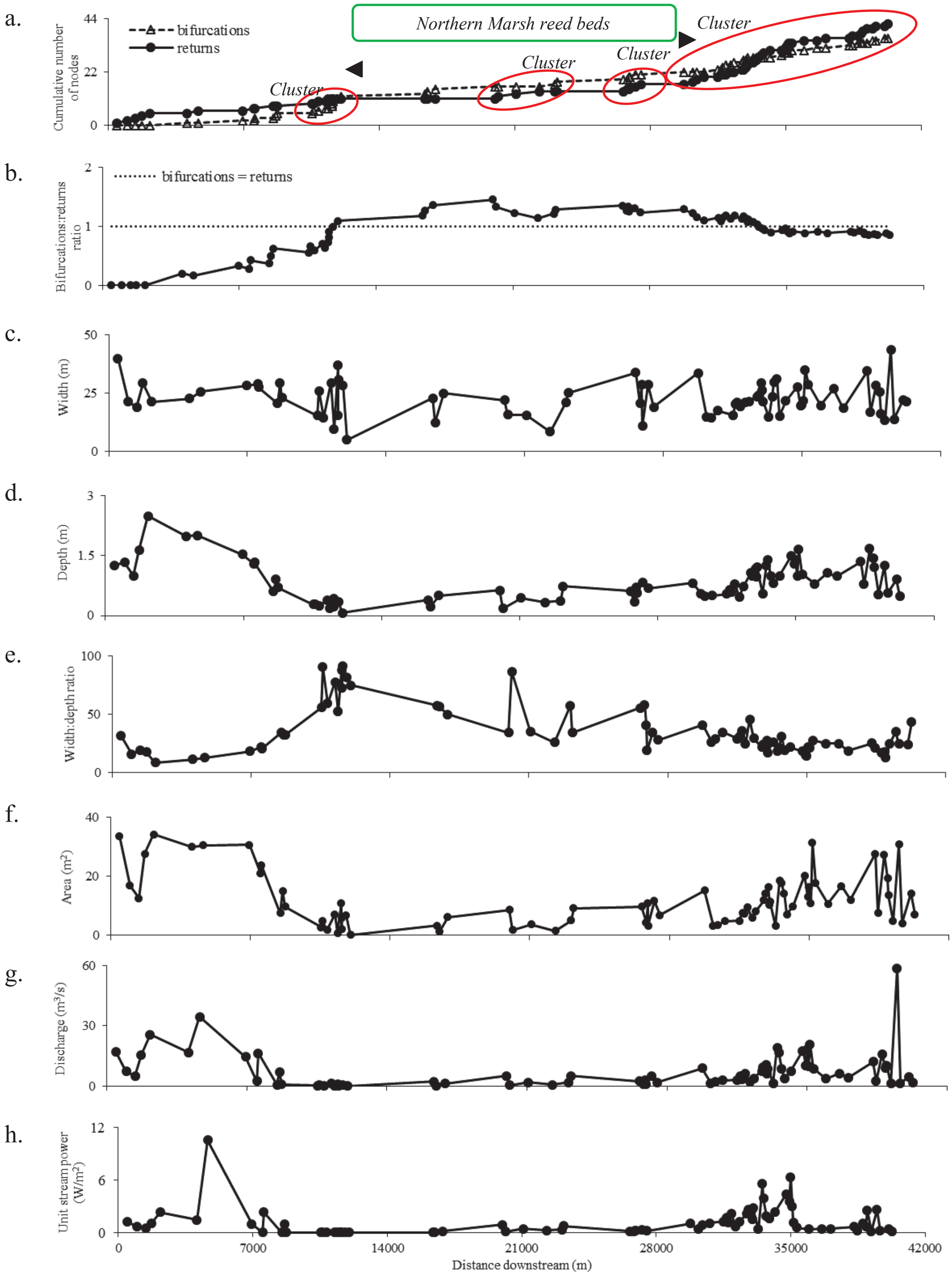

Figure 5.19 Downstream trends along the Macquarie River in the Northern Marshes for the distribution of bifurcation and return nodes (a), bifurcation:return ratio (b), channel bankfull width (c), channel bankfull depth (d), channel width:depth ratio (e), channel bankfull cross-sectional area (f), bankfull discharge (g) and unit stream power (h). The symbol ◄ represents a point of channel termination, and the symbol ► represents a point of channel reformation. Distance downstream on the X-axis is derived from the start of the polyline for this channel, shown in Figure 5.7.

5.6.2.2 Bora Creek

Channel bifurcations initially exceed returns along Bora Creek, until ~12 km downstream (between 6 to 12 km extensive reed beds exist) where a cluster of returns occur which causes the bifurcation:return ratio become closer to and then fall below 1 (Figures 5.20a and 5.20b). Bifurcations and returns occur in clusters from ~12 to 15 km and from ~18 to 21 km downstream (Figure 5.20a). Channel bankfull width, bankfull depth and bankfull cross-sectional area are fairly constant within upper half of the channel and are highly variable within the lower half (Figures 5.20c, 5.20d and 5.20f). Width:depth ratio is also highly variable in the lower half of the channel (Figure 5.20e). Discharge and unit stream power follow the same trends as channel width, depth and area, and are highly variable but generally both are lower where the channel becomes smaller (Figures 5.20g and 5.20h). There are significant positive correlations between channel width and area, depth and area, and significant negative correlation between width:depth ratio and unit stream power for Bora Creek (Appendix 2; Figure A2.13).

5.6.3 Eastern Macquarie Marshes

5.6.3.1 Long Plain Cowal

Channel bifurcations initially exceed returns along Long Plain Cowal, until ~25 km downstream where a cluster of returns occur which causes the bifurcation:return ratio become below 1 and then again it moved above 1 when a cluster of bifurcations occur (Figures 5.21a and 5.21b). Bifurcations and returns occur in small clusters along the whole channel, although the number of bifurcations and returns increase gradually downstream (Figure 5.21a). Channel bankfull width, bankfull depth and bankfull cross-sectional area are all highly variable, and depth and area decrease slightly downstream and there are noticeable local jumps in area and area at the beginning of the reach and ~31 km downstream (Figures 5.21c, 5.21d and 5.21f). Width:depth ratio is also highly variable (Figure 5.21e), as are discharge and unit stream power (Figures 5.21g and 5.21h). There are significant positive correlations between channel width and depth, width and area, width and discharge, width and unit stream power depth and area, and significant negative correlation between width:depth ratio and unit stream power for Long Plain Cowal (Appendix 2; Figure A2.13).

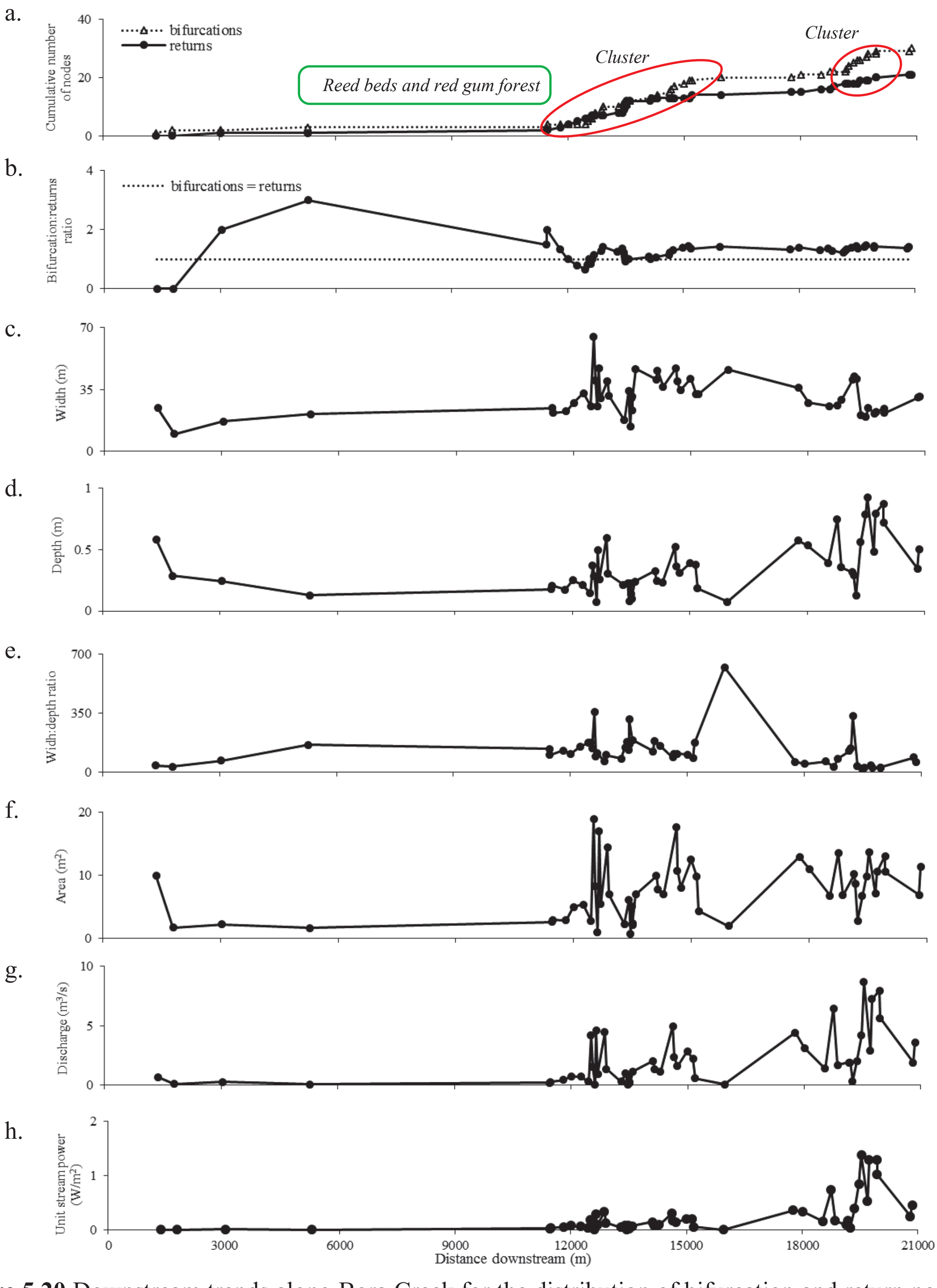

Figure 5.20 Downstream trends along Bora Creek for the distribution of bifurcation and return nodes (a), bifurcation:return ratio (b), channel bankfull width (c), channel bankfull depth (d), channel width:depth ratio (e), channel bankfull cross-sectional area (f), bankfull discharge (g) and unit stream power (h). Distance downstream on the X-axis is derived from the start of the polyline for this channel, shown in Figure 5.7.

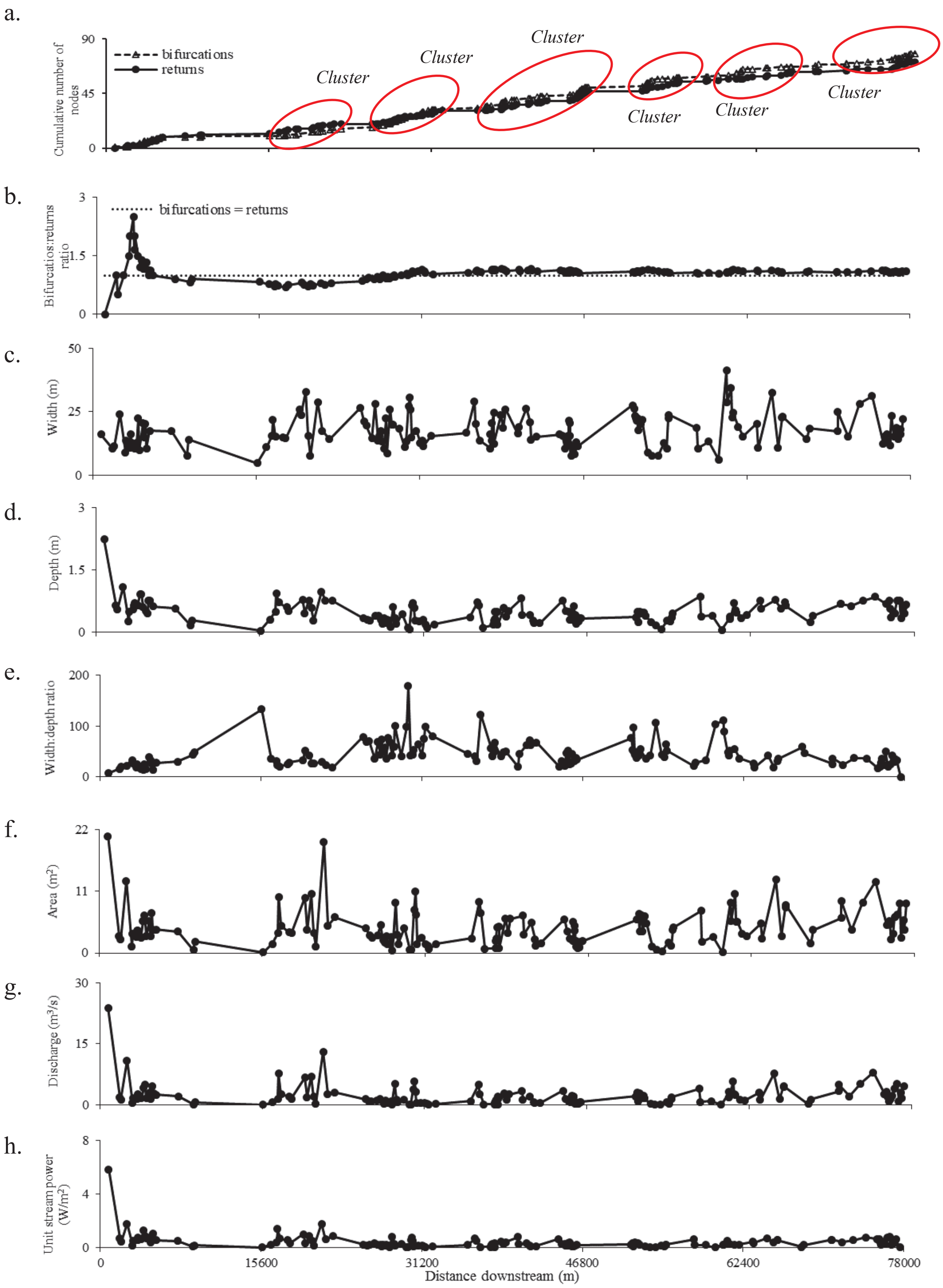

Figure 5.21 Downstream trends along Long Plain Cowal for the distribution of bifurcation and return nodes (a), bifurcation:return ratio (b), channel bankfull width (c), channel bankfull depth (d), channel width:depth ratio (e), channel bankfull cross-sectional area (f), bankfull discharge (g) and unit stream power (h). Distance downstream on the X-axis is derived from the start of the polyline for this channel, shown in Figure 5.7.

5.6.3.2 Gum Cowal

Channel returns briefly exceed returns along Gum Cowal, until ~8 km downstream where a cluster of bifurcations occur which causes the bifurcation:return ratio become closer to 1 (Figures 5.22a and 5.22b). Bifurcation and return clusters do occur, however, the number of bifurcations and returns increase gradually along the whole reach with a marked increase between ~15 to ~20 km (Figure 5.22a). Channel bankfull width, bankfull depth and bankfull cross-sectional area are highly variable, but decrease slightly downstream (Figures 5.22c, 5.22d and 5.22f). Width:depth ratio is fairly constant along the whole reach except for the end of the reach with a jump where channel becomes wider (Figure 5.22e). Discharge and unit stream power follow the same downstream trends as channel width, depth and area, and both are lower where the channel becomes smaller (Figure 5.22g and 5.22h). There are significant positive correlations between channel width and depth, width and area, width and discharge, width and unit stream power depth and area, and significant negative correlation between width:depth ratio and unit stream power for Gum Cowal (Appendix 2; Figure A2.15).

5.6.3.3 Terrigal Creek

Channel bifurcations and returns are relatively balanced along Terrigal Creek, although small clusters occur at ~12, 16, 24, 32 and ~40 km which cause the bifurcation:return ratio fluctuate around 1 (Figures 5.23a and 5.23b). Channel bankfull width, bankfull depth and bankfull cross-sectional area are highly variable, particularly at the end of the reach, and there are no clear downstream trends for any of these parameters (Figures 5.23c, 5.23d and 5.23f). Width:depth ratio is also highly variable (Figure 5.23e), as are discharge and unit stream power (Figures 5.23g and 5.23h). There are significant positive correlations between channel width and depth, width and area, width and discharge, width and unit stream power, depth and area, and significant negative correlation between width:depth ratio and unit stream power for Terrigal Creek (Appendix 2; Figure A2.16).

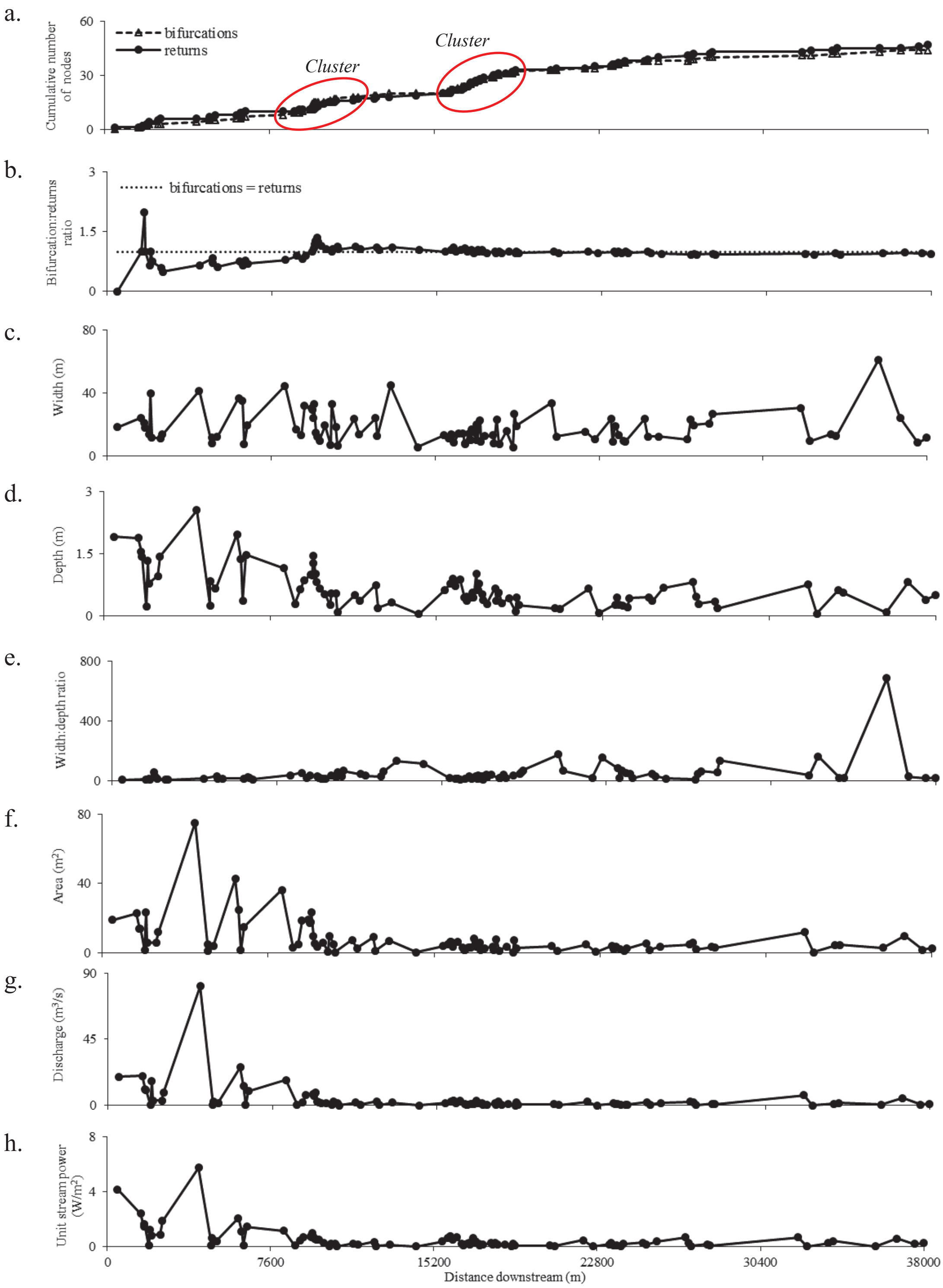

Figure 5.22 Downstream trends along Gum Cowal for the distribution of bifurcation and return nodes (a), bifurcation:return ratio (b), channel bankfull width (c), channel bankfull depth (d), channel width:depth ratio (e), channel bankfull cross-sectional area (f), bankfull discharge (g) and unit stream power (h). Distance downstream on the X-axis is derived from the start of the polyline for this channel, shown in Figure 5.7.

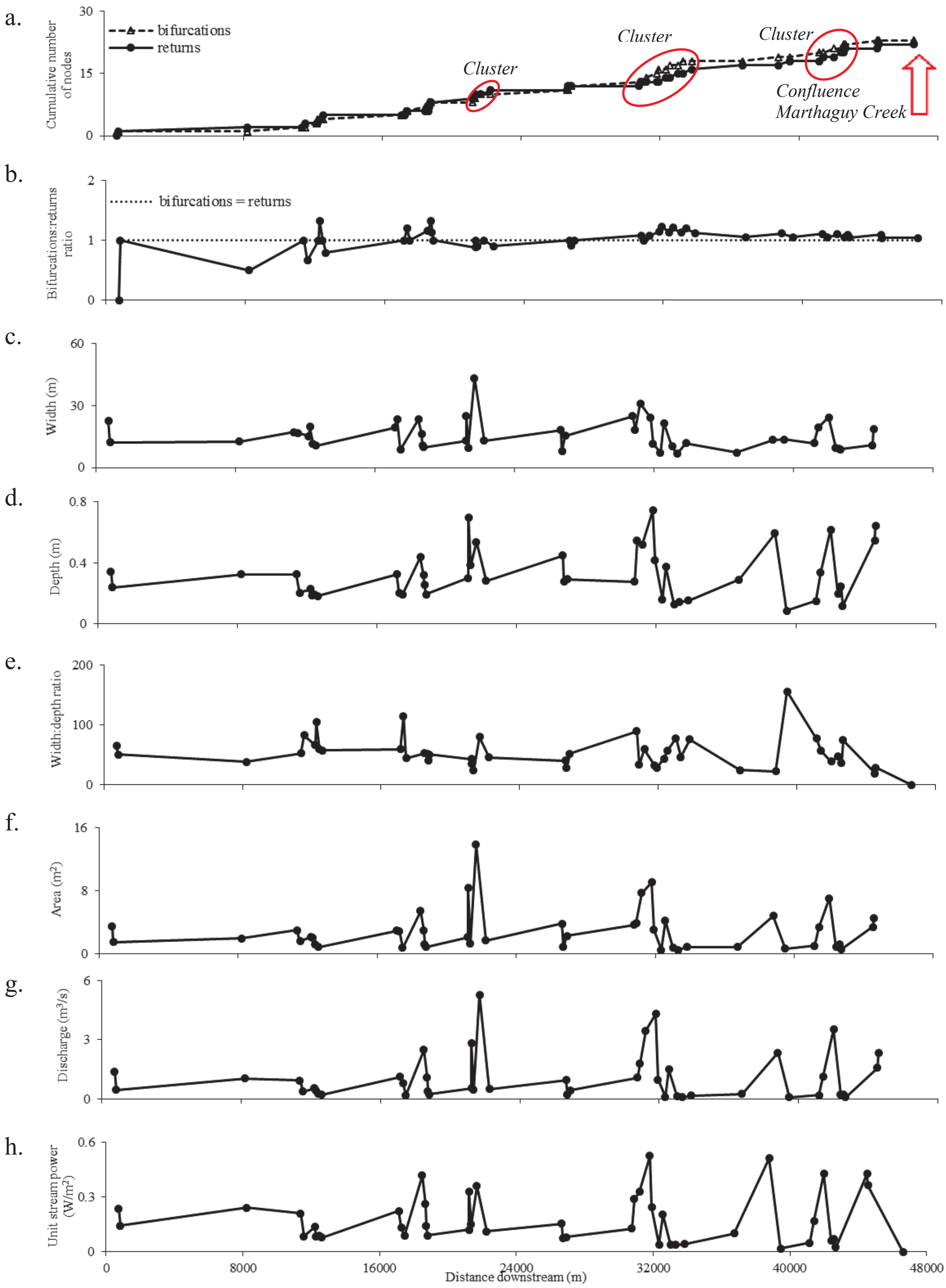

Figure 5.22 Downstream trends along Terrigal Creek for the distribution of bifurcation and return nodes (a), bifurcation:return ratio (b), channel bankfull width (c), channel bankfull depth (d), channel width:depth ratio (e), channel bankfull cross-sectional area (f), bankfull discharge (g) and unit stream power (h). Distance downstream on the X-axis is derived from the start of the polyline for this channel, shown in Figure 5.7.

5.7 Interpretation

The pattern of main channels demonstrates the dominance of anastomosing reaches in the Macquarie Marshes, and the vast majority of channels were between 10-20 m wide and less than 1 m deep. Channels in the Southern Macquarie Marshes are the largest in the system and account for ~50% of bifurcations and returns in overall, meaning that the Southern Marshes are more channelized and has a more complex channel arrangement than either the Northern or Eastern Macquarie Marshes. Returns outnumber bifurcations in the whole system and in each sub-system in the Macquarie Marshes, showing that while many bifurcations occur, these instances of channel splitting are balanced by channels re-joining downstream, in most cases. Bifurcations cause a local increase in the size and capacity of channels in terms of their combined bankfull width and cross-sectional area, while channel depth remains fairly stable throughout the system, despite the position of bifurcations. In contrast, returns effectively show the opposite by leading to reductions in combined channel size at confluences, thereby offsetting any increases gained at upstream bifurcations.

While bankfull discharge and unit stream power were highly variable throughout the system, the largest discharge and stream power estimates occurred in the Southern Macquarie Marshes, which is also the most channelized part of the system. Importantly, combined discharge and stream power at bifurcations typically exceeded those at returns in the Southern and Eastern Macquarie Marshes, demonstrating the positive influence of channel splitting in maintaining and enhancing hydraulic conditions in these parts of the systems. In contrast, discharge and stream power at returns tend to exceed those at bifurcations in the Northern Marshes, where outflowing channels leave the northern end of the system. This suggests that bifurcations help channels to more effectively transmit water and sediments locally, while, at the scale of the sub-systems and the whole system, returns are essential for outflowing channels to reform and continue downstream. Channels in the Macquarie Marshes mostly have bankfull discharge less than 5 m^3/s and unit stream power less than 1 W/m^2, showing that on the whole the system is very low energy and most likely has little capacity for major episodes of sediment reworking and transport. While sediment transport and the role of overbank flows were not modelled, it is highly likely that local increases in sediment transport occur at bifurcations (cf. Frings & Kleinhans, 2008), while declines occur at returns, perhaps influenced by flows returning from the floodplain that contain high concentrations of sediment.

While channel bankfull discharge and unit stream power provide a valuable insight into the hydro-geomorphological character of the Macquarie Marshes, including general downstream declines in the main channels and variations associated with major bifurcation and return points, overbank flooding and backwater effects may also influence hydrology at some sites. Flow velocity is reduced when floodwaters overtop the banks of a river. Backwater effects are most likely to occur when water on the floodplain and in wetlands becomes impounded (e.g. in depressions, or due to earth levees or dense vegetation) and starts to recirculate. When this occurs, the flood pulse is delayed due to a reduction in flow velocity, which encourages the development of slow-moving or standing waterbodies upstream that affect the duration and amplitude of the flood (Stevaux et al., 2020). Water that is standing or recirculating on the floodplain may be lost to evapotranspiration, or may rejoin channels downstream. These processes have not been studied in the Macquarie Marshes, but in low-gradient systems when flow dynamics may be controlled by the slope of the water surface instead of the slope of the channels, backwater effects are quite important (Stevaux et al., 2020). In the Macquarie Marshes, this would be particularly important at return points where the capacity of the downstream channel is less than the capacity of the upstream joining streams.

Nevertheless, downstream analysis of channel geometry and other morphometrics demonstrates the role of distributary and tributary flows associated with bifurcations and returns that affect hydraulic and geomorphological character leading to changes in channel capacity (even taking into account the limitations of the methods by employing conservative thresholds of difference in channel bankfull width, depth and cross-sectional area). Although all channels had highly variable bankfull width, depth, cross-sectional area, width:depth ratio, discharge and stream power, almost all exhibited some form of downstream decline in size and hydraulic character Despite this overall decline, channel maintenance and reformation occurred when clusters of bifurcations were balanced by clusters of returns. Thus, the bifurcation:return ratio can be used as a parameter to group river reaches of similar character and behaviour.

Where bifurcations were dominant (bifurcation:return ratio consistently above 1), channels tended to split multiple times as they formed distributary channels and/or broke down in wetlands, before some channels eventually reconverged downstream of the wetlands. Channels of this type became wider and shallower downstream, which markedly increased the width:depth ratio which would allow for a greater spread of water and sediment on the floodplain and into wetlands. Examples of where this occurred include Macquarie River upstream Monkeygar Creek and Bora Creek, which are major feeder channels for the two main areas of wetlands in the Southern and Northern sections of the Macquarie Marshes (Figure 5.23a). In other cases, where returns were dominant (bifurcation:return ratio consistently below 1), channels accumulated flow and did not terminate in wetlands. Examples include the Macquarie River downstream of the Old Macquarie River and Oxley Break (Figure 5.23b).

The majority of channels exhibited an initial dominance of bifurcations, which were ultimately outnumbered or superseded by returns (leading to a bifurcation:return ratio above 1 that returned to and then dropped below 1 downstream). Examples include the Old Macquarie River, Mole Marsh, The Breakaway, Monkeygar Creek, Monkey Creek, Bulgeraga Creek, Back Swamp and Buckiinguy Creek (Figure 5.23c). The Macquarie River in the Northern Marshes shows a different behaviour where returns were dominant (bifurcation:return ratio below 1) and then bifurcations became dominant (bifurcation:return ratio above 1) which led to channel breakdown. In the lower reach, returns again dominated the system (bifurcation:return ratio close to and below 1) where channels flowed out of the Macquarie Marshes (Figure 5.23d). Other reaches had very few obvious trends in channel capacity or hydraulic conditions downstream, and so for these it is difficult to interpret the broader controls on or patterns of channel maintenance, or overall decline. These rivers typically had bifurcations that were balanced by returns (bifurcation:return ratio hovered around 1). Examples of this fluctuating character and behaviour include Long Plain Cowal, Gum Cowal and Terrigal Creek (Figure 5.23e). Some river reaches incorporate larger (wider, perhaps shallower) palaeochannels that could upset the typical downstream declining trends in some channels, for example along Gum Cowal and Long Plain Cowal, but the role of palaeochannels in influencing modern channel character has not been quantitatively investigated in this study.

These changes may be inferred as being related to equilibrium (i.e. channel maintenance) or non-equilibrium (i.e. channel enlargement, decline and/or termination) channel conditions. Overall, the numerous, and approximately balanced, number of bifurcations and returns within the system, and within the majority of reaches studied within the sub-systems, help the Macquarie River to recover its channel capacity (i.e. size, particularly width) and to provide a hydraulic advantage for channel maintenance in the Macquarie Marshes. Channel depth is fairly constant throughout the system, but it is clear that channels become very shallow where they split and terminate in wetlands and become increasingly deep as they flow out of wetlands. These channel conditions occur in response to the low imposed discharge and stream power in the system, which suggests that channel adjustment processes should occur slowly, on the whole.

It remains to be seen, however, whether the spatial patterns and downstream distribution of bifurcations and returns in the Macquarie Marshes, and the hydro-geomorphic character of the channels themselves, have remained relatively constant or have experienced major changes over time. While the aforementioned changes in spatial patterns and distributions are very difficult to determine without previous high-resolution elevation data (e.g. there is no LiDAR data for the system that pre-dates 2008), analysis of channel cross-sections that have been surveyed on the ground using traditional methods during the recent historical period can be used to assess whether significant recent historical channel changes have occurred. Such an analysis would allow differences in channel bankfull width, depth and cross-sectional area to be quantified together with associated hydraulic factors, and then linked back to the relative position of the channels, and their bifurcations and returns, in the system (see Chapter 6).

a. Bifurcation dominant (split/spread flow)

Macquarie River upstream Monkeygar Creek

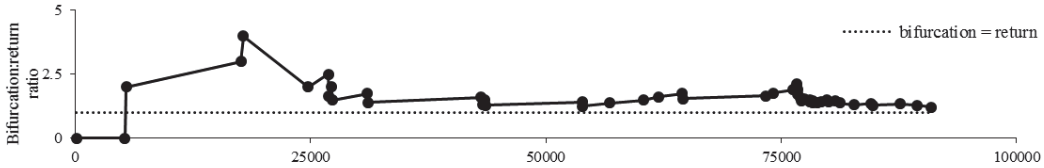

Bora Creek

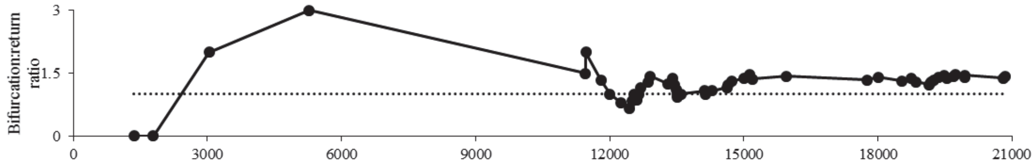

b. Return dominant (draw/accumulate flow)

Macquarie River downstream Old Macquarie River

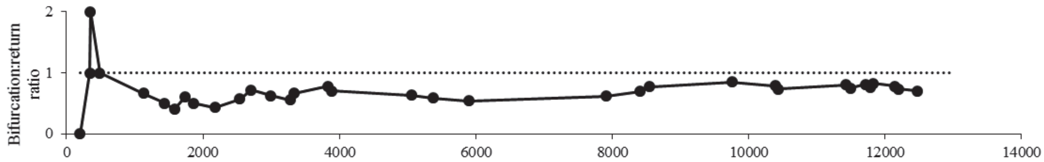

Oxley Break

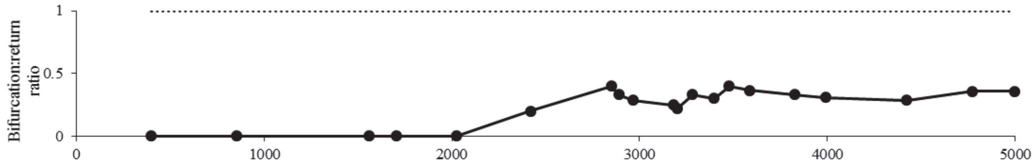

c. Bifurcations superseded by returns (split/spread then draw/accumulate flow)

Old Macquarie River

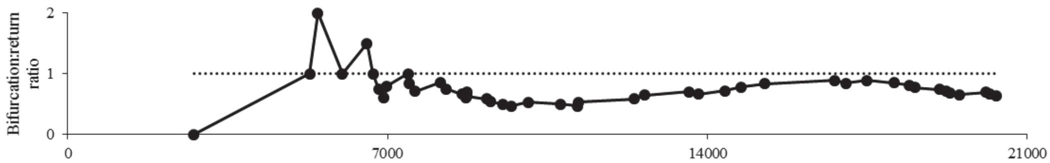

Mole Marsh

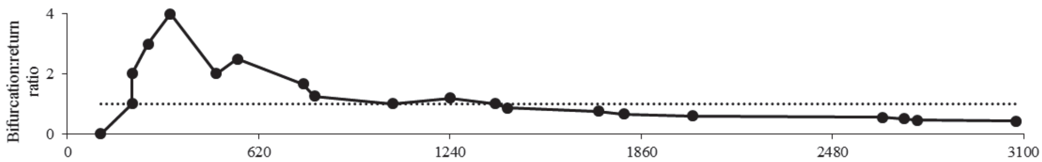

The Breakaway

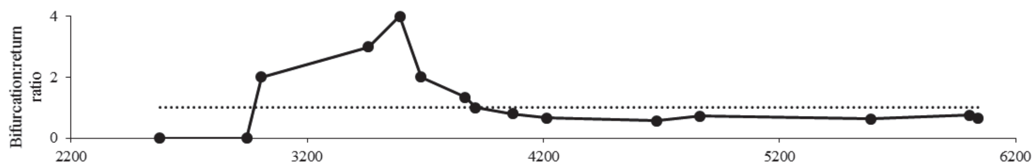

Monkeygar Creek

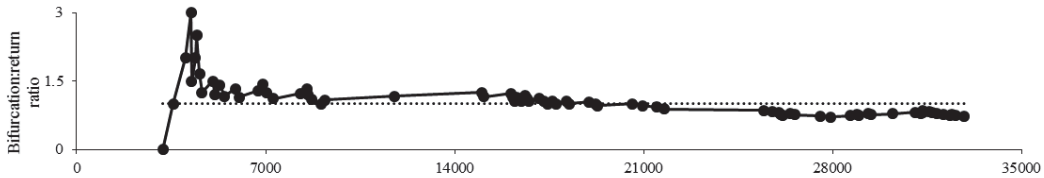

Monkey Creek

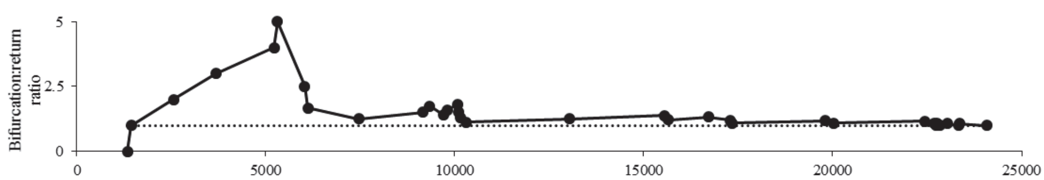

Figure 5.23 continued over page.

c. *continued*

Bulgeraga Creek

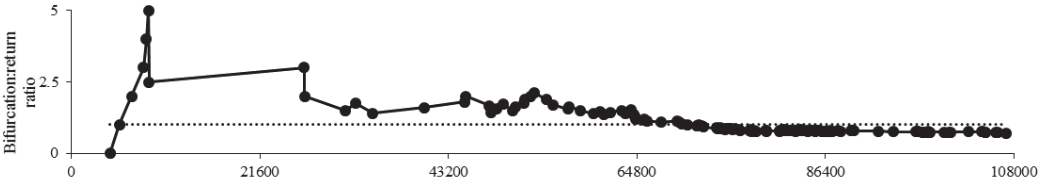

Back Swamp

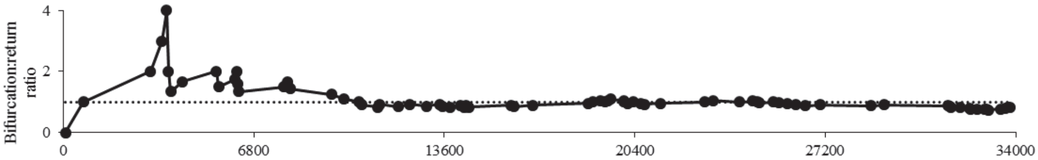

Buckiinguy Creek

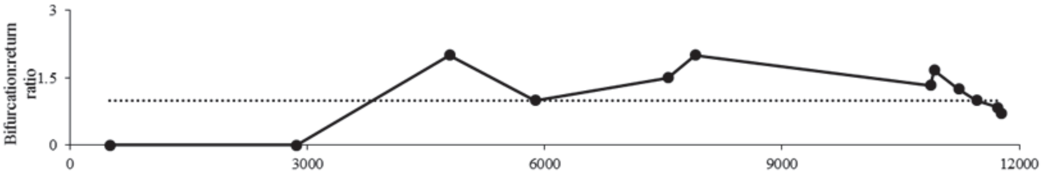

d. Returns- bifurcations- returns (draw/accumulate then split/spread, then draw/accumulate flow)

Macquarie River in the Northern Marshes

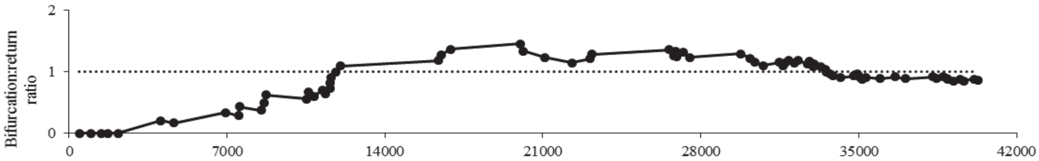

e. Bifurcations and returns balanced (transmit flow)

Long Plain Cowal

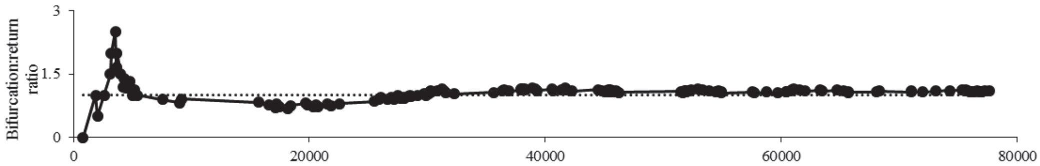

Gum Cowal

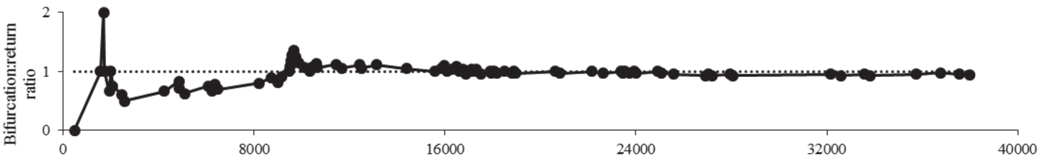

Terrigal Creek

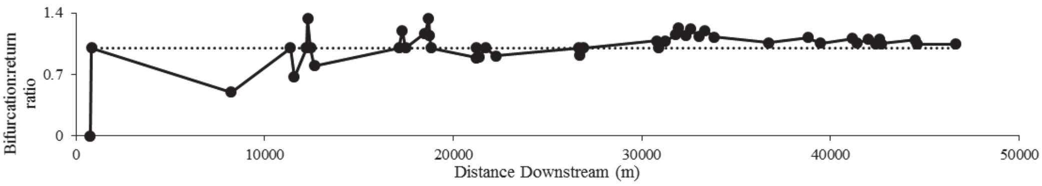

Figure 5.23 River reaches in the Macquarie Marshes grouped by bifurcation:ratio trends, where bifurcations are dominant (a), returns are dominant (b), bifurcations are superseded by returns (c), returns are superseded by bifurcations before returns (d) and where bifurcations and returns are balanced (d). Distance downstream on the X-axis is derived from the start of the polyline for this channel, shown in Figure 5.7.

5.8 Summary

This chapter presented a detailed description of the geomorphic and hydraulic character of the Macquarie Mrashes and its sub-systems affected by channel bifurcations and returns. A LiDAR-derived DEM was used to quantify the number, location and spatial distribution of bifurcations and returns scattered among the main river channels in the Macquarie Marshes, leading to channel maintenance in the system on the whole. Analysis for sixteen channels demonstrated the key downstream changes in morphometric and hydraulic character leading to channel continuation or termination. Although bifurcations and returns affect channel capacity, particularly at local scales, they tend to maintain the dynamic equilibrium conditions of the whole system. In the next chapter, recent historical and contemporary channel cross-section data and analysis of morphological change at the sub-system scale of the Southern Macquarie Marshes is presented to investigate the role of channel erosion as a key part of channel adjustment in the system.

Chapter 6: Recent historical channel adjustment in the Southern Macquarie Marshes

6.1 Introduction

This chapter investigates historical channel adjustment in the Southern Macquarie Marshes. Changes in the geomorphic and hydraulic character of key channels are described from 1992 to 2018, and a synthesis of recent historical channel adjustments are presented. The analysis was undertaken for the Macquarie River upstream of Monkeygar Creek, Monkeygar Creek, The Breakaway, the Old Macquarie River and the Macquarie River downstream of the Old Macquarie River (Figure 6.1). Channel morphometric parameters including bankfull width, depth, area, width:depth ratio, bed height and bank height were compared using topographic data derived from channel cross-section surveys in 1992 (Brereton, 1994), transects extracted from a LiDAR-derived DEM from 2008 and channel cross-section surveys from 2018. In this chapter, the following aims of this thesis are addressed:

2. *To define the geometric configuration and hydraulic behaviour of channels leading to channel maintenance, avulsion and breakdown in the southern Macquarie Marshes;*
3. *To identify historical and contemporary trajectories of channel behaviour in hyper-avulsive reaches of the Southern Macquarie Marshes and to explain the role of erosion in the system.*

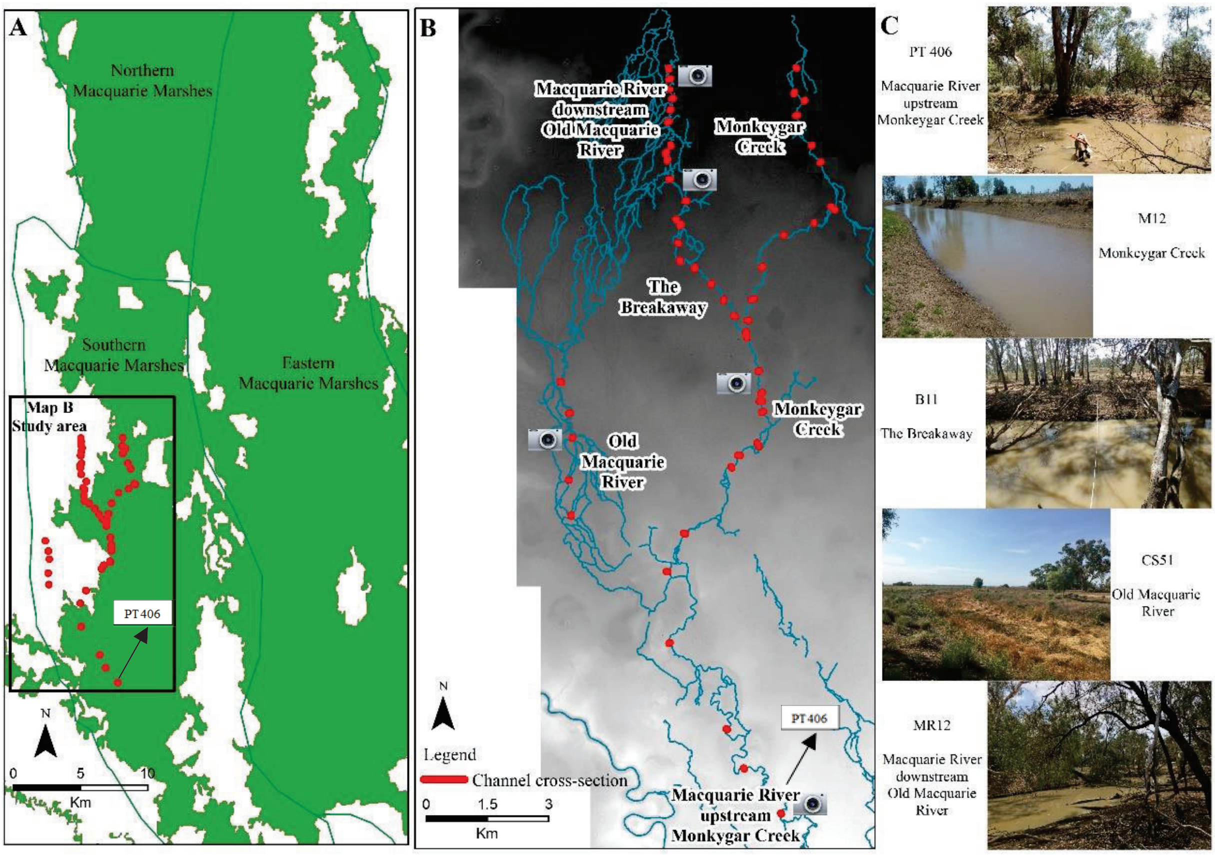

Figure 6.1 Map of the study area in the Southern Macquarie Marshes (A), cross-section surveys in 1992 (Brereton, 1994), 2018, and extracted from LiDAR-derived DEM for 2008 along key reaches (B), and images of example cross-sections surveyed in the field. Distance downstream is measured from PT406.

6.2 Channel morphology and hydrology

6.2.1 Macquarie River upstream of Monkeygar Creek

The Macquarie River upstream of Monkeygar Creek in the Southern Macquarie Marshes has a sinuous, meandering trunk stream with several branches. In this region, the Macquarie River experiences a downstream decline in discharge and stream power due to natural losses from evapotranspiration, infiltration and dispersal of flow into secondary channels and onto the floodplain, leading to a mostly anastomosing pattern of channels (Ralph and Hesse, 2010). An example of a cross-section transect on the Macquarie River upstream Monkeygar Creek is shown in Figure 6.2.

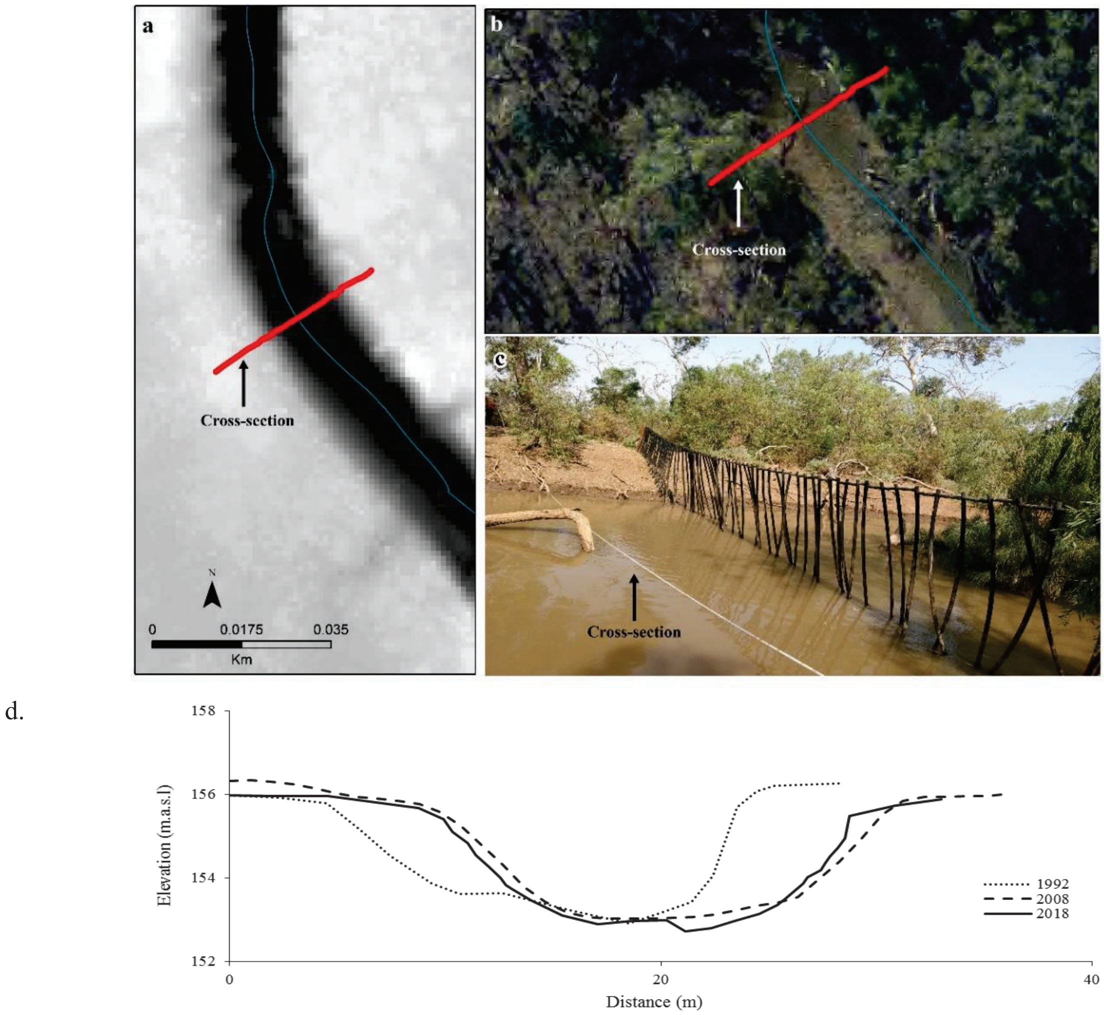

Figure 6.2 Site MY289 located on the Macquarie River upstream of Monkeygar Creek as seen on LiDAR-derived DEM (a), aerial imagery (b) and on the ground (c) and cross-section profile data from 1992 (Brereton, 1994), 2008 and 2018 (d). All cross-sections are presented looking downstream.

Analysis of bed and bank height along the Macquarie River upstream of Monkeygar Creek shows a steady decline in the distance downstream, with little variation over the three time slices (Figures 6.3a and 6.3b). Comparison of channel bankfull width, depth, width:depth ratio and cross-sectional area shows that these metrics have also remained stable over the 26-year period from 1992 to 2018 (Figures 6.3c, 6.3d, 6.3e and 6.3f). The downstream trends for these parameters have also not changed significantly over time, with channel width, depth, width:depth and area increasing slightly in the lower reach of the channel following the confluence of Buckiinguy Return. Bankfull discharge and unit stream power are also stable from 1992 to 2018, and both increase slightly in the lower reach when compared downstream (Figures 6.3g and 6.3h).

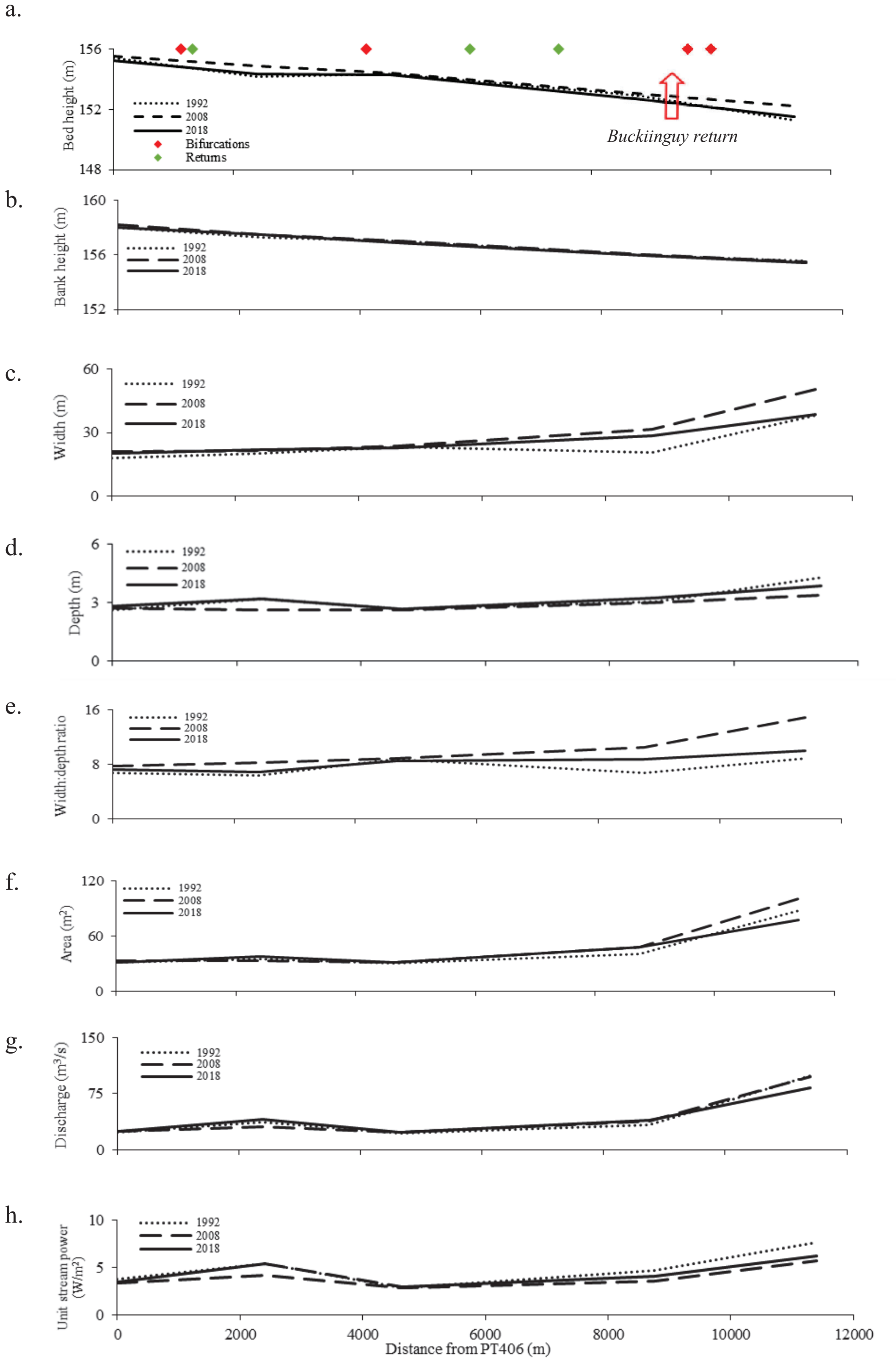

Figure 6.3 The longitudinal profile of bed height (a), bank height (b), channel width (c), channel depth (d), width to depth ratio (e), channel cross-sectional area (f), bankfull discharge (g) and unit stream power (h) for the Macquarie River upstream of Monkeygar Creek in 1992 (Brereton, 1994), 2008 and 2018. The location of PT406 is shown in Figure 6.1A and 6.1B.

6.2.2 Monkeygar Creek

Monkeygar Creek is the main arm of the Macquarie River in the Southern Macquarie Marshes. Previous studies have shown that channel morphology altered significantly in this reach over the last 50 years due to erosion (channel deepening and widening) and knickpoint retreat (channel erosion cutting back upstream due to a step-change in topography on the channel bed) (Brereton 1994; Ralph et al., 2011; Ralph et al. 2016; Yonge and Hesse, 2009). Monkeygar Creek is now a continuous, low-sinuosity channel, which initially formed as a discontinuous branch of the Macquarie River, then enlarged in length prior to 1963 and became deeply channelized in the early 1990s (Ralph et al. 2016). Monkeygar Creek feeds several distributary channels and wetlands including Little Monkeygar, The Breakaway, Monkeygar Marsh and Willancorah Swamp. An example of a cross-section transect on Monkeygar Creek is shown in Figure 6.4.

d.

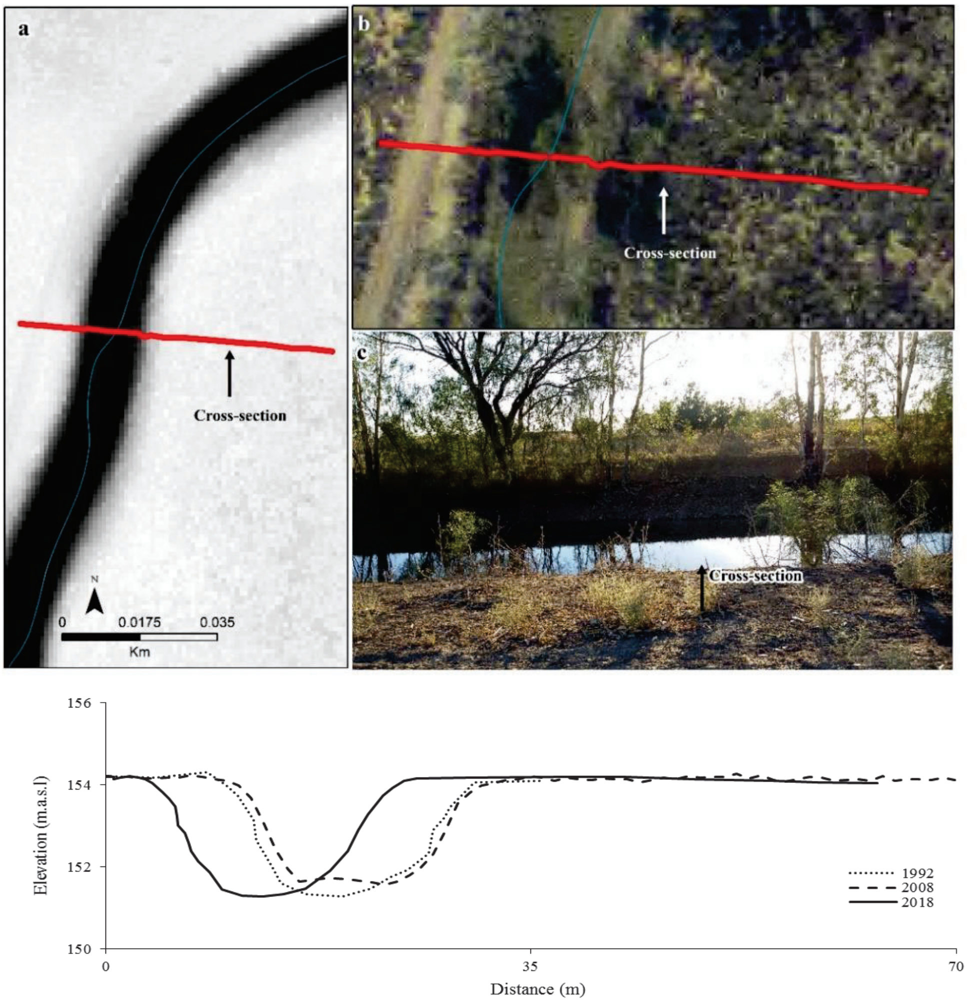

Figure 6.4 Site M5 located on Monkeygar Creek as seen on LiDAR-derived DEM (a), aerial imagery (b) and on the ground (c) and cross-section profile data from 1992 (Brereton, 1994), 2008 and 2018 (d).

Channel bed and bank heights on Monkeygar Creek have changed very little between 1992 and 2018 (Figures 6.5a and 6.5b). Channel width varies over time at some cross-sections, but there is not a consistent trend of channel widening or narrowing in any reach (Figure 6.5c). A rapid increase in width occurs at 15 km, which is located before the bifurcation of Little Monkeygar, and an increase from 23 to 29 km, which is where the return channels from Monkey Marsh enter. Channel depth and cross-sectional area have exhibited minor changes from 1992 to 2018, and width:depth has decreased over time in the channel (Figures 6.5c, 6.5d, 6.5e and 6.5f). Overall, the discharge and stream power have declined slightly over time (Figures 6.5g and 6.5h).

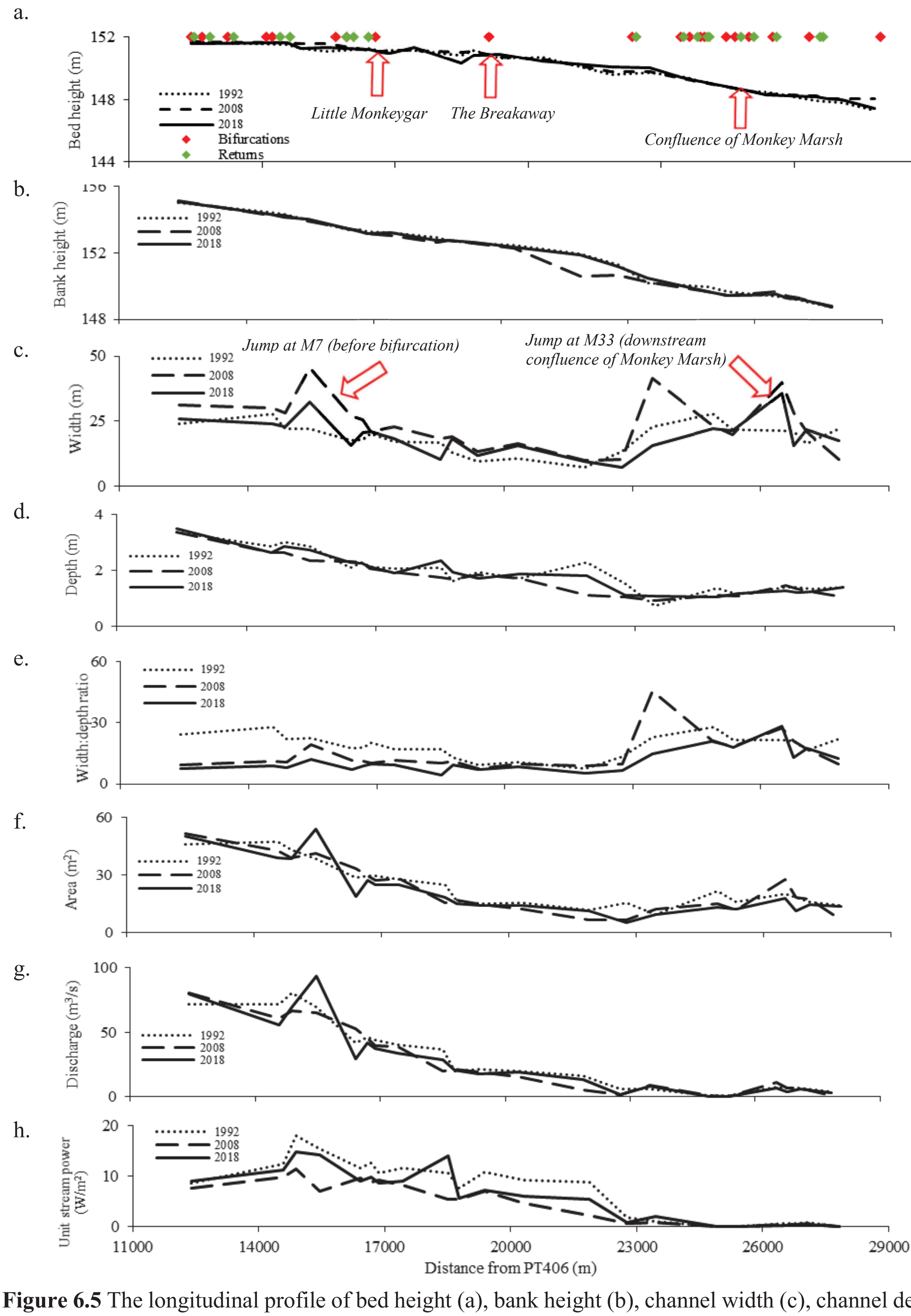

Figure 6.5 The longitudinal profile of bed height (a), bank height (b), channel width (c), channel depth (d), width to depth ratio (e), channel cross-sectional area (f), bankfull discharge (g) and unit stream power (h) for Monkeygar Creek in 1992 (Brereton, 1994), 2008 and 2018. The location of PT406 is shown in Figure 6.1A and 6.1B.

6.2.3 The Breakaway

The Breakaway is an important avulsion from Monkeygar Creek that directs flows back into the Old Macquarie River. The Breakaway was initially a discontinuous drainage line in Monkeygar Marsh in circa 1949 (Ralph et al. 2016). The Breakaway then enlarged during the 1950s, becoming almost continuous to the Old Macquarie River from the 1970s. Floods in the 1990s served to further enlarge the channel, particularly deepening it as erosion and knickpoints retreating upstream cut into the floodplain (Brereton, 1994; Ralph et al. 2016). An example of a cross-section transect on The Breakaway is shown in Figure 6.6.

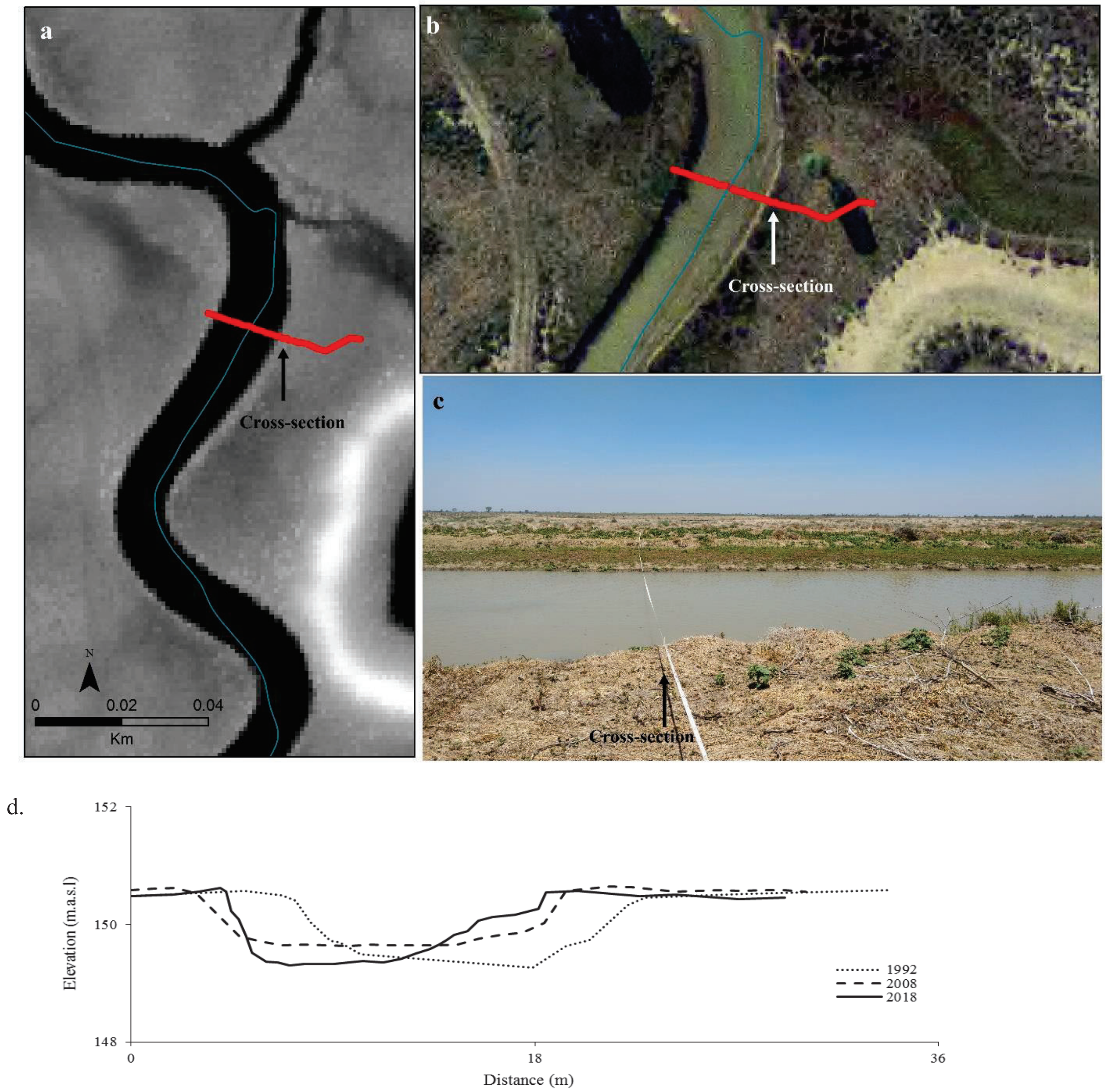

Figure 6.6 Site B10 located on The Breakaway as seen on LiDAR-derived DEM (a), aerial imagery (b) and on the ground (c) and cross-section profile data from 1992 (Brereton, 1994), 2008 and 2018 (d).

Bed and bank height remained almost stable along The Breakaway between 1992 and 2018 (Figures 6.7a and 6.7b). Channel width, however, increased significantly over time, particularly in the upper 4 km of the channel (Figure 6.7c). Channel depth has also increased slightly in the upper and middle reaches (Figure

6.7d), while width:depth ratio and cross-sectional area have increased, over time, as the width increased (Figures 6.7e and 6.7f). Bankfull discharge also increased in the upper and middle reaches, while unit stream power generally declined from 1992 to 2018 due to the widening of the channel (Figure 6.7).

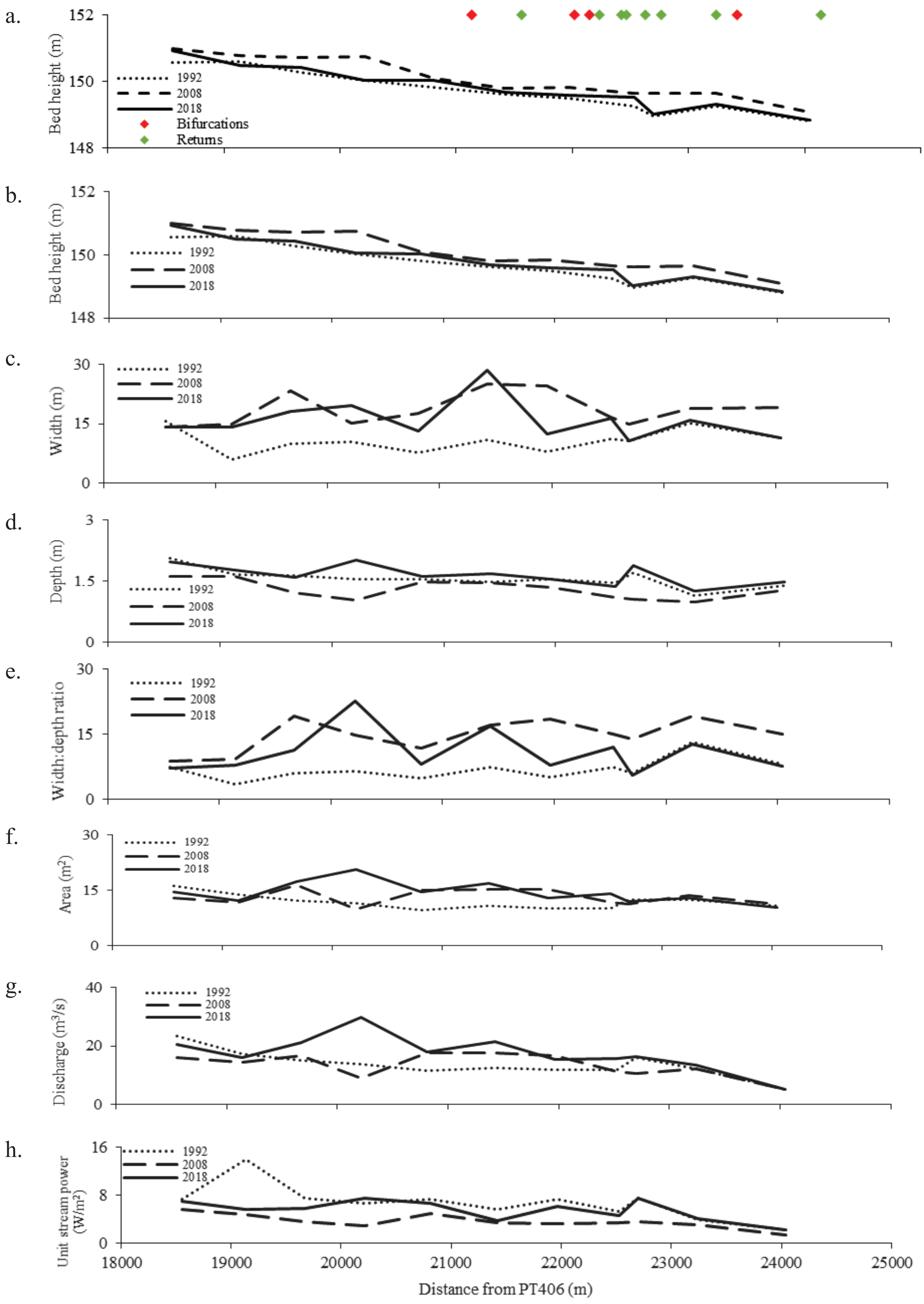

Figure 6.7 The longitudinal profile of bed height (a), bank height (b), channel width (c), channel depth (d), width to depth ratio (e), channel cross-sectional area (f), bankfull discharge (g) and unit stream power (h) for The Breakaway in 1992 (Brereton, 1994), 2008 and 2018. The location of PT406 is shown in Figure 6.1A and 6.1B.

6.2.4 Old Macquarie River

The Old Macquarie River comprises a reformed channel of the Macquarie trunk stream downstream of the Terminus Marsh, which now receives irregular discharge. This reach previously inundated large parts of the southern Nature Reserve and Willie Marsh upstream of Mole Marsh, and now feeds into a lower section of the Macquarie River, which eventually runs into Mole Marsh. An example of a cross-section transect on the Old Macquarie River is shown in Figure 6.8.

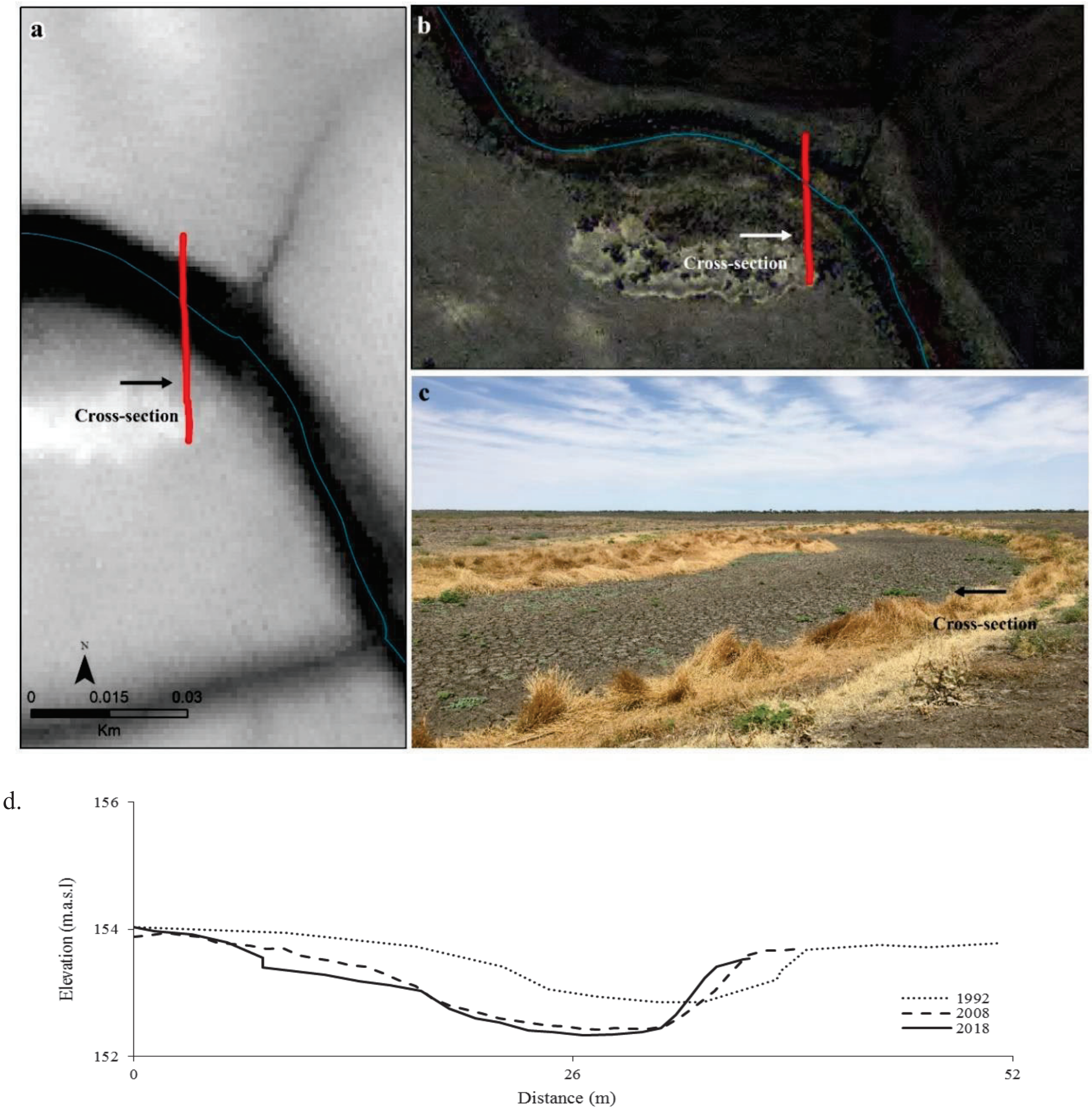

Figure 6.8 Site CS3 located on the Old Macquarie River as seen on LiDAR-derived DEM (a), aerial imagery (b) and on the ground (c) and cross-section profile data from 1992 (Brereton, 1994), 2008 and 2018 (d).

Channel bed height has remained stable along the Old Macquarie River (Figure 6.9a). Bank height has increased in middle and lower reach over the 26-year period from 1992 to 2018 (Figure 6.9b). Channel width decreased in the middle reach, but channel depth remained constant along the whole reach (Figures 6.9c and 6.9d). Width:depth ratio and cross-sectional area decreased in the middle reach, while cross-sectional area increased in the lower reach (Figures 6.9e and 6.9f). Bankfull discharge has shown minor changes from 1992 to 2018, decreased in places where channel width and area declined, and increased where channel width and area increased, while unit stream power generally increased in this period (Figures 6.9g and 6.9h).

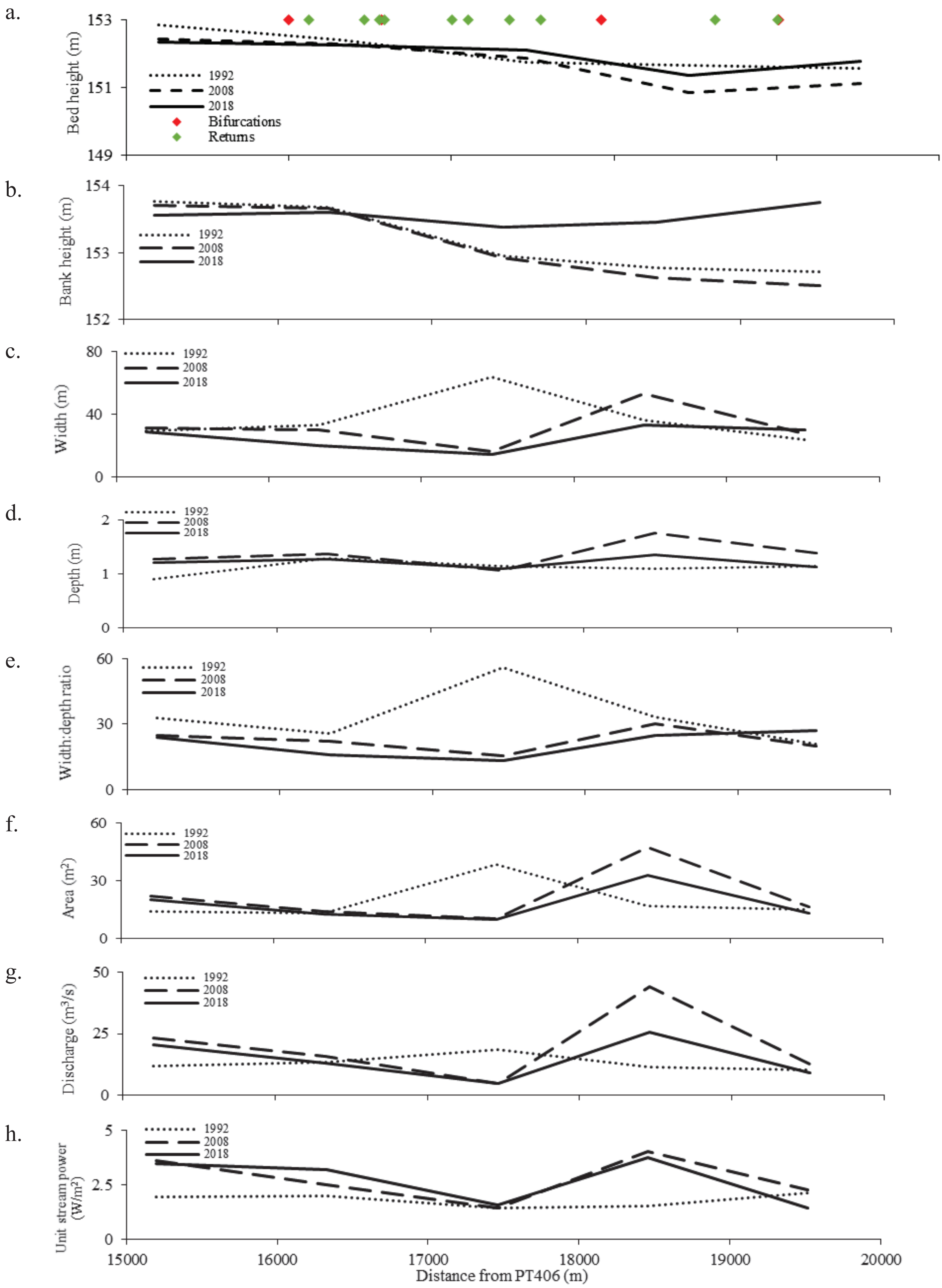

Figure 6.9 The longitudinal profile of bed height (a), bank height (b), channel width (c), channel depth (d), width to depth ratio (e), channel cross-sectional area (f), bankfull discharge (g) and unit stream power (h) for the Old Macquarie River in 1992 (Brereton, 1994), 2008 and 2018. The location of PT406 is shown in Figure 6.1A and 6.1B.

6.2.5 Macquarie River downstream of the Old Macquarie River

The main channel of the Macquarie River reforms downstream of the old Macquarie River where The Breakaway joins the trunk stream, bringing flow from Monkeygar Creek. An example of a cross-section transect on the Macquarie River downstream of the Old Macquarie is shown in Figure 6.10. Channel bed and bank height remained fairly consistent along the Macquarie River downstream of the Old Macquarie River from 1992 to 2018 (Figures 6.11a and 6.11b). Channel width and depth, width:depth ratio and cross-sectional area all varied over time at some cross-sections, but there were no consistent trends of channel widening or narrowing in any reach (Figures 6.11c, 6.11d, 6.11e and 6.11f). Bankfull discharge also varied over time at some cross-sections, showing a reduction in some places and an increase in others, while unit stream power remained almost constant over the 26-year period (Figures 6.11g and 6.11h).

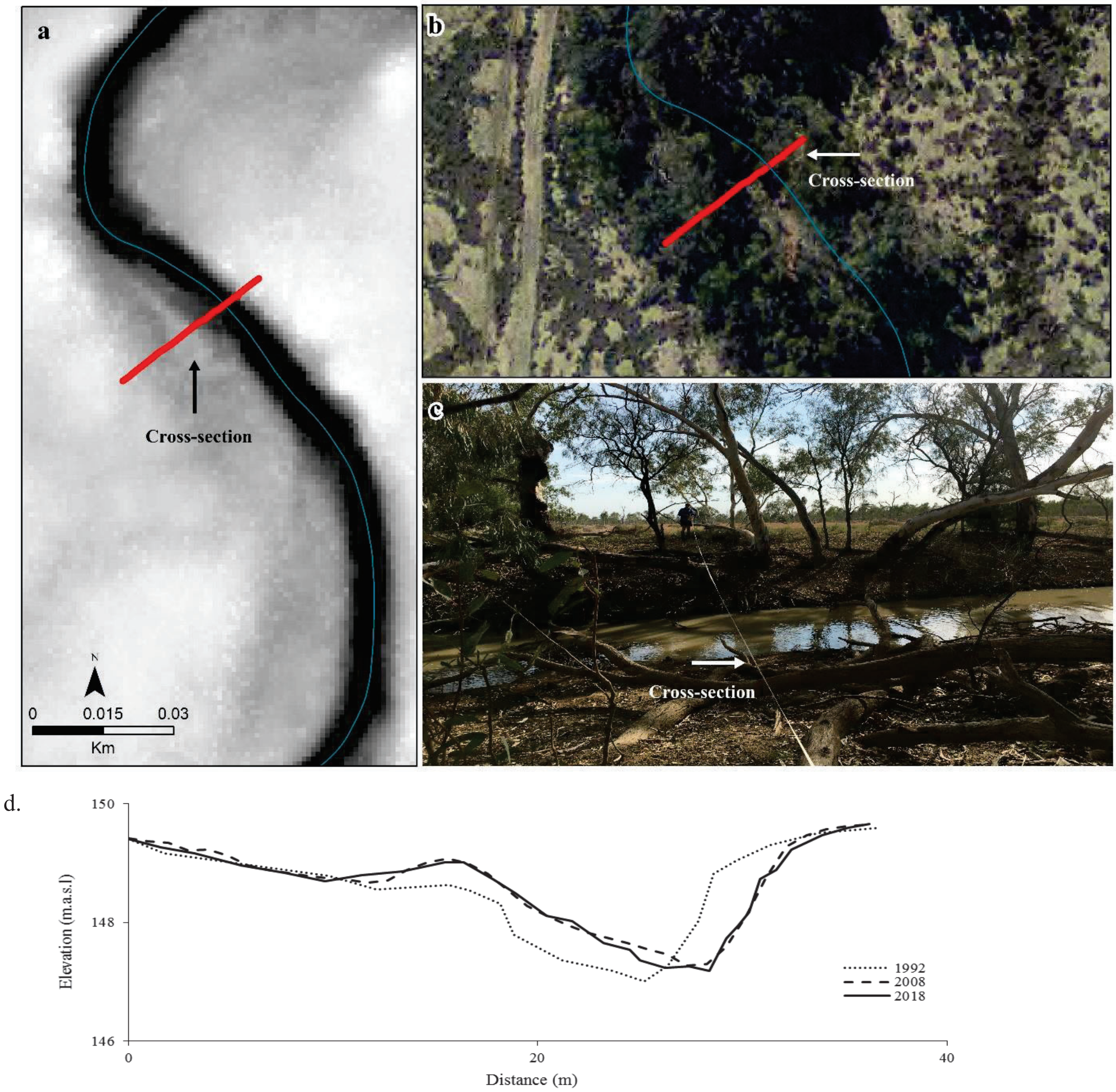

Figure 6.10 Site MR4 located on the Macquarie River downstream of the Old Macquarie River as seen on LiDAR-derived DEM (a), aerial imagery (b) and on the ground (c) and cross-section profile data from 1992 (Brereton, 1994), 2008 and 2018 (d).

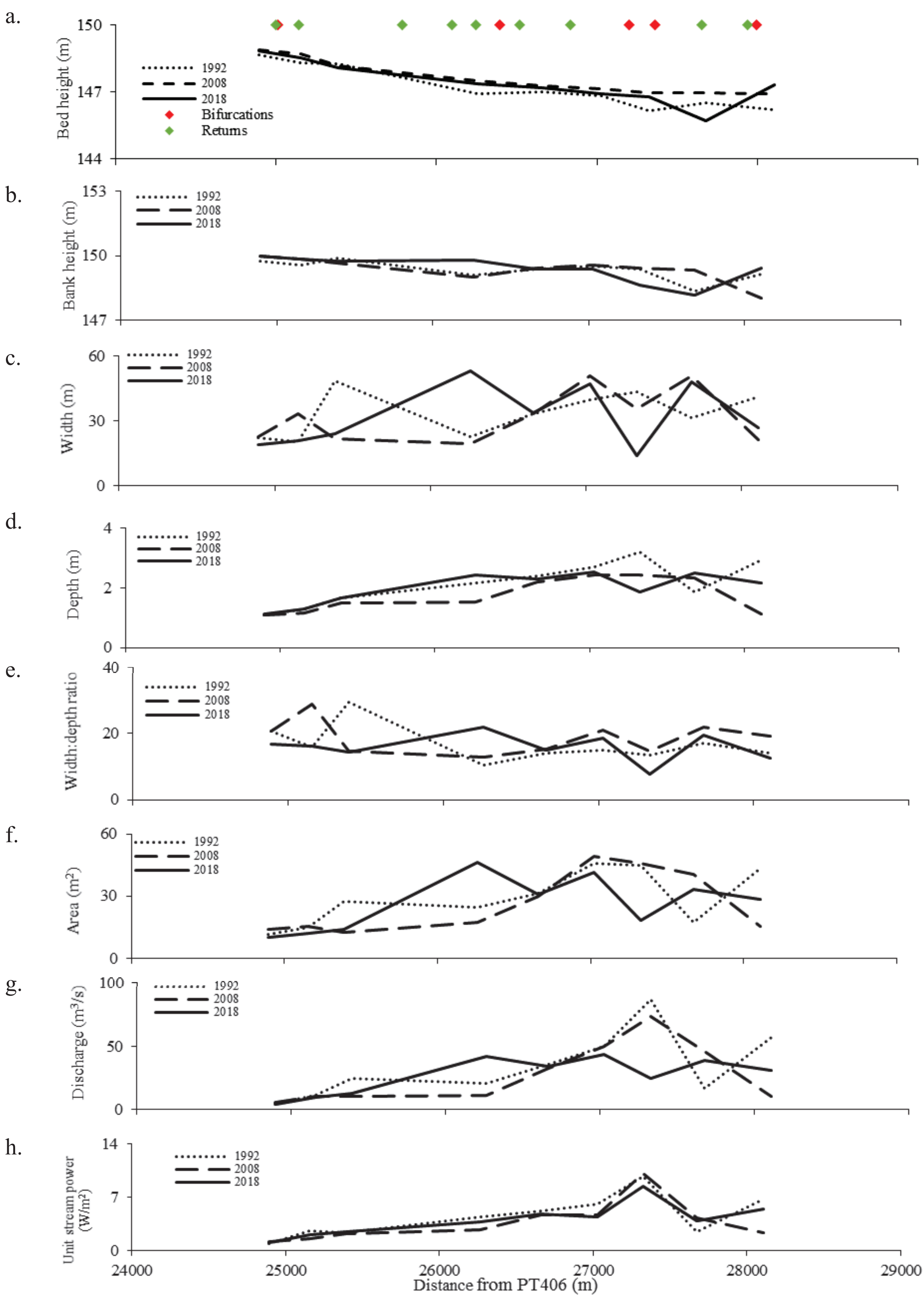

Figure 6.11 The longitudinal profile of bed height (a), bank height (b), channel width (c), channel depth (d), width to depth ratio (e), channel cross-sectional area (f), bankfull discharge (g) and unit stream power (h) for the Macquarie River downstream Old Macquarie in 1992 (Brereton, 1994), 2008 and 2018. The location of PT406 is shown in Figure 6.1A and 6.1B.

6.3 Historical changes at key bifurcations

Several anabranches and distributary channels occur in the Macquarie Marshes, yet before this research project, very few channels at bifurcation points have ever been measured in terms of their channel morphology. However, Ralph (2008) did conduct topographic surveys of channels at two major bifurcation points in 2004. In this section, adjustments in the morphometric and hydraulic character of these two bifurcation points are presented for the period from 2004 to 2018, including where Buckiinguy Creek avulses from the Macquarie River and where The Breakaway avulses from Monkeygar Creek.

6.3.1 Bifurcation of The Breakaway from Monkeygar Creek

The Breakaway diverges from Monkeygar Creek and eventually joins the Macquarie River approximately 7 km downstream. A comparison of the morphology and size of the channels at this avulsion point between 2004 and 2018 are summarised in Table 6.1 and shown in Figure 6.12. These results show that the Monkeygar Creek channel upstream of the avulsion has become 17% narrower and 23% deeper, with a 3% larger cross-sectional area and 32% lower width:depth, while also having 17% greater bankfull discharge and 40% greater unit stream power after 14 years. The two branches downstream of the avulsion point have also changed. The Breakaway channel has become 25% wider and 19% deeper. It has increased by 9% in both cross-sectional area and width:depth ratio and has increased by 19% in discharge and 40% in unit stream power. Monkeygar Creek downstream of the bifurcation has declined by 29% in width, 10% in area and 39% in width:depth ratio, increased by 20% in depth, and maintained its discharge and unit stream power (Table 6.1).

Table 6.1 Comparison of geometric and hydraulic factors at The Breakaway-Monkeygar bifurcation between 2008 and 2018.

Transect	Year	Width (m)	Depth (m)	Area (m^2)	Width:depth ratio	Discharge (m^3/s)	Unit stream power (W/m^2)
Upstream Monkeygar Creek	2008	18.6	1.7	19.8	11	25.3	6.7
	2018	15.4	2.1	20.4	7.5	29.5	9.4
	% change	-17.2%	23.5%	3%	-31.8%	16.6%	40.3%
The Breakaway	2008	14.1	1.6	13.6	8.6	16.9	5.3
	2018	17.6	1.9	14.8	9.4	20.1	7.4
	% change	24.8%	18.8%	8.8%	9.3%	18.9%	39.6%
Downstream Monkeygar Creek	2008	11.9	1.5	10.8	7.7	12.9	5.9
	2018	8.5	1.8	9.7	4.7	12.8	5.6
	% change	-28.6%	20%	-10.2%	-39%	-0.8%	-5.1%

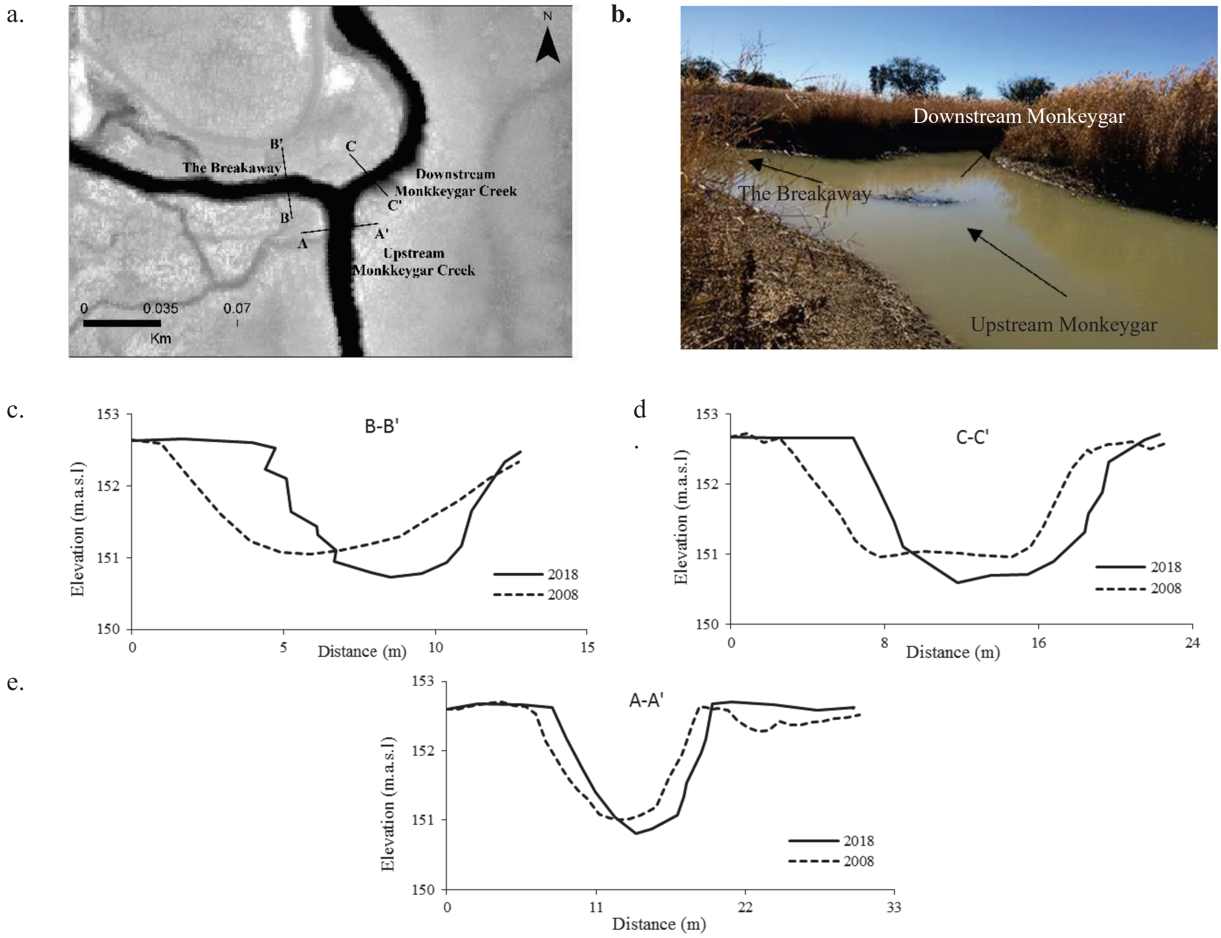

Figure 6.12 Location of the transects at The Breakaway-Monkeygar Creek bifurcation (a), bifurcation as observed in the field (b), transect on The Breakaway (c), transect on the downstream reach of Monkeygar Creek (d) and the transect on the upstream reach of Monkeygar Creek (e).

6.3.2 Bifurcation of Buckiinguy Creek from the Macquarie River

Buckiinguy Creek diverges from the Macquarie River in an anastomosing reach and flows from Buckiinguy eventually re-join the Macquarie River approximately 5 km downstream, via Buckiinguy Swamp and its return channels. A comparison of the morphology and size of the channels at this avulsion point between 2004 and 2018 are summarised in Table 6.2 and shown in Figure 6.13. These results show that the Macquarie River channel upstream of the avulsion has become 14% narrower and 44% deeper, with a 16% larger cross-sectional area and 38% lower width:depth ratio, while also having a 45% greater bankfull discharge and 68% greater unit stream power after 14 years. The two branches downstream of the avulsion point have also changed. The Buckiinguy Creek channel has become 29% narrower and 5% deeper. It has decreased by 21% in cross-sectional area, 34% in width:depth ratio and 18% in discharge and has increased by 14% in unit stream power. The Macquarie River channel downstream of the bifurcation has declined by 17% in width, 33% in area, 23% in width:depth ratio, 30% in discharge and 17% in unit stream power; although, it has increased by 7% in depth between 2004 and 2018 (Table 6.2).

Table 6.2 Comparison of geometric and hydraulic factors at the Buckiinguy Creek-Macquarie River bifurcation between 2008 and 2018.

Transect	Year	Width (m)	Depth (m)	Area (m^2)	Width:depth ratio	Discharge (m^3/s)	Unit stream power (W/m^2)
Upstream	2008	20.9	1.6	20.3	12.7	4.69	0.22
Macquarie	2018	18	2.3	23.5	7.9	6.79	0.37
River	% change	-13.9%	43.8%	15.8%	-37.8%	44.8%	68.2%
Buckiinguy	2008	13.5	1.9	14.6	7.1	4.59	0.5
Creek	2018	9.6	2	11.5	4.7	3.75	0.57
	% change	-28.9%	5.3%	-21.2%	-33.8%	-18.3%	14%
Downstream	2008	16.1	1.5	13.5	10.9	2.92	0.18
Macquarie	2018	13.4	1.6	9.1	8.4	2.06	0.15
River	% change	-16.8%	6.7%	-32.6%	-22.9%	-29.5%	-16.7%

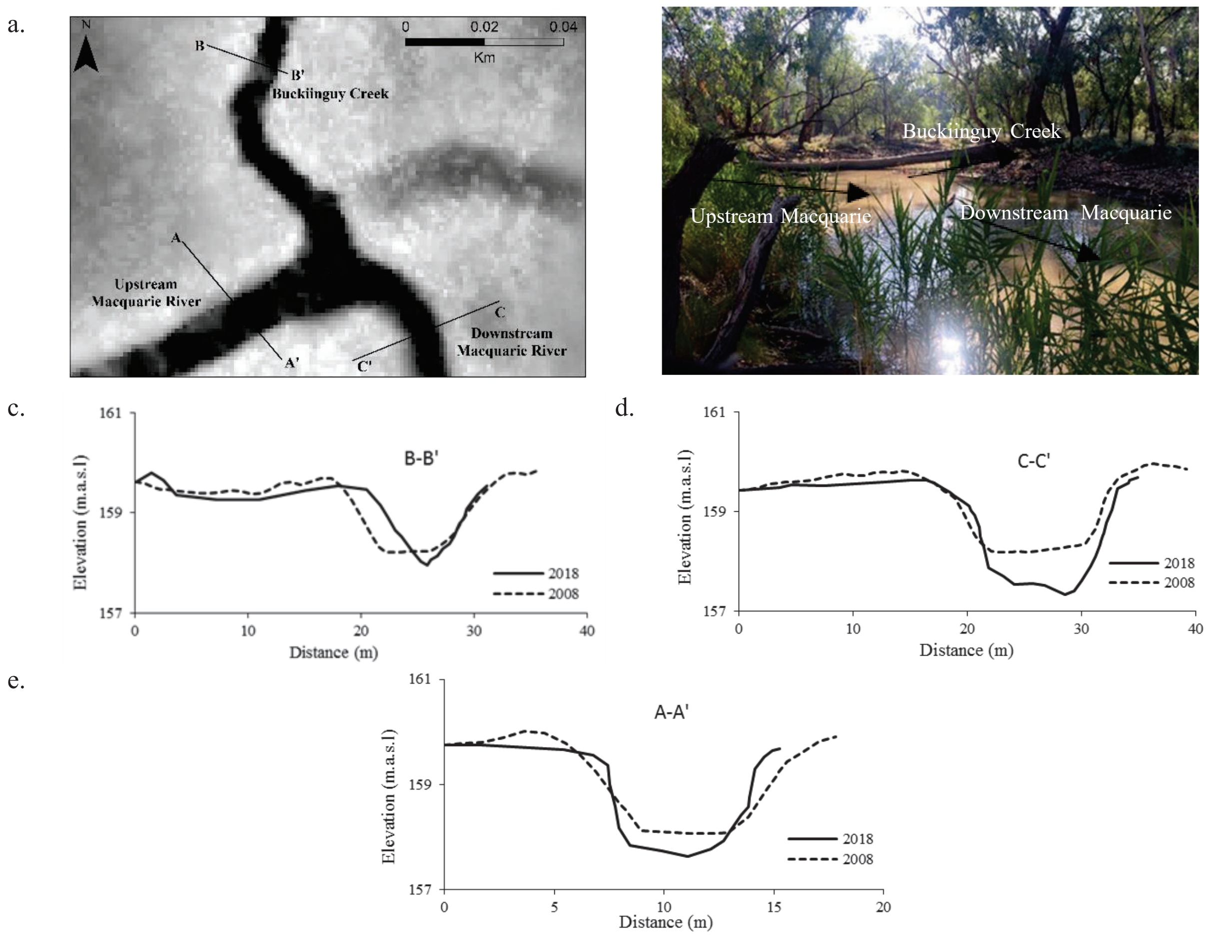

Figure 6.13 Location of the transects at the Buckiinguy Creek-Macquarie River bifurcation (a), bifurcation observed in the field (b), transect on Buckiinguy Creek (c), transect on the downstream reach of the Macquarie River (d) and the transect on the upstream reach of the Macquarie River (e).

6.4 Synthesis of historical channel adjustments

The most pronounced adjustments in channel size from 1992 to 2018 occurred along The Breakaway, which enlarged in channel cross-sectional area between 29 and 95% (Figure 6.14a). Most of the cross-sections on Monkeygar Creek experienced reductions in channel area, some as much as -34%, while channel area in the Macquarie River upstream of Monkeygar Creek increased in places up to 29%. Changes in channel area in the Old Macquarie River, and the Macquarie River downstream of the Old Macquarie, were quite variable, with no consistent trends in channel enlargement or contraction over time (Figure 6.14a).

Bankfull discharge along The Breakaway has increased the most with changes up to 135% (Figure 6.14b). Most of the Monkeygar Creek cross-sections experienced decreases in bankfull discharge of between -45 and 0%, while discharge in the Macquarie River upstream of Monkeygar Creek mostly increased by up to 53%. Discharge in the Old Macquarie River was variable over time and discharge in the Macquarie River downstream of the Old Macquarie River mostly decreased between 1992 and 2018 (Figure 6.14b).

Unit stream power generally declined in The Breakaway from 1992 to 2018 due to widening of the channel (Figure 6.14c). Unit stream power along Monkeygar Creek also decreased with changes between -59 and -32%. Most of the cross-sections on the Macquarie River upstream of Monkeygar Creek also experienced declines in stream power of between -32 and 0%. Unit stream power increased the most along the Old Macquarie River with changes from 31 to 145%. The Macquarie River downstream of the Old Macquarie River had variable changes in stream power over time (Figure 6.14c).

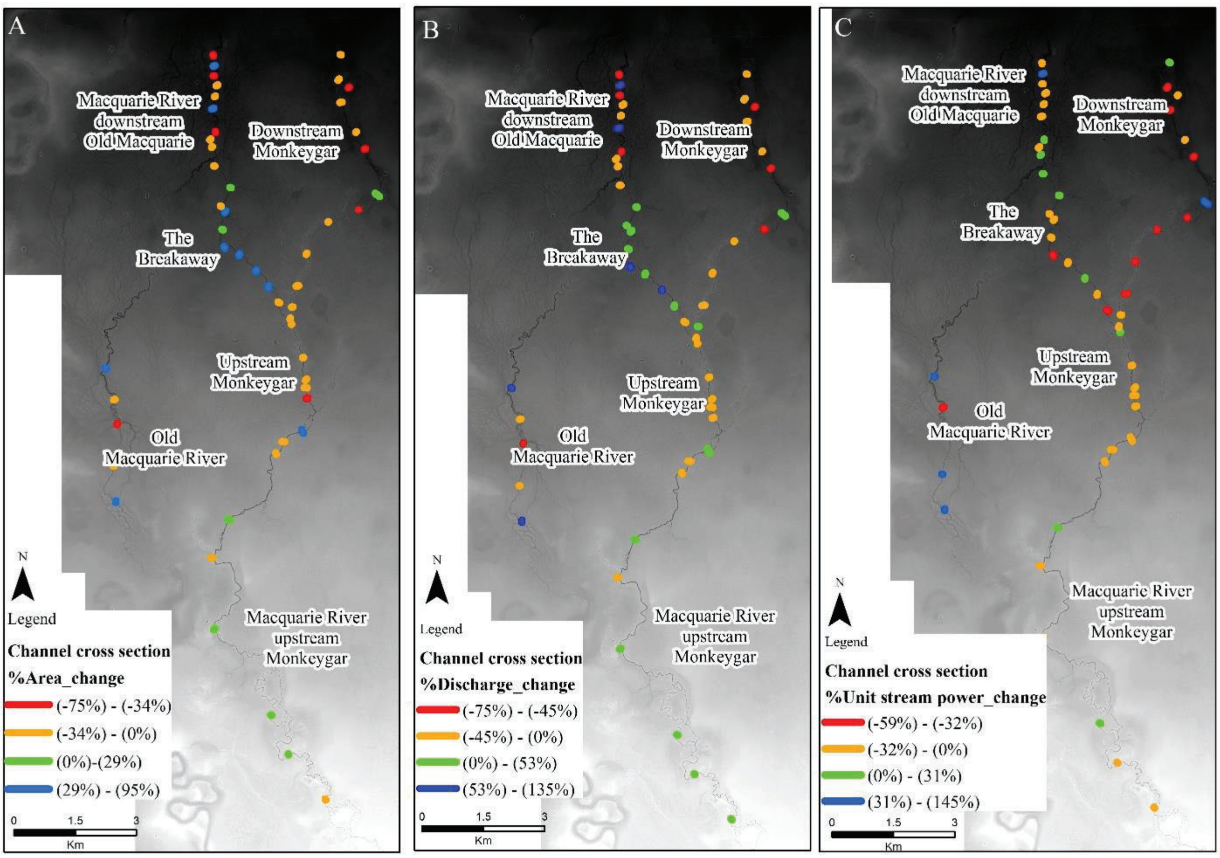

Figure 6.14 Changes in channel cross-sectional area (A), bankfull discharge (B) and unit stream power (C) for the period between 1992 and 2018 along Macquarie River upstream of Monkeygar, Monkeygar Creek, The Breakaway, Old Macquarie River and Macquarie River downstream of the Old Macquarie River.

Channel width increases were also pronounced in the Macquarie River upstream of Monkeygar Creek and through The Breakaway to the beginning of the Macquarie River downstream of the Old Macquarie River. A general reduction in channel width occurred in Monkeygar Creek and the Old Macquarie River. Other channel geometric parameters including bed and bank height and depth were stable in the Southern Macquarie Marshes. Therefore, adjustments in channel area, width-depth ratio, bankfull discharge and unit stream power were mostly affected by local and reach-scale changes in channel width.

At the two key bifurcation points studied, it is clear that both channels upstream of the avulsion points became narrower and deeper over 14 years (Monkeygar upstream: 17% narrower and 23% deeper; Macquarie River upstream: 14% narrower and 44% deeper), and that this translated into increases in channel area and reductions in width:depth ratio (Monkeygar upstream: 3% larger area and 32% lower width:depth; Macquarie River upstream: 16% larger area and 38% lower width:depth). This also translated into changes in hydraulic conditions, with Monkeygar upstream having 17% greater bankfull discharge and 40% greater unit stream power, and the Macquarie upstream having 45% greater discharge and 68% greater unit stream power.

The avulsion channels downstream of the bifurcations behaved differently, however, with The Breakaway off Monkeygar enlarging (25% wider, 19% deeper, 9% greater area and 9% greater width:depth) while Buckiinguy off the Macquarie River decreased in capacity (29% narrower, 5% deeper, 21% lower area and 34% lower width:depth). This translated into The Breakaway increasing by 19% in bankfull discharge and 40% in unit stream power, while Buckiinguy Creek decreased by 18% in discharge and increased by 14% in unit stream power.

Downstream of the bifurcations on the main channels, Monkeygar Creek after The Breakaway declined in capacity (29% narrower, 10% lower area and 39% lower width:depth) but increased in depth (20% deeper) and maintained its bankfull discharge and unit stream power. The Macquarie River after Buckiinguy declined in capacity (17% narrower, 33% lower area and 23% lower width:depth) and in hydraulic conditions (30% lower discharge and 17% lower unit stream power).

6.5 Interpretation

6.5.1 Historical adjustments in channel morphology and hydraulic conditions

Analysis of historical channel adjustment in the Southern Macquarie Marshes from 1992 to 2018 demonstrates that, except for channel expansion and enhanced bankfull discharge in The Breakaway and in places in the Old Macquarie River, and some less pronounced reductions in channel size and discharge in Monkeygar Creek, major changes were not observed in the morphological character of the rivers studied. The overall trend, however, is one of increasing channelization in the system during the period studied. This interpretation of channel adjustments focusses on the overall comparison of changes between 1992 and 2018, because, in several cases, elevation data and subsequent metrics for 2008 obtained from the LiDAR-derived DEM were either much more variable, or quite different at specific locations, than the data derived from field measurements of cross-sections in 1992 and 2018. This is most likely to be an artefact of the LiDAR-derived DEM source data from 2008, which has greater vertical and horizontal inaccuracies than manual topographic surveys, and is known to contain some errors due to dense vegetation and/or water in places throughout the wetlands.

There is a direct relationship between increases in channel size (usually due to increases in channel width) and greater bankfull discharge conditions that could enhance the potential for channels to transmit water and sediment more efficiently. This is reflected by the unit stream power estimates, which also vary according to channel size; for example, channels (including Monkeygar Creek and the Macquarie River upstream of key bifurcations) became narrower and deeper leading to greater channel area, bankfull discharge and stream power. The Breakaway also enlarged significantly in channel capacity, leading to greater bankfull discharge and unit stream power conditions. However, unit stream power does not necessarily depend on the total channel size, rather, changes in width:depth ratio are critical. For example, Buckiinguy Creek off the Macquarie River decreased in capacity and discharge, yet still increased in unit stream power. Therefore, changes in channel width play a critical role in changing the rate of energy dissipation against the bed and banks, leading to changes in the potential for erosion and channelization to occur. This means that if an increase in channel size mostly depends on an increase in channel width (width:depth ratio increases), then this may cause a reduction in unit stream power.

A major implication of the increases in channel capacity and associated increases in bankfull discharge in several channels, particularly in The Breakaway, is that in most cases in 2018 it would take greater flows to achieve bankfull conditions at the same location than it would have in 1992. The impact of this is that the ability and/or likelihood of overbank flows has declined in this part of the Macquarie Marshes since 1992. Since overbank flows are essential for maintenance of the surrounding wetlands, this could be a major issue for habitat and biodiversity.

6.5.2 Historical adjustments at bifurcations

An analysis of historical morphological and hydrological changes at two avulsion points provided different scenarios of channel behaviour. Both channels entering the bifurcations have experienced channel enlargement with associated increases in hydraulic conditions, probably related to channel expansion along the lower Macquarie River more broadly. This channel expansion may be due to the dominance of low-level flows in the system during prolonged droughts (for example, from 2002 to 2009), and to flows that concentrate their energy within the banks and may lead to bed erosion and bank undercutting. Where The Breakaway avulses from Monkeygar Creek, it is clear that channel enlargement and flow capture has occurred in The Breakaway, causing a reduction in channel capacity in the downstream reach of Monkeygar Creek (probably due to a combination of in-channel sedimentation and vegetation growth).

However, where Buckiinguy Creek avulses from the main Macquarie River, both downstream branches have experienced channel contraction and a net reduction in bankfull discharge. This may mean that another branch of the Macquarie River in this anastomosing reach may be slowly taking flow from the branch that presently feeds Buckiinguy Creek. The areas where these avulsions occur also have different types of vegetation (The Breakaway has more marsh with in-channel and floodplain reeds, while Buckiinguy has river red gum woodland with in-channel reeds) so it would translate that vegetation and other factors will affect the modes and impacts of the bifurcations leading to anastomosis or channel breakdown. Nevertheless, the avulsions seem to be well-established and it is likely that the system is adjusting to a new level of stabilisation, which equates to a new dynamic equilibrium. This would define a medium-term dynamic equilibrium in this system.

6.6 Summary

This chapter quantified the morphometric and hydraulic characteristics of channels in the Southern Macquarie Marshes and presented evidence of recent historical channel change using data from two field surveys in 1992 and 2018, and LiDAR-derived DEM in 2008. Evidence for channel expansion and contraction was found in the system, and channelization seems to be the general trend in this part of the Macquarie Marshes, leading to the need for greater flows to achieve bankfull discharge conditions in 2018, as opposed to 1992. Key bifurcations are slowly adjusting their morphology in response to wider changes to the flow in the system. In the next chapter, key sites along hyper-avulsive reaches in the Southern Macquarie Marshes are investigated to identify contemporary trajectories of channel behaviour and to rank channels according to the likelihood and consequences of channel change.

Chapter 7: Rapid assessment of key hazards and risks associated with channels in the Southern Macquarie Marshes

7.1 Introduction

This chapter presents the findings of the erosion risk assessments that were undertaken at 20 sites in 2012 and 2018. Erosion is particularly harmful to wetland ecosystems where channels become so deep and wide that the surrounding floodplain is cut off from overbank flows (i.e. where wetlands become disconnected from the channels). Sedimentation is also considered a problem, for example, where sediment plugs lead to channels becoming infilled and choked with vegetation, causing flow diversion. Both erosion and sedimentation are pronounced in the Southern Macquarie Marshes, and so observations of erosion, sedimentation and channel change, and an interpretation of the likely impacts of these processes, allow key sites to be identified as priority sites for monitoring and management. The following aims are addressed:

3. *To identify contemporary trajectories of channel behaviour in hyper-avulsive reaches of the Southern Macquarie Marshes and to explain the role of erosion in the system;*
4. *To assess erosion and sediment deposition risk at key sites in the Southern Macquarie Marshes and to rank channels according to the likelihood and consequences of channel change.*

7.2 Site conditions during the rapid assessment fieldwork

Twenty sites (including three observations at each site, spaced <50 m downstream) in the Southern Macquarie Marshes were assessed visually for evidence of erosion and sedimentation in 2018 (Figures 7.1 and 7.2). These assessments were repeats of those originally conducted in 2012, when 19 sites were identified by Ralph et al. (2013) for erosion risk assessment using feedback from landholders and wetland managers, as well as previous geomorphic research and local knowledge of the area. An additional site was identified in 2013 by Oyston et al. (2014) as being of particular significance and as a threat due to erosion near Buckiinguy Swamp; it was added to the list created by Ralph et al. (2013) and included in this research.

Site accessibility and visibility required for visual assessments are influenced by the flow conditions at the time of the field visits, as are some of the findings, such as water quality and interpretations of bank stability based on measurements of bank strength in dry (or wet) bank sediments. Flow in the Macquarie River was different during the two field seasons; in 2012 there was moderate flow in the system, with discharge >1000 ML/day at Oxley (Figure 7.3). In contrast, in 2018, flow was lower throughout the Macquarie Marshes, with discharge <500 ML/day at Oxley. Flow was not measured directly at the field sites, but relative measures were noted including when the bed and lower/middle/upper banks were wet or actually inundated. Generally, in 2012, the upper one-third of the banks were exposed for visual assessment and the lower two-thirds of the banks and the bed were underwater (and, therefore, unable to be assessed visually); whereas in 2018, most sites had flow over the bed and up to the lower one-third of the banks only, and the top two-thirds of the banks were exposed for rapid field assessment (Figure 7.4).

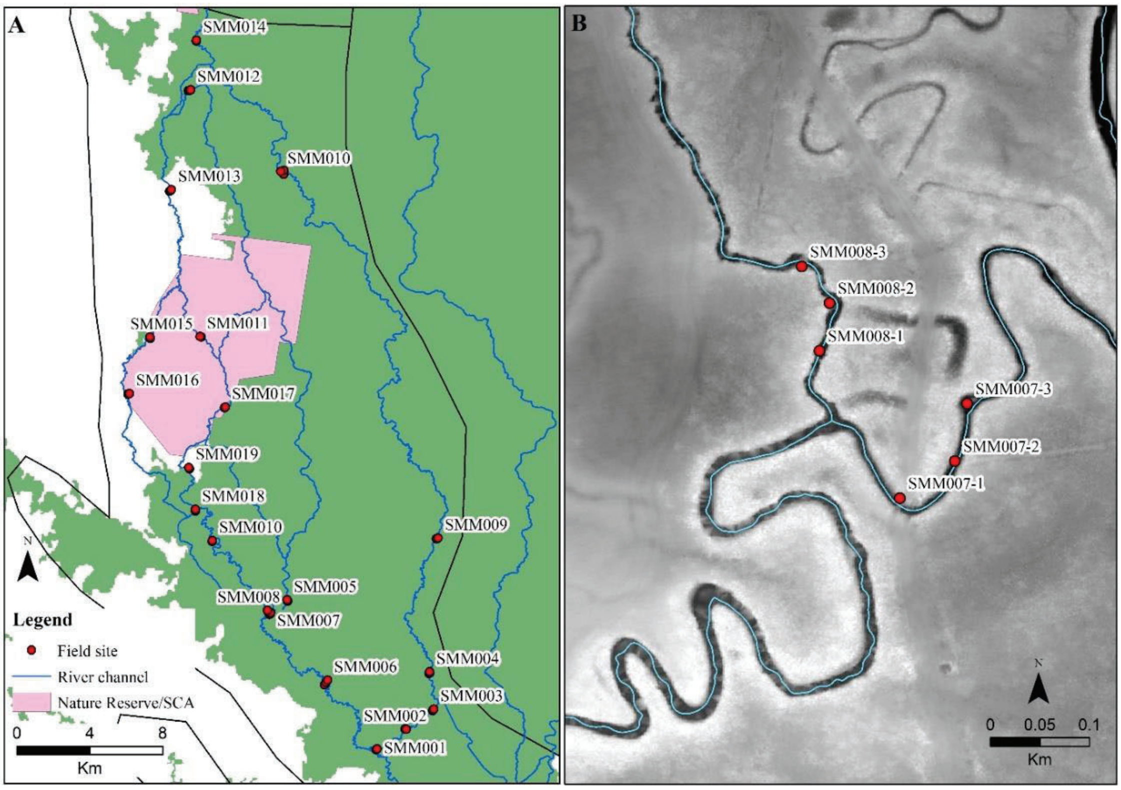

Figure 7.1 Rapid assessment site locations in the Southern Macquarie Marshes (a) and an example of three observations taken in downstream order at two sites, SMM007 and SMM008 (b).

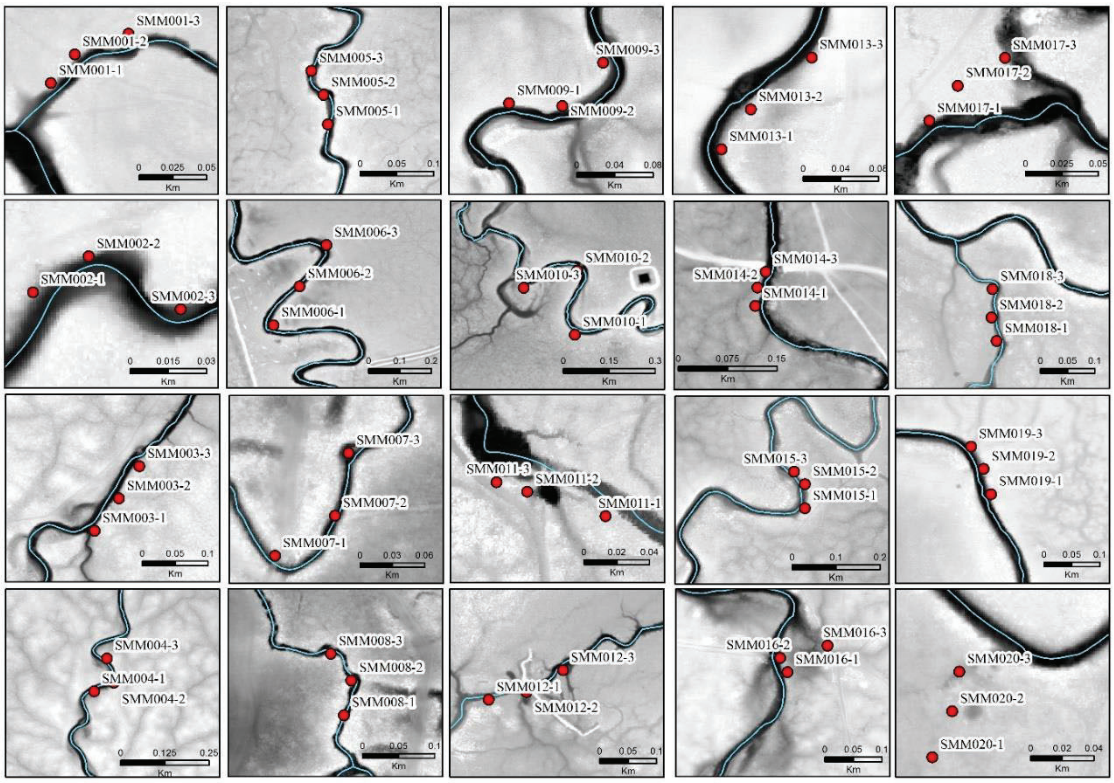

Figure 7.2 Maps of all rapid assessment sites in the Southern Macquarie Marshes (locations shown on Figure 7.1a and listed in Table 7.1).

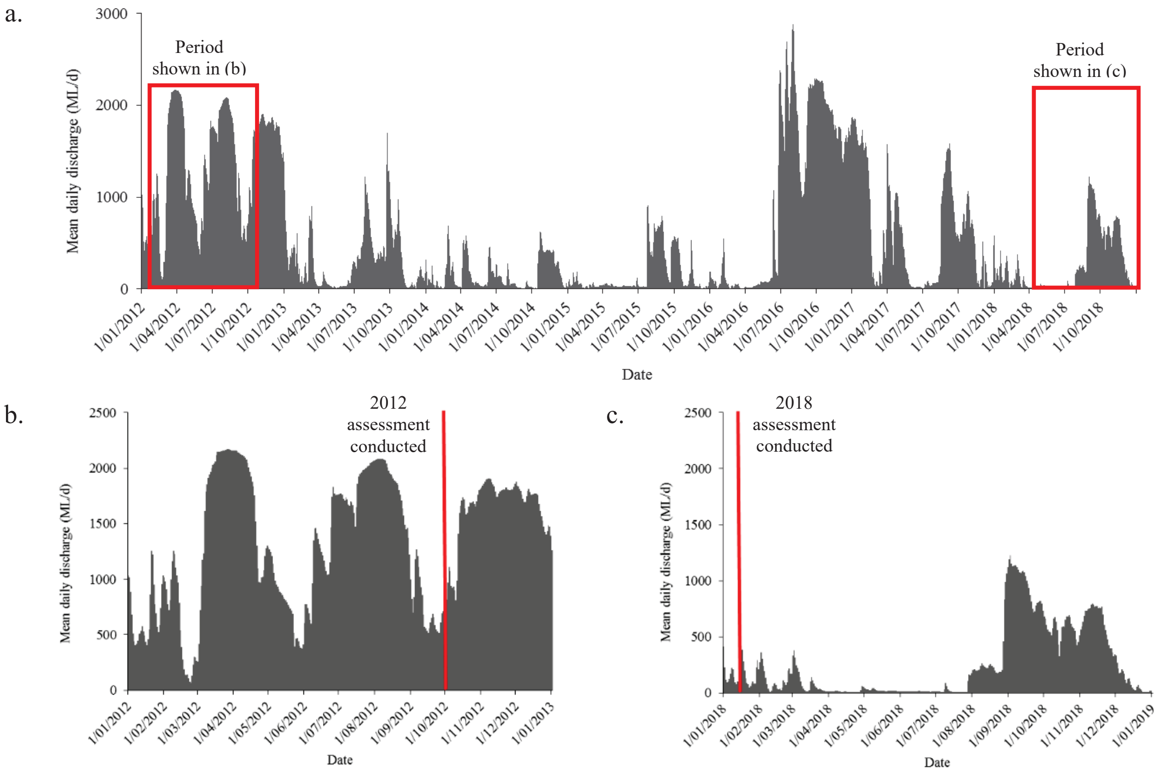

Figure 7.3 Discharge at Oxley Station (421022), entering the Southern Macquarie Marshes from 2012 to 2018 (a), discharge at Oxley from January to December 2012 (b) and discharge at Oxley from January to December 2018 (c). Red lines show the timing of rapid field assessments. Data from WaterNSW (2019).

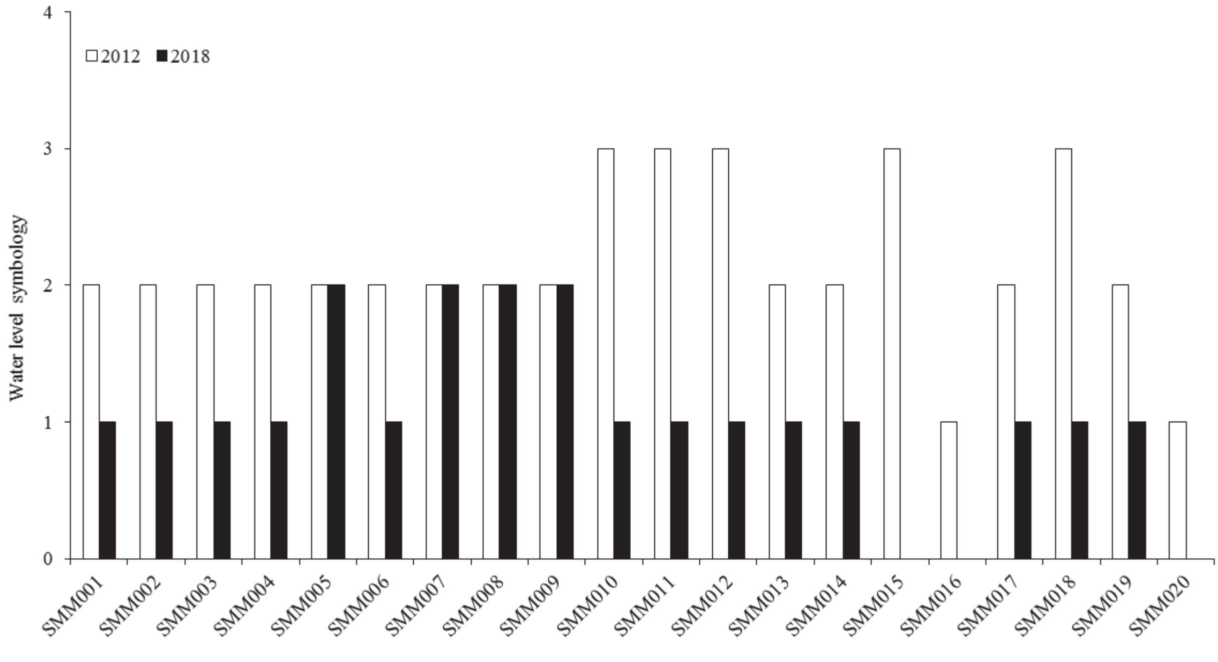

Figure 7.4 Water level at the rapid assessment study areas at the time of the field visits. Water level symbology: 0 = Channel dry and no water, 1 = Bed and lower banks covered by water, 2 = Bed and lower-middle banks covered by water, 3 = Bed and middle-upper banks covered by water and 4 = Overbank flow. Data from 2012 (Ralph et al., 2013).

Water temperature varied at the sites depending on the time of sampling (for example, morning, midday and evening) and other local factors, such as shading, turbidity and the velocity of flow (these contributing factors are not measured at the field sites). The 2018 survey was performed during summer when the Old Macquarie River and other sites were dry; therefore, the water quality parameters could not be measured for these sites. The pH of the water ranged from 7.8 to 8.5 (Table 7.1), and none of the sites exceeded the ANZECC (2000) trigger value for lowland river ecosystems of pH 9.0. Electrical conductivity (EC) results were in the upper normal range for freshwater systems at most sites and were higher on average in 2012. Comparison of mean values of pH and EC in 2012 and 2018 show consistency overall, and there were no systematic variations or strong correlations at the sites for pH in 2012 and 2018, or EC in 2012 and 2018 (Figure 7.5).

Table 7.1 Summary of the water conditions in the Southern Macquarie Marshes during 2012 and 2018.

Channel	**Site code**	**Water condition**					
		2012			**2018**		
		Temp. (˚C)	**pH**	**EC (µS/cm)**	**Temp. (˚C)**	**pH**	**EC (µS/cm)**
Upper Oxley Break	SMM001	19.8	8.3	424	-	-	-
Middle Oxley Break	SMM002	19.8	8.3	410	-	-	-
Lower Oxley Break	SMM003	18.3	8.3	417	21	8.5	355
Bulgeraga Creek downstream of Oxley Break	SMM004	18.9	8.4	400	-	8.5	590
Monkey Creek	SMM005	19.0	8.3	417	27.3	8	295
Macquarie River downstream of Oxley Break and upstream of Monkey Creek	SMM006	17.4	8.2	412	27	8	298
Macquarie River downstream of Monkey Creek and downstream of Buckiinguy Creek	SMM007	18.3	8.4	410	22.7	7.9	211
Buckiinguy Creek	SMM008	18.3	8	413	24.8	7.9	290
Bulgeraga Creek downstream of Oxley Break	SMM009	19.6	8.5	402	-	8.4	657
Bulgeraga Creek at Willancorah (downstream of Gibson Way)	SMM010	17	8.2	426	25.5	8.2	313
The Breakaway	SMM011	19.5	8.1	445	-	8.4	668
The Mole reed bed outflow channels	SMM012	16.6	8.1	454	dry	dry	dry
Macquarie River at Maxwelton and The Mole	SMM013	16.6	8.2	444	23	7.8	362
Macquarie River at Pillicawarrina	SMM014	19.1	8.2	440	26.8	8.3	381
Old Macquarie River in Nature Reserve (near Willie)	SMM015	16.5	8.1	618	dry	dry	dry
Old Macquarie River in Nature Reserve (Boss' Crossing)	SMM016	15.8	7.9	684	dry	dry	dry
Monkeygar Creek upstream of The Breakaway in Nature Reserve	SMM017	17.7	8.2	413	22.7	8.1	225
Buckiinguy Return and Buckiinguy Runner	SMM018	11.4	8.2	503	23.8	7.9	438
Macquarie River downstream of Monkey Creek and downstream of Buckiinguy Creek	SMM019	15.6	8.4	409	27	8.2	326
Buckiinguy Swamp (knickpoint at eastern outlet)	SMM020*	-	-	-	dry	dry	dry
Mean value (standard deviation)		**17.6 (2.0)**	**8.2 (0.2)**	**449.5 (75.7)**	**24.7 (2.2)**	**8.2 (0.2)**	**386.4 (149.2)**

Notes: Data from 2012 (Ralph et al., 2013). *Site added in 2013 (Oyston et al., 2014).

a.

b.

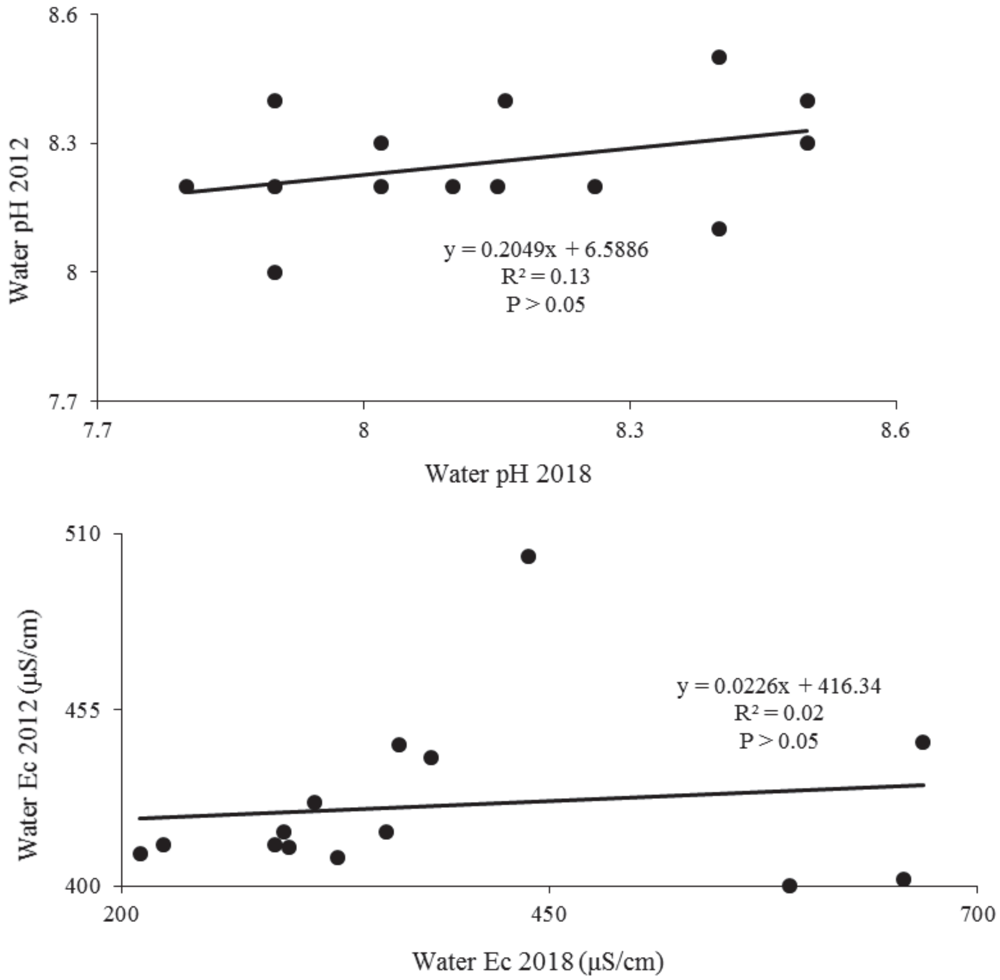

Figure 7.5 Correlation of pH (a) and EC (b) in 2012 and 2018 at the rapid assessment sites. Data from 2012 (Ralph et al., 2013).

7.3 Geomorphic assessment

7.3.1 Visual assessment of features indicating erosion and sedimentation

Various geomorphic features, such as flow entry and exit points, anthropogenic modifications, vegetation cover and roughness were investigated at the study sites and compared with the previous results from 2012. Bank morphology and the presence/absence and position of flow entry and exit points were stable over this short-term timescale (i.e. 2012-2018). Other sites exhibited only small changes, except for the small earth weir that was located at Macquarie River downstream of Buckiinguy Creek (SMM007), which was removed or destroyed by flooding between 2012 and 2018 (Figures 7.6a and 7.6b). Small tracks were also observed at SMM010 and SMM011 in 2018 (Table 7.2). At almost all the sites there was a consistent decline in roughness (Manning's n) between 2012 and 2018, which takes into account vegetation cover, substrate type, river planform and sinuosity, among other factors. Of the factors contributing to Manning's n, vegetation was the only one that changed at the sites, being less dense in 2018 than in 2012 due to drought.

a.

b.

Figure 7.6 Macquarie River downstream of Buckiinguy Creek (SMM007) looking upstream in 2012 when the earth weir was present (a) and in 2018 (b) when the earth weir was absent. Photographs by Tim Ralph.

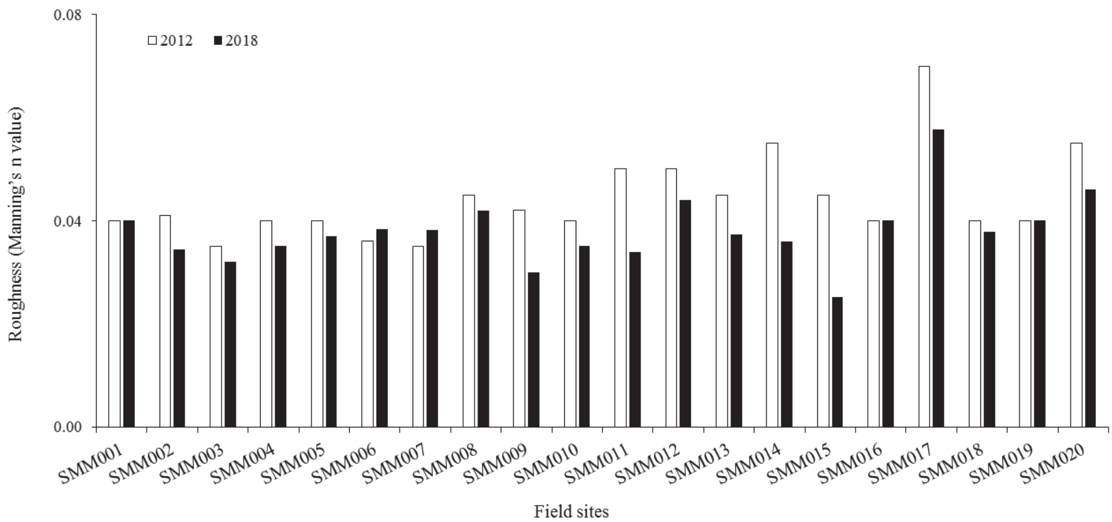

Figure 7.7 Comparisons of roughness (Manning's n value) at the field sites in 2012 and 2018. Data from 2012 (Ralph et al., 2013).

Table 7.2 Summary of major geomorphic features in 2012 and 2018 in the Southern Macquarie Marshes.

Site code	Bank shape	Modification		Roughness (Manning's n value)		Vegetation	Flow entry and exit points
	2012 & 2018	2012	2018	2012	2018	2012 & 2018	2012 & 2018
SMM001	S, V, U	Track u/s	Track u/s	0.040	0.040	RRG, debris	Entry d/s
SMM002	S	-	-	0.041	0.035	RRG, debris	Exit u/s, d/s
SMM003	S, V	-	-	0.035	0.032	RRG, debris	Entry u/s, d/s
SMM004	S, V	-	-	0.040	0.035	RRG, grass	Entry u/s, d/s; Exit u/s, d/s
SMM005	S, V	Bridge u/s	Bridge u/s	0.040	0.037	RRG, debris	-
SMM006	S	-	-	0.036	0.038	RRG, grass	Entry u/s, d/s
SMM007	S	Earth weir	Track	0.035	0.038	RRG, debris	Exit d/s
SMM008	S, V	-	-	0.045	0.042	RRG, debris	-
SMM009	S, V	-	-	0.042	0.030	Grass, debris	Entry d/s
SMM010	S	-	Track	0.040	0.035	RRG, debris	Entry d/s; Exit d/s
SMM011	S, V, U	Rock Weir	Rock Weir, Track	0.050	0.034	Grass, debris	Entry u/s, d/s; Exit d/s
SMM012	S, V	Rock weir, artificial banks	Rock weir, artificial banks	0.050	0.044	Reeds, grass	Entry u/s, d/s; Exit u/s, d/s
SMM013	S, V	Willows	Willows	0.045	0.037	RRG, debris	Entry u/s, d/s; Exit u/s, d/s
SMM014	S, V, U	Bridge d/s	Bridge d/s	0.055	0.036	RRG, debris	Entry u/s, d/s
SMM015	S	-	-	0.045	0.025	RRG, grass	Exit u/s, d/s
SMM016	S	Track	Track, culvert	0.040	0.040	RRG, grass, debris	Entry u/s, d/s; Exit u/s
SMM017	S, V	Willows	Willows	0.070	0.058	RRG, debris	Entry u/s, d/s; Exit u/s, d/s
SMM018	S	Rock weir u/s	Rock weir u/s	0.040	0.038	RRG, debris	Entry u/s, d/s
SMM019	S	Bridge	Bridge	0.040	0.040	RRG, debris	Exit d/s
SMM020	S	Weir, Track	Weir, Track	0.055	0.046	RRG, grass, debris	Entry

Notes: 'S' = Sloping, 'V' = Vertical, 'U' = Undercut, 'd/s' = Downstream, 'u/s' = Upstream, 'RRG' = River red gum (the rapid assessment form and explanations of these categories can be found in Appendix 1); Orange = Change. Data from 2012 (Ralph et al., 2013).

Erosion, sedimentation and sub-aerial features were also surveyed and compared in 2012 and 2018. Erosion features noted during assessments include exposed knickpoints, ledges or benches, bank breaches, bank retreat (general face sour), bank rilling (scour down face), bank failure (slumping or toppling), bank undercutting and exposed tree roots (Figure 7.8a). Sedimentation features represent unconsolidated sediment in the channel (Figure 7.8b), channel blockages, benches or bars, natural levees, splays (overbank or on the floodplain) and recent overbank deposition. Sub-aerial features include tunnelling (holes at the top of the bank; Figure 7.8c), compaction, animal trails (trampling or pugging) and other disturbances. For these processes, 'minor' means they occupy or affect <10% of channel or banks, 'moderate' refers to 10 to 25% and 'major' means >25% impact. However, the definitions of these terms vary for other features (Appendix 1). Erosional features were mostly consistent between surveys, although erosion was more pronounced in 2018 at SMM005, SMM008 and SMM020. SMM001, SMM003, SMM004, SMM006 and SMM014 had a reduction in erosion features since 2012. For sedimentation, most sites had no change or a slight increase in depositional features, while sub-aerial features were highly variable (Table 7.3).

Oyston et al. (2014) monitored erosion at a knickpoint at the north eastern perimeter of site SMM020 from 2013 to 2014 using a combination of topographic surveys, erosion pin surveys and fixed-point time-lapse photography. They found significant and highly variable rates of erosion (for example, headcut retreat rates from 2 to 29.5 mm/day; equating to 0.73 to 10.7 m/year) and significant changes in channel morphology (for example, width change varied at sites during the study from a 71% reduction to a 13% gain, and depth varied from a 85% reduction to a 25% gain) (Oyston et al., 2014). This site was again surveyed in 2018 and the results showed an increase in erosional features and moderate sub-aerial features (Figure 7.8d).

Table 7.3 Summary of erosion, sedimentation and sub-aerial features in 2012 and 2018.

Site code	Erosional features		Sediment deposition features		Sub-aerial features	
	2012	2018	2012	2018	2012	2018
SMM001	Major	Moderate	-	Moderate	Moderate	Major
SMM002	Major	Major	-	Minor	Minor	Minor
SMM003	Moderate	Minor	-	Minor	Moderate	Minor
SMM004	Major	Moderate	Major	Moderate	Moderate	Moderate
SMM005	Moderate	Major	Moderate	Minor	Moderate	-
SMM006	Moderate	Minor	Moderate	Moderate	Moderate	Moderate
SMM007	Moderate	Moderate	Moderate	Moderate	Minor	Minor
SMM008	Minor	Moderate	-	Minor	-	Minor
SMM009	Major	Major	Moderate	Moderate	Moderate	Minor
SMM010	Moderate	Moderate	Minor	Minor	Moderate	Minor
SMM011	Major	Major	Minor	Moderate	Minor	Moderate
SMM012	Major	Major	Moderate	-	Major	Major
SMM013	Minor	Minor	Moderate	Moderate	Moderate	Moderate
SMM014	Major	Moderate	-	Minor	-	-
SMM015	-	-	-	-	-	Minor
SMM016	Minor	Minor	-	Minor	Moderate	Moderate
SMM017	Moderate	Moderate	Minor	Moderate	Minor	Moderate
SMM018	-	-	-	-	-	Minor
SMM019	Minor	Minor	-	-	Minor	Minor
SMM020	-	Major	-	Minor	-	Moderate

Notes: White = No change, Orange = Increase, Green = Decrease. Data from 2012 (Ralph et al., 2013).

a.

b.

c.

d.

Figure 7.8 Photographs from 2018 of exposed tree roots at upper Oxley Break (SMM001) showing evidence of erosion (a), unconsolidated sediment in the channel at middle Oxley Break (SMM002) showing sedimentation (b), tunnelling and cracking on the bank at Bulgeraga Creek downstream of Oxley Break (SMM004) showing sub-aerial processes, and the eroding knickpoint and widening channel at the north-eastern outlet of Buckiinguy Swamp (SMM020) (d).

7.3.2 Assessment of bank strength

All of the channel banks in the Southern Macquarie Marshes are dominated by muddy sediment (i.e. clay and silt; <63 μm). Soil surface conditions and bank strength was assessed using two factors, undrained shear strength and compressive strength. These differed between the field sites and changed slightly over the six years from 2012 to 2018 (Table 7.4). 'Undrained shear strength' is a term used to describe the amount of horizontal pressure that a soil or sediment can undergo before it normalises the pore water pressure and dissipates (Ralph et al., 2013). The results from 2012 show that the majority of upper bank sediments (dry when sampled) had moderate or relatively high shear strength (>60 kPa), while the middle bank sediments (wet when sampled) had low or very low shear strength (<30 kPa). Shear strength measurements of the same banks in 2018 show lower values of upper bank shear strength for most of the sites (Figure 7.9). However, sites SMM006, SMM012, SMM016, SMM019 and SMM020 had higher upper bank shear strength in 2018. Site SMM009 on Bulgeraga Creek and site SMM012 at The Mole reed bed outflow channels experienced the lowest and highest value of shear strength in 2018, respectively. The greatest decline in upper bank shear strength in six years occurred at site SMM009 and the greatest increase in upper bank shear strength during the assessment period occurred at site SMM020 (Figure 7.9). The middle bank sediments showed significantly higher values of shear strength in 2018 compared with 2012 (Figure 7.10). However, sites SMM005, SMM007, SMM008 and SMM009 had lower values in 2018 compared to 2012. Site SMM007 on the Macquarie River downstream of Monkey Creek and downstream of Buckiinguy Creek and site SMM011 at The Breakaway experienced the lowest and highest values in 2018, respectively. The most negative change for upper bank shear strength in six years was at site SMM007 and the most positive change during the assessment period occurred at site SMM011 (Figure 7.10).

'Compressive strength' represents the degree of compressive pressure (downward pressure) that a soil or sediment can sustain without severe compaction. The results from 2012 show that the majority of upper bank sediments had moderate or relatively high compressive strength (>3.5 kg/cm^2), while all of the middle bank sediments had very low compressive strength (<1 kg/cm^2) since they were wet when sampled. The results from 2018 show an overall reduction in upper bank compressive strength (Figure 7.11). However, sites SMM015, SMM016 and SMM020 show an increase in compressive strength in the upper bank. Sites SMM002 and SMM011 showed the lowest and highest values in 2018, respectively. The greatest change in compressive strength in upper bank sediments occurred at site SMM020 (Figure 7.11). Middle bank compressive strength was significantly higher at all sites in 2018 (Figure 7.12). However, sites SMM005, SMM007 and SMM008 all had similarly low values. The greatest change in compressive strength in middle bank sediment occurred at site SMM020 (Figure 7.12).

The relationship between compressive and shear strength for all bank sediments are significant and show that the sites with higher shear strength also tend to have higher compressive strength, both in 2012 (Figure 7.13a) and in 2018 (Figure 7.13b). It is also clear that dry bank sediments have higher shear and compressive strength than wet bank sediment.

Table 7.4 Summary of bank sediment composition and strength in 2012 and 2018 for the Southern Macquarie Marshes.

Site code	Soil surface condition at top of bank		Upper bank				Middle bank			
	2012	2018	Undrained shear strength (kPa; mean ± SE)		Compressive strength (kg/cm^2; mean ± SE)		Undrained shear strength (kPa; mean ± SE)		Compressive strength (kg/cm^2; mean ± SE)	
			2012	2018	2012	2018	2012	2018	2012	2018
SMM001	Small cracks	-	88 ±6.6	69.7±10.8	>5	3.5±0.6	11.7±1.5	59.2±6.7	0.2±0.1	2.3±0.4
SMM002	Deep cracks	Small cracks	43.3±7	43.5±5.3	2.8±0.7	1.1±0.1	14±2.3	46.5±11.1	0.1±0.03	1.3±0.4
SMM003	Small cracks	Large cracks	47.7±5.5	38.7±6.2	4.2±0.4	1.1±0.2	12.3±1.6	36.7±5.1	0.2±0.1	0.9±0.1
SMM004	Large cracks	Friable topsoil/very hard subsoil	62±9.6	44.2±10.9	>5	2.1±0.5	18.7±3.6	40.3±16.2	0.1±0.1	2.5±0.7
SMM005	Small cracks	Small cracks	88.7±11.8	48.5±10.5	4.5±0.2	1.4±0.3	15.7±1.2	13.7±1.2	0.1±0.04	0
SMM006	Small cracks	-	72.3±14	76.3±7.3	4.4±0.3	2.5±0.8	13.7±2.9	65±17.6	0.03±0.02	2.7±0.7
SMM007	Cracks	-	67.7±6.3	55±7.6	>5	2.2±0.6	16±2.3	9±1.3	0.3±0.1	0
SMM008	Small cracks	-	100.8±6.8	58±8.2	4.7±0.2	2.7±0.5	17.5±2	11.7±1.1	0.03±0.03	0
SMM009	Small cracks	Small cracks	106.7±6.4	26.5±5.9	>5	2±0.5	13.3±2.8	12.2±2.5	0.1±0.1	0.2±0.2
SMM010	Small cracks	Small cracks	>115	84.2±6.1	>5	1.9±0.6	17.7±2.5	77.5±6.4	0.1±0.04	1.2±0.2
SMM011	Small cracks	Small cracks	108.8±6.3	99.3±20.7	no data	3.9±0.8	17.2±3	100±20	no data	4.3±0.2
SMM012	Small cracks	Small cracks	99±11.1	105±11.9	3.8±0.5	3.5±0.3	19.8±3.8	93.8±16	0.3±0.1	3.9±0.3
SMM013	Small cracks	Small cracks	83.5±8.5	68.5±5.8	2.4±0.7	1.2±0.4	12±1.9	59.7±10.8	0.1±0.04	1.5±0.3
SMM014	-	-	71.7±6.5	68.3±16.4	4.3±0.4	2±0.6	14.8±0.7	60.7±16.7	0.03±0.03	2±0.0
SMM015	Small cracks	Small cracks	88.8±9.3	60.7±3.5	1.3±0.4	1.7±0.3	12.3±2	75.3±13.4	0.2±0.1	3.3±0.7
SMM016	Small cracks	Small cracks	68.3±7.2	81±19.3	0.8±0.1	2.3±0.7	27.3±6.7	54.7±11.3	0.7±0.4	2.7±0.1
SMM017	Small cracks	-	70.7±14.5	47±7.6	2.6±0.7	1.9±0.4	12±4.6	55±17.7	0.03±0.03	2.4±0.7
SMM018	Small cracks	Large cracks	81.5±9.3	75±2.9	3.1±0.6	2.2±0.3	17.7±3.4	75.7±7.4	0.2±0.1	1.9±0.6
SMM019	Small cracks	Small cracks	77.2±13.5	92.7±17.1	4±0.4	2±1	12.8±2.4	78±18.9	0.2±0.1	3.7±0.1
SMM020*	-	Cracks (dry topsoil all over site)	21.9±1.9	90.8±10.7	0.22±0.05	3.6±0.5	20±2.33	86.7±12.4	0.17±0.05	2.8±0.5

Notes: Data from 2012 (Ralph et al., 2013). *Data from Oyston et al. (2014).

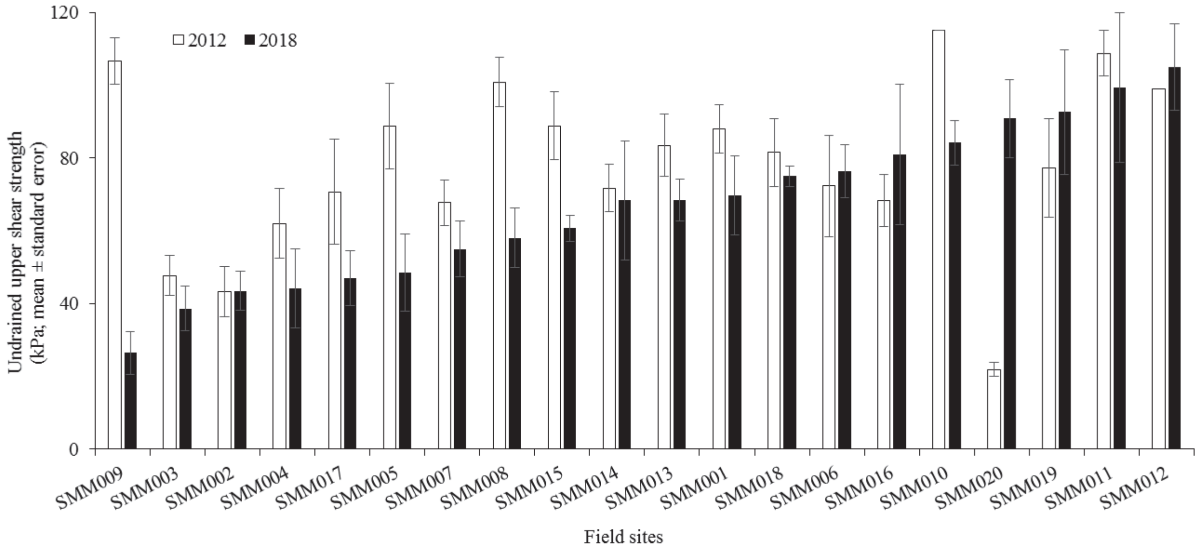

Figure 7.9 Undrained shear strength results for upper bank sediments in 2012 and 2018, ranked in ascending order based on 2018 data. Data from 2012 (Ralph et al., 2013).

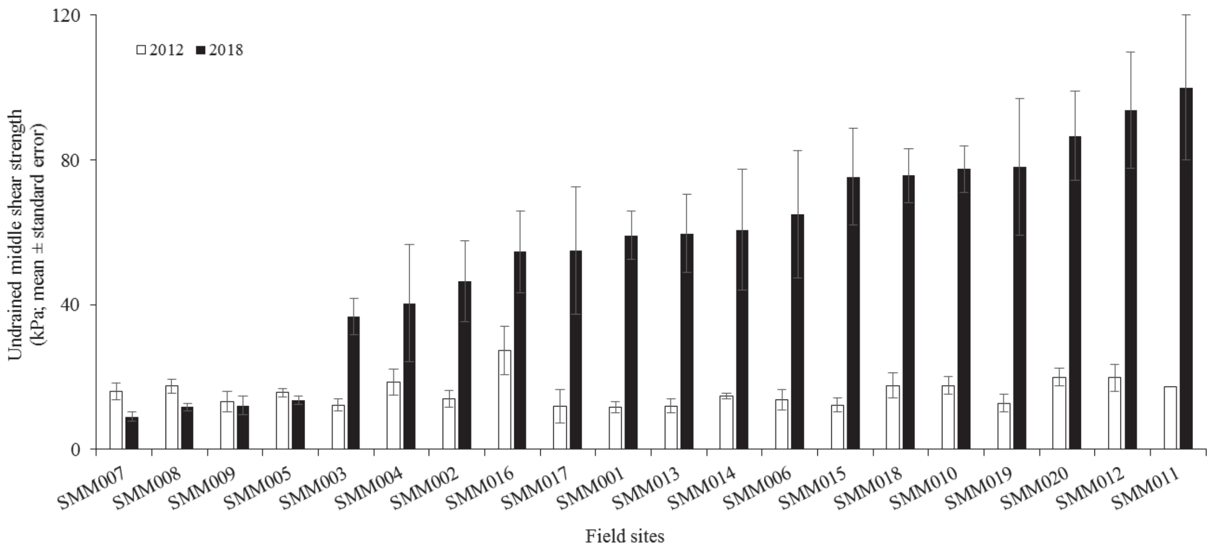

Figure 7.10 Undrained shear strength results for middle bank sediments in 2012 and 2018, ranked in ascending order based on 2018 data. Data from 2012 (Ralph et al., 2013).

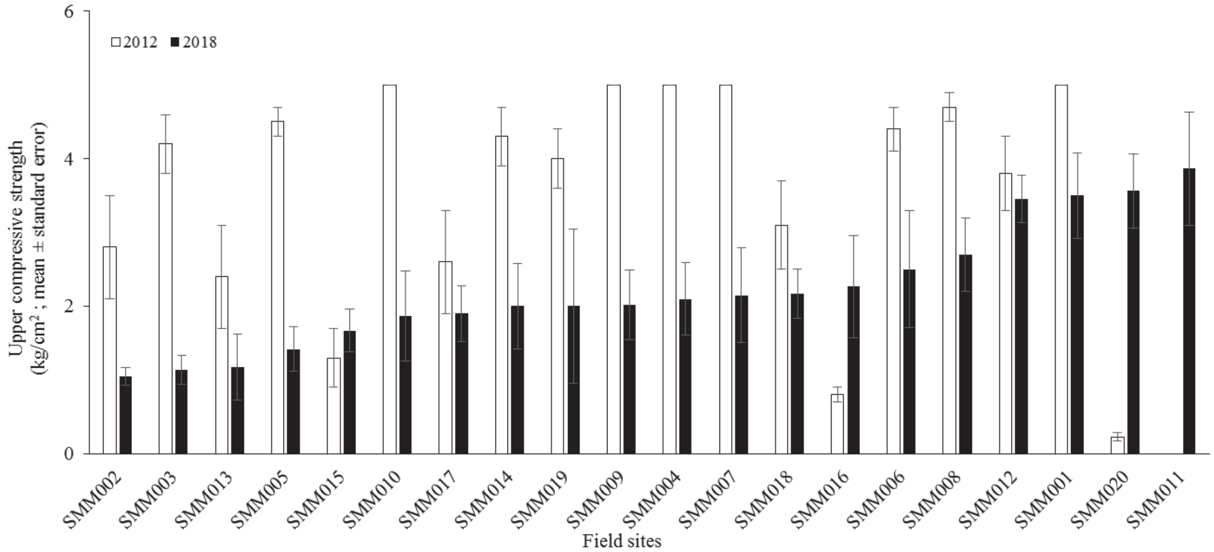

Figure 7.11 Compressive strength results for upper bank sediments in 2012 and 2018, ranked in ascending order based on 2018 data. Data from 2012 (Ralph et al., 2013).

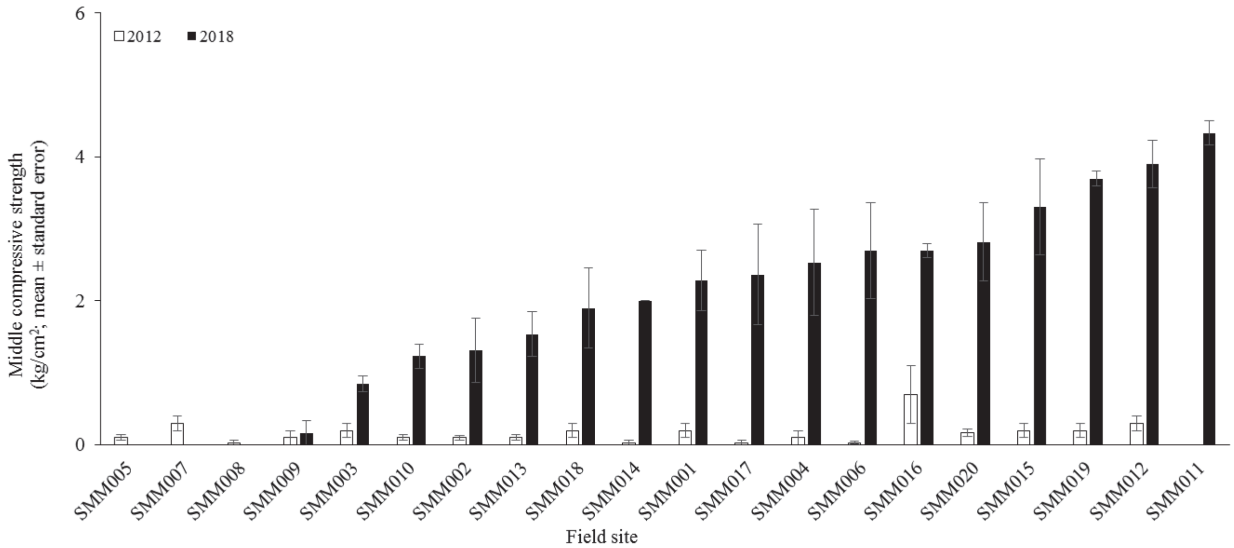

Figure 7.12 Compressive strength results for middle bank sediments in 2012 and 2018, ranked in ascending order based on 2018 data. Data from 2012 (Ralph et al., 2013).

a.

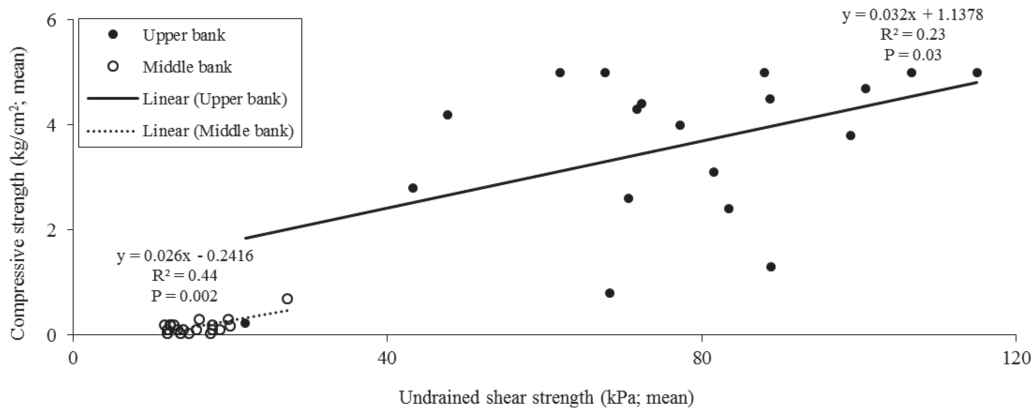

b.

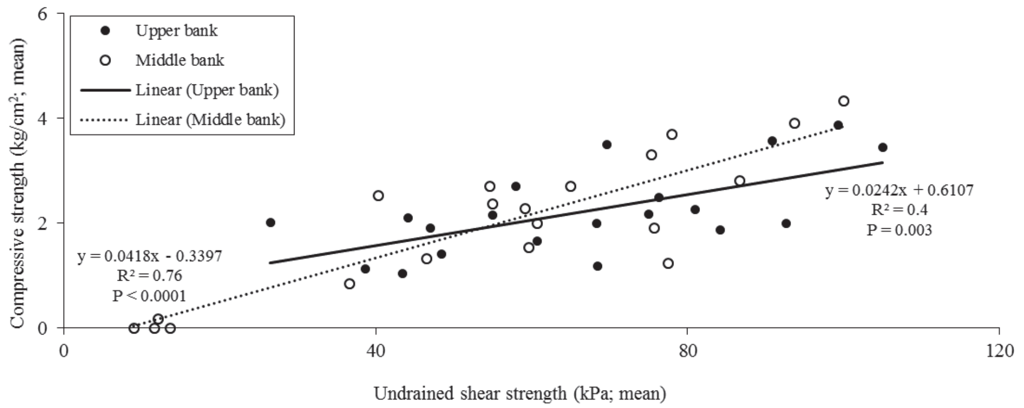

Figure 7.13 Relationship between undrained shear strength and compressive strength in upper and middle bank sediments at the field sites in (a) 2012 and (b) 2018. Data from 2012 (Ralph et al., 2013).

7.4 Erosion risk assessment matrix

Evidence of erosion, sedimentation and other features, and diagnostic criteria identified within a channel or on the floodplain, can guide risk assessments for erosion and channel change in a large and complex floodplain wetland system like the Macquarie Marshes. A risk assessment framework was developed for the Southern Macquarie Marshes by Ralph et al. (2013), and here the results from 2012 and 2018 are compared. The protocol first defines the hazards posed by erosion, then the likelihood of those hazards occurring, and then the consequences of the hazards occurring (see methods in Chapter 3, Section 3.5). The magnitude of risk posed by the hazards is then determined. For each channel of interest in the Southern Macquarie Marshes, a level of likelihood (from 1 to 5; Table 7.5) and a level of consequence (from 1 to 5; Table 7.6) are defined in 2012 and 2018. An erosion risk assessment matrix was then built based on the combination of the levels of likelihood and consequence (Table 7.7).

Table 7.5 Likelihood of key hazards associated with channels in the Southern Macquarie Marshes in 2012 and 2018.

Channel	Site code	Key hazards													
		Bed erosion		Bank erosion		Flow capture		In-channel sedimentation		Channel blockage		Breakaway formation		New channel formation	
		2012	2018	2012	2018	2012	2018	2012	2018	2012	2018	2012	2018	2012	2018
Oxley Break	SMM001	5	5	5	5	5	5	1	1	3	5	2	1	2	1
	SMM002	5	4	5	5	4	4	2	2	2	2	3	3	3	2
	SMM003	5	3	5	4	4	4	3	1	2	1	1	1	1	1
Bulgeraga Creek downstream of Oxley Break	SMM004	3	4	4	4	3	4	2	1	1	1	2	1	2	1
	SMM009	3	3	4	3	3	3	2	2	1	1	2	2	2	1
Bulgeraga Creek at Willancorah (downstream of Gibson Way)	SMM010	2	1	4	4	2	3	1	2	1	3	2	2	2	2
Macquarie River downstream of Oxley Break and upstream of Monkey Creek	SMM006	2	3	2	4	1	3	2	2	1	2	2	1	2	1
Monkey Creek	SMM005	3	4	4	4	3	4	3	2	3	3	2	1	2	1
Buckiinguy Creek	SMM008	4	3	4	4	5	4	2	2	2	4	4	4	4	4
Buckiinguy Return and Buckiinguy Runner	SMM018	4	2	5	3	4	3	2	2	2	4	2	1	2	1
Macquarie River downstream of Monkey Creek and downstream of Buckiinguy Creek	SMM007	2	2	2	3	2	3	5	2	5	4	4	4	4	4
	SMM019	2	2	3	3	2	3	2	1	2	1	2	2	2	1
Monkeygar Creek upstream of The Breakaway in Nature Reserve	SMM017	4	3	5	4	4	4	2	2	2	3	3	4	3	4
The Breakaway	SMM011	5	4	5	4	5	4	4	2	4	4	5	4	4	4
Old Macquarie River in Nature Reserve (Boss' crossing)	SMM016	1	1	1	1	2	1	5	5	2	3	2	2	2	1
Old Macquarie River in Nature Reserve (near Willie)	SMM015	1	1	1	1	2	1	5	2	2	1	2	2	2	1
Macquarie River at Maxwelton and The Mole	SMM013	2	2	3	1	1	1	2	2	1	2	2	2	2	2
The Mole reed bed outflow channels	SMM012	5	2	5	2	5	1	4	2	5	4	4	3	4	2
Macquarie River at Pillicawarrina	SMM014	2	2	3	3	1	2	1	1	1	3	1	1	1	1
Buckiinguy Swamp (knickpoint at eastern outlet)*	SMM020	5	5	5	5	5	5	2	2	1	4	1	3	2	4

Notes: 1 = Rare; 2 = Unlikely; 3 = Possible; 4 = Likely; 5 = Almost certain (see Table 6.6 for definitions of the levels of likelihood). Data from 2012 (Ralph et al., 2013).

Table 7.6 Consequences of key hazards associated with channels in the Southern Macquarie Marshes in 2012 and 2018.

Channel	Site code	Key hazards													
		Bed erosion		Bank erosion		Flow capture		In-channel sedimentation		Channel blockage		Breakaway formation		New channel formation	
		2012	2018	2012	2018	2012	2018	2012	2018	2012	2018	2012	2018	2012	2018
Oxley Break	SMM001	4	4	4	4	4	4	1	1	2	4	2	1	3	1
	SMM002	4	3	3	3	3	4	1	3	2	2	2	2	3	2
	SMM003	4	3	3	3	3	3	1	1	2	1	2	2	2	1
Bulgeraga Creek downstream of Oxley Break	SMM004	4	4	3	4	3	4	2	1	2	2	2	1	2	1
	SMM009	4	3	3	3	3	3	2	2	1	1	1	1	2	1
Bulgeraga Creek at Willancorah (downstream of Gibson Way)	SMM010	2	1	2	3	2	3	1	1	1	2	1	2	2	1
Macquarie River downstream of Oxley Break and upstream of Monkey Creek	SMM006	3	3	3	3	2	3	1	2	1	2	2	1	4	1
Monkey Creek	SMM005	3	3	3	3	4	3	4	2	3	3	3	2	4	1
Buckiinguy Creek	SMM008	4	4	4	4	4	4	4	2	4	3	4	4	4	4
Buckiinguy Return and Buckiinguy Runner	SMM018	4	1	4	2	4	2	2	1	2	4	2	1	2	1
Macquarie River downstream of Monkey Creek and downstream of Buckiinguy Creek	SMM007	2	2	2	2	3	2	4	2	4	3	4	4	4	4
	SMM019	2	2	2	3	2	3	2	1	2	1	3	2	3	1
Monkeygar Creek upstream of The Breakaway in Nature Reserve	SMM017	4	4	4	4	4	4	2	2	2	3	4	4	4	4
The Breakaway	SMM011	4	4	4	4	4	5	3	4	3	3	3	4	4	4
Old Macquarie River in Nature Reserve (Boss' crossing)	SMM016	3	2	3	2	3	2	3	4	3	2	2	2	4	1
Old Macquarie River in Nature Reserve (near Willie)	SMM015	1	1	1	1	2	1	1	1	2	1	2	1	4	1
Macquarie River at Maxwelton and The Mole	SMM013	3	2	3	1	2	2	1	2	3	2	3	3	4	13
The Mole reed bed outflow channels	SMM012	4	1	4	1	4	2	4	2	4	4	4	3	4	2
Macquarie River at Pillicawarrina	SMM014	1	2	1	2	2	2	1	1	2	2	3	2	4	1
Buckiinguy Swamp (knickpoint at eastern outlet)	SMM020	4	4	4	4	4	5	2	2	2	4	1	3	1	5

Notes: 1 = Insignificant; 2 = Minor; 3 = Moderate; 4 = Major; 5 = Extreme (see Table 6.7 for definitions of the levels of consequence). Data from 2012 (Ralph et al., 2013).

Table 7.7 Risk assessment of key hazards associated with channels in the Southern Macquarie Marshes in 2012 and 2018.

Channel	Site code	Bed erosion 2012	Bed erosion 2018	Bank erosion 2012	Bank erosion 2018	Flow capture 2012	Flow capture 2018	In-channel sedimentation 2012	In-channel sedimentation 2018	Channel blockage 2012	Channel blockage 2018	Breakaway formation 2012	Breakaway formation 2018	New channel formation 2012	New channel formation 2018
Oxley Break	SMM001	VH	VH	VH	VH	VH	VH	VL	VL	L	VH	L	VL	M	VL
	SMM002	VH	M	H	H	M	H	VL	M	L	L	L	L	M	L
	SMM003	VH	M	H	M	M	M	L	VL	L	VL	VL	VL	VL	VL
Bulgeraga Creek downstream of Oxley Break	SMM004	H	H	M	H	M	H	L	VL	VL	VL	L	VL	L	VL
	SMM009	H	M	M	M	M	M	L	L	VL	VL	VL	VL	L	VL
Bulgeraga Creek at Willancorah (downstream of Gibson Way)	SMM010	L	VL	M	M	L	M	VL	VL	VL	L	VL	L	L	VL
Macquarie River downstream of Oxley Break and upstream of Monkey Creek	SMM006	M	M	M	M	VL	L	VL	L	VL	L	L	VL	M	VL
Monkey Creek	SMM005	M	M	M	M	H	L	H	L	M	M	M	VL	M	VL
Buckiinguy Creek	SMM008	H	H	H	H	VH	L	M	L	M	M	H	H	H	H
Buckiinguy Return and Buckiinguy Runner	SMM018	H	VL	VH	L	H	VL	L	VL	L	H	L	VL	L	VL
Macquarie River downstream of Monkey Creek and downstream of Buckiinguy Creek	SMM007	L	L	L	L	M	L	VH	L	VH	M	H	H	H	H
	SMM019	L	L	L	M	L	VL	L	VL	L	VL	M	L	M	VL
Monkeygar Creek upstream of The Breakaway in Nature Reserve	SMM017	H	H	VH	H	H	L	L	L	L	M	H	H	H	H
The Breakaway	SMM011	VH	H	VH	H	VH	VH	M	M	M	M	H	H	H	H
Old Macquarie River in Nature Reserve (Boss' crossing)	SMM016	L	VL	L	VL	M	VH	H	VH	M	L	L	L	M	VL
Old Macquarie River in Nature Reserve (near Willie)	SMM015	VL	VL	VL	VL	L	VL	L	VL	L	VL	L	VL	M	VL
Macquarie River at Maxwelton and The Mole	SMM013	M	L	M	VL	VL	L	VL	L	L	L	M	M	M	M
The Mole reed bed outflow channels	SMM012	VH	VL	VH	VL	VH	L	H	L	VH	H	H	M	H	L
Macquarie River at Pillicawarrina	SMM014	VL	L	L	L	VL	VL	VL	VL	VL	L	L	VL	M	VL
Buckiinguy Swamp (knickpoint at eastern outlet)	SMM020	VH	VH	VH	VH	VH	VH	L	L	VL	H	VL	M	VL	VH

Notes: VL= Very low; L = Low; M = Medium; H = High; VH = Very high (see Table 6.8 for definitions of the levels of consequence) Colour guide: White = no change, Orange = increase and Green = decrease. Data from 2012 (Ralph et al., 2013).

7.5 Site risk ranking

Based on the erosion risk assessment (Tables 7.5, 7.6 and 7.7), the sites in the Southern Macquarie Marshes were ranked according to their risk factors (Table 7.8). Results showed that The Mole reed bed outflow channel (SMM012), which was ranked at the highest risk level in 2012, has been replaced by the knickpoint at the eastern outlet in Buckiinguy Swamp (SMM020) in 2018. The Breakaway, Buckiinguy Creek, Monkeygar Creek upstream of The Breakaway in Nature Reserve, Oxley Break and Macquarie River downstream of Monkey Creek and downstream of Buckiinguy Creek are still positioned in the top one-third for risk of erosion, with a minor increase for the Macquarie River and a minor decrease for Monkeygar Creek. In the middle of the ranked list, Bulgeraga Creek at Willancorah moved up from rank 16 to rank 9, while Buckiinguy Return and Buckiinguy Runner and the Macquarie River downstream of Oxley Break and upstream of Monkey Creek moved down 5 and 7 ranks, respectively. Furthermore, Monkey Creek and Bulgeraga Creek downstream of Oxley Break moved slightly towards a higher risk ranking. Among the last third of the ranking list, there was a reduction in erosion risk in the Old Macquarie River in Nature Reserve and Macquarie River, whereas the Old Macquarie River in Nature Reserve (near Willie) ranked in the lowest position and the Macquarie River at Maxwelton and The Mole and Macquarie River downstream of Monkey Creek and downstream of Buckiinguy Creek had a reduced risk ranking (Table 7.8).

Table 7.8 Ranked list of sites at risk from key hazards in the Southern Macquarie Marshes in 2012 and 2018.

Rank in 2012	Site code	Channel	Rank in 2018	Site code	Channel
1	SMM012	The Mole reed bed outflow channels	1	SMM020	Buckiinguy Swamp (knickpoint at eastern outlet)
2	SMM011	The Breakaway	2	SMM011	The Breakaway
3	SMM008	Buckiinguy Creek	3	SMM008	Buckiinguy Creek
4	SMM007	Macquarie River downstream of Monkey Creek and downstream of Buckiinguy Creek	4	SMM017	Monkeygar Creek upstream of The Breakaway in Nature Reserve
5	SMM002	Middle Oxley Break	5	SMM001	Upper Oxley Break
6	SMM017	Monkeygar Creek upstream of The Breakaway in Nature Reserve	6	SMM002	Middle Oxley Break
7	SMM001	Upper Oxley Break	7	SMM007	Macquarie River downstream of Monkey Creek and downstream of Buckiinguy Creek
8	SMM018	Buckiinguy Return and Buckiinguy Runner	8	SMM005	Monkey Creek
9	SMM003	Lower Oxley Break	9	SMM010	Bulgeraga Creek at Willancorah (downstream of Gibson Way)
10	SMM005	Monkey Creek	10	SMM004	Bulgeraga Creek downstream of Oxley Break
11	SMM004	Bulgeraga Creek downstream of Oxley Break	11	SMM006	Macquarie River downstream of Oxley Break and upstream of Monkey Creek
12	SMM009	Bulgeraga Creek downstream of Oxley Break	12	SMM012	The Mole reed bed outflow channels
13	SMM016	Old Macquarie River in Nature Reserve (Boss' crossing)	13	SMM018	Buckiinguy Return and Buckiinguy Runner
14	SMM019	Macquarie River downstream of Monkey Creek and downstream of Buckiinguy Creek	14	SMM003	Lower Oxley Break
15	SMM015	Old Macquarie River in Nature Reserve (near Willie)	15	SMM009	Bulgeraga Creek downstream of Oxley Break
16	SMM010	Bulgeraga Creek at Willancorah (downstream of Gibson Way)	16	SMM016	Old Macquarie River in Nature Reserve (Boss' Crossing)
17	SMM013	Macquarie River at Maxwelton and The Mole	17	SMM019	Macquarie River downstream of Monkey Creek and downstream of Buckiinguy Creek
18	SMM006	Macquarie River downstream of Oxley Break and upstream of Monkey Creek	18	SMM014	Macquarie River at Pillicawarrina
19	SMM014	Macquarie River at Pillicawarrina	19	SMM013	Macquarie River at Maxwelton and The Mole
20	-	-	20	SMM015	Old Macquarie River in Nature Reserve (near Willie)

Notes: Data from 2012 (Ralph et al., 2013), although a risk ranking site list was not provided in that report.

7.6 Site prioritisation for future monitoring, evaluation and management

Based on the erosion risk assessment and ranking (Table 7.8), high priority, medium priority and low priority sites were identified for 2012 (Table 7.9) and 2018 (Table 7.10). High priority sites are those where erosion or sedimentation are likely to have a major effect on flow distribution and channel integrity, and so should be further assessed for potential works and management interventions. Medium priority sites are those where erosion or sedimentation are expected to have only a minor effect on flow distribution and channel integrity. In low priority sites, erosion and sedimentation may occur, but are likely to have a negligible effect on flow distribution and channel integrity.

Table 7.9 The level of priority of sites in the Southern Macquarie Marshes in 2012.

Priority level	Sites
High	Oxley Break Bulgeraga Creek downstream of Oxley Break Buckiinguy Creek Buckiinguy Return and Buckiinguy Runner Macquarie River downstream of Monkey Creek and downstream of Buckiinguy Creek Monkeygar Creek upstream of The Breakaway in Nature Reserve The Breakaway The Mole reed bed outflow channels
Medium	Monkey Creek Old Macquarie River in Nature Reserve (Boss' crossing) Old Macquarie River in Nature Reserve (near Willie) Macquarie River at Maxwelton and The Mole (downstream of Gibson Way) Macquarie River downstream of Oxley Break and upstream of Monkey Creek
Low	Bulgeraga Creek at Willancorah (downstream of Gibson Way) Macquarie River at Pillicawarrina

Notes: Data from 2012 (Ralph et al., 2013).

Table 7.10 The level of priority of sites in the Southern Macquarie Marshes in 2018.

Priority level	Sites
High	Oxley Break Buckiinguy Creek Buckiinguy Swamp (knickpoint at eastern outlet) Macquarie River downstream of Monkey Creek and downstream of Buckiinguy Creek Monkeygar Creek upstream of The Breakaway in Nature Reserve The Breakaway Monkey Creek
Medium	Bulgeraga Creek at Willancorah (downstream of Gibson Way) Bulgeraga Creek downstream of Oxley Break Macquarie River downstream of Oxley Break and upstream of Monkey Creek The Mole reed bed outflow channels Buckiinguy Return and Buckiinguy Runner
Low	Old Macquarie River in Nature Reserve (Boss' crossing) Old Macquarie River in Nature Reserve (near Willie) Macquarie River at Pillicawarrina Macquarie River at Maxwelton and The Mole (downstream of Gibson Way)

7.7 Interpretation

In the six-year period between 2012 and 2018, fairly minor changes in physical characteristics linked to erosion and sedimentation occurred at the 20 rapid assessment field sites in the Southern Macquarie Marshes. During this time, there were significant flows in the system in both 2012 and 2016, which could increase the risk of erosion should the system be primed for change ahead of and at those times of higher flows. The flows themselves play a critical role in water quality conditions, which are used by a wide range of species of fauna and flora in the Macquarie Marshes. Electrical conductivity (EC) results showed this parameter to be in the upper normal range for freshwater systems at most sites, while pH remained below the ANZECC (2000) trigger value for lowland river ecosystems.

Throughout the system, erosion processes occurred leading to various minor changes in channel and bank morphology, while sedimentation also occurred, and visual estimates of these changes confirmed which sites had undergone the most impact from erosion and deposition. Exposed tree roots, bank retreat, bank rilling, tunnelling and cracking, ledges, exposed knickpoints and bank failure by toppling are the most visible processes of erosion and sub-aerial processes in the Southern Macquarie Marshes. Conversely, channel blockage (for example, from woody debris), development of low natural levees and benches are evidence of sedimentation in this area. Soil compaction, anthropogenic tracks and animal trampling are other features affecting erosion risk assessment at the study sites.

Roughness (Manning's n) varied between the sites; this was mainly due to vegetation cover, which was an especially important factor since sediment properties and other key factors did not vary greatly between sites. Most of the sites in 2012 had higher roughness due the climate regime and flow conditions in that year (Ralph et al., 2013), which led to more vegetation compared to the drier situation in 2018 which was during a prolonged drought.

It is clear that the soil moisture content strongly influences measures of bank strength, with dry bank sediments being stronger than wet bank sediments in terms of their shear and compressive strength. It could be concluded that higher flows may lead to reduced shear and compressive bank strength due to wetting, and therefore, an increase in the likelihood of bank erosion. However, some channels did not have evidence of erosion even though they had low bank strength values; this suggests the importance of other factors affecting channel erosion risk. Indeed, since the Macquarie Marshes sediments are dominated by mud, silt and clay, and are very cohesive, disaggregation is also likely to strongly influence bank erosion, as would bank trampling and disturbance, tunnelling, riling and cracking. Therefore, soil shear and compressive strength measures alone do not completely define the nature of the banks and their erosion potential.

Findings from the rapid risk assessment demonstrate that several channels experienced minor changes during the six-year period between assessments (i.e. negligible short-term change), including Monkey Creek, Bulgeraga Creek, the Old Macquarie River and Macquarie River. These channels were typically of low to medium concern for future assessment, monitoring and evaluation. Others, such as Oxley Break, Buckiinguy Creek, The Breakaway and Monkeygar Creek had some evidence of channel change due to erosion and/or sedimentation. Furthermore, because of their position in the system and the wetland associated with them, they were consistently ranked as sites of risk, and are of high importance for future assessment, monitoring and evaluation.

However, the results showed that knickpoint retreat and channel expansion due to erosion at Buckiinguy Swamp is a significant threatening process, and this site in 2018 was determined to have the highest level of risk for future detrimental change in the Southern Macquarie Marshes. These results also confirmed that erosion caused by knickpoint retreat and other channelization processes are variable over short timescales, and at different parts of the system. Therefore, erosion processes are critical for the formation, growth and development of new channels leading to avulsion in the floodplain wetlands.

7.8 Summary

This chapter presented the findings of repeated erosion risk assessments undertaken at 20 sites in 2012 (Ralph et al., 2013) and 2018 in the Southern Macquarie Marshes. Key factors affecting bank strength, roughness and channel erosion potential were examined, and sites were assessed and ranked in terms of their erosion risk and their priority for future monitoring and management. This demonstrated the variability and importance of short-term processes, such as bank erosion and knickpoint retreat, in creating and modifying channels in the Macquarie Marshes. In next the chapter, the main findings of the thesis are synthesised and discussed.

Chapter 8: Discussion

8.1 Introduction

This chapter synthesises the main findings and key trends identified in the previous results chapters and discusses the processes of channel change and the importance of bifurcation, avulsion and erosion in multi-channelled rivers and floodplain wetlands within the context of current literature. The chapter addresses the final aim of the thesis:

5. *To synthesise and understand channel patterns and channel change processes in the Macquarie Marshes that are relevant for water and wetland management.*

First, spatial patterns of channels and bifurcation and return nodes and their influence on channel morphology and hydraulics are discussed, which ultimately leads to a consideration of the maintenance of channel capacity in many river-reaches of the Macquarie Marshes. Contrasting channel conditions in the low-energy, multi-channelled floodplain wetlands are highlighted, as well as the trends and thresholds for channel bankfull discharge and unit stream power. Then, historical and contemporary channel adjustment in the hyper-avulsive reaches of the system are discussed, before bank strength, roughness and other key factors affecting erodibility and erosion risk are evaluated. High priority sites for consideration of erosion, sedimentation, changes in flow and channel geometric and hydraulic character are reviewed for the Macquarie Marshes. Finally, the relationships between erosion, bifurcation and avulsion in multi-channelled rivers and floodplain wetlands, as identified in this research, are compared with similar systems at a global scale, and dominant internal and external drivers of change in these systems are discussed.

8.2 Discussion of key findings

8.2.1 Bifurcations and returns associated with channel maintenance in the Macquarie Marshes

In geomorphology, it is important to understand whether a river system is in a dynamic equilibrium condition or not, and whether alluvial channels can, and do, maintain their capacity to transport flow and sediment efficiently (Blom et al., 2017; Zhou et al., 2017). It is fundamental to investigate how conditions vary from reach to reach in a system and to assess how channel cross-sections adjust in terms of their morphology to balance rates of sediment erosion, transport and deposition (Ruiz-Villanueva et al., 2016). Bifurcation and return nodes play a vital role in routing sediment from upstream to downstream branches of rivers and wetlands (Bolla Pittaluga et al., 2003; Kleinhans, 2010). The Macquarie Marshes, as a multi-channelled river system with a predominantly anastomosing channel pattern, exhibit a series of channel bifurcation and return nodes along the reaches in the Southern, Northern and Eastern Macquarie Marshes. The highest density of channel bifurcation and return nodes occurs in the western part of the Southern Macquarie Marshes where the Macquarie River splits into several major branches (including Monkey Creek, Buckiinguy Creek and Monkeygar Creek), before forming the Old Macquarie River, which receives return flow from Monkeygar Creek via The Breakaway and continues (as the Macquarie River) downstream and into the Northern Macquarie Marshes. Similarly, a high concentration of bifurcation and return nodes occur in the northern section of the Northern Macquarie Marshes, where numerous channels reconverge to take flow out of the system to the north. Overall, return nodes dominate over bifurcation points throughout the Macquarie Marshes, although the morphometric data from these nodes show some clear trends in terms of the effects of channel splitting and convergence on the overall channel capacity and maintenance.

The Southern Macquarie Marshes has the lowest bifurcation:return ratio (0.86), demonstrating the dominance of return points in this sub-system despite the presence of several large distributary channels. Conversely, the Northern and Eastern Macquarie Marshes both have higher bifurcation:return ratios (0.94-0.98), demonstrating the relative balance of divergent and convergent channels in these areas. The largest channels (in terms of bankfull width, depth and cross-sectional area) and steepest channels (i.e. slope) occur in the Southern Macquarie Marshes, which means that these channels also have the greatest flow potential (i.e. bankfull discharge) and energy (i.e. unit stream power). Throughout the system, channels are usually wider at bifurcation nodes, and narrower at return nodes, while discharge and stream power within the channels tend to follow the same trend. In some places, however, such as the outflow points of Buckiinguy Swamp and the downstream reaches of the Northern Macquarie Marshes, many channels reconverge downstream of reed beds, and the discharge at these returns exceeds that at nearby bifurcations. It is difficult to determine what the effect of flows returning from the surface of the floodplains and wetlands are in the system because these tend to be highly variable and were not directly assessed or modelled in this research. Nevertheless, according to fundamental principles in hydrology and geomorphology, it can be assumed that when and where flows go over bank, they dissipate their energy on the floodplain and that significant infiltration and evapotranspiration also occurs (Zwoliński, 1992). This would lead to a net loss of discharge and stream power in the system, which helps to explain the downstream declining size of channels throughout the Macquarie Marshes, and also the propensity for smaller channels to occur at return nodes.

Bifurcations help channels to more effectively transmit water and sediments locally, while, at the scale of the sub-systems and the whole Macquarie Marshes, returns are essential for outflowing channels to reform and continue downstream. Development of bifurcation and return nodes throughout the Macquarie Marshes demonstrates the importance of the local bed slope and roughness (since bed slope is variable and roughness is generally moderate in channels, but higher in reed beds and elsewhere on the floodplain). The results suggest that channels develop a system with a higher bifurcation:return ratio with smaller channels to transport sediment at lower bed slope. However, channels are wider where a higher bifurcation:return ratio occurs (with the same bed slope) because bifurcations mainly lead to increases in total channel width and depth, while returns lead to reductions in channel capacity. Overall, however, returns are especially important for the channel maintenance and the hydraulic character of the Macquarie Marshes. The occurrence of more returns in the outflowing reaches of the Southern and Northern Macquarie Marshes helps the system to increase hydraulic conditions in the channels and to transfer water and sediments downstream. Indeed, returns play an important role in controlling the morphology and sedimentology character of a system by controlling sediment distribution at and downstream of river confluences (Lisenby and Fryirs, 2017).

Channels in the Macquarie Marshes are mostly capable of maintaining their flow and morphology, despite bankfull discharge being predominantly less than 5 m^3/s, and only a few channels have a higher discharge than 5-50 m^3/s. Moreover, the dominant rate of energy dissipation against the bed and banks per unit channel width, as defined by unit stream power, is less than 1 W/m^2 for the whole system, which increases somewhat in the Southern Macquarie Marshes (up to 5 W/m^2). Therefore, the dominant morphological and hydraulic characteristics for channels in the Macquarie Marshes, and possibly the minimum conditions required for dynamic equilibrium and maintenance of channel capacity, can be defined as channels that are: 10-20 m in width and approximately 1 m deep, 10 m^2 in cross-sectional area, 5 m^3/s in bankfull discharge and 1 w/m^2 in unit stream power. These major findings mean that if channels fall below these hydrogeomorphic thresholds, they risk a shift to non-equilibrium conditions and will likely suffer a dramatic decline in size, flow and sediment transport efficiency, which could lead to channel breakdown and termination in some places.

Most of the channels in the Macquarie Marshes are maintaining their size and, therefore, their flow capacity, despite having multiple bifurcations. While, in most cases, bifurcations split/spread water and sediment, the channels receive significant return channels that accumulate flow further downstream, and only in a few places do channels terminate. The net effect of most bifurcations is to increase channel size and unit stream power, while at returns (at the system scale), channel size and stream power generally decline. Therefore, since only a relatively small proportion of the major channels terminate on the floodplain and in wetlands, there is a fine balance between bifurcations and returns that leads to a general dominance of channel capacity maintenance throughout the system.

Spatial patterns of distributary and tributary flows along each reach provide different scenarios of river character that can be synthesised in terms of bifurcation:return ratios. A conceptual model is presented in Figure 8.1 to show the different scenarios of bifurcation:return ratio trends downstream and their relationships with channel capacity and flow energy. Channels branch and split their flow when bifurcations dominate the system and the bifurcation:return ratio remains above 1 (Figure 8.1a). This is the case for the Macquarie River upstream of Monkeygar Creek, where the Macquarie River trunk stream bifurcates and forms the multi-channelled pattern in the Southern Macquarie Marshes. Channels can accumulate flow when returns are dominant in the system and the bifurcation:return ratio remains below 1 (Figure 8.1b). This is the case for the Macquarie River downstream Old Macquarie River; to confluence downstream and to be continued as a main trunk stream. However, some reaches could exhibit both patterns where initially bifurcations dominated the system (bifurcation:return ratio above 1) and were then superseded by returns leading to a bifurcation:return ratio below 1 (Figure 8.1c). This is the most common scenario in the Southern Macquarie Marshes, where major avulsions are stabilising and heading to an equilibrium condition. In an opposite pattern, an alternate dominance of returns and bifurcations occur, where initially returns dominate the system (bifurcation:return ratio below 1), and then more flows spread causing an increase in the bifurcation:return ratio (to above 1) and the accumulating flow again reduces the bifurcation:return ratio close to, or below, 1 (Figure 8.1d). This scenario is visible in the Macquarie River in the Northern Macquarie Marshes, where a series of channels from the Southern Macquarie Marshes combine before splitting again to spread water in the Northern Macquarie Marshes via the Macquarie River, and then accumulate to take flows out of the northern end of the Macquarie Marshes. In the last pattern, channels had bifurcations that were balanced by returns (bifurcation:return ratio hovered around 1) (Figure 8.1e). This scenario was dominant within the Eastern Macquarie Marshes and the reoccupied palaeochannels of Gum Cowal and Long Plain Cowal that help the system to transmit flow more efficiency.

a. Bifurcation:return >1: Split/spread flow	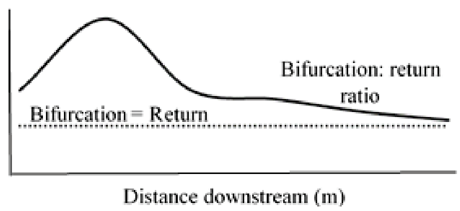
b. Bifurcation:return <1: Draw/accumulate flow	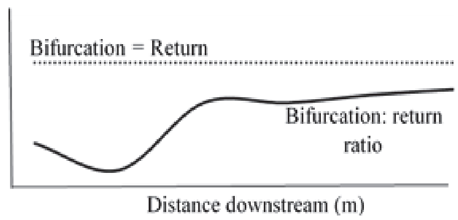
c. Bifurcation:return >1 then <1: Split/spread then draw/accumulate flow	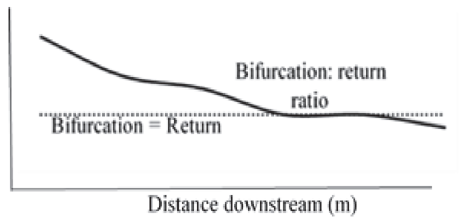
d. Bifurcation:return <1 then >1 then <1: Draw/accumulate then split/spread then draw/accumulate flow	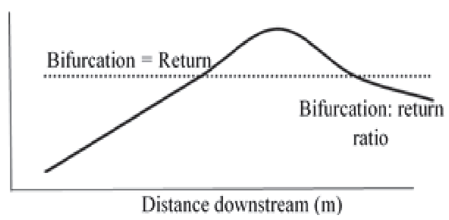
e. Bifurcation:return ~1: Transmit flow	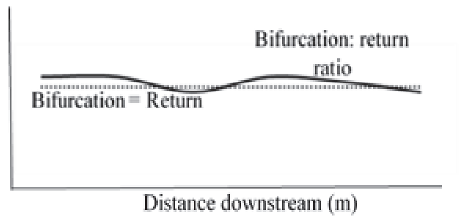

Figure 8.1 Conceptual model of the different scenarios of bifurcation:return ratio trends downstream, and their relationships with channel capacity and flow energy.

The analysis of channel bifurcation and return nodes in this system reveals that a balanced number of nodes help the system to both lose and recover its channel capacity in order to improve its hydraulic character and to achieve channel maintenance. Moreover, previous research has showed that erosion, sedimentation and avulsion affect the location of wetlands, particularly the active wetlands surrounding the Old Macquarie River and around Monkeygar Creek, which have changed since the 1940s (Ralph et al., 2016). Also, the palaeochannels of the Macquarie River surrounding the Macquarie Marshes have reduced in size and competence during the Holocene in response to greater discharge variability and overall declines in high energy flows, leading to channel breakdown, flood out and wetland formation (Hesse et al., 2018). Despite the presence of channel breakdown and termination, channels in the modern system display an anastomosing pattern more than a distributary pattern, and the dominance of return nodes reduces the probability of channel breakdown and avulsion in this system. Channels in this low-energy system appear to balance their form by adjusting their sinuosity and the number of channels (i.e. bifurcations leading to anastomosis and distributary channel formation) where they cannot adjust their depth. This serves to maintain the overall channel continuity, as well as the flow and sediment transport capacity, through the Macquarie Marshes, which translates to the maintenance of channel capacity and a dominance of intrinsic processes that operate in a dynamic equilibrium over the long-term.

8.2.2 Historical and contemporary channel adjustment

LiDAR-derived DEM is an important tool for understanding fluvial geomorphology and measuring the size and shape of channels (Bizzi et al., 2016). Comparison of channel geomorphic character in the Southern Macquarie Marshes within a seven-year period in this study (from 2008 to 2015) showed that trunk streams and tributary channels that provide the majority of flow and incoming discharge exhibit channel expansion, while bifurcation and distributary channels mostly exhibited contraction in the short-term. Channel expansion is related to erosion, while channel contraction is related to sediment deposition and vegetation encroachment into the channels. However, an analysis of the DEM of Differences (DoD) could not resolve fine-scale channel adjustment over a short timeframe due to the limitation of threshold accuracy and low-gradient nature of the Macquarie Marshes, leading to unreliable results in dense vegetated and/or inundated areas.

A downstream analysis of geomorphic and hydraulic character of channels in the Southern Macquarie Marshes for 1992 and 2018 based on channel cross-sections showed a general decline in channel size, discharge and stream power downstream, although bankfull channel width, depth, cross-sectional area, discharge and unit stream power were highly variable. However, in some channels a downstream increase in size and hydraulic capacity was observed mainly where major returns channels occurred, which is critical to most channels in the system maintaining their continuity and anastomosing pattern (i.e. confluence of the Buckiinguy Return channel and the Macquarie River upstream of Monkeygar Creek; confluence of Monkey Creek and Monkeygar Creek; confluence of The Breakaway and the Old Macquarie River).

The analysis of historical channel adjustment in the Southern Macquarie Marshes in the 26-year period between cross-section surveys demonstrates the significant increase in channel size along The Breakaway. The Breakaway's cross-sectional area enlarged by 29 to 95%, while the nearby branch of Monkeygar Creek experienced reductions in channel area of almost -34%. This equates to increases in bankfull discharge along The Breakaway of up to 135%, while Monkeygar Creek experienced decreases in bankfull discharge of between -45 and 0%. The Breakaway therefore continues to have the ability to capture flow from Monkeygar Creek, and it is the major feeder channel of the Old Macquarie River, which continues to the reformed trunk stream of the Macquarie River further downstream. Channel size is also an important factor in terms of sediment connectivity (Lisenby and Fryirs, 2017), and these results suggest that The Breakaway is adjusting its shape to maintain and enhance the hydrological and sediment connectivity throughout the system. Ralph et al. (2016) summarised the period of transition of The Breakaway from a discontinuous flow path in the mid-20th century to a continuous channel in the late-20th century due to erosion and channel expansion from floods. The findings in this thesis confirm the prediction of Ralph et al. (2016) that The Breakaway will likely supersede Monkeygar Creek due to continuing channel enlargement and flow capture.

Channel bankfull width and depth affect channel cross-sectional area; although both were highly variable in the system. Bed and bank heights were the most consistent factors in the Southern Macquarie Marshes. This means that channel depth is the least affected parameter within the historical timeframe of the analysis. Channel width, which is the more important metric for the determination of unit stream power, is more liable to change. There is a direct relationship between an increase in channel size (due to an increase in channel width/and or depth) and an increase in bankfull discharge conditions that could affect the ability of channels to transmit water and sediment more efficiently. However, in the event that an increase in channel size occurred mostly due to a change in channel depth, while width remained the same, then unit stream power may decline. Therefore, in such a scenario, the width:depth ratio could have a negative relationship with unit stream power. Based on these findings, although wider and deeper channels are more likely to have greater capability to transfer water and sediment, the probability of sedimentation increase in wider channels with less stream power and deeper channels leads to a higher risk of channel erosion in some places.

The analysis of historical morphological and hydraulic changes at two key avulsion points in the Southern Macquarie Marshes, Monkeygar Creek-The Breakaway and Macquarie River-Buckiinguy Creek, helps to define the characteristics of bifurcating channels and how they adjust over time during avulsion. Both of the main channels upstream of the avulsion points became narrower and deeper over 14 years, which is indicative of continuing channelization in the system. Channel size and bankfull discharge decreased in both branches downstream of the avulsion point of Buckiinguy Creek from the Macquarie River. The reduction in channel capacity refers to decreases in channel width; so, the width:depth ratio decreased in both channels and unit stream power increased in Buckiinguy Creek but decreased in the Macquarie River. Furthermore, bankfull discharge declined in both of the downstream branches. These results show how subtle changes in width:depth ratio can affect channels differently. The overall decline in bankfull discharge capacity at the Macquarie River-Buckiinguy Creek avulsion node suggests that another branch of the Macquarie River in this anastomosing reach may be taking flow from the branch that feeds Buckiinguy Creek. Further downstream, superelevation of Monkeygar Creek primed the system prior to The Breakaway avulsion in the Southern Macquarie Marshes (Ralph and Hesse, 2010). At this avulsion, The Breakaway channel has increased in size and Monkeygar Creek has become smaller. This is a situation where a system is adapting to the new channelization pattern. Unit stream power has increased in The Breakaway and decreased in Monkeygar Creek downstream of the avulsion, which could put Monkeygar Creek at risk of abandonment. Vegetation and roughness are also important factors, with The Breakaway having more herbaceous marsh cover with in-channel and floodplain reeds, whereas Buckiinguy Creek has river red gum woodland with far less in-channel reeds.

Overall, with the exception for key changes around The Breakaway and related channels, major channel changes were not observed or measured in the 26-year historical period. Previous studies show that several new avulsions have occurred since the 1890s that led to changes in the channels and floodplain wetland boundaries and the abandonment of wetlands in some areas during the 20th century (Ralph et al., 2016). The findings from this thesis show that several of these avulsions are now fairly stable. This suggests that the system is adjusting, over time, to a new level of channelization through a new dynamic equilibrium following the major disturbances caused by European alterations to land and water management (Ralph, 2008). This demonstrates the capability of channels to maintain themselves in the medium-term through erosion and sedimentation processes linked to a dynamic equilibrium.

While bifurcations have the ability to lead to distributary or anastomosing channel patterns, anastomosis clearly dominates this system. Multi-channelled floodplain wetlands, such as the Macquarie Marshes, provide a unique habitat for fauna and flora, and changes in geometric and hydraulic character of channels in the Southern Macquarie Marshes affect this habitat. A major implication of the increases in channel capacity and the associated increases in bankfull discharge in several channels, particularly in The Breakaway, is that it would take greater flows to achieve bankfull conditions compared with those in 1992. Therefore, the ability and/or likelihood of overbank flows has declined in the Southern Macquarie Marshes in the last 26 years. Overbank flows are essential for the maintenance of surrounding wetlands (Kobayashi et al., 2013) and excessive channel enlargement may lead to the abandonment of these vital aquatic features.

8.2.3 Channel erosion risk evaluation

Erosion (causing channel enlargement and/or avulsion) and sedimentation (causing contraction and/or flow diversion) are critical elements leading to channel changes in the Macquarie Marshes. Erosion risk analysis is mainly based on visual evidence of erosion, although various factors affect the potential for erosion in the system. This analysis showed that most of the geomorphic parameters remained stable at 20 sites in the Southern Macquarie Marshes in the six-year period between assessments (for example, bank shape) and that no new flow entry or exit points occurred at any of the sites. Roughness did decline systematically over time, which mainly reflected the impact of drought on vegetation cover and type in 2018. Although previous measurements showed that channel cross-sections and planform have not changed greatly in the Southern Macquarie Marshes (for example, variation of cross-section and degree of meandering), over the last six years, minor changes in erosion, sedimentation and sub-aerial features were visible. The most significant was the continued development and enlargement of the knickpoint at the outlet of Buckiinguy Swamp. In terms of bank strength, the presence of water plays a vital role where increased flow reduces the shear and compressive strength parameters and increases the risk of bank erosion. However, the nature of the very cohesive muddy sediments (i.e. silt and clay) and their ability to resist disaggregation (see Oyston et al., 2014) also influence bank erosion risk.

The interpretation of the likely hazards and risks posed by erosion and sedimentation processes helped to identify priority sites for monitoring and management. A comparison of site erosion risk rankings from 2012 (Ralph et al., 2013) and 2018 (this study) showed that most of the higher risk channels have maintained that status, although the order has changed slightly. The eroding knickpoint at Buckiinguy Swamp was deemed to be the site with the highest risk. Previous studies of channel erosion and sedimentation in Buckiinguy Swamp showed the tendency of channels to change morphology at active knickpoints under flood pulse conditions (Oyston et al., 2014). The combination of vertical incision and rapid retreat of the knickpoint at the eastern outlet in this area increased the level of risk. The Breakaway and Monkeygar Creek clearly also had evidence of channel change, and so both channels increased in risk ranking. The Mole reed bed outflow channels decreased in risk ranking, reflecting the generally stable condition of the channels there over the period of assessments.

Overall, major channel changes were not observed and measured in the short period of the risk assessments, but time will tell whether some of the higher risk channels do change more significantly. It is clear that accelerated rates of erosion usually cause channels to become deeper, wider and/or more continuously channelized, but channel formation only occurs in some places (for example, at Buckiinguy Swamp through the knickpoint retreat). The major findings show that channels are maintaining their form and function as conduits of flow and sediment transport through short-term dynamic equilibrium, while rapid changes to channels (for examples, incision and knickpoint retreat) may threaten wetland stability more than the generally slow channel expansion due to changes in width, and are therefore of greater risk to the system.

8.2.4 Synthesis of channel morphology and change

Although major avulsions in the Macquarie Marshes have caused channels to shift and floodplain wetlands to adjust over time, leading to channel breakdown and termination in some cases, this system on the whole is in a dynamic equilibrium condition and anastomosis is the dominant channel pattern. However, in places where channels do terminate (for example, Monkeygar Creek in Willancorah Swamp, Buckiinguy Creek in Buckiinguy Swamp ad Macquarie River in the Northern Macquarie Marshes), or where knickpoints cut through the floodplain (for example, Buckiinguy Swamp), the system is in a non-equilibrium state. This investigation of historical change in the Southern Macquarie Marshes defined the trajectory of channel adjustment. In this system, the formation of new channels starts the process of bifurcation and/or avulsion, and this temporarily puts the system out of its dynamic equilibrium in this location until the channel has time to adjust to the new conditions and to regain its equilibrium. However, new channels that terminate or join palaeochannels and leave the Macquarie Marshes altogether are out of dynamic equilibrium. In contrast, new channels that re-join the main channel and contribute to the maintenance of the channel size and discharge capacity still sit within the system's dynamic equilibrium. Therefore, the dominant pattern of return nodes throughout the Macquarie Marshes helps to conserve the equilibrium condition in this system.

8.3 The role of bifurcations, avulsion and erosion in multi-channelled rivers

8.3.1 Bifurcations, returns and channel adjustment in anastomosing systems

Channel bifurcations, avulsion and erosion are natural processes within multi-channelled rivers that affect formation and development of floodplain wetlands in these systems. This research showed that bifurcations help channels to more effectively transmit water (and sediments) locally, while, at the scale of the sub-systems and of the whole system, returns are essential for outflowing channels to reform and continue downstream. Previous studies demonstrated bifurcations as fundamental features in multi-channelled river systems that affect water and sediment transfer downstream based on the geometric character of the bifurcation (Bolla Pittaluga et al., 2003). Burge (2006) emphasized the dynamic behaviour of bifurcations and their impact on the characteristics of anabranching systems, where both stable and unstable bifurcations were observed in the Renous River in New Brunswick, Canada. Stable bifurcation scenarios comply with the majority of the findings in this research, where channels widened at bifurcations, causing sediment and water to be divided into branches downstream, while unstable bifurcation scenarios lead to non-uniform flow distribution and changing sediment transport patterns over time at bifurcation nodes, leading to significant deposition in a single branch (Burge, 2006). This is the case in The Breakaway where it avulses from Monkeygar Creek, which is slowly contracting as channel expansion along The Breakaway continues. Anabranches linked to unstable bifurcations could recover their stability if they have the ability to adjust their sinuosity, slope and/or channel capacity, or they could be abandoned if they become blocked by vegetation and/or sediment (or, for example, woody debris or ice jams in different systems) leading to a marked reduction in discharge and stream power. Kleinhans et al. (2013) defined stability in bifurcations when flow and sediment division are maintained during branching, and where fluctuating patterns in channels are affected by variations in discharge entering the system, but without systematic changes over time. Although channels can adjust, particularly in width as this thesis has shown, major morphological changes do not occur at stable bifurcations. Otherwise, unstable bifurcations that could lead to channel avulsion in lowland plains mostly re-join downstream and form an anastomosing pattern (Kleinhans et al., 2013). This pattern can remain for a long period, even during rapid avulsion and abandonment, but in a relatively unstable condition, until channels can efficiently redistribute water and sediment (Nanson, 2013).

Anastomosing rivers are defined as a type of dynamic equilibrium channel pattern (Nanson and Knighton, 1996) but are considered a non-equilibrium channel pattern when extrinsic disturbances affect the system (Makaske, 2001). Anabranching is associated with dynamic equilibrium conditions when channel geometry and hydraulic character become adjusted to balance the capability of water and sediment transport (Nanson and Knighton, 1996). However, Huang and Nanson (2000) state that not all anabranching systems achieve a stable equilibrium condition based on sediment transport enhancement. Huang and Nanson (2007) explained the relation between flow resistance and sediment transport in conveying sediment loads to maintain a systems equilibrium. In their study, channel slope was introduced as the initial parameter to adjust, however, in low slope environments, a reduction in channel width:depth ratio (in particular reduction in channel width), together with more channels in an anabranching pattern, can enhance flow efficiency. In another study from Latrubesse (2008), anabranching systems were shown to achieve efficient ways of moving water and sediment over low gradients. However, increasing the number of anabranches could lead to a reduction in transport capacity when the channel width cannot be significantly reduced (for example, in the Upper Columbia River in British Columbia, Canada) (Huang and Nanson, 2007). Nanson (2013) also showed that stable anabranches form where vertical accretion is slow and that this can then lead to equilibrium conditions.

Previous studies on the Macquarie Marshes revealed that channels experienced major avulsions in the historical period (Ralph et al., 2016) that disrupted the single-thread Macquarie River channel (Hesse et al., 2018) and in places converted it into an anastomosing pattern. The findings of this thesis showed that the majority of channels comprising the anastomosing pattern in the Macquarie Marshes (including most bifurcation and return nodes) are now stabilised and that the system is in a dynamic equilibrium state.

8.3.2 Contrasting character in distributive fluvial systems

Distributive fluvial systems (DFS) exhibit a single or multi-channelled river pattern where channels diverge downstream. They develop in all climate systems but, in particular, large, multi-channelled DFS are reported in dryland regions (Davidson et al., 2013). Although anabranching and distributary patterns arise from the same suite of hydrogeomorphic processes, the frequency of channel abandonment (due to avulsion) and the condition of channel boundaries determine the final pattern of the systems (Jerolmack and Mohrig, 2007). Indeed, non-equilibrium conditions in avulsing anabranching systems provide a base for DFS (Nanson and Huang, 2017), or else DFS form from a series of distributary streams (Fielding et al., 2012). Davidson et al. (2013) documented the breakdown of the main trunk stream into smaller distributary channels in a DFS that lead to channel termination in many cases. This would suggest a difference in sediment regimes where DFS are dominated by sediment deposition (Nanson and Huang, 2017). Avulsion was investigated in the Taquari River, Brazil, and the results showed that avulsion in this DFS caused a reduction in channel size in the primary channel due to rapid sedimentation (Buehler et al., 2011).

Weissmann et al. (2010) defined the difference between DFS and tributary fluvial systems. Their results for 700 cases showed that in DFS, channels have a radial pattern from the apex of the DFS (Sambrook Smith et al., 2010) and that they bifurcate downstream, leading to reductions in channel size and increases in floodplain area:channel ratio; while in tributary systems, discharge and channel size increase downstream (Weissmann et al., 2010). The DFS on the Gwydir floodplain, south-eastern Australia, exhibits a reduction in channel capacity followed by a decline in discharge in a distributary pattern (Pietsch et al., 2013). The Gregory River (Australia), Kur River (Russia) and Zambezi River (Namibia) are examples of this type of DFS around the world (Davidson et al., 2013). The Gwydir, Lachlan and Loddon are examples of DFS with floodouts and wetlands in Murray-Darling Basin (Hesse et al., 2018).

At the broadest scale, the 74,000 km^2 Macquarie alluvial plain comprising the Macquarie River, Macquarie Marshes and more than 50 palaeochannels can be considered a DFS (Hesse et al., 2018). The Macquarie Marshes occur where they do because of the breakdown in the lower Macquarie River within the DFS, which forms a complex set of flood outs and wetlands fed by the modern Macquarie River (Hesse et al., 2018). However, this thesis has demonstrated that, within the ~2,000 km^2 area of the Macquarie Marshes, anastomosing channels that serve to maintain flow, rather than distribute it, dominate over distributary channels.

8.4 Internal and external drivers of fluvial change

8.4.1 Internal mechanisms of channel change

Various intrinsic factors influence multi-channelled rivers and floodplain wetlands, including bank erosion leading to channel widening, sediment deposition causing reduction in channel capacity and braiding and channel avulsion (Yochum et al., 2017). Interactions between floodplain conditions and channel parameters (i.e. hydrology and geometry) define the broad characteristics of a system and its tendency for erosion and/or deposition (Hajek and Edmonds, 2014). Erosion is a natural process in rivers and floodplain wetlands that causes channel formation and development over time. Changes in the rates of channel adjustment (for example, accelerated erosion leading to channel enlargement) affect the flow distribution and location of aquatic habitats in these systems. Different types of erosion, including incision, widening and knickpoint retreat, are known to affect channel formation and evolution in floodplain wetlands (Oyston et al., 2014). A study of the South African drylands showed that knickpoint migrations lead to the formation of straight and deep channels, which could cause wetland abandonment (Tooth, 2018). Similarly, the risk of erosion has been demonstrated in the Macquarie Marshes in this thesis, where knickpoint retreat and channel enlargement occur in channels susceptible to significant erosion over time. Sediment deposition also occurs in rivers and floodplain wetlands causing channel infilling, development of in-stream depositional geomorphic units over time and topographic development on the floodplain. In the Macquarie Marshes, rates of sedimentation near major channels greatly exceed those on the distal floodplain, leading to gradient advantages for channel banks to be breached, which forms bifurcations and sometimes leads to avulsions

(Ralph, 2008; Ralph et al., 2011). As another example, sedimentation has been identified as the main reason for channel change leading to narrower reaches in the Talar River, Iran (Yousefi et al., 2017).

Erosion and sedimentation combine to influence avulsion (Jones and Schumm, 1999). River patterns also vary in response to channel avulsion and the related processes of self-adjustment through erosion and sedimentation that affect geometric and hydraulic character of the channels (Huang and Nanson, 2007). Studies have shown that avulsion is the dominant mechanism for the formation of new channels in both single and multi-channelled systems (Jerolmack and Mohrig, 2007), and that anastomosing patterns can form by avulsion due to in-channel deposition (Nanson and Knighton, 1996). Ralph and Hesse (2010) determined the important role of avulsion in the formation and abandonment of channels and distribution of floodwaters in the Southern Macquarie Marshes. Ralph (2008) demonstrated that avulsion and channel breakdown are pivotal processes in the formation and evolution of the system as a whole. Avulsion is a key control factor of the anastomosing pattern of the Narew River, Poland, which has had a slow but constant extinction of anabranches leading to a switch in river channel behaviour and the emerging dominance of a single-thread pattern in recent decades (Marcinkowski et al., 2018). Historical studies in the Yellow River, China, show that seven major avulsions affect 250,000 km^2 of this system (Slingerland and Smith, 2004). However, this river has mainly a single-thread channel due to the high degree of channel migration caused by bank erosion (Jerolmack and Mohrig, 2007). Avulsions control sediment and water dispersal in the long-term (Mohrig et al., 2000). For example, in the Saskatchewan River, Canada, avulsions guide flow to different parts of the marshes, leading to some areas of the system being abandoned while other parts are rejuvenated and adjust in channel form and hydraulic character to the new sediment and water regime (Smith et al., 1989).

Intrinsic processes play an important role in the system. These processes lead channels to form as bifurcations and return patterns and help them to maintain their geometric and hydraulic character. This would provide a dynamic equilibrium condition for the system.

8.4.2 External mechanisms of channel change

Various extrinsic factors (i.e. tectonic activity, lithology, climate change, sea level rise, land use change and human interference) control the structure and characteristics of multi-channelled rivers and floodplain wetlands (Larkin et al., 2017; Tooth, 2018). For example, change in local base levels in response to tectonic faulting, resistance of bed-rock outcrops and blocking by aeolian or fluvial sedimentation, are all key external controls on river character and behaviour in low energy conditions in dryland floodplain wetlands (Larkin et al., 2017). A study of Wakkerstroom Vlei, South Africa, considered the interaction between geological (i.e. bed-rock bevelling) and geomorphic conditions along with vegetation to control wetland formation (Joubert and Ellery, 2013). Human interference is also a critical element in river stabilisation, but also can cause instability. In the Karkheh River, Iran, human disturbances influenced two important river avulsions in this system, where artificial irrigation canals affected the flow divergence and led to high sedimentation rates (Heyvaert et al., 2012). Irrigation and dam construction have reduced the annual flows and peak discharge of the Rio Grande, United States, and have led to a reduction in channel size and avulsion (Tooth, 2000).

Climate regimes and climate change also play an important role in wetland character and this factor could control wetland hydrological regimes and geomorphological adjustments at a large scale (Lisenby et al., 2019; Rolls et al., 2018). Climate affects flow characteristics and has a particularly significant impact on runoff and flood inundation leading to changes in the ecological resilience of rivers and wetlands (Sandi et al., 2019). Rivers responding to climate change may be predictable or not, however, one of the remarkable changes that may occur is planform transition from a continuous, single-thread pattern to a multi-channelled river system pattern; an example of which has been documented for the Macquarie River during the Holocene period (Hesse et al., 2018). The Macquarie Marshes have also experienced impacts of climate change, such as reduced water availability leading to reduced flood frequency, which has resulted in low-level flows and increased in-channel erosion (Rogers et al., 2010). It is as yet unknown what geomorphological changes may occur in the Macquarie Marshes due to anthropogenic climate change, but destabilisation of bifurcation and return nodes and avulsive channels may occur, leading to a subtle (or perhaps pronounced) change in the internal dynamic equilibrium conditions documented by this thesis.

Extrinsic processes that cause major channel changes (for example, avulsions) play an important role in the character of a system. These processes could lead a system to shift to a new state or dynamic equilibrium when avulsions maintain channels and/or older channels are abandoned.

8.4.3 Prediction of channel change in complex fluvial systems

The outcomes of this research provide a comprehensive understanding of bifurcation, return and channel behaviour in the Macquarie Marshes during the past few decades, effectively documenting the medium- and short-term changes in the system due to channelization and channel adjustment. However, the Macquarie Marshes and similar floodplain wetlands are affected by a combination of biological, ecological, hydrological and geomorphological processes. Therefore, modelling approaches are required to predict the likelihood and rates of processes influencing channel changes over longer timeframes, and into the future.

Based on the modelling review in Chapter 2, hydrodynamic and morphodynamic models are practical for predicting erosion and sedimentation processes, bank erosion, channel hydrology and channel geometric character in response to intrinsic and extrinsic parameters within long-time periods. For example, CFDs could be applied to predict the rates of erosion and sedimentation likely to occur in response to different scenarios of climate change in the Macquarie Marshes considering the medium- and short-term character and behaviour of the system shown by this research. Alluvial architecture models would also prove useful for predicting the impacts of channel erosion and sedimentation that may lead to avulsion in the system. Moreover, a combination of information from flood patterns (simulated by hydrodynamic models) and system responses to flood situations could be helpful for system management.

8.5 Summary

This chapter has synthesised and discussed the major findings of this thesis. It has demonstrated the processes and history of channel change that have created a relative balance between geometric and hydraulic parameters in this multi-channelled river system that have led to a dominance of dynamic equilibrium fluvial conditions. It is clear that the character of the Macquarie Marshes and the mode of channel change that occurs in response to erosion and sedimentation is reflected in other similar systems worldwide. The impact of bifurcation and return nodes and channel avulsion in forming the anastomosing patterns in the Macquarie Marshes was also compared and contrasted with distributive fluvial systems. Overall, understanding the mix of intrinsic and extrinsic factors influencing channel change is critical. Furthermore, the application of modelling techniques combined with physical assessments to predict the future behaviour of complex fluvial systems will also prove extremely important. In the final chapter, the major findings of the thesis will be summarised and conclusions presented.

Chapter 9: Conclusion

9.1 Introduction

This chapter summarises the major findings of this thesis and shows how these findings address the aims of the research. Suggestions for future research are outlined to guide further investigations and quantifications of patterns and processes of biophysical change in multi-channelled rivers and floodplain wetlands.

9.2 Major findings

The main goal of the thesis was to understand the key patterns and processes of channel change and to define the behaviour of channel bifurcation and avulsion and other modes of channel adjustment by investigating the multi-channelled floodplain wetlands of the Macquarie Marshes. The major findings of this thesis are directly related to the aims of the research.

Aim 1: To quantify the spatial patterns of channels and determine the distribution of channel bifurcation and return nodes along major channels within the Macquarie Marshes.

This thesis has documented the anastomosing pattern of channels within the Macquarie Marshes, and quantified the numerous points of channel bifurcation and return nodes (889 and 997 nodes, respectively) that act to split and recombine flow within the complex network of channels and wetlands (see Chapter 5). The whole system and sub-systems (Southern, Northern and Eastern Macquarie Marshes) had more return nodes than bifurcations, and the Southern Macquarie Marshes exhibited more channelization with larger channels compared to the Northern and Eastern Macquarie Marshes. This pattern was repeated for the majority of river-reaches in the system, showing that channel bifurcations were balanced by returns downstream in most areas. In exceptional cases, bifurcations were not matched by returns, and in these cases, the channels tended to break down and terminate in wetlands on the floodplain.

Aim 2: To define the geomorphic configuration and hydraulic behaviour of channels leading to channel maintenance, avulsion and breakdown in the Macquarie Marshes.

This thesis has demonstrated that the channel size and flow capacity increased due to channel bifurcation, and that these gains were typically balanced or dominated by reductions in the combined channel size at confluences downstream (see Chapter 5). Together, this led to a dominance of channel maintenance throughout the system. Bankfull discharge and unit stream power at bifurcations exceeded the discharge and stream power in single channels and at return points. In the Southern and Eastern Macquarie Marshes, this has allowed the channels to transmit water and sediment effectively. Where a channel has reformed, such as in the Northern Macquarie Marshes, they have continued downstream and eventually formed outflowing channels that leave the end of the (sub)system. Therefore, channel capacity and bankfull discharge have a direct relationship that is critical for the efficient transmission of water and sediment. However, unit stream power was found to have a negative relationship with channel width, rather than total capacity, demonstrating the importance of channel width in influencing flows and stream power in the system.

The analysis of channel bifurcations and returns associated with channel geometric and hydraulic behaviour showed that channel maintenance and reformation occurred when clusters of bifurcations were balanced by clusters of returns. The bifurcation:return ratio for the Macquarie River upstream of Monkeygar Creek and Bora Creek was consistently above 1, which showed the tendency for distributary channels and/or channel breakdown to occur in the wetlands, while channels of this type became wider and shallower downstream. The bifurcation:return ratio for the Macquarie River downstream of the Old Macquarie River and Oxley Break was consistently below 1, which showed the tendency for accumulating flow and no opportunity for channel termination in the wetlands. The majority of channels, including the Old Macquarie River, Mole Marsh, The Breakaway, Monkeygar Creek, Monkey Creek, Bulgeraga Creek, Back Swamp and Buckiinguy Creek, had a bifurcation:return ratio that was initially above 1 and then dropped to below 1, showing how the bifurcations are superseded by the returns when the spread flow tends to be accumulated again. In contrast, the bifurcation:return ratio for the Macquarie River in the Northern Macquarie Marshes was initially below 1 and increased to above 1 where the channels break down, but then dropped again to below 1 as the channels reformed and continued downstream to the end of the system. The bifurcation:return ratio for Long Plain Cowal, Gum Cowal and Terrigal Creek hovered around 1, which showed a balanced situation with no significant dispersal or accumulation of flow.

Aim 3: To identify historical and contemporary trajectories of channel behaviour in hyper-avulsive reaches of the Southern Macquarie Marshes and to explain the role of erosion in the system.

This thesis has demonstrated that trunk streams and return reaches in the Southern Macquarie Marshes tend to have experienced expansion due to erosion, while bifurcation reaches in the system mostly experienced contraction due to sediment deposition in the short-term (i.e. seven years from 2008 to 2015; see Chapter 4). The Breakaway and places along the Old Macquarie River have enlarged in channel capacity, while Monkeygar Creek and the Macquarie River downstream of the Old Macquarie River experienced channel contraction. However, major changes in the morphological character of the rivers studied were not measured within the 26-year period between cross-section surveys (i.e. 1992 to 2018; see Chapter 6). A direct relationship between channel size and bankfull discharge was demonstrated and, in particular, channel width was found to have an effect on unit stream power. Therefore, in places where channels have enlarged, greater flow is required to achieve bankfull conditions and the affect this would have on the surrounding wetlands would depend on the overbank flow. Morphometric and hydraulic conditions at major avulsion nodes were shown to be different, leading to channel breakdown or anastomosing patterns. The Breakaway, which bifurcates from Monkeygar Creek, has increased in channel size and discharge capacity at the expense of Monkeygar Creek. Buckiinguy Creek, which bifurcates from the Macquarie River, has actually experienced a reduction in channel size and discharge capacity. This is potentially related to the process of channel abandonment in this area.

Aim 4: To assess erosion and sediment deposition risk at key sites in the Southern Macquarie Marshes and to rank channels according to the likelihood and consequences of channel change.

This thesis has demonstrated that most of the sites in the Southern Macquarie Marshes experienced few modifications due to erosion or sedimentation and are therefore maintained in the short-term (six years; see Chapter 7). However, the knickpoint at Buckiinguy Swamp was shown to be retreating quickly, which has led to new channels forming in this area. Therefore, knickpoint retreat is an especially important type of erosion that can cause rapid morphological change, and potentially rapid hydrological and ecological change, leading to a new level of channelization and avulsion in the system. Sites that were ranked as being of high risk include Buckiinguy Swamp (knickpoint at eastern outlet), Oxley Break, Buckiinguy Creek, Macquarie River downstream of Monkey Creek and downstream of Buckiinguy Creek, Monkeygar Creek upstream of The Breakaway in Nature Reserve, The Breakaway and Monkey Creek. Other sites were ranked as having moderate or low risk, including Bulgeraga Creek, Macquarie River downstream of Oxley Break and upstream of Monkey Creek, Macquarie River at Pillicawarrina and at Maxwelton, The Mole reed bed outflow channels, Buckiinguy Return and Buckiinguy Runner, Old Macquarie River in Nature Reserve and The Mole. The process of erosion risk assessment and site ranking is useful for river and wetland management in places where rapid and/or impactful changes occur, and where conservation and management actions may be required to address chronic or acute issues.

Aim 5: To synthesise and understand channel patterns and channel change processes in the Macquarie Marshes that are relevant for water and wetland management.

This thesis has demonstrated that there is balance of bifurcations and returns throughout most of the Macquarie Marshes, and that the anastomosing channels are, on the whole, being maintained in the system. Despite some key places where rapid channel adjustment has occurred and/or where channels have broken down and terminated in wetlands on the floodplain, the majority of systems experienced moderate or mild change over the short-term. However, while previous studies showed that avulsions have been frequent during the historical period, this research confirmed that those previous avulsions have most likely reached, or are approaching, a new level of stabilisation in the medium-term; that is, a dynamic equilibrium condition. Moreover, the Macquarie River trunk stream appears to be recovering its capacity and improving its hydraulic conditions to provide channel maintenance conditions in the long-term within the Macquarie Marshes system. Whether channel maintenance continues and is balanced by flood outs in wetlands, or whether increasing channelization occurs leading to wetland decline, remains to be seen, measured or modelled.

9.3 Directions for future research

This study leads to several potential pathways for future research in multi-channelled rivers and floodplain wetlands. These options are listed below:

1. Modelling sediment transport in bifurcating channels and the role of overbank flows within the major reaches of the Macquarie Marshes, and/or other similar systems.
2. Investigating the role of palaeochannels in influencing modern channel character, for example, whether inherited width and depth influences channel maintenance and/or breakdown in this type of system.
3. Investigating role and impact of vegetation on anastomosis or channel breakdown, for example, the influence of changing roughness in flood and drought cycles and the associated type and rate of channel adjustment due to erosion and/or sedimentation.
4. Investigating parameters that lead to bank erosion (rather than shear and compressive strength), for example, measuring and modelling the impacts of animal trampling, flow regime change and artificial bank and other stream restoration works.
5. Modelling channel bifurcation and return nodes to assess the real-time morphodynamic processes that influence channel formation and enlargement and the fine-scale adjustment of geomorphic units and how they behave through a system.

References

ANZECC 2000, *Australian and New Zealand guidelines for fresh and marine water quality: volume 2, aquatic ecosystems*, Australian and New Zealand Environment and Conservation Council (ANZECC) and Agriculture and Resource Management Council of Australia and New Zealand, Canberra, Australia.

Arcement, GJ & Schneider, VR 1989, 'Guide for selecting Manning's roughness coefficients for natural channels and flood plains'.

Arnaud, F, Piégay, H, Béal, D, Collery, P, Vaudor, L. & Rollet, AJ 2017, 'Monitoring gravel augmentation in a large regulated river and implications for process-based restoration', *Earth Surface Processes and Landforms*, vol. *42*, no. 13, pp. 2147-2166.

AS/NZS 4360 2004, *Risk Management*, Joint Australian/New Zealand Standard (AS/NZS 4360).

Bagarello, V, Ferro, V, Keesstra, S, Comino, JR, Pulido, M & Cerdà, A 2018, 'Testing simple scaling in soil erosion processes at plot scale', *Catena*, vol. 167, pp. 171-180.

Balaguer-Puig, M, Marqués-Mateu, Á, Lerma, JL & Ibáñez-Asensio, S 2017, 'Quantifying small-magnitude soil erosion: geomorphic change detection at plot scale', *Land Degradation & Development*, vol. 29, no. 3, pp. 825-834.

Bandyopadhyay, S & De, SK 2017, 'Estimation of bank erosion of the Haora River and proposition of bank erosion vulnerability zonation model', in S Bandyopadhyay & SK De, *Human Interference on River Health: a study on the Haora River, Tripura, India*, Springer International Publishing, Switzerland, pp. 141-167.

Barnes, HH 1849, 'Roughness characteristics of natural channels', *US Geol, Survey, Water Supply Paper*.

Belletti, B, Dufour, S & Piégay, H 2013, 'What is the relative effect of space and time to explain the braided river width and island patterns at a regional scale?', *River Research and Applications*, vol. 31 no. 1, pp. 1-15.

Beneš, B, Těšínský, V, Hornyš, J & Bhatia, SK 2006, 'Hydraulic erosion', *Computer Animation and Virtual Worlds*, vol. 172, no. 2, pp. 99-108.

Bezak, N, Grigillo, D, Rusjan, S, Šraj, M, Urbancic, T, Trajkovski, KK, Petrovic, D & Mikoš, M 2015, *Sediment budget estimation in a small torrential catchment using DEM of difference approach*, conference paper, European Geosciences Union General Assembly (EGU 2015) 12-17 April, Vienna, Austria.

Bezak, N, Grigillo, D, Urbančič, T, Mikoš, M, Petrovič, D & Rusjan, S 2017, 'Geomorphic response detection and quantification in a steep forested torrent', *Geomorphology*, vol. 291, pp. 33-44.

Bizzi, S, Demarchi, L, Grabowski, RC, Weissteiner, CJ & Van de Bund, W 2016, 'The use of remote sensing to characterise hydromorphological properties of European rivers', *Aquatic Sciences*, vol. 78, no. 1, pp. 57-70.

Blom, A, Arkesteijn, L, Chavarrías, V & Viparelli, E 2017, 'The equilibrium alluvial river under variable flow and its channel-forming discharge', *Journal of Geophysical Research: Earth Surface*, vol. 122, no. 10, pp. 1924-1948.

Bogoni, M, Putti, M & Lanzoni, S 2017, 'Modeling meander morphodynamics over self-formed heterogeneous floodplains', *Water Resources Research*, vol. 53, no. 6, pp. 5137-5157.

Boix-Fayos, C, Martínez-Mena, M, Arnau-Rosalén, E, Calvo-Cases, A, Castillo, V & Albaladejo, J 2006, 'Measuring soil erosion by field plots: understanding the sources of variation, *Earth-Science Reviews*, vol. 78, no. 3-4, pp. 267-285.

Bolla Pittaluga, M, Repetto, R & Tubino, M 2003, 'Channel bifurcation in braided rivers: equilibrium configurations and stability', *Water Resources Research*, vol. 39, no. 3, pp. 1046-1058.

Bolton, DK, Coops, NC & Wulder, MA 2015, 'Characterizing residual structure and forest recovery following high-severity fire in the western boreal of Canada using Landsat time-series and airborne lidar data', *Remote Sensing of Environment*, vol. 163, pp. 48-60.

Brasington, J, Rumsby, B & Mcvey, R 2000, 'Monitoring and modelling morphological change in a braided gravel-bed river using high resolution GPS-based survey, *Earth Surface Processes and Landforms: The Journal of the British Geomorphological Research Group*, vol. 25, no. 9, pp. 973-990.

Bravard, JP 2010, 'Discontinuities in braided patterns: the River Rhône from Geneva to the Camargue delta before river training', *Geomorphology*, vol. 117, no. 3-4, pp. 219-233.

Brazier, R 2004, 'Quantifying soil erosion by water in the UK: a review of monitoring and modelling approaches', *Progress in Physical Geography: Earth and Environment*, vol. 28, no. 3, pp. 340-365.

Brereton, GJ 1994, *An investigation into the impact of erosion in the Southern Macquarie Marshes*, *Macquarie Marshes Management Strategy, Stage 1, Biophysical Investigations, Natural Resources Management Strategy Project,* Department of Water Resources, Dubbo, New South Wales, Australia.

Brogan, DJ, Nelson, PA & Macdonald, LH 2015, *Quantifying erosion and deposition patterns using airborne LiDAR following the 2012 High Park Fire and 2013 Colorado Flood*, conference proceedings, American Geophysical Union (2015 AGU Fall Meeting), 14-18 December, San Francisco, United States of America.

Buehler, HA, Weissmann, GS, Scuderi, LA & Hartley, AJ 2011, 'Spatial and temporal evolution of an avulsion on the Taquari River distributive fluvial system from satellite image analysis', *Journal of Sedimentary Research*, vol. 81, no. 8, pp. 630-640.

Burge, LM 2006, 'Stability, morphology and surface grain size patterns of channel bifurcation in gravel–cobble bedded anabranching rivers', *Earth Surface Processes and Landforms*, vol. 31, no. 10, pp. 1211-1226.

Cahoon, DR & Turner, RE 1989, 'Accretion and canal impacts in a rapidly subsiding wetland II. Feldspar marker horizon technique', *Estuaries*, vol. 12, no. 4, pp. 260-268.

Chaplot, V & Le Bissonnais, Y 2000, 'Field measurements of interrill erosion under different slopes and plot sizes', *Earth Surface Processes and Landforms: The Journal of the British Geomorphological Research Group*, vol. 25, no. 2, pp. 145-153.

Charlton, ME, Large, ARG & Fuller, IC 2003, 'Application of airborne LiDAR in river environments: the River Coquet, Northumberland, UK', *Earth Surface Processes and Landforms: The Journal of the British Geomorphological Research Group*, vol. 28, no. 3, pp. 299-306.

Coulthard, TJ & Van De Wiel, MJ 2012, 'Modelling river history and evolution', *Philosophical Transactions of the Royal Society of London A: Mathematical, Physical and Engineering Sciences*, no. 370, pp. 2123-2142.

Coulthard, TJ, Neal, JC, Bates, PD, Ramirez, J, Almeida, GA & Hancock, GR 2013, 'Integrating the LISFLOOD-FP 2D hydrodynamic model with the CAESAR model: implications for modelling landscape evolution', *Earth Surface Processes and Landforms*, vol. 38, no. 15, pp. 1897-1906.

Couper, P, Stott, T & Maddock, I 2002, 'Insights into river bank erosion processes derived from analysis of negative erosion-pin recordings: observations from three recent UK studies', *Earth Surface Processes and Landforms*, vol. 27, no. 1, pp. 59-79.

Croke, J, Todd, P, Thompson, C, Watson, F, Denham, R & Khanal, G 2013, 'The use of multi temporal LiDAR to assess basin-scale erosion and deposition following the catastrophic January 2011 Lockyer flood, SE Queensland, Australia', *Geomorphology*, vol. 184, pp. 111-126.

Croke, J, Todd, P, Thompson, C, Watson, F, Denham, R & Khanal, G 2013, 'The use of multi temporal LiDAR to assess basin-scale erosion and deposition following the catastrophic January 2011 Lockyer flood, SE Queensland, Australia', *Geomorphology*, vol. 184, pp. 111-126.

Cunningham, AG, Lillycrop, W, Guenther, GC & Brooks, MW 2016, 'Shallow water laser bathymetry: accomplishments and applications, *US Army Corps of Engineers Mobile United States*, AD1003834.

Dackombe, RV & Gardiner, V 1983, *Geomorphological field manual*, Allen & Unwin, Crows Nest, Australia.

Davidson, SK, Hartley, AJ, Weissmann, GS, Nichols, GJ & Scuderi, LA 2013, 'Geomorphic elements on modern distributive fluvial systems', *Geomorphology*, vol. 180-181, pp. 82-95.

De Rose, RC & Basher, LR 2011, 'Measurement of river bank and cliff erosion from sequential LIDAR and historical aerial photography', *Geomorphology*, vol. 126, no. 1-2, pp. 132-147.

Deng, ZQ & Singh, VP 1999, 'Mechanism and conditions for change in channel pattern', *Journal of Hydraulic Research*, vol. 37, no. 4, pp. 465-478.

Devia, GK, Ganasri, B & Dwarakish, G 2015, 'A review on hydrological models', *Aquatic Procedia*, vol. 4, pp. 1001-1007.

Di Baldassarre, G, Schumann, G & Bates, P 2009, 'Near real time satellite imagery to support and verify timely flood modelling', *Hydrological Processes: An International Journal*, vol. 23, no. 5, pp. 799-803.

Elmi, O, Tourian, M & Sneeuw, N 2016, 'Dynamic river masks from multi-temporal satellite imagery: an automatic algorithm using graph cuts optimization', *Remote Sensing*, vol. 8, no. 12, pp. 1005.

Elmi, O, Tourian, MJ & Sneeuw, N 2015, 'River discharge estimation using channel width from satellite imagery', *IEEE International Geoscience and Remote Sensing Symposium (IGARSS)*, 26-31 July, Milan, Italy.

Fang, N, Wang, L & Shi, Z 2017, 'Runoff and soil erosion of field plots in a subtropical mountainous region of China', *Journal of Hydrology*, vol. 552, pp. 387-395.

Farebrother, W & Ralph, TJ 2017, 'Semi-automated delineation of reticulate channel networks in low-gradient floodplain wetlands using LiDAR-derived DEMs', *In T. J. Ralph (Ed.), WIDS2017 Dynamic Landscapes: proceedings of the Wetlands in Drylands Research Network Conference*, Sydney, Australia: Macquarie University, pp. 11-12.

Farrell, KM 2001, ‘Geomorphology, facies architecture, and high-resolution, non-marine sequence stratigraphy in avulsion deposits, Cumberland Marshes, Saskatchewan’, *Sedimentary Geology*, vol. 139, no. 2, pp. 93-150.

Fielding, CR, Ashworth, PJ, Best, JL, Prokocki, EW & Smith, GHS 2012, ‘Tributary, distributary and other fluvial patterns: what really represents the norm in the continental rock record?’, *Sedimentary Geology*, vol. 261-262, pp. 15-32.

Fonstad, MA, Dietrich, JT, Courville, BC, Jensen, JL & Carbonneau, PE 2013, ‘Topographic structure from motion: a new development in photogrammetric measurement’, *Earth Surface Processes and Landforms*, vol. 38, no. 4, pp. 421-430.

Foucher, A, Salvador-Blanes, S, Vandromme, R, Cerdan, O & Desmet, M 2017, ‘Quantification of bank erosion in a drained agricultural lowland catchment’, *Hydrological Processes*, vol. 31, no. 6, pp. 1424-1437.

Frings, RM & Kleinhans, MG 2008, ‘Complex variations in sediment transport at three large river bifurcations during discharge waves in the river Rhine’, *Sedimentology*, vol. *55,* no. 5, pp. 1145-1171.

Fryirs, KA, Ralph, TJ, Larkin, ZT, Tooth, S, Humphries, M, Mccarthy, T, Hesse, PP & Mosimanyana, E 2018, ‘A nested hierarchical perspective to enhance interpretations and communication in fluvial geomorphology for use in water resources management: lessons from the Okavango Delta, Botswana’, *The Geographical Journal*, vol. 184, no. 2, pp. 192-207.

Fuller, I, Passmore, D, Heritage, G, Large, A, Milan, D & Brewer, P 2002, ‘Annual sediment budgets in an unstable gravel-bed river: the River Coquet, northern England’, *Geological Society, London, Special Publications*, vol. 191, no. 1, pp. 115-131.

Fuller, IC, Large, AR, Charlton, ME, Heritage, GL & Milan, DJ 2003, ‘Reach-scale sediment transfers: an evaluation of two morphological budgeting approaches’, *Earth Surface Processes and Landforms: The Journal of the British Geomorphological Research Group*, vol. 28, no. 8, pp. 889-903.

Gell, P, Fluin, J, Tibby, J, Hancock, G, Harrison, J, Zawadzki, A, Haynes, D, Khanum, S, Little, F & Walsh, B 2009, ‘Anthropogenic acceleration of sediment accretion in lowland floodplain wetlands, Murray–Darling Basin, Australia’, *Geomorphology*, vol. 108, no. 1-2, pp. 122-126.

Genç, L, Dewitt, B & Smith, S 2004, ‘Determination of wetland vegetation height with LIDAR’, *Turkish Journal of Agriculture and Forestry*, vol. 28, no. 1, pp. 63-71.

Gibling, MR, Nanson, GC & Maroulis, JC 1998, 'Anastomosing river sedimentation in the Channel Country of central Australia', *Sedimentology*, vol. 45, no. 3, pp. 595-619.

Gobeyn, S, Van Wesemael, A, Neal, J, Lievens, H, Van Eerdenbrugh, K, De Vleeschouwer, N, Vernieuwe, H, Schumann, GJP, Di Baldassarre, G, De Baets, B, Bates, PD & Verhoest NEC 2017, 'Impact of the timing of a SAR image acquisition on the calibration of a flood inundation model', *Advances in Water Resources*, vol. 100, pp. 126-138.

GRASS Development Team 2018, *GRASS GIS 7.0.7svn Reference Manual: r.watershed*, viewed June 2017 to March 2019, https://grass.osgeo.org/grass70/manuals/r.watershed.html

Greaves, HE, Vierling, LA, Eitel, JU, Boelman, NT, Magney, TS, Prager, CM & Griffin, KL 2017, 'Applying terrestrial lidar for evaluation and calibration of airborne lidar-derived shrub biomass estimates in Arctic tundra', *Remote Sensing Letters*, vol. 8, no. 2, pp. 175-184.

Grenfell, MC 2012, Dynamics and morphodynamic implications of chute channels in large, sand-bed meandering rivers, postdoctoral thesis, University of Exeter, United Kingdom.

Grenfell, MC 2015, 'Section 6.4: dGPS', in SJ Cook, LE Clarke & JM Nield (eds), *Geomorphological Techniques (Online Edition)*, British Society for Geomorphology, London, United Kingdom.

Gupta, A & Liew, SC 2007, 'The Mekong from satellite imagery: a quick look at a large river', *Geomorphology*, vol. 85, no. 3-4, pp. 259-274.

Gupta, A, Hock, L, Xiaojing, H & Ping, C 2002, 'Evaluation of part of the Mekong River using satellite imagery', *Geomorphology*, vol. 44, no. 3-4, pp. 221-239.

Gurnell, AM, Morrissey, IP, Boitsidis, AJ, Bark, T, Clifford, NJ, Petts, GE & Thompson, K 2006, 'Initial adjustments within a new river channel: interactions between fluvial processes, colonizing vegetation, and bank profile development', *Environmental Management*, vol. 38, no. 4, pp. 580-596.

Hajek, EA & Edmonds, DA 2014, 'Is river avulsion style controlled by floodplain morphodynamics?', *Geology*, vol. 42, no. 3, pp. 199-202.

Hajek, EA & Wolinsky, MA 2012, 'Simplified process modeling of river avulsion and alluvial architecture: connecting models and field data', *Sedimentary Geology*, vol. 257, pp. 1-30.

Hancock, G, Willgoose, G & Evans, K 2002, 'Testing of the SIBERIA landscape evolution model using the Tin Camp Creek, Northern Territory, Australia, field catchment', *Earth Surface Processes and Landforms: The Journal of the British Geomorphological Research Group*, vol. 27, no. 2, pp. 125-143.

Henshaw, AJ, Thorne, CR & Clifford, NJ 2013, 'Identifying causes and controls of river bank erosion in a British upland catchment', *Catena*, vol. 100, pp. 107-119.

Heritage, G, Milan, D & Entwistle, N 2016, *Alluvial anastomosed channels: the preferred channel type on active UK rivers*, conference paper, 11th International Symposium on Ecohydraulics (ISE 2016), 7-12 February, Melbourne, Australia.

Hesse, PP, Williams, R, Ralph, TJ, Fryirs, KA, Larkin, ZT, Westaway, KE & Farebrother, W 2018, 'Palaeohydrology of lowland rivers in the Murray-Darling Basin, Australia', *Quaternary Science Reviews*, vol. 200, pp. 85-105.

Hesse, PP, Williams, R, Ralph, TJ, Larkin, ZT, Fryirs, KA, Westaway, KE & Yonge, D 2018, 'Dramatic reduction in size of the lowland Macquarie River in response to Late Quaternary climate-driven hydrologic change', *Quaternary Research*, vol. 90, no. 2, pp. 360-379.

Heyvaert, VM, Walstra, J, Verkinderen, P, Weerts, HJ & Ooghe, B 2012, 'The role of human interference on the channel shifting of the Karkheh River in the Lower Khuzestan plain (Mesopotamia, SW Iran)', *Quaternary International*, vol. 251, pp. 52-63.

Hooke, J & Mant, J 2000, 'Geomorphological impacts of a flood event on ephemeral channels in SE Spain', *Geomorphology*, vol. 34, no. 3-4, pp. 163-180.

Huang, C, Peng, Y, Lang, M, Yeo, IY & Mccarty, G 2014, 'Wetland inundation mapping and change monitoring using Landsat and airborne LiDAR data', *Remote Sensing of Environment*, vol. 141, pp. 231-242.

Huang, HQ & Nanson, GC 2000, 'Hydraulic geometry and maximum flow efficiency as products of the principle of least action', *Earth Surface Processes and Landforms*, vol. 25, no. 1, pp. 1-16.

Huang, HQ & Nanson, GC 2007, 'Why some alluvial rivers develop an anabranching pattern', *Water Resources Research*, vol. 43, no. 7, doi:10.1029/2006wr005223.

Hupp, CR, Schenk, ER, Kroes, DE, Willard, DA, Townsend, PA & Peet, RK 2015, 'Patterns of floodplain sediment deposition along the regulated lower Roanoke River, North Carolina: annual, decadal, centennial scales', *Geomorphology*, vol. 228, pp. 666-680.

Jain, V & Sinha, R 2003, ‘Hyperavulsive-anabranching Baghmati river system, north Bihar plains, eastern India’, *Zeitschrift für Geomorphologie*, vol. 47, no. 1, pp. 101-116.

Jain, V & Sinha, R 2004, ‘Fluvial dynamics of an anabranching river system in Himalayan foreland basin, Baghmati river, north Bihar plains, India’, *Geomorphology*, vol. 60, no. 1-2, pp. 147-170.

Javernick, L, Brasington, J & Caruso, B 2014, ‘Modeling the topography of shallow braided rivers using Structure-from-Motion photogrammetry’, *Geomorphology*, vol. 213, no. 166-182.

Jerolmack, DJ & Mohrig, D 2007, ‘Conditions for branching in depositional rivers’, *Geology*, vol. 35, no. 5, pp. 463-466.

Jones, AF, Brewer, PA, Johnstone, E & Macklin, MG 2007, ‘High-resolution interpretative geomorphological mapping of river valley environments using airborne LiDAR data’, *Earth Surface Processes and Landforms*, vol. 32, no. 10, pp. 1574-1592.

Jones, LS & Schumm, SA 1999, ‘Causes of avulsion: an overview’, in *Fluvial Sedimentology VI*, International Association of Sedimentologists, Blackwell Science Ltd, United Kingdom, pp. 171-178.

Joubert, R & Ellery, W 2013, ‘Controls on the formation of Wakkerstroom Vlei, Mpumalanga province, South Africa’, *African Journal of Aquatic Science*, vol. 38, no. 2, pp. 135-151.

Kamintzis, JE, Irvine-Fynn, T, Holt, T, Jones, JPP, Tooth, S, Griffiths, H & Hubbard, B 2019, ‘Knickpoint evolution in a supraglacial stream’, *Geografiska Annaler: Series A, Physical Geography*, vol. 101, no. 2, pp. 118-135.

Kearney, S, Fonte, SJ, García, E & Smukler, SM 2018, ‘Improving the utility of erosion pins: absolute value of pin height change as an indicator of relative erosion’, *Catena*, vol. 163, pp. 427-432.

Kelleway, JJ, Cavanaugh, K, Rogers, K, Feller, IC, Ens, E, Doughty, C & Saintilan, N 2017, ‘Review of the ecosystem service implications of mangrove encroachment into salt marshes’, *Global change biology*, vol. 23, no. 10, pp. 3967-3983.

Kimiaghalam, N, Goharrokhi, M & Clark, SP 2016, ‘Assessment of wide river characteristics using an acoustic Doppler current profiler’, *Journal of Hydrologic Engineering*, vol. 21, no. 12, pp. 06016012.

Kingsford, R & Thomas, R 2004, ‘Destruction of wetlands and waterbird populations by dams and irrigation on the Murrumbidgee River in arid Australia’, *Environmental Management*, vol. 34, no. 3, pp. 383-396.

Kingsford, RT & Auld, KM 2005, 'Waterbird breeding and environmental flow management in the Macquarie Marshes, arid Australia', *River Research and Applications*, vol. 21, no. 2-3, pp. 187-200.

Kingsford, RT & Thomas, RF 1995, 'The Macquarie Marshes in arid Australia and their waterbirds: a 50-year history of decline', *Environmental Management*, vol. 19, no. 6, pp. 867-878.

Kleinhans, MG 2010, 'Sorting out river channel patterns', *Progress in Physical Geography*, vol. 34, no. 3, pp. 287-326.

Kleinhans, MG, Ferguson, RI, Lane, SN & Hardy, RJ 2013, 'Splitting rivers at their seams: bifurcations and avulsion', *Earth Surface Processes and Landforms*, vol. 38, no. 1, pp. 47-61.

Kleinhans, MG, Weerts, HJ & Cohen, KM 2010, 'Avulsion in action: reconstruction and modelling sedimentation pace and upstream flood water levels following a Medieval tidal-river diversion catastrophe (Biesbosch, The Netherlands, 1421–1750AD)', *Geomorphology*, vol. 118, no. 1-2, pp. 65-79.

Knaus, RM & Van Gent, DL 1989, 'Accretion and canal impacts in a rapidly subsiding wetland. III. A new soil horizon marker method for measuring recent accretion', *Estuaries*, vol. 12, no. 4, pp. 269-283.

Kobayashi, T, Ralph, TJ, Ryder, DS & Hunter, SJ 2013, 'Gross primary productivity of phytoplankton and planktonic respiration in inland floodplain wetlands of southeast Australia: habitat-dependent patterns and regulating processes', *Ecological Research*, vol. 28, no. 5, pp. 833-843.

Lallias-Tacon, S, Liébault, F & Piégay, H 2017, 'Use of airborne LiDAR and historical aerial photos for characterising the history of braided river floodplain morphology and vegetation responses', *Catena*, vol. 149, pp. 742-759.

Larkin, ZT, Ralph, TJ, Tooth, S & Mccarthy, T 2016, 'The interplay between extrinsic and intrinsic controls in determining floodplain wetland characteristics in the South African drylands', *Earth Surface Processes and Landforms*, vol. 42, no. 7, pp. 1092-1109.

Larkin, ZT, Tooth, S, Ralph, TJ, Duller, GA, Mccarthy, T, Keen-Zebert, A & Humphries, MS 2017, 'Timescales, mechanisms, and controls of incisional avulsions in floodplain wetlands: insights from the Tshwane River, semiarid South Africa', *Geomorphology*, vol. 283, pp. 158-172.

Latrubesse, EM 2008, 'Patterns of anabranching channels: the ultimate end-member adjustment of mega rivers', *Geomorphology*, vol. 101, no. 1-2, pp. 130-145.

Lauer, JW, Echterling, C, Lenhart, C, Belmont, P & Rausch, R 2017, 'Air-photo based change in channel width in the Minnesota River basin: modes of adjustment and implications for sediment budget', *Geomorphology*, vol. 297, pp. 170-184.

Lawler, DM 1991, 'A new technique for the automatic monitoring of erosion and deposition rates', *Water Resources Research*, vol. 27, no. 8, pp. 2125-2128.

Lawler, DM 1993, 'The measurement of river bank erosion and lateral channel change: a review', *Earth Surface Processes and Landforms*, vol. 18, no. 9, pp. 777-821.

Lawler, DM, West, JR, Couperthwaite, JS & Mitchell, SB 2001, 'Application of a novel automatic erosion and deposition monitoring system at a channel bank site on the tidal River Trent, U.K', *Estuarine, Coastal and Shelf Science*, vol. 53, no. 2, pp. 237-247.

Lea, DM & Legleiter, CJ 2016, 'Mapping spatial patterns of stream power and channel change along a gravel-bed river in northern Yellowstone', *Geomorphology*, vol. 252, pp. 66-79.

Lefsky, MA, Cohen, W, Acker, S, Parker, GG, Spies, T & Harding, D 1999, 'Lidar remote sensing of the canopy structure and biophysical properties of Douglas-fir western hemlock forests', *Remote Sensing of Environment*, vol. 70, no. 3, pp. 339-361.

Lisenby, PE, Fryirs, KA 2017, 'Sedimentologically significant tributaries: catchment-scale controls on sediment (dis) connectivity in the Lockyer Valley, SEQ, Australia', *Earth Surface Processes and Landforms*, vol. 42, no. 10, pp. 1493-1504.

Li, J, Bristow, CS, Luthi, SM & Donselaar, ME 2015, 'Dryland anabranching river morphodynamics: Río Capilla, Salar de Uyuni, Bolivia' *Geomorphology*, vol. 250, pp. 282–297.

Li, J, Grenfell, MC, Wei, H, Tooth, S & Ngiem, S 2020, 'Chute cutoff-driven abandonment and sedimentation of meander bends along a fine-grained, non-vegetated, ephemeral river on the Bolivian Altiplano', *Geomorphology*, vol. *350*, pp. 106917.

Lisenby, PE, Tooth, S & Ralph, TJ 2019, 'Product vs. process? The role of geomorphology in wetland characterization', *Science of the Total Environment*, vol. 663, pp. 980-991.

Liu, J, Clift, PD, Yan, W, Chen, Z, Chen, H, Xiang, R & Wang, D 2014, 'Modern transport and deposition of settling particles in the northern South China Sea: sediment trap evidence adjacent to Xisha Trough', *Deep Sea Research Part I: Oceanographic Research Papers*, vol. 93, pp. 145-155.

Lovric, N & Tosic, R 2016, ‘Assessment of bank erosion, accretion and channel shifting using remote sensing and GIS: case study–lower course of the Bosna River’, *Quaestiones Geographicae*, vol. 35, no. 1, pp. 81-92.

Lu, S, Zhang, L, Guo, S, Fan, L, Meng, J & Wang, G 2016, ‘Forty years' channel change on the Yongdinghe River, China: patterns and causes’, *International Journal of River Basin Management*, vol. 14, no. 2, pp. 183-193.

Makaske, B 2001, ‘Anastomosing rivers: a review of their classification, origin and sedimentary products, *Earth-Science Reviews*, vol. 53, no. 3-4, pp. 149-196.

Malik, I & Matyja, M 2008, ‘Bank erosion history of a mountain stream determined by means of anatomical changes in exposed tree roots over the last 100 years (Bílá Opava River — Czech Republic)’, *Geomorphology*, vol. 98, no. 1-2, pp. 126-142.

Marcinkowski, P, Giełczewski, M & Okruszko, T 2018, ‘Where might the hands-off protection strategy of anastomosing rivers lead? A case study of Narew National Park’, *Polish Journal of Environmental Studies*, vol. 27, no. 6, pp. 2647-2658.

Marks, K & Bates, P 2000, ‘Integration of high-resolution topographic data with floodplain flow models’, *Hydrological Processes*, vol. 14, no. 11-12, pp. 2109-2122.

Matsubara, Y & Howard, AD 2014, ‘Modeling planform evolution of a mud-dominated meandering river: Quinn River, Nevada, USA’, *Earth Surface Processes and Landforms*, vol. 39, no. 10, pp. 1365-1377.

Meng, X, Wang, H, Cai, S, Zhang, X, Leng, G, Lei, X, Shi, C, Liu, S & Shang Y 2016, ‘The China meteorological assimilation driving datasets for the SWAT model (CMADS) and it's application in China: a case study in Heihe River Basin’, *Preprints*, doi:10.20944/preprints201612.0091.v2.

Middlemann, MH (ed) 2007, *Natural hazards in Australia: identifying risk analysis requirements*, Geoscience Australia, Department of Transport and Regional Services, Canberra, Australia.

Milan, DJ, Heritage, GL, Large, ARG & Fuller, IC 2011, ‘Filtering spatial error from DEMs: implications for morphological change estimation’, *Geomorphology*, vol. 125, no. 1, pp. 160-171.

Mohrig, D, Heller, PL, Paola, C & Lyons, WJ 2000, ‘Interpreting avulsion process from ancient alluvial sequences: Guadalope-Matarranya system (northern Spain) and Wasatch Formation (western Colorado)’, *Geological Society of America Bulletin*, vol. 112, no. 12, pp. 1787-1803.

Morsy, MM, O'neil, GL, Goodall, JL & Hassan, G 2017, *Computational Enhancements for the Virginia Department of Transportation Regional River Severe Storm (R^2S^2) Model*, Virginia Transportation Research Council, Charlottsville, Virginia.

Murray, AB & Paola, C 1994, ‘A cellular model of braided rivers’, *Nature*, vol. 371, pp. 54-57.

Murray, AB & Paola, C 1997, ‘Properties of a cellular braided-stream model’, *Earth Surface Processes and Landforms*, vol. 22, no. 11, pp. 1001-1025.

Murray-Darling Basin Authority (MDBA) 2011, *Acid Sulfate soils in the Murray-darling Basin*, Murray-Darling Basin Authority, Canberra, Australia.

Murray-Darling Basin Authority(MDBA) 2012, *Assessment of environmental water requirements for the proposed Basin Plan: Macquarie Marshes*, Murray-Darling Basin Authority, Canberra, Australia.

Musa, Z, Popescu, I & Mynett, A 2015, ‘A review of applications of satellite SAR, optical, altimetry and DEM data for surface water modelling, mapping and parameter estimation’, *Hydrology and Earth System Sciences*, vol. 19, no. 9, pp. 3755-3769.

Nabi, M, Vriend, DH, Mosselman, E, Sloff, C & Shimizu, Y 2012, ‘Detailed simulation of morphodynamics: 1. hydrodynamic model’, *Water Resources Research*, vol. 48, no. 12, doi:10.1029/2012WR011911.

Nanson, G 2013, ‘9.19 Anabranching and anastomosing rivers’, *Reference Module in Earth Systems and Environmental Sciences: Treatise on Geomorphology*, vol. 9, pp. 330-345.

Nanson, GC, Huang, HQ 2017, ‘Self-adjustment in rivers: evidence for least action as the primary control of alluvial-channel form and process’, *Earth Surface Processes and Landforms*, vol. 42, no. 4, pp. 575-594,

Nanson, GC, Knighton, AD 1996, ‘Anabranching rivers: their cause, character and classification’, *Earth Surface Processes and Landforms*, vol. 21, no. 3, pp. 217-239.

Nicholas, AP 2013, ‘Modelling the continuum of river channel patterns’, *Earth Surface Processes and Landforms*, vol. 38, no. 10, pp. 1187-1196.

Office of Environment and Heritage (OEH) 2008, *J221527 NSW DECC Central Wetlands LiDAR*, Office of Environment and Heritage, Sydney, Australia.

Oyston, SM, Ralph, TJ & Hesse, PP 2014, 'Cutting down, back and out: assessment of channel erosion in a sensitive floodplain wetland', in G Vietz, ID Rutherfurd & R Hughes (editors), *Proceedings of the 7th Australian Stream Managament Conference*, 27-30 July, Townsville, Queensland, pp. 143-149.

Palmer, JA, Schilling, KE, Isenhart, TM, Schultz, RC, Tomer, MD 2014, 'Streambank erosion rates and loads within a single watershed: bridging the gap between temporal and spatial scales', *Geomorphology*, vol. 209, pp. 66-78.

Papanicolaou, AT, Wilson, CG, Tsakiris, AG, Sutarto, TE, Bertrand, F, Rinaldi, M, Dey, S & Langendoen, E 2017, 'Understanding mass fluvial erosion along a bank profile: using PEEP technology for quantifying retreat lengths and identifying event timing', *Earth Surface Processes and Landforms*, vol. 42, no. 11, pp. 1717-1732.

Patel, DP, Ramirez, JA, Srivastava, PK, Bray, M & Han, D 2017, 'Assessment of flood inundation mapping of Surat city by coupled 1D/2D hydrodynamic modeling: a case application of the new HEC-RAS 5', *Natural Hazards*, vol. 89, no. 1, pp. 93-130.

Patro, S, Chatterjee, C, Mohanty, S, Singh, R & Raghuwanshi, N 2009, 'Flood inundation modeling using MIKE FLOOD and remote sensing data', *Journal of the Indian Society of Remote Sensing*, vol. 37, no. 1, pp. 107-118.

Peyer, KE, Morris, M & Sellers, WI 2015, 'Subject-specific body segment parameter estimation using 3D photogrammetry with multiple cameras', *PeerJ*, vol. 3. https://doi.org/10.7717/peerj.831.

Piermattei, L, Carturan, L & Guarnieri, A 2015, 'Use of terrestrial photogrammetry based on structure-from-motion for mass balance estimation of a small glacier in the Italian alps', *Earth Surface Processes and Landforms*, vol. 40, no. 13, pp. 1791-1802.

Pietsch, TJ, Nanson, GC & Olley, JM 2013, 'Late Quaternary changes in flow-regime on the Gwydir distributive fluvial system, southeastern Australia', *Quaternary Science Reviews*, vol. 69, pp. 168-180.

Rădoane, M, Perșoiu, I, Chiriloaei, F, Cristea, I & Robu, D 2017, 'Styles of channel adjustments in the last 150 years', in M Rădoane & A Vespremeanu-Stroe, *Landform Dynamics and Evolution in Romania*, Springer Geography, Springer, Cham, Switzerland, pp. 489-518.

Ralph, T, Kobayashi, T, García, A, Hesse, P, Yonge, D, Bleakley, N & Ingleton, T 2011, 'Paleoecological responses to avulsion and floodplain evolution in a semiarid Australian freshwater wetland', *Australian Journal of Earth Sciences*, vol. 58, no. 1, pp. 75-91.

Ralph, TJ & Hesse, PP 2010, 'Downstream hydrogeomorphic changes along the Macquarie River, southeastern Australia, leading to channel breakdown and floodplain wetlands', *Geomorphology*, vol. 118, no. 1-2, pp. 48-64.

Ralph, TJ 2008, Channel breakdown and floodplain wetland morphodynamics in the Macquarie Marshes, south-eastern Australia, postdoctoral thesis, Macquarie University, Sydney.

Ralph, TJ, Barma, D, Hesse, P, Outhet, D, Davies, B & Wettin, P 2013, *Southern Macquarie Marshes geomorphic restoration scoping study*, Acess Macquarie Ltd, Sydney, Australia.

Ralph, TJ, Hesse, PP & Kobayashi, T 2016, 'Wandering wetlands: spatial patterns of historical channel and floodplain change in the Ramsar-listed Macquarie Marshes, Australia', *Marine and Freshwater Research*, vol. 67, no. 6, pp. 782-802.

Rayburg, S, Thoms, M & Neave, M 2009, 'A comparison of digital elevation models generated from different data sources', *Geomorphology*, vol. 106, no. 3–4, pp. 261-270.

Refsgaard, JC 1997, 'Parameterisation, calibration and validation of distributed hydrological models', *Journal of Hydrology*, vol. 198, no. 1-4, pp. 69-97.

Reutebuch, SE, Mcgaughey, RJ, Andersen, HE & Carson, WW 2003, 'Accuracy of a high-resolution lidar terrain model under a conifer forest canopy', *Canadian Journal of Remote Sensing*, vol. 29, no. 5, pp. 527-535.

Reynolds, JM 2011, *An introduction to applied and environmental geophysics*, John Wiley & Sons, United States of America.

Rodriguez, JF, Bombardelli, FA, García, MH, Frothingham, KM, Rhoads, BL & Abad, JD 2004, 'High-resolution numerical simulation of flow through a highly sinuous river reach', *Water Resources Management*, vol. 18, no. 3, pp. 177-199.

Rogers, K & Ralph, TJ 2011, *Floodplain wetland biota in the Murray-Darling Basin: water and habitat requirements*, CSIRO Publishing, Clayton, Australia.

Rogers, K, Ralph, T & Imgraben, S 2010, *Water requirements of biota, geomorphology and climate change in the Macquarie Marshes, Ecosystem Response Modelling in the Murray-Darling Basin*, CSIRO Publishing, Melbourne, Australia.

Rolls, RJ, Heino, J, Ryder, DS, Chessman, BC, Growns, IO, Thompson, RM & Gido, KB 2018, 'Scaling biodiversity responses to hydrological regimes', *Biological Reviews*, vol. 93, no. 2, pp. 971-995.

Rooth, J & Stevenson, J 2000, 'Sediment deposition patterns in Phragmites australiscommunities: implications for coastal areas threatened by rising sea-level', *Wetlands Ecology and Management*, vol. 8, no. 2-3, pp. 173-183.

Rousseau, YY, Biron, PM & Van De Wiel, MJ 2016, 'Sensitivity of simulated flow fields and bathymetries in meandering channels to the choice of a morphodynamic model', *Earth Surface Processes and Landforms*, vol. 41, no. 9, pp. 1169-1184.

Rowland, JC, Shelef, E, Pope, PA, Muss, J, Gangodagamage, C, Brumby, SP & Wilson, CJ 2016, 'A morphology independent methodology for quantifying planview river change and characteristics from remotely sensed imagery', *Remote Sensing of Environment*, vol. 184, pp. 212-228.

Roy, S & Sahu, AS 2015, 'Quaternary tectonic control on channel morphology over sedimentary low land: a case study in the Ajay-Damodar interfluve of Eastern India', *Geoscience Frontiers*, vol. 6, no. 6, pp. 927-946.

Ruiz-Villanueva, V, Piégay, H, Gurnell, AM, Marston, RA and Stoffel, M 2016, 'Recent advances quantifying the large wood dynamics in river basins: new methods and remaining challenges', *Reviews of Geophysics*, vol. 54, no. 3, pp. 611-652.

Sambrook Smith, GH, Best, JL, Ashworth, PJ, Fielding, CR, Goodbred, SL & Prokocki, EW 2010, 'Fluvial form in modern continental sedimentary basins: distributive fluvial systems: COMMENT', *Geology*, vol. 38, no. 12, pp. e230-e230.

Sandi, SG, Saco, PM, Saintilan, N, Wen, L, Riccardi, G, Kuczera, G, Willgoose, G & Rodríguez, JF 2019, 'Detecting inundation thresholds for dryland wetland vulnerability', *Advances in Water Resources*, vol. 128, pp. 168-182.

Savage, JTS, Pianosi, F, Bates, P, Freer, J & Wagener, T 2016, 'Quantifying the importance of spatial resolution and other factors through global sensitivity analysis of a flood inundation model', *Water Resources Research*, vol. 52, no. 11, pp. 9146-9163.

Savic, R, Ondrasek, G, Letic, L, Nikolic, V & Tanaskovik, V 2017, 'Nutrients accumulation in drainage channel sediments', *International Journal of Sediment Research*, vol. 32, no. 2, pp. 180-185.

Schoorl, J, Sonneveld, M & Veldkamp, A 2000, 'Three-dimensional landscape process modelling: the effect of DEM resolution', *Earth Surface Processes and Landforms*, vol. 25, no. 9, pp. 1025-1034.

Seoane, M, Rodriguez, J, Saco, P & Rojas, SS 2015, *A geomorphological modelling approach for landscape evolution analysis of the Macquarie Marshes, Australia*, conference paper, IAHR World Congress, 28 June – 3 July, The Hague, Natherlends.

Sinha, R, Mohanta, H, Jain, V & Tandon, S 2017, 'Geomorphic diversity as a river management tool and its application to the Ganga River, India', *River Research and Applications*, vol. 33, no. 7, pp. 1156-1176.

Slingerland, R & Smith, N D 2004, 'River avulsions and their deposits', *Annual Review of Earth and Planetary Sciences*, vol. 32, pp. 257-285.

Smets, T, Poesen, J & Bochet, E 2008, 'Impact of plot length on the effectiveness of different soil-surface covers in reducing runoff and soil loss by water, Progress in Physical Geography', vol. 32, no. 6, pp. 654-677.

Smith, MW & Vericat, D 2015, 'From experimental plots to experimental landscapes: topography, erosion and deposition in sub-humid badlands from structure-from-motion photogrammetry', *Earth Surface Processes and Landforms*, vol. 40, no. 12, pp. 1656-1671.

Smith, ND, Cross, TA, Dufficy, JP & Clough, SR 1989, 'Anatomy of an avulsion', *Sedimentology*, vol. 36, no. 1, pp. 1-23.

Starek, MJ 2016, 'Light detection and ranging (LIDAR), in MJ Kennish (ed.), *Encyclopedia of Estuaries*, Springer Science & Business Media, Dordrecht, Netherlands, pp. 383-384.

Steiger, J, Gurnell, A & Goodson, J 2003, 'Quantifying and characterizing contemporary riparian sedimentation', *River Research and Applications*, vol. 19, no. 4, pp. 335-352.

Stevaux, JC, de Azevedo Macedo, H, Assine, ML & Silva, A 2020, 'Changing fluvial styles and backwater flooding along the Upper Paraguay River plains in the Brazilian Pantanal wetland', *Geomorphology*, vol. 350, pp.106906.

Tarolli, P 2014, 'High-resolution topography for understanding Earth surface processes: opportunities and challenges', *Geomorphology*, vol. 216, pp. 295-312.

Teng, J, Jakeman, A, Vaze, J, Croke, BF, Dutta, D & Kim, S 2017, 'Flood inundation modelling: a review of methods, recent advances and uncertainty analysis', *Environmental Modelling & Software*, vol. 90, pp. 201-216.

Thomas, RF, Kingsford, RT, Lu, Y & Hunter, SJ 2011, 'Landsat mapping of annual inundation (1979–2006) of the Macquarie Marshes in semi-arid Australia', *International Journal of Remote Sensing*, vol. 32, no. 16, pp. 4545-4569.

Thomas, RF, Kingsford, RT, Lu, Y, Cox, SJ, Sims, NC & Hunter, SJ 2015, 'Mapping inundation in the heterogeneous floodplain wetlands of the Macquarie Marshes, using Landsat Thematic Mapper', *Journal of Hydrology*, vol. 524, pp. 194-213.

Tooth, S 1999, 'Downstream changes in floodplain character on the Northern Plains of arid central Australia', in ND Smith & J Rogers (eds.), *Fluvial Sedimentology VI*, International Association of Sedimentologists, Blackwell Science Ltd, United Kingdom, pp. 93-112.

Tooth, S & Nanson, GC 2000, 'The role of vegetation in the formation of anabranching channels in an ephemeral river, Northern plains, arid central Australia', *Hydrological processes*, vol *14*, no 16-17, pp. 3099-3117.

Tooth, S 2000, 'Process, form and change in dryland rivers: a review of recent research', *Earth-Science Reviews*, vol. 51, no. 1-4, pp. 67-107.

Tooth, S 2018, 'The geomorphology of wetlands in drylands: resilience, nonresilience, or…?', *Geomorphology*, vol. 305, pp. 33-48.

Tourian, M, Elmi, O, Mohammadnejad, A & Sneeuw, N 2017, 'Estimating river depth from SWOT-type observables obtained by satellite altimetry and imagery', *Water*, vol. 9, no. 10, pp. 753.

Trimble, SW 1997, 'Contribution of stream channel erosion to sediment yield from an urbanizing watershed', *Science*, vol. 278, no. 5342, 1442-1444.

Turowski, JM & Cook, KL 2017, 'Field techniques for measuring bedrock erosion and denudation', *Earth Surface Processes and Landforms*, vol. 42, no. 1, pp. 109-127.

Van De Wiel, MJ, Coulthard, TJ, Macklin, MG & Lewin, J 2011, 'Modelling the response of river systems to environmental change: progress, problems and prospects for palaeo-environmental reconstructions', *Earth-Science Reviews*, vol. 104, no. 1-3, pp. 167-185.

WaterNSW 2019, *WaterNSW,* viewed March 2019, https://www.waternsw.com.au/

Weissmann, G, Hartley, A, Nichols, G, Scuderi, L, Olson, M, Buehler, H & Banteah, R 2010, 'Fluvial form in modern continental sedimentary basins: distributive fluvial systems', *Geology*, vol. 38, no. 1, pp. 39-42.

Wellen, C, Arhonditsis, GB, Long, T & Boyd, D 2014, 'Quantifying the uncertainty of nonpoint source attribution in distributed water quality models: a Bayesian assessment of SWAT's sediment export predictions', *Journal of Hydrology*, vol. 519, pp. 3353-3368.

Wen, L, Ralph, T, Hosking, T, Barma, D & Saintilan, N 2013, *Assessing stream restoration works in the southern Macquarie Marshes using hydrodynamic modeling*, conference paper, 20th International Congress on Modelling and Simulation, 1-6 December, Adelaide, Australia.

Westoby, MJ, Brasington, J, Glasser, NF, Hambrey, MJ & Reynolds, JM 2012, ''Structure-from-Motion'photogrammetry: a low-cost, effective tool for geoscience applications', *Geomorphology*, vol. 179, pp. 300-314.

Wheaton, JM, Brasington, J, Darby, SE & Sear, DA 2010, 'Accounting for uncertainty in DEMs from repeat topographic surveys: improved sediment budgets', *Earth Surface Processes and Landforms*, vol. 35, no. 2, pp. 136-156.

Willgoose, G, Bras, RL & Rodriguez-Iturbe, I 1991, 'A coupled channel network growth and hillslope evolution model: 1. theory', *Water Resources Research*, vol. 27, no. 7, pp. 1671-1684.

Williams, RD, Brasington, J & Hicks, DM 2016, 'Numerical modelling of braided river morphodynamics: review and future challenges', *Geography Compass*, vol. 10, no. 3, pp. 102-127.

Wood, M, Hostache, R, Neal, J, Wagener, T, Giustarini, L, Chini, M, Corato, G, Matgen, P & Bates, P 2016, 'Calibration of channel depth and friction parameters in the LISFLOOD-FP hydraulic model using medium-resolution SAR data and identifiability techniques', *Hydrology and Earth System Sciences*, vol. 20, no. 12, pp. 4983.

Wright, L 1977, 'Sediment transport and deposition at river mouths: a synthesis', *Geological Society of America Bulletin*, vol. 88, no. 6, pp. 857-868.

Xia, J, Guangqian, W & Baosheng, W 2004, 'Two-dimensional numerical modeling of the longitudinal and lateral channel deformations in alluvial rivers', *Science in China Series E: Technological Sciences*, vol. 471, pp. 199-211.

Xue, B, Keming, M, Liu, Y, Jieyu, Z & Xiaolei, Z 2008, 'Differences of ecological functions inside and outside the wetland nature reserves in Sanjiang Plain, China', *Acta Ecologica Sinica*, vol. 28, no. 2, pp. 620-626.

Yang, SL, Xu, KH, Milliman, JD, Yang, HF & Wu, CS 2015, 'Decline of Yangtze River water and sediment discharge: impact from natural and anthropogenic changes', *Scientific Reports*, vol. 5, 12581, doi: 10.1038/srep12581.

Yang, X, Damen, MC & Van Zuidam, RA 1999, 'Satellite remote sensing and GIS for the analysis of channel migration changes in the active Yellow River Delta, China', *International Journal of Applied Earth Observation and Geoinformation*, vol. 1, no. 2, pp. 146-157.

Yochum, SE, Sholtes, JS, Scott, JA & Bledsoe, BP 2017, 'Stream power framework for predicting geomorphic change: the 2013 Colorado Front Range flood', *Geomorphology*, vol. 292, pp. 178-192.

Yonge, D & Hesse, P 2009, 'Geomorphic environments, drainage breakdown, and channel and floodplain evolution on the lower Macquarie River, central-western New South Wales', *Australian Journal of Earth Sciences*, vol. 56, no. S1, pp. S35-S53.

Yousefi, S, Moradi, HR, Pourghasemi, HR & Khatami, R 2017, 'Assessment of floodplain landuse and channel morphology within meandering reach of the Talar River in Iran using GIS and aerial photographs', *Geocarto International*, vol. 33, no. 12, pp. 1367-1380.

Zedler, JB & Kercher, S 2004, 'Causes and consequences of invasive plants in wetlands: opportunities, opportunists, and outcomes', *Critical Reviews in Plant sciences*, vol. 23, no. 5, pp. 431-452.

Zhou, Z, Coco, G, Townend, I, Olabarrieta, M, Van Der Wegen, M, Gong, Z, D'alpaos, A, Gao, S, Jaffe, BE, Gelfenbaum, G & He, Q 2017, 'Is "morphodynamic equilibrium" an oxymoron?', *Earth-Science Reviews*, vol. 165, pp. 257-267.

Zwoliński, Z 1992, 'Sedimentology and geomorphology of overbank flows on meandering river floodplains', *Geomorphology*, vol. 4, no. 6, pp. 367-379.

Appendix 1: Geomorphology Site Assessment form

Geomorphology Site Assessment Form

MACQUARIE UNIVERSITY SYDNEY ~ AUSTRALIA

Page 1
Tim Ralph
05.10.12

Date / Assessor			
Wetland / Site ID		**Property**	
Channel / Reach		**Contact**	

GPS (WGS'84) - *Site 1*	*Deg. Min. Sec.*	S		E	
GPS (WGS'84) - *Site 2*	*Deg. Min. Sec.*	S		E	
GPS (WGS'84) - *Site 3*	*Deg. Min. Sec.*	S		E	

Site Photographs	*ID number*	**Bend**	*Site 1*	*Site 2*	*Site 3*	**Water Level**	*Site 1*	*Site 2*	*Site 3*
View upstream from site		Inner				Dry (no water)			
View downstream from site		Outer				Low (bed covered)			
View across channel (L/R bank)		Straight				Med (to bank mid)			
View across floodplain (L/R bank)		Floodout				High (to bank top)			
Other:		No channel				Overbank			

Planform Sketch (looking from above)
Show cross section ($S_{1,2,3}$) and vertical profiles ($V_{1,2,3}$)

Scale (m) ***N***

Cross Section Sketch (looking downstream)

Include all geomorphic units >2 m², plus: X log jam; → flow; photo; • S; ○ V

Bankfull width (m):
Channel depth (m):

Modifications	0	1	2
Bank stability works			
Channel excavations			
Dam / weir			
Artificial bank			
Road / track			
Culvert / pipe			
Other:			
Other:			

Impact of Works		0	1	2
Wk 1				
Wk 2				
Wk 3				

Debris	0	1	2
Large / woody			
Small / herbaceous			
Other:			

Bank Shape	*Site 1*		*Site 2*		*Site 3*	
Bank morphology						
	(left)	(right)	(left)	(right)	(left)	(right)

Erosional Features (circle and score)	0	1	2
Thalweg is narrow / incised / inset			
Exposed knickpoint / substrate			
Ledges / eroded benches			
Bank breaches / gaps			
Bank retreat (general face scour)			
Bank rilling / fluting (scour down face)			
Bank failure by slumping / toppling			
Bank undercutting / tree roots exposed			

Sub-Aerial Features (circle and score)	0	1	2
Tunnelling (holes at top of bank)			
Compaction (any cause)			
Animal trails / trampling / pugging			
Carp / other disturbance			

Sedimentation Features	0	1	2
Unconsolidated sediment			
In-channel blockages			
Benches / bars			
Natural levees			
Splays (overbank / floodplain)			
Recent overbank deposition			

Flow Entry and Exit Points	0	1	2
In-flowing gully / tributary			
--> depth (deepest)			
--> extent (longest)			
--> slope (steepest)			
Bank breach / distributary			
--> depth (deepest)			
--> extent (longest)			
--> slope (steepest)			
Other:			

Geomorphology Site Assessment Form

MACQUARIE UNIVERSITY SYDNEY ~ AUSTRALIA | Page 2 | *Tim Ralph*

Vegetation (visual estimate)	Habitat (A/R/T)		Structure (H/G/S/T)		Ground cover (%)		Dom. Species
	Left bank	*Right bank*	*Left bank*	*Right bank*	*Left bank*	*Right bank*	(N or A)
Channel							
Edge of water							
Bank							
Proximal floodplain							
Medial floodplain							
Other:							

Notes/Sketch:

Roughness (visual estimate)	n_0	n_1	n_2	n_3	n_4	m_5	n
Manning's n							
	(material)	(irregularity)	(variation)	(obstructions)	(vegetation)	(sinuosity)	(overall)

Water (PCTestr35)	*Site 1*	*Site 2*	*Site 3*	
Temp (°C)				Notes:
pH				
EC (μS/cm)				

Soil Surface (tick if present)	*Site 1*	*Site 2*	*Site 3*	
Cracking				Notes:
Biotic crust				
Salt crust				
Saline discharge				

Bank Sediment (Folk class)	*Site 1*	*Site 2*	*Site 3*	
Upper 1/3 of bank				Notes:
Middle 1/3 of bank				
Lower 1/3 of bank				

Bank Shear (shear vane)	*Site 1*	*Site 2*	*Site 3*	
Upper 1/3 of bank				Notes:
Middle 1/3 of bank				
Lower 1/3 of bank				

Bank Compression (penetr.)	*Site 1*	*Site 2*	*Site 3*	
Upper 1/3 of bank				Notes:
Middle 1/3 of bank				
Lower 1/3 of bank				

DBD Samples (collect & bag)	*Site 1*	*Site 2*	*Site 3*	
Upper 1/3 of bank				Notes:
Middle 1/3 of bank				
Lower 1/3 of bank				

Additional Notes:

Indicator	Score	Descriptor
		MACQUARIE UNIVERSITY SYDNEY ~ AUSTRALIA — Page 3 — *Tim Ralph*
Modifications	**All categories**	
(Use % cover charts on page 4)	0	Single, small (occupies or affects <10% of channel or banks)
	1	Single, large (occupies or affects >10% of channel or banks)
	2	Multiple, or composite (occupy or affect >25% of channel or banks)
Impact of Works	**All categories**	
	0	Minor, or positive (few adverse effects, no monitoring needed)
	1	Moderate (observed or potential adverse effects, needs monitoring)
	2	Major (serious adverse effects, needs modification/monitoring)
Debris	**All categories**	
(Use % cover charts on page 4)	0	Minor (occupies or affects <10% of channel or banks)
	1	Moderate (occupies or affects 10 to 25% of channel or banks)
	2	Major (occupies or affects >25% of channel or banks)
Bank Shape	**Basic Units**	**Composite Examples**
(Right bank example shown)	Undercut U; Vertical V; Sloping S; Benched B; Fluted F	Vert/Slope V/S; Slope/Vert/Undercut S/V/U

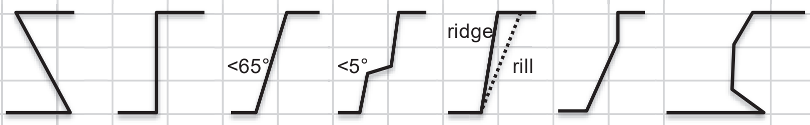

** Adapted from: Crouch, R.J. and Blong, R.J. 1989. Zeitschrift für Geomorphologie 33, 291-305.*

Indicator	Score	Descriptor
Erosional Features	**All categories**	
(Use % cover charts on page 4)	0	Minor (occupies or affects <10% of channel or banks)
	1	Moderate (occupies or affects 10 to 25% of channel or banks)
	2	Major (occupies or affects >25% of channel or banks)
Sub-Aerial Features	**All categories**	
(Use % cover charts on page 4)	0	Minor (occupies or affects <10% of channel or banks)
	1	Moderate (occupies or affects 10 to 25% of channel or banks)
	2	Major (occupies or affects >25% of channel or banks)
Sedimentation Features	**Unconsolidated sediment**	
(Use % cover charts on page 4)	0	Minor (<25cm deep and occupies <10% of channel)
	1	Moderate (25 to 50cm deep and occupies 10 to 25% of channel)
	2	Major (>50cm deep and occupies >25% of channel)
	All other categories	
	0	Minor (occupies or affects <10% of channel or floodplain)
	1	Moderate (occupies or affects 10 to 25% of channel or floodplain)
	2	Major (occupies or affects >25% of channel or floodplain)
Flow Entry and Exit Points	**In-flowing gully / tributary and bank breach / distributary**	
(Use % cover charts on page 4)	0	Single, small (occupies or affects <10% of channel or banks)
	1	Single, large (occupies or affects >10% of channel or banks)
	2	Multiple, or composite (occupy or affect >25% of channel or banks)
--> depth (deepest)	0	Minor (<10cm deep)
	1	Moderate (10 to 50cm deep)
	2	Major (>50cm deep)
--> extent (longest)	0	Minor (extends <10m on floodplain)
	1	Moderate (extends 10 to 25m on floodplain)
	2	Major (extends >25m on floodplain)
--> slope (steepest)	0	Minor (approximates the cross-floodplain slope)
	1	Moderate (exceeds the cross-floodplain slope by >10 degrees)
	2	Major (exceeds the cross-floodplain slope by >20 degrees)

Indicator	**Score**	**Descriptor**	MACQUARIE UNIVERSITY SYDNEY ~ AUSTRALIA	Page 4
				Tim Ralph

Vegetation

Habitat Type		**Structural Type**		**Dominant Species**	
A	Aquatic	H	Herbs (<1 m herbaceous)	N	Native
R	Riparian	G	Grasses (<1 m herbaceaous tufts)	A	Alien
T	Terrestrial	S	Shrubs (<2 m woody)		
		T	Trees (>2 m woody)		

10% cover (black)

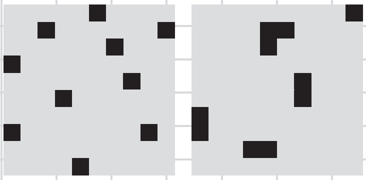

25% cover (black)

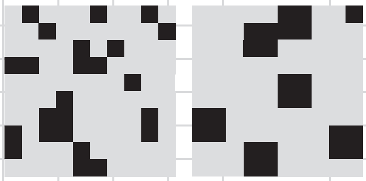

Roughness

Manning's n, the resistance (aka roughness) coefficient, can be estimated via the component method*, where a range of parameters can be estimated then summed together. This method is unsuitable for large channels (with R>~5 m) and care must be taken to avoid double counting channel characteristics in the various components.

Manning's n is estimated from: $\mathbf{n = m_5 (n_0 + n_1 + n_2 + n_3 + n_4)}$ where:

n_0 = a value for the material of a straight uniform channel

n_1 = a factor for surface irregularities

n_2 = a factor for variations in the shape and size of the channel cross-section

n_3 = a factor for obstructions

n_4 = a factor for vegetation

m_5 = a multiplier for channel meandering (sinuosity)

Material, n_0		**Degree of surface irregularity, n_1**	
earth	0.020	smooth	0.000
rock	0.025	minor (e.g. minor slumping)	0.005
fine gravel	0.024	moderate (e.g. moderate slumping)	0.010
coarse gravel	0.028	severe (e.g. badly slumped, or irregular bedrock)	0.020

Variation of channel cross-section, n_2		**Relative effect of obstructions (debris, roots, boulders etc), n_3**	
gradual	0.000	negligible	0.000
alternating occasionally	0.005	minor	0.010-0.015
alternating frequently	0.010-0.015	appreciable	0.020-0.030
		severe	0.040-0.060

Vegetation, n_4		**Degree of meandering, m_5**	
none	0.000	minor (sinuosity < 1.2)	1.00
low	0.005-0.010	appreciable (sinuosity 1.2-1.5)	1.15
medium	0.010-0.025	severe (sinuosity > 1.5)	1.30
high	0.025-0.050		
very high	0.050-0.100		

* *Adapted from: Gardiner, V. and Dackombe, R.V. 1983. Geomorphological field manual. Allen and Unwin, London.*

Bank Sediment

Folk Classes

Folk texture classes to be determined according to the following key*:

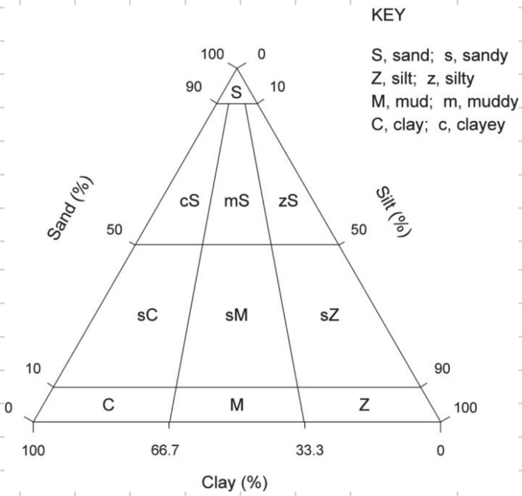

* *Adapted from Folk, R.L.1974. Petrology of Sedimentary Rocks.*

Appendix 2: Plots of relation between geometric and hydraulic parameters

1. Southern Macquarie Marshes

1.1 Macquarie River upstream Monkeygar

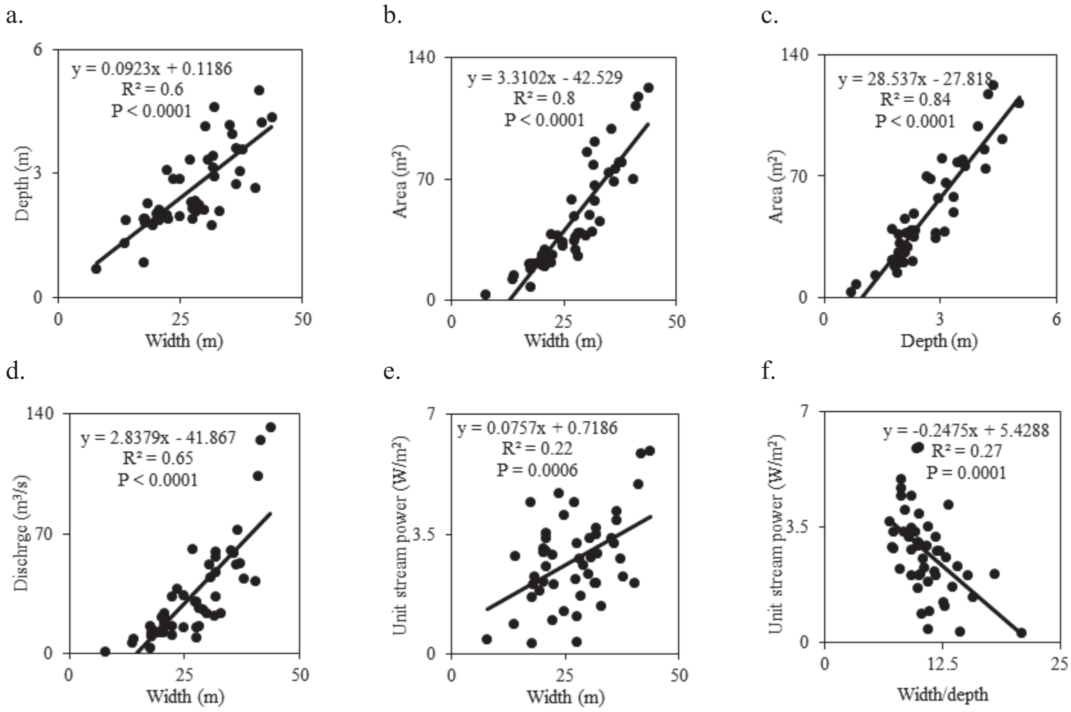

Figure A2.1 Relation between depth and width (a) area and width (b) area and depth (c) discharge and width (d) unit stream power and width (e) and unit stream power and width:depth ratio (f) in the Macquarie River upstream of Monkeygar Creek.

1.2 Buckiinguy Creek

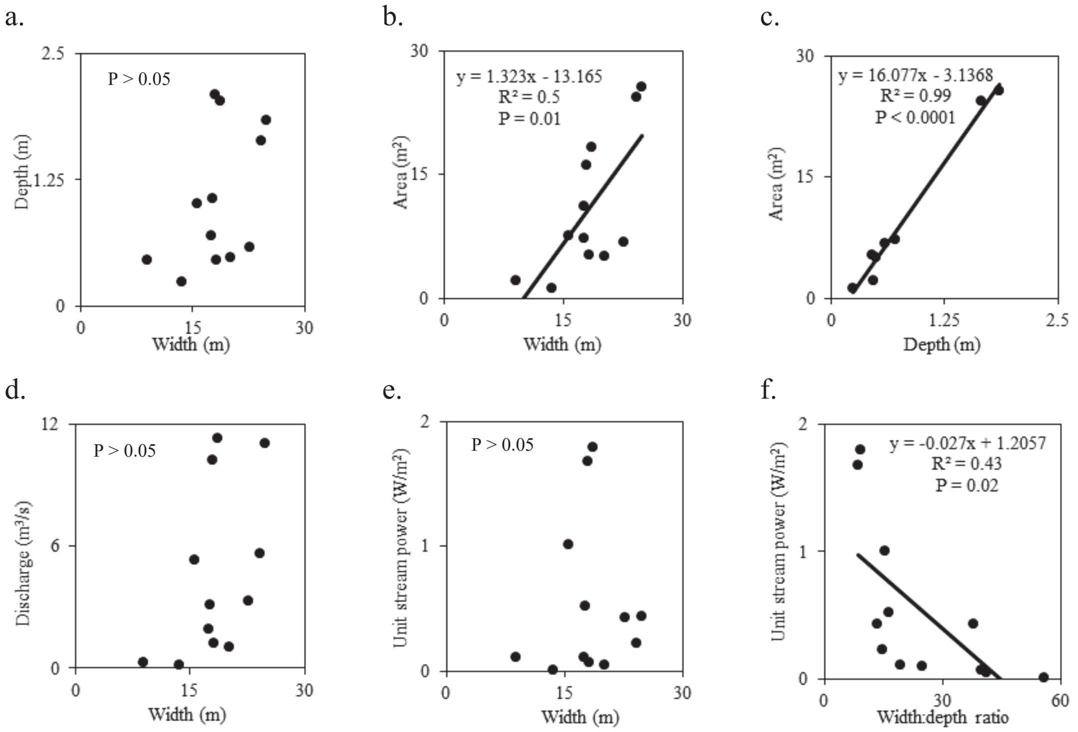

Figure A2.2 Relation between depth and width (a) area and width (b) area and depth (c) discharge and width (d) unit stream power and width (e) and unit stream power and width:depth ratio (f) in the Bukiinguy Creek.

1.3 Old Macquarie River

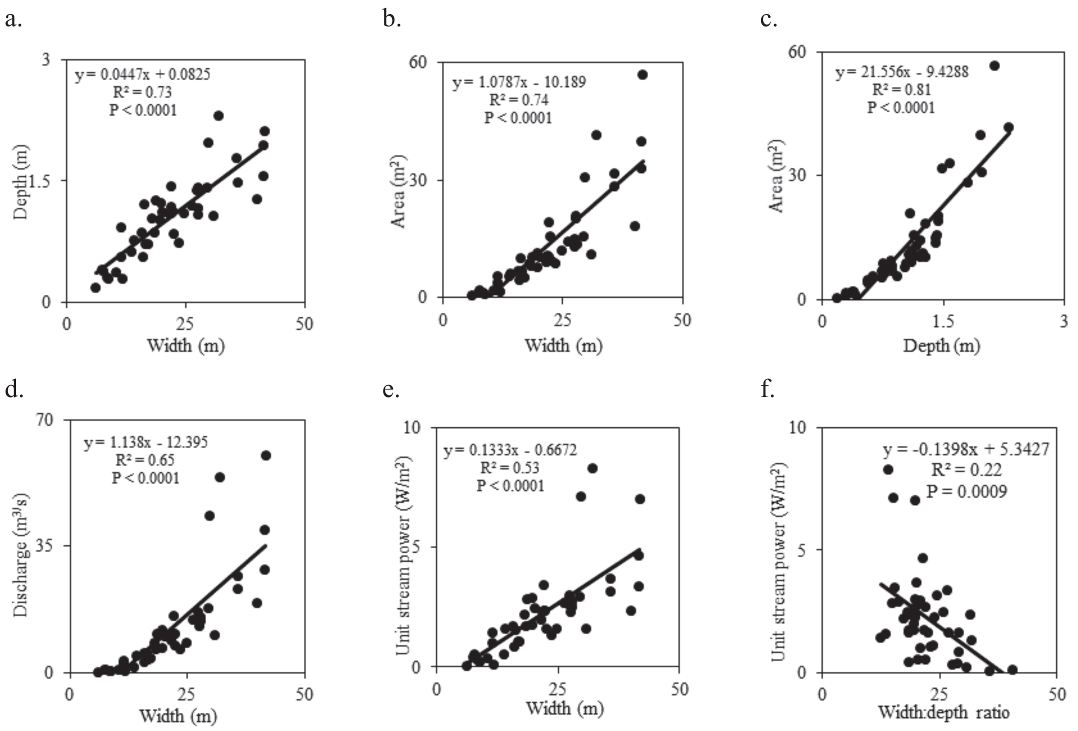

Figure A2.3 Relation between depth and width (a) area and width (b) area and depth (c) discharge and width (d) unit stream power and width (e) and unit stream power and width:depth ratio (f) in the Old Macquarie River.

1.4 Macquarie River downstream Old Macquarie River

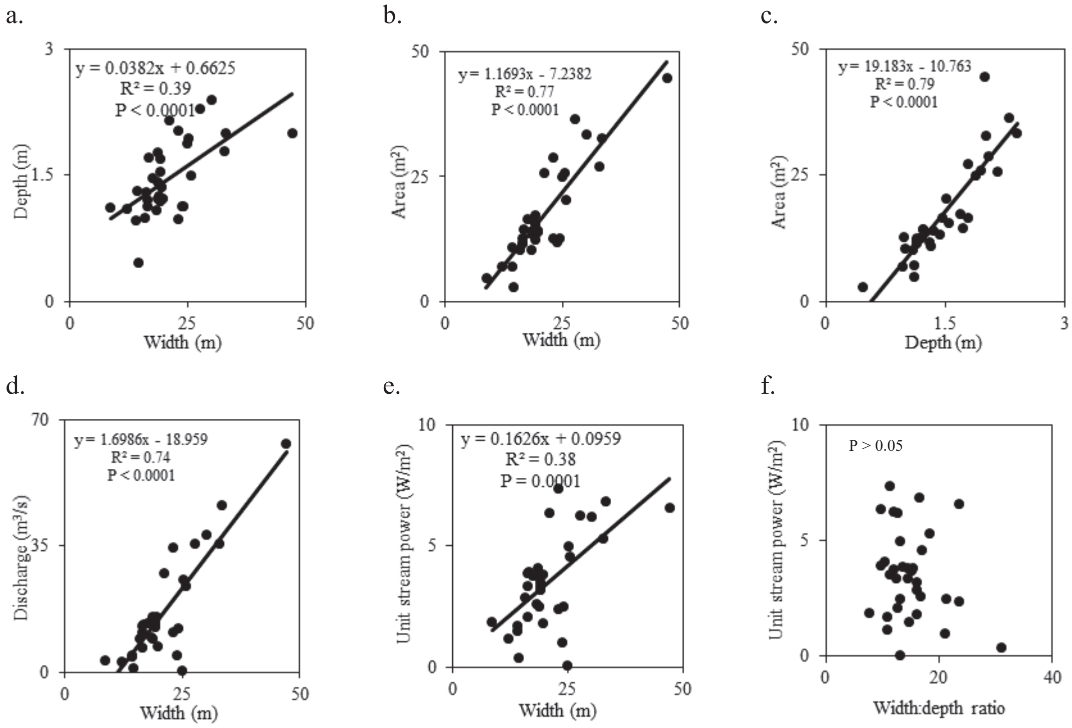

Figure A2.4 Relation between depth and width (a) area and width (b) area and depth (c) discharge and width (d) unit stream power and width (e) and unit stream power and width:depth ratio (f) in the Macquarie River downstream of Old Macquarie River.

1.5 Mole Marsh

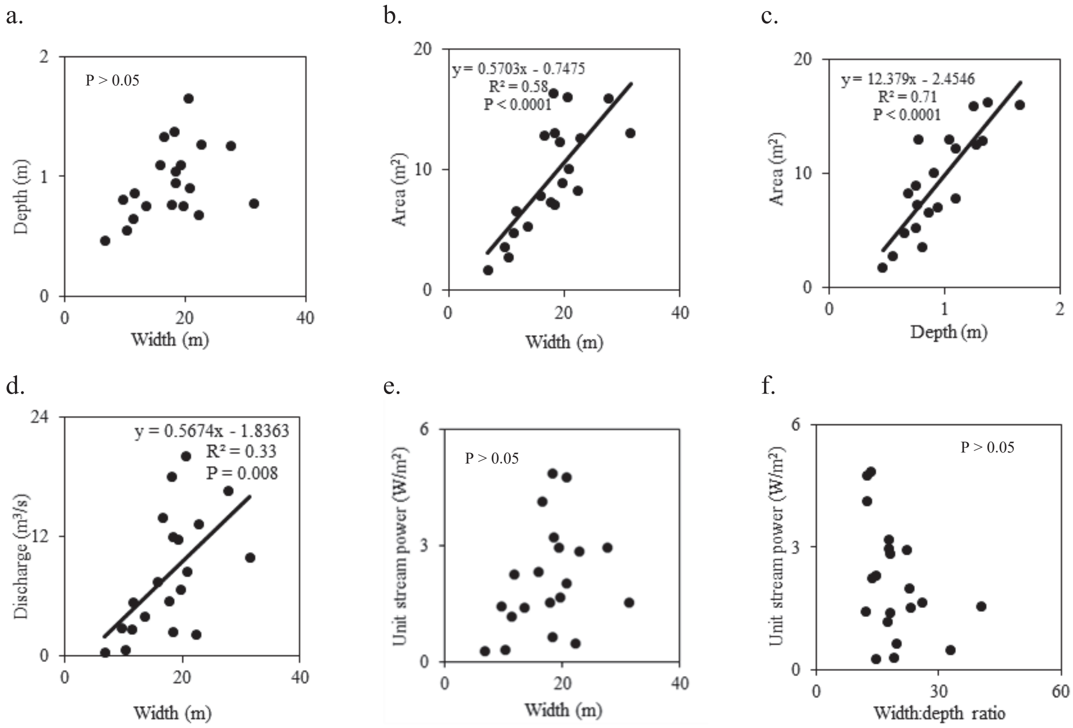

Figure A2.5 Relation between depth and width (a) area and width (b) area and depth (c) discharge and width (d) unit stream power and width (e) and unit stream power and width:depth ratio (f) in the Mole Marsh.

1.6 The Breakaway

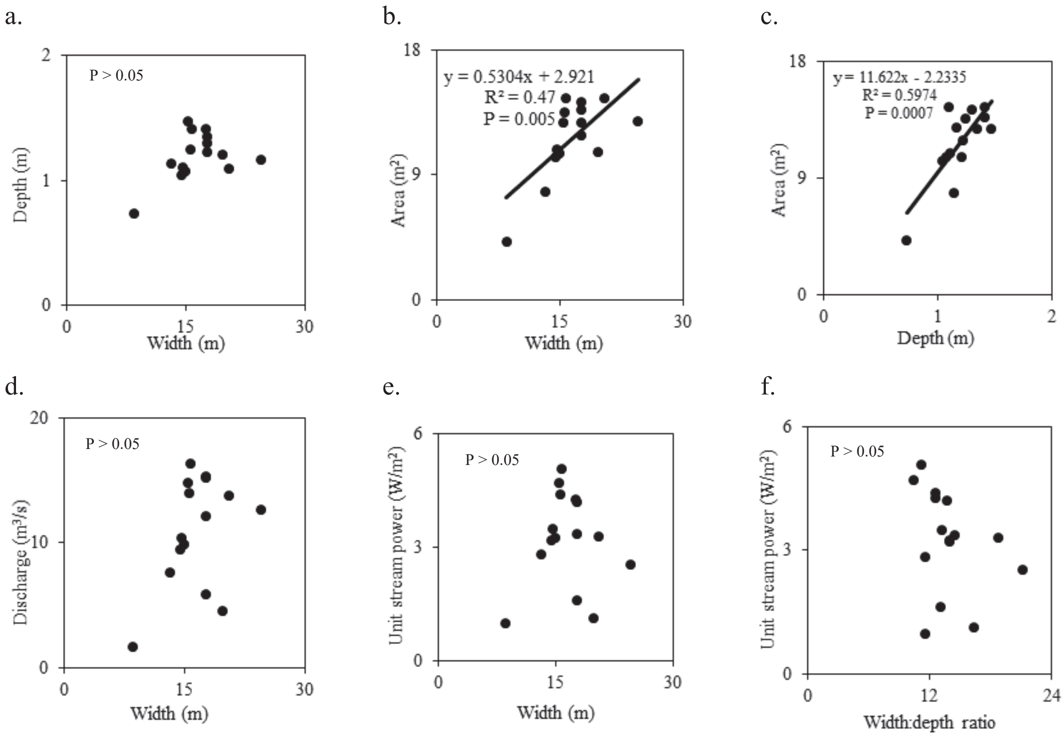

Figure A2.6 Relation between depth and width (a) area and width (b) area and depth (c) discharge and width (d) unit stream power and width (e) and unit stream power and width:depth ratio (f) in The Breakaway.

1.7 Monkeygar Creek

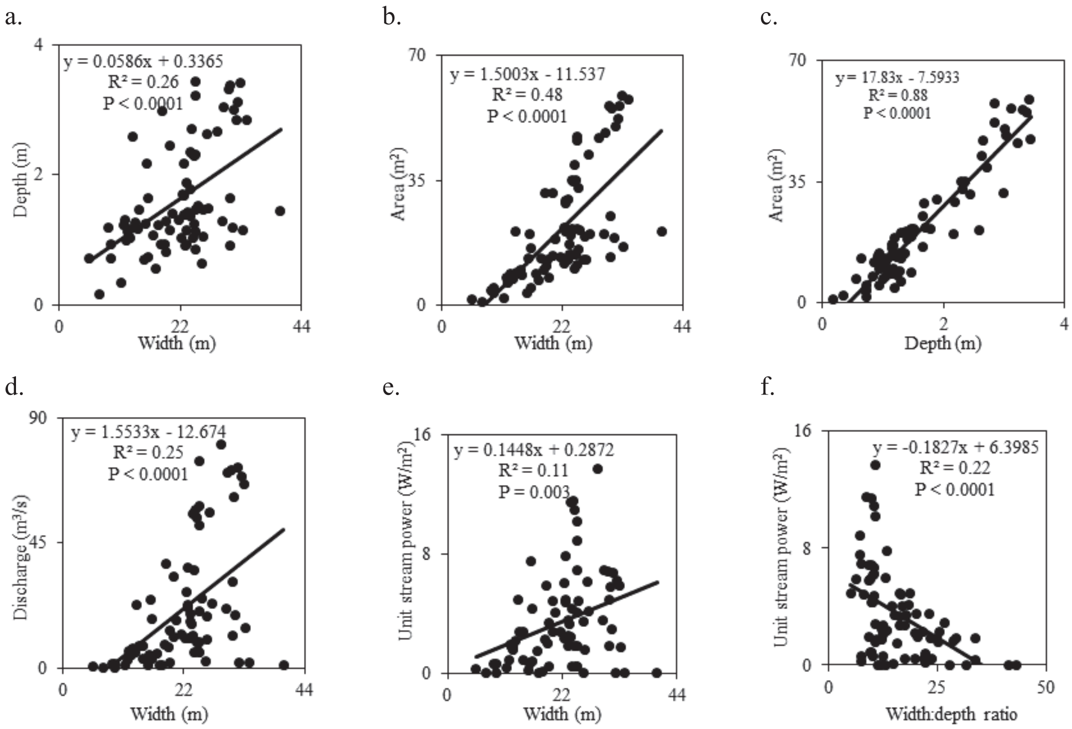

Figure A2.7 Relation between depth and width (a) area and width (b) area and depth (c) discharge and width (d) unit stream power and width (e) and unit stream power and width:depth ratio (f) in the Monkeygar Creek.

1.8 Monkey Creek

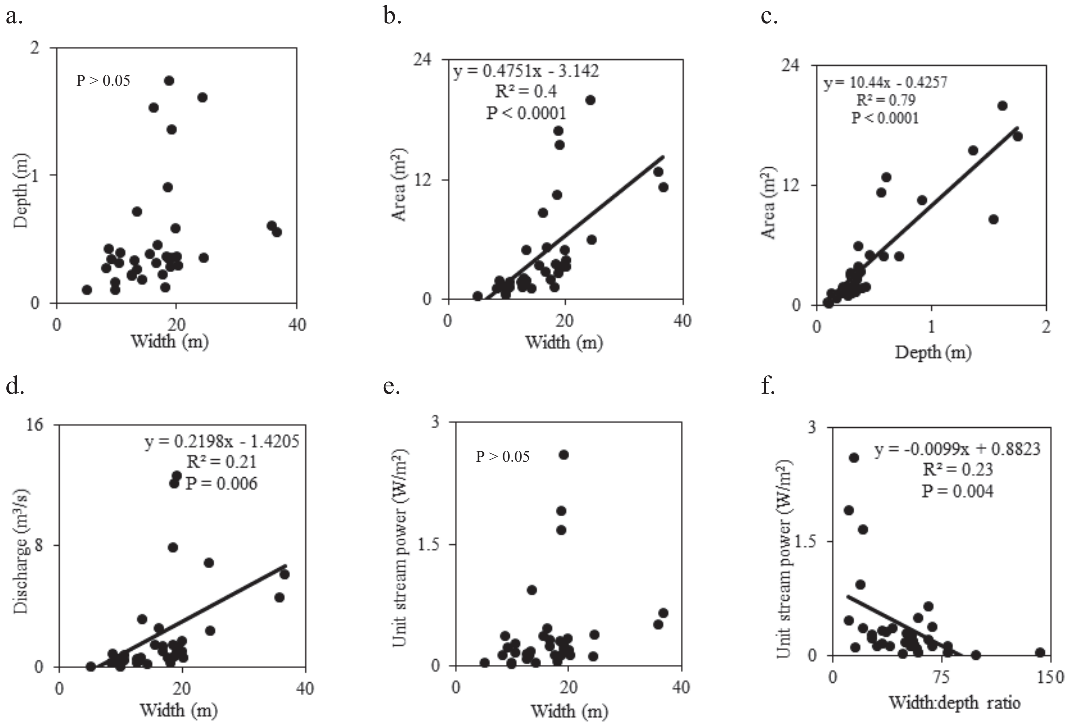

Figure A2.8 Relation between depth and width (a) area and width (b) area and depth (c) discharge and width (d) unit stream power and width (e) and unit stream power and width:depth ratio (f) in the Monkey Creek.

1.9 Oxley Break

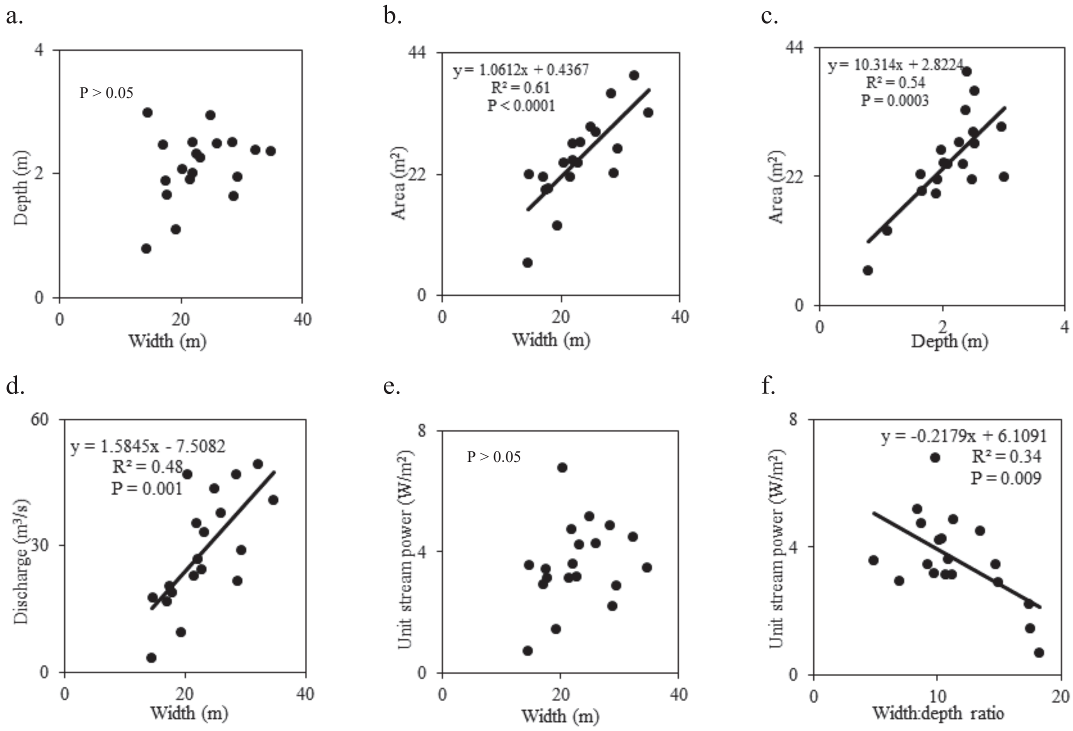

Figure A2.9 Relation between depth and width (a) area and width (b) area and depth (c) discharge and width (d) unit stream power and width (e) and unit stream power and width:depth ratio (f) in the Oxley Break.

1.10 Bulgeraga Creek

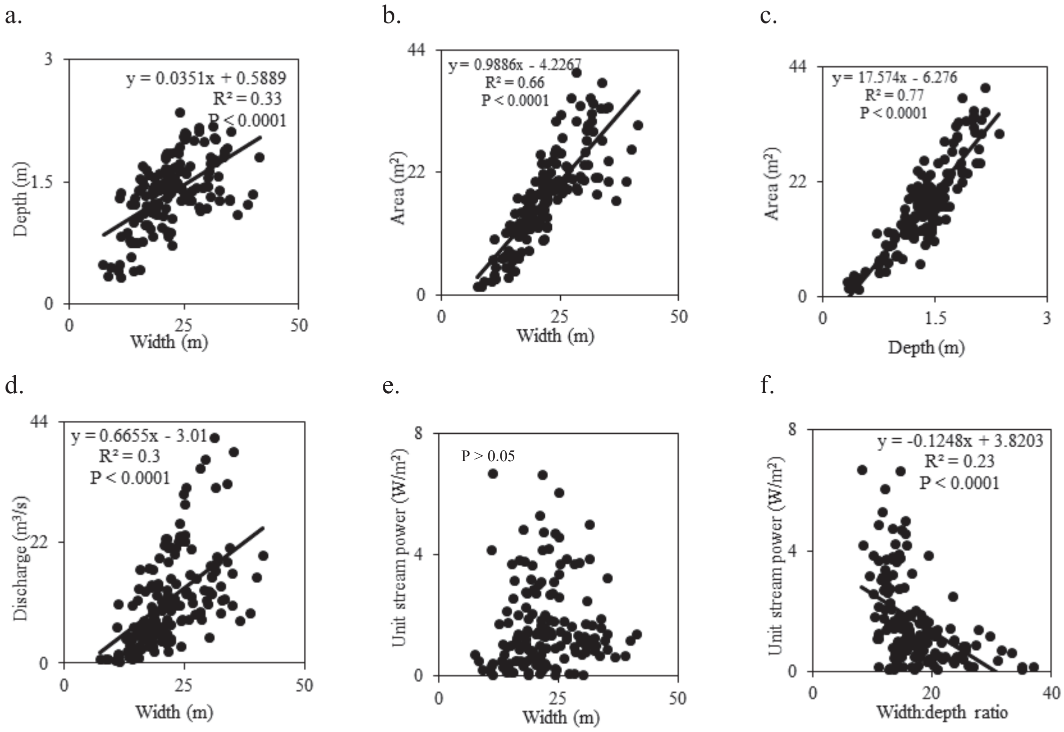

Figure A2.10 Relation between depth and width (a) area and width (b) area and depth (c) discharge and width (d) unit stream power and width (e) and unit stream power and width:depth ratio (f) in the Bulgeraga Creek.

1.11 Back Swamp

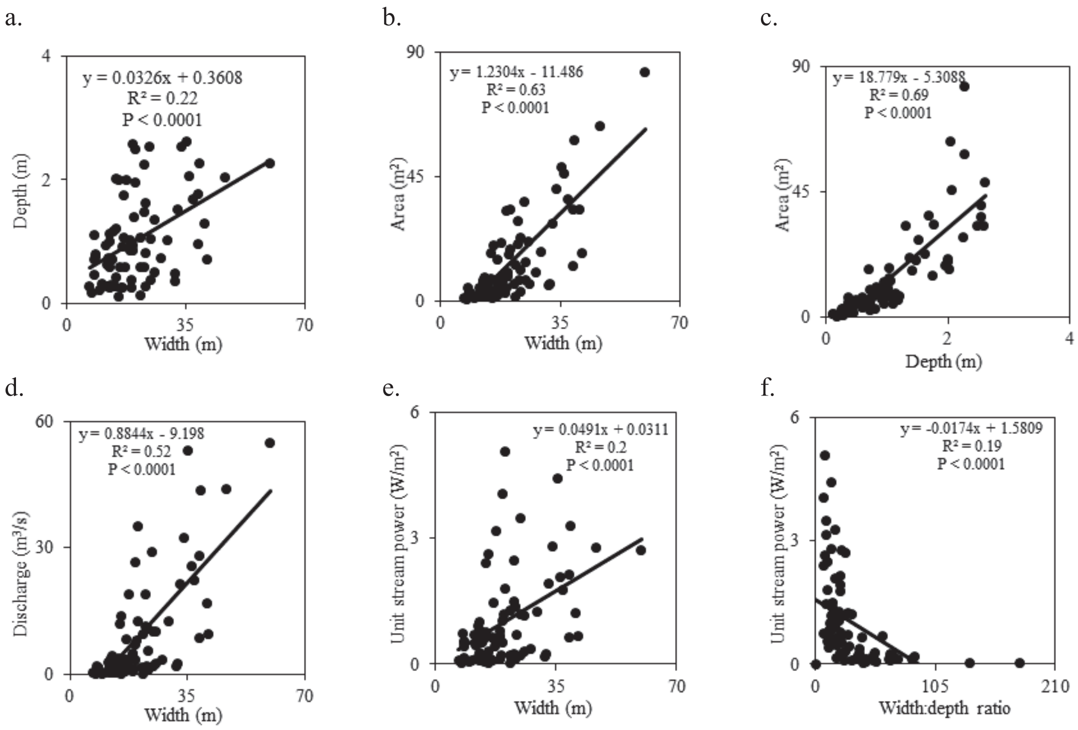

Figure A2.11 Relation between depth and width (a) area and width (b) area and depth (c) discharge and width (d) unit stream power and width (e) and unit stream power and width:depth ratio (f) in the Back Swamp.

2. Northern Macquarie Marshes

2.1 Macquarie River

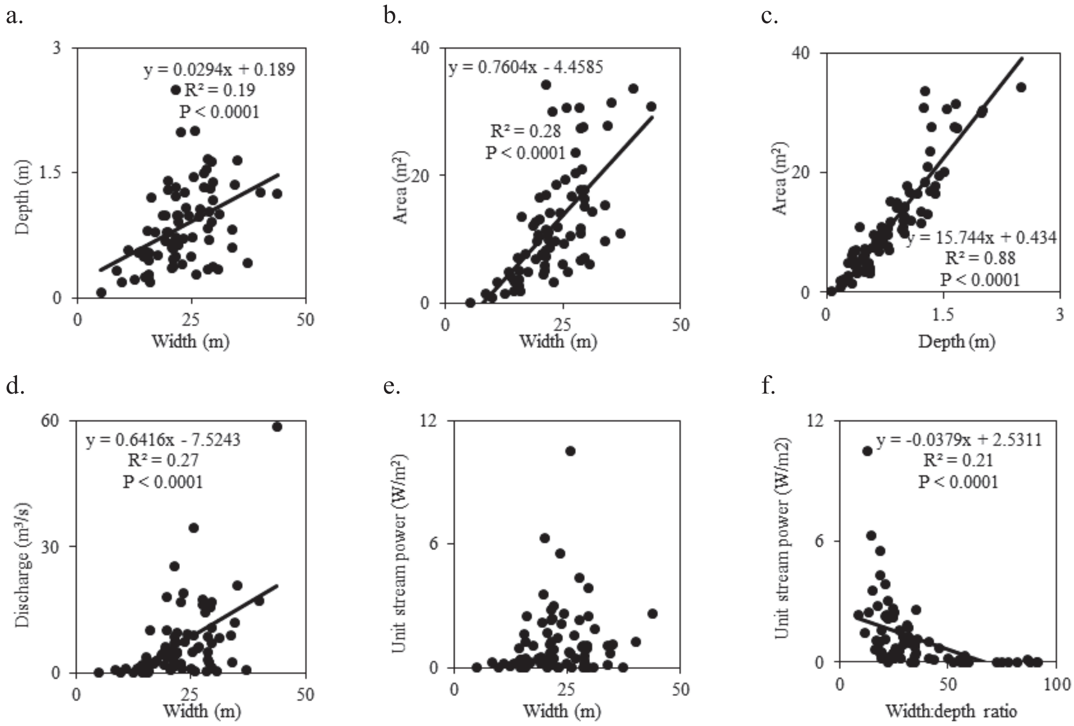

Figure A2.12 Relation between depth and width (a) area and width (b) area and depth (c) discharge and width (d) unit stream power and width (e) and unit stream power and width:depth ratio (f) in the Macquarie River in the Northern Marshes.

2.2 Bora Creek

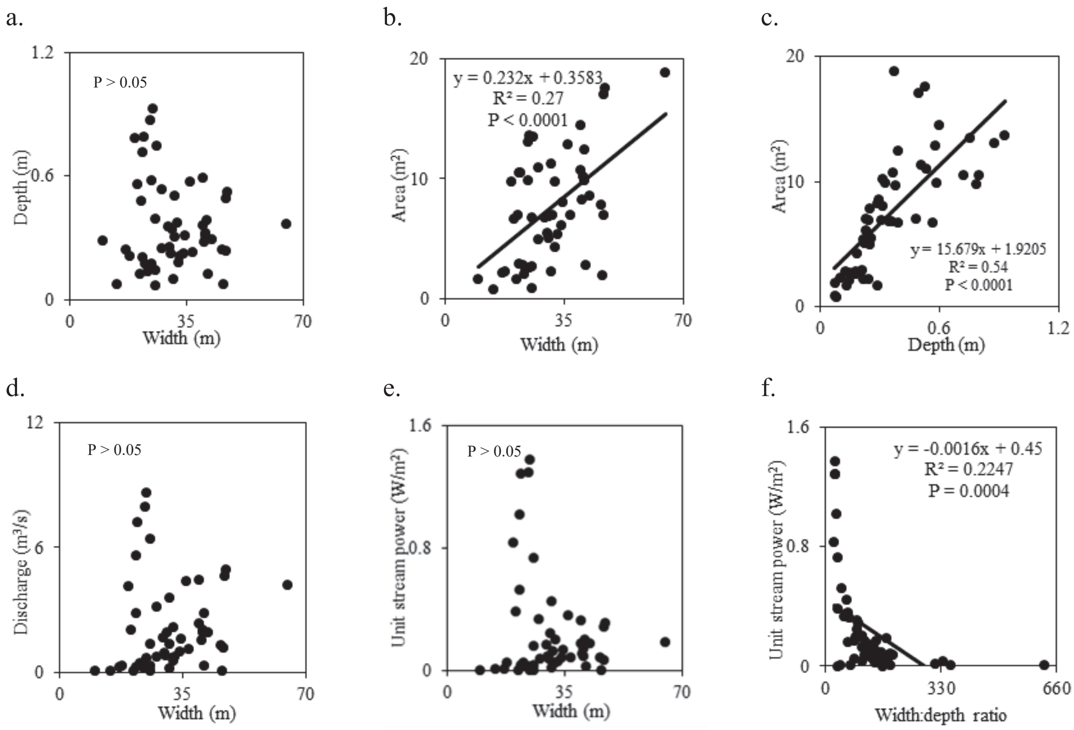

Figure A2.13 Relation between depth and width (a) area and width (b) area and depth (c) discharge and width (d) unit stream power and width (e) and unit stream power and width:depth ratio (f) in the Bora Creek.

3. Eastern Macquarie Marshes

3.1 Long Plain Cowal

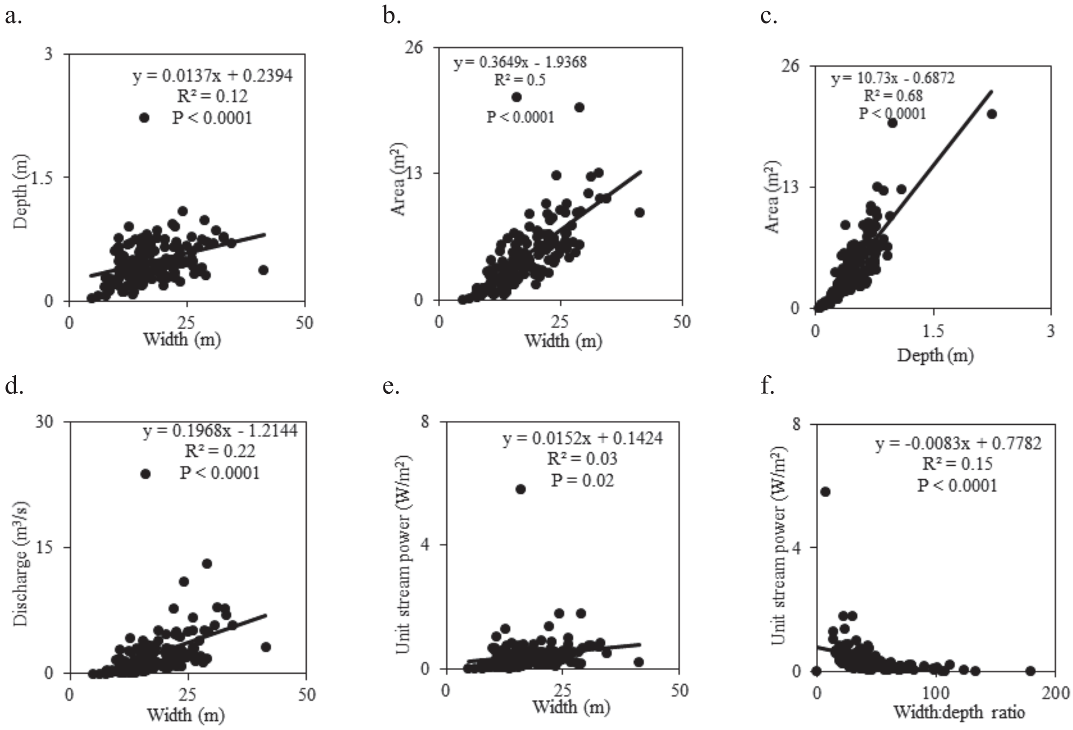

Figure A2.14 Relation between depth and width (a) area and width (b) area and depth (c) discharge and width (d) unit stream power and width (e) and unit stream power and width:depth ratio (f) in the Long Plain Cowal.

3.2 Gum Cowal

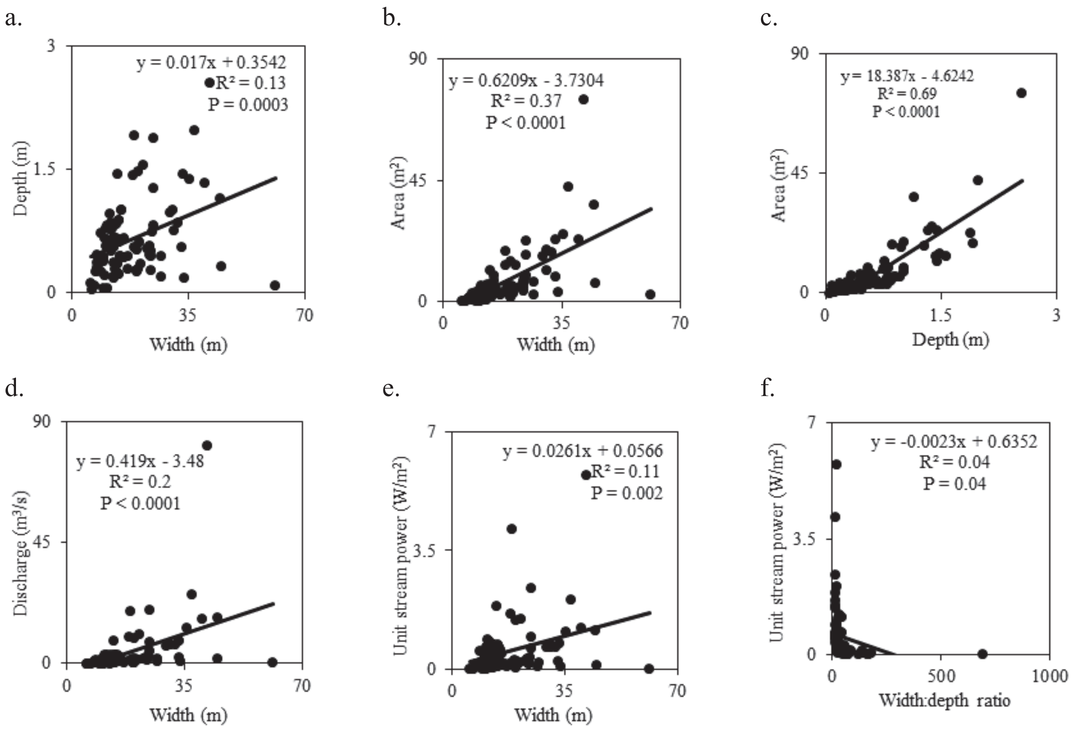

Figure A2.15 Relation between depth and width (a) area and width (b) area and depth (c) discharge and width (d) unit stream power and width (e) and unit stream power and width:depth ratio (f) in the Gum Cowal.

3.3 Terrigal Creek

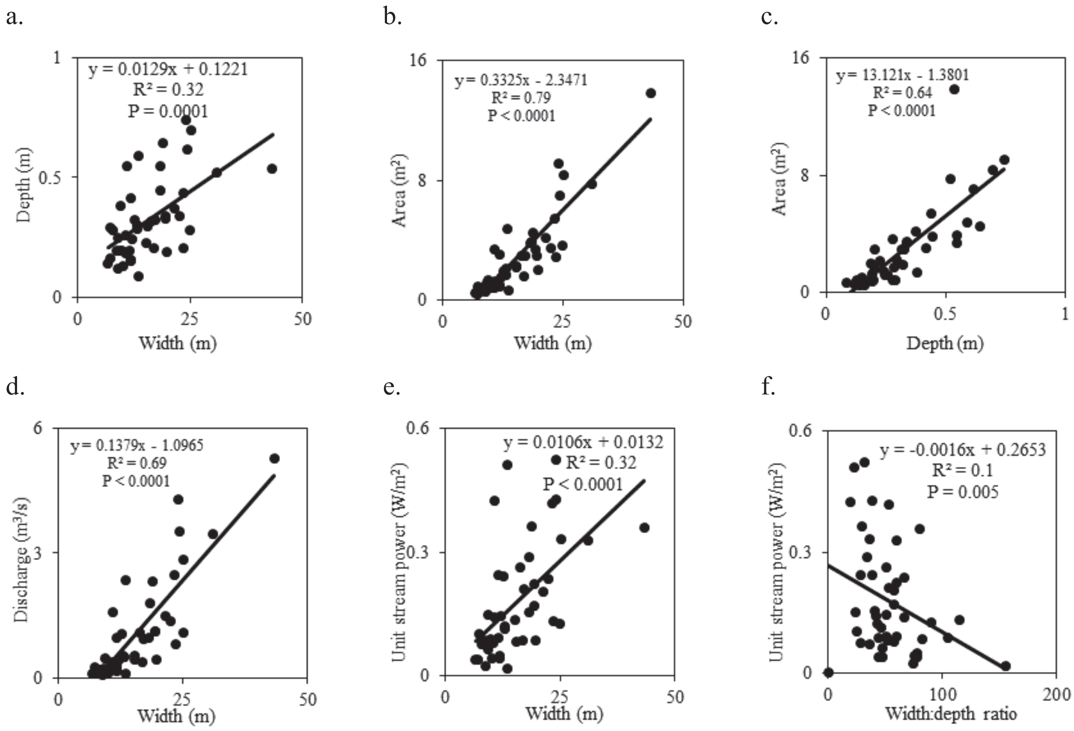

Figure A2.16 Relation between depth and width (a) area and width (b) area and depth (c) discharge and width (d) unit stream power and width (e) and unit stream power and width:depth ratio (f) in the Terrigal Creek.